NATIONAL COOPERATIVE HIGHWAY RESEARCH PROGRAM

DRAFT FINAL REPORT

EVALUATION OF ABUTMENT-SCOUR EQUATIONS FROM NCHRP PROJECTS 24-15(2) AND 24-20 USING LABORATORY AND FIELD DATA

NCHRP 24-20(2)

Stephen T. Benedict
U.S. Geological Survey
Clemson, South Carolina 29631
USA

Subject Areas
Highway and Facility Design • Bridges, Other Structures, and Hydraulic and Hydrology •Soils, Geology, and Foundations • Materials and Construction

Research Sponsored by the American Association of State Highway and Transportation Officials in Cooperation with the Federal Highway Administration

TRANSPORTATION RESEARCH BOARD
WASHINGTON, D.C.
June 2015
www.TRB.org

EVALUATION OF ABUTMENT-SCOUR EQUATIONS FROM NCHRP PROJECTS 24-15(2) AND 24-20 USING LABORATORY AND FIELD DATA

EXECUTIVE SUMMARY

Problem Statement

The National Cooperative Highway Research Program (NCHRP) sponsored several projects for the development of new abutment-scour prediction methods in cohesive and non-cohesive sediments. These projects include:

1. NCHRP Project 24-15(2): Abutment Scour in Cohesive Soils[1]

2. NCHRP Project 24-20 Prediction of Scour at Bridge Abutments[2]

The NCHRP 24-15(2) and NCHRP 24-20 Projects represent extensive efforts to develop new methods for predicting abutment scour, and with the completion of these investigations, there is a need to test and evaluate their performance with field data. This analysis will help identify strengths, weaknesses, and limitations associated with the newly developed scour prediction methods, and will provide guidance to the practitioner for the application of these methods.

Project Objectives

The primary objectives of this investigation were to test and evaluate the performance of the abutment-scour prediction methods developed in the NCHRP Projects 24-15(2) and 24-20, using field measurements collected by the U.S. Geological Survey (USGS). To confirm prediction patterns observed in the field data, laboratory measurements from previous investigations also were applied to the newly developed methods. Results from the analysis were used to identify

---

[1] Briaud, J.-L., Chen, H.-C., Chang, K.-A., Oh, S.J., and Chen, X. (2009). "Abutment Scour in Cohesive Material." NCHRP Report 24-15(2), Transportation Research Board, National Research Council, Washington, D.C.

[2] Ettema, R., Nakato, T., and Muste, N. (2010). "Estimation of scour depth at bridge abutments." Draft final report, NCHRP Report 24-20, National Cooperative Highway Research Program, Transportation Research Board, Washington, D.C.

performance characteristics for each scour prediction method, note potential ways to improve performance, and provide limited guidance to the practitioner for application of these methods. Additionally this investigation aligns with a recommendation from NCHRP Project 24-27(02), a review of the state of knowledge regarding abutment scour, that more data on abutment scour be obtained and used to illuminate scour and evaluate methods for estimating scour depth.

Field and Laboratory Data

A literature review was done to identify potential sources of abutment-scour data, and selected data, including 329 field and 514 laboratory measurements of abutment scour, were compiled into a database. All of the field data were collected by the USGS and included 15 measurements from the USGS National Bridge Scour Database[3], 92 measurements from the moderate-gradient streams of the South Carolina Piedmont having cohesive sediments[4], 106 measurements from the low-gradient streams of the South Carolina Coastal Plain (none are tidally influenced) generally having sandy[4], non-cohesive sediments, 93 measurements from the small, steep-gradient streams of Maine having coarse sediments[5], and 23 measurements from the low-gradient streams of the Alabama Black Prairie Belt having cohesive sediments[6]. Most of these data are historical scour measurements, similar to post-flood measurements, and are assumed to represent the maximum abutment-scour depth that has occurred at the bridge since construction. The field data are largely associated with clear-water scour conditions where sediments do not refill the scour holes as flood waters recede, making them appropriate sites for historical scour measurements. Because the scour measurements were made during low-flow conditions, one-dimensional flow models were used to estimate the hydraulic properties. The measurement characteristics associated with the field data (post flood) and the estimated hydraulics will

---

3 U.S. Geological Survey (2001). "National bridge scour database." (http://water.usgs.gov/osw/techniques/bs/BSDMS/index.html).

4 Benedict, S.T. (2003). "Clear-water abutment and contraction scour in the coastal plain and Piedmont provinces of South Carolina, 1996-99." Water-Resources Investigations Report 03-4064, U.S. Geological Survey, Columbia, South Carolina.

5 Lombard, P.J., and Hodgkins, G.A. (2008). "Comparison of observed and predicted abutment scour at selected bridges in Maine." Scientific Investigations Report 2008–5099, U.S. Geological Survey, Reston, VA.

6 Lee, K.G., and Hedgecock, T.S. (2008). "Clear-water contraction scour at selected bridge sites in the Black Prairie Belt of the Coastal Plain in Alabama, 2006." Scientific Investigations Report 2007–5260 U.S. Geological Survey, Reston, VA.

introduce some error into these measurements, making them less than ideal. It also is notable that field conditions associated with the USGS field data will frequently deviate from the simple models of the laboratory; therefore, the scour patterns in the laboratory and field data will differ in some measure. In particular, the small to moderate drainage areas associated with most of the USGS field data will tend to have peak-flow durations lasting only hours, likely preventing the attainment of equilibrium abutment-scour depths comparable to those of the laboratory, where peak flows may continue for days. Additionally, sediments in the field are typically non-uniform in grain size and often have some measure of cohesion. Furthermore, field sediments often have subsurface scour-resistant layers that impede or limit scour. These field characteristics are distinctly different from the non-cohesive sediments of the laboratory and will tend to reduce scour depth. The limitations and characteristics associated with the USGS field data make these data less than ideal for evaluating laboratory-derived scour prediction equations. While the limitations are acknowledged, it is currently (2015) the best available set of field data, and the large number of measurements (329) should be sufficient to gain insights into the general trends of abutment scour in the field setting.

In addition to field data, 514 laboratory measurements of abutment scour from selected authors, including 359 measurements from Palaviccini[7], 74 measurements from Sturm[8], 19 measurements from the NCHRP 24-15(2) investigation[1], and 62 measurements from the NCHRP 24-20 investigation[2], were incorporated into the database. The Palaviccini data consist of measurements of live-bed and clear-water abutment scour in non-cohesive sediments compiled from selected investigations conducted prior to 1990. The measurements were collected in rectangular flumes with rigid abutment models. The Sturm data consist of clear-water abutment scour in non-cohesive sediments collected in compound channels with rigid abutment models. The NCHRP 24-15(2) data consist of clear-water abutment scour in cohesive sediments collected in compound and rectangular channels with rigid abutment models. The NCHRP 24-20 data consist of live-bed and clear-water abutment scour in non-cohesive sediments collected in compound and rectangular channels. The NCHRP 24-20 investigation

---

7 Palaviccini, M. (1993). "Predictor model for bridge abutments. PhD Thesis, The Catholic University of America, Washington, D.C.

8 Sturm, T.W. (2004). "Enhanced abutment scour studies for compound channels." Report No. FHWA-RD-99-156, Federal Highway Administration, McLean, VA.

used a combination of erodible and non-erodible floodplains, embankments, and abutment substructures thought to better represent field conditions, and as such, are distinctly different from the other data. The varying characteristics of the laboratory data will influence their performance when applied to scour prediction equations, and this should be kept in mind when reviewing the results of this investigation.

Comparison of Dimensionless Variables for Field and Laboratory Data

Scour prediction equations developed from small-scale laboratory investigations are typically scaled to the field through the development of equations associated with dimensionless variables. To assure the success of a laboratory-derived equation, the range of the dimensionless variables associated with the laboratory data should approximate the typical range found in the field. To gain perspective, percentile plots of selected dimensionless variables that are commonly used in the analysis of abutment scour were developed for the field and laboratory data. The dimensionless variables included relative abutment length (L/y_1), relative scour depth (y_{sadj}/y_1) adjusted for abutment shape, unit discharge ratio (q_2/q_1), relative sediment size ($L/D50$), the approach Froude number (Fr_1), and the ratio of embankment length blocking flow to the floodplain width (L/B_f). The percentile plots helped identify typical ranges associated with selected explanatory variables for the laboratory and field data. It was notable that the laboratory data did not include the higher range of embankment lengths and flow contractions found in the field where potential for scour is greatest, indicating that the equations derived from the laboratory data may incompletely include the effects of abutment length on abutment scour and, therefore, possibly underpredict scour for such conditions. This limitation in the laboratory data is largely due to the challenges of modeling long embankments that produce large contractions of flow in the laboratory setting. The upper bounds of relative scour depth (scour depth divided by flow depth) for laboratory and field data also were compared, showing that laboratory models have an upper bound of about 11 while the upper bound of the field data was only 4.2. While many factors likely contribute to the smaller relative abutment-scour depths in the field data, the non-uniform sediments and short flow durations found in the field, in conjunction with the rigid

abutment models associated with most of the laboratory data, are thought to be prominent reasons for the laboratory and field discrepancies.

Analysis and General Conclusions

To assure appropriate application of the NCHRP 24-15(2) and 24-20 prediction methods to the field and laboratory data, the principal investigators for each method were consulted during the development of the application procedures and provided opportunity to review the documented procedures along with preliminary results. The application procedures were applied to each respective method using the selected laboratory and field data. The results from this application were incorporated into selected scatter plots to display the relations of predicted and measured scour, as well as prediction residuals with respect to selected explanatory variables. While the results associated with the field data were of primary concern in this investigation, the laboratory results were useful to confirm and better understand the field data results. General conclusions for each method follow.

NCHRP 24-15(2)

The NCHRP 24-15(2) prediction method was originally developed for predicting abutment scour in cohesive sediments. The abutment models used in this investigation consisted of rigid structures having vertical-wall substructures that extended fully into the surrounding sediments. Results from this investigation indicate that the equation will perform best for cohesive sediments, but will produce some underpredictions. In contrast, the method yields frequent, and at times excessive underprediction in the field data with non-cohesive sediments, and this is of concern. Poor estimates of the increased flow velocities at the abutment from the one-dimensional flow models is a factor that likely contributes, in part, to the patterns of underprediction in the NCHRP 24-15(2) prediction method. However, the analysis indicates that some of the underprediction is associated with selected correction factors (channel geometry, abutment location, abutment shape, and Reynolds number) and that additional analysis and modification of those factors could substantially improve performance.

NCHRP 24-20

The NCHRP 24-20 prediction method was originally developed for predicting abutment scour in non-cohesive sediments. A unique feature of the NCHRP 24-20 investigation was the use of erodible embankments and abutments to better simulate conditions found in the field. The analysis of the NCHRP 24-20 method indicates that it reflects the general trend of the non-cohesive field data, with predicted scour depth generally increasing as measured scour depth increases and with the scatter about the line-of-agreement being relatively small. This pattern suggests that the NCHRP 24-20 method is, in some measure, capturing the scour processes for the non-cohesive field data. However, as measured scour depth increases beyond 10 feet, underprediction increases, which is of concern. Multiple factors likely contribute to this pattern of underprediction, including poor estimates of the increased flow velocities at the abutment from the one-dimensional flow models and intact rather than eroded abutments. Many of the underpredictions in the field data are associated with intact abutments classified as Scour Condition B. The intact abutments differ from the erodible embankment/abutment models for Scour Condition B in the NCHRP 24-20 investigations, possibly contributing to the underprediction. The limitations and uncertainty of the field data make it difficult to confidently conclude the cause of the underprediction. Because many of the underpredictions in the field data are associated with densely-vegetated floodplains, relatively long abutments, and large flow contractions, where the potential for scour is large, caution must be used when applying the NCHRP 24-20 method to such field conditions.

With respect to cohesive sediments, there is infrequent underprediction, but overprediction is excessive at times. While the NCHRP 24-20 method can be adapted for application to cohesive and non-cohesive sediments, its current formulation is for non-cohesive sediments. Therefore, the excessive overprediction in cohesive sediments is to be expected.

Recommendation for Additional Analysis

The analysis of the NCHRP 24-15(2) and NCHRP 24-20 prediction methods with laboratory and field data provided valuable insights into the performance characteristics of these methods. For both methods, there are some patterns of underprediction that are of concern. Because of the

limitations in the field data as well as limitations associated with the derivations of each method, identifying the factors that cause the underprediction is difficult. However, further analysis could help identify likely sources of the error and thus improve the performance of each method. With this objective in mind, the following recommendations for each method are made.

NCHRP 24-15(2)

- Evaluate the sensitivity of the NCHRP 24-15(2) method to flow velocity by using two-dimensional flow models for selected sites in the USGS field data. This would help determine if the underprediction is primarily associated with poor estimates of the velocity from the one-dimensional models.

- The analysis in this investigation indicates that modification of selected correction factors in the NCHRP 24-15(2) method would substantially improve equation performance. Further review and analysis of these correction factors should be made, and modifications should be adopted as deemed appropriate.

- The NCHRP 24-15(2) method notes that the Erosion Function Apparatus (EFA) test is an alternate method for estimating sediment critical velocity (V_c). It may be beneficial to evaluate the sensitivity of predicted scour for V_c determined from an EFA test in contrast to V_c determined from the recommended empirical method.

- Evaluate an appropriate safety factor.

NCHRP 24-20

- Evaluate the sensitivity of the method to flow velocity by using two-dimensional flow models for selected sites in the USGS field data. This would help determine if the underprediction is primarily associated with poor estimates of the velocity from the one-dimensional models.

- Using the analysis based on two-dimensional models, evaluate the influence of relatively long abutments to determine if incorporating an adjustment factor in the NCHRP 24-20 for such abutments would be appropriate to minimize the potential for underprediction.

- Using the analysis based on two-dimensional models, evaluate the amplification factor for field conditions where the abutment/embankment remains intact to determine if adjustments to the amplification factor may be needed.

- Using the analysis based on two-dimensional models, in conjunction with the other data, evaluate an appropriate safety factor.

- While the theory of the NCHRP 24-20 method is applicable to both non-cohesive and cohesive sediments, its current formulation has yet to be adapted to cohesive sediments. Therefore, it is recommended that consideration be given to developing a formulation appropriate for cohesive sediments.

- The NCHRP 24-20 method uses an estimate of contraction scour to predict abutment scour. Current methods for predicting contraction scour are based on simplified equations that do not capture the complexity of the field. Therefore, it would be beneficial to conduct research to advance the understanding of, and the methods used for estimating contraction scour. Such research should evaluate contraction geometry (including abutment length and asymmetry of abutment lengths), and channel and floodplain roughness characteristics commonly found in the field. The Laursen method does not fully account for these conditions.

ACKNOWLEDGEMENTS

This report was prepared under NCHRP Project 24-20(2) by the U.S. Geological Survey. The research was conducted by Stephen Benedict, a hydrologist with the U.S. Geological Survey, under a sole source contract with the National Cooperative Highway Research Program. Assistance regarding the procedures for applying the methods presented in NCHRP 24-15(2) and 24-20 were provided by the Principal Investigators, Dr. Jean-Louis Briaud, professor in the Department of Civil Engineering at Texas A&M University, and Dr. Robert Ettema, professor in the Department of Civil and Architectural Engineering at the University of Wyoming, respectively.

The NCHRP Panel, listed below, provided technical and editorial suggestions for this investigation, and their contributions are gratefully acknowledged.

Panel Members:

David Reynaud, Senior Program Officer, NCHRP

Larry A. Arneson

Bart Bergendahl

Stanley R. Davis

Daryl James Greer

J. Sterling Jones

Arthur C. Miller

Richard A. Phillips

Amy Ronnfeldt

Larry J. Tolfa

Mehmet T. Tumay

Njoroge W. Wainaina

ABSTRACT

The National Cooperative Highway Research Program (NCHRP) sponsored the NCHRP 24-15(2) and NCHRP 24-20 Projects to investigate abutment scour in cohesive and non-cohesive sediments, respectively. These investigations represent extensive efforts to collect and evaluate laboratory data, leading to the development of new methods for predicting abutment scour. To evaluate these new methods, the U.S. Geological Survey, in cooperation with the NCHRP, conducted an investigation to analyze their performance by using laboratory and field data. These data included approximately 500 laboratory and 330 field measurements of abutment scour, providing a large and diverse dataset for assessing prediction performance. The analysis provides insights into the strengths, weaknesses, and limitations associated with the newly developed scour prediction methods, providing guidance to the practitioner for their application.

TABLE OF CONTENTS

EXECUTIVE SUMMARY ii

ACKNOWLEDGEMENTS x

ABSTRACT xi

TABLE OF CONTENTS xii

LIST OF FIGURES xvi

LIST OF TABLES xxviii

LIST OF SYMBOLS xxix

CHAPTER 1 INTRODUCTION AND OVERVIEW OF ABUTMENT-SCOUR DATA 1-1

1.1 Introduction 1-1
1.1.1 Project Objective 1-2
1.1.2 Approach 1-2
1.1.3 Report Organization 1-3

1.2 Field Data 1-3
1.2.1 South Carolina Data 1-4
1.2.2 Maine Data 1-10
1.2.3 Alabama Data 1-13
1.2.4 National Bridge Scour Database 1-15
1.2.5 Limitations 1-19

1.3 Laboratory Data 1-22
1.3.1 Adjustment for Abutment Shape 1-26
1.3.2 Upper Bound of Laboratory Data 1-27

1.4 Comparison of Field and Laboratory Data 1-30
1.4.1 Percentile Plots of Selected Dimensionless Variables 1-30
1.4.2 Upper Bound of Abutment Scour 1-40
1.4.3 Abutment Scour with Respect to the Geometric Contraction Ratio 1-43
1.4.4 Unit Discharge Ratio 1-46

CHAPTER 2 APPLICATION PROCEDURE FOR THE NCHRP 24-20 PREDICTION METHOD 2-1

2.1 Introduction 2-1

2.2 Summary of NCHRP 24-20 Scour Prediction Method 2-1

2.3 General Procedure for Application of NCHRP 24-20 to the Laboratory and the USGS Field Data 2-12

CHAPTER 3 APPLICATION OF THE NCHRP 24-20 PREDICTION METHOD TO LABORATORY AND FIELD DATA 3-1

3.1 Introduction 3-1

3.2 Analysis of the Laboratory Data 3-3
3.2.1 Relation of Measured and Predicted Scour 3-3
3.2.2 Prediction Residuals with Respect to Selected Explanatory Variables 3-7
i. Prediction Residuals with Respect to q_2 3-7
ii. Prediction Residuals with Respect to q_2/q_1 3-10
iii. Prediction Residuals with Respect to *D50* 3-11
iv. Prediction Residuals with Respect to L/y_1 3-11
v. Prediction Residuals with Respect to y_1 3-14
vi. Prediction Residuals with Respect to α 3-14

3.3 Analysis of the USGS Field Data 3-17
3.3.1 Measured and Predicted Scour for the USGS Field Data 3-17
3.3.2 Prediction Residuals with Respect to Selected Variables 3-23
i. Prediction Residuals with Respect to q_2 3-23
ii. Prediction Residuals with Respect to q_2/q_1 3-25
iii. Prediction Residuals with Respect to *D50* 3-26
iv. Prediction Residuals with Respect to L/y_1 3-27
v. Prediction Residuals with Respect to y_1 3-27
vi. Prediction Residuals with Respect to α 3-29

3.4 Evaluation of the Amplification Factor 3-30
3.4.1 Determination of the Required Amplification Factor 3-36

3.5 Prediction Trends for Cohesive and Non-Cohesive Sediments 3-41

3.6 Alternate Critical-Velocity Methods for Estimating Clear-Water Contraction Scour 3-43
3.6.1 Fortier and Scobey Maximum Permissible Velocity 3-44
3.6.2 The Neill Critical-Velocity Curve 3-48
3.6.3 The Vanoni Critical-Velocity Curve 3-50
3.6.4 Application of Alternate Critical Velocities to the NCHRP 24-20 Method for Clear-Water Scour Sites 3-51

3.7 Assessment of the NCHRP 24-20 Prediction Method 3-57
3.7.1 Strengths 3-57
3.7.2 Weaknesses 3-58
3.7.3 Recommendations for Additional Analysis 3-61
3.7.4 General Application Guidance 3-64

CHAPTER 4 APPLICATION PROCEDURE FOR THE NCHRP 24-15(2) PREDICTION METHOD 4-1

4.1 Introduction 4-1

4.2 Summary of NCHRP 24-15(2) Scour Prediction Method 4-1

4.3 General Procedure for Application of NCHRP 24-15(2) to the Laboratory and the USGS Field Data 4-7

CHAPTER 5 APPLICATION OF THE NCHRP 24-15(2) PREDICTION METHOD TO LABORATORY AND FIELD DATA 5-1

5.1 Introduction 5-1

5.2 Analysis of the Laboratory Data 5-2
5.2.1 Relation of Measured and Predicted Scour 5-3
5.2.2 Influence of Selected Explanatory Variables on Predicted Scour 5-8
5.2.3 Prediction Residuals with Respect to Selected Explanatory Variables 5-13
i. Prediction Residuals with Respect to $D50$, V_c, and Fr_c 5-13
ii. Prediction Residuals with Respect to Fr_{f2} and $7.94(1.65Fr_{f2} - Fr_c)$ 5-18
iii. Prediction Residuals with Respect to Re_{f2} and K_{Re} 5-20
iv. Prediction Residuals with Respect to K_1, K_2, K_G, and K_L 5-24

5.3 Analysis of the USGS Field Data 5-39
5.3.1 Relation of Measured and Predicted Scour 5-39
5.3.2 Influence of Selected Explanatory Variables on Predicted Scour 5-44
5.3.3 Prediction Residuals with Respect to Selected Explanatory Variables 5-50
i. Prediction Residuals with Respect to $D50$, V_c, and Fr_c 5-50
ii. Prediction Residuals with Respect to Fr_{f2} and $7.94(1.65Fr_{f2} - Fr_c)$ 5-54
iii. Prediction Residuals with Respect to Re_{f2} and K_{Re} 5-57
iv. Prediction Residuals with Respect to K_1, K_2, K_G, K_L, and K_p 5-59
v. Prediction Residuals with Respect to Relative Abutment Length (L/y_{f1}) 5-64
5.3.4 Prediction Trends for Cohesive and Non-Cohesive Sediments 5-67
5.3.5 Alternate Critical-Velocity Methods for Estimating Clear-Water Contraction Scour 5-69

5.4 Assessment of the NCHRP 24-15(2) Prediction Method 5-72
5.4.1 Strengths 5-72
5.4.2 Weaknesses 5-73
5.4.3 Recommendations for Improving Method 5-75
5.4.4 General Application Guidance 5-79

CHAPTER 6 COMPARISON OF RESULTS FOR NCHRP 24-20 AND NCHRP 24-15(2) AND CONCLUSIONS 6-1

6.1 Introduction 6-1

6.2 Performance in the Laboratory Data 6-1
6.2.1 Residual Patterns Associated with the NCHRP 24-20 Prediction Method 6-2
6.2.2 Residual Patterns Associated with the NCHRP 24-15(2) Prediction Method 6-3

6.3 Performance in the Field Data 6-8
6.3.1 Residual Patterns Associated with the NCHRP 24-20 Prediction Method 6-8
6.3.2 Residual Relations Associated with the NCHRP 24-15(2) Prediction Method 6-13

6.4 Conclusions 6-15
6.4.1 Summary of Conclusions for NCHRP 24-20 6-16
6.4.2 Summary of Conclusions for NCHRP 24-15(2) 6-18

REFERENCES R-1

LIST OF FIGURES

Figure 1-1. Percentile plot of bridge lengths for bridges in South Carolina crossing water. 1-5

Figure 1-2. Typical cross section for bridges with setback abutments (from Benedict, 2003). 1-7

Figure 1-3. General plan and profile for bridges with setback abutments (from Benedict, 2003). 1-8

Figure 1-4. Typical cross section for bridges crossing swampy channels or for floodplain relief bridges (from Benedict, 2003)..... 1-9

Figure 1-5. Typical cross section for bridge abutment/embankment with definition of selected variables from tables 1-1 through 1-4 (modified from Ettema et al., 2010)..... 1-9

Figure 1-6. Percentile plot of bridge lengths for bridges in Maine crossing water..... 1-11

Figure 1- 7. Typical cross section for abutment protruding into main channel (from Benedict, 2003). 1-11

Figure 1- 8. Example of abutments protruding into main channel at East Branch of the Wesserunsett Stream at Athens, Maine (from Lombard and Hodgkins, 2008). 1-12

Figure 1-9. Percentile plot of bridge lengths for bridges in Alabama crossing water..... 1-14

Figure 1- 10. A floodplain relief bridge at Cottonwood Creek crossing of County Road 12, Hale County, Alabama (from Lee and Hedgecock, 2008). 1-15

Figure 1- 11. Relation of the relative scour depth to relative flow depth, with respect to abutment length, for selected laboratory data..... 1-29

Figure 1- 12. Relation of the relative scour depth to relative abutment length, with respect to flow depth, for selected laboratory data. 1-29

Figure 1-13. Percentile plots for the relative abutment length (L/y_1) for selected field and laboratory data. 1-36

Figure 1-14. Percentile plots for the relative abutment scour (y_{sadj}/ y_1) for selected field and laboratory data. 1-36

Figure 1-15. Percentile plots for the unit discharge ratio (q_2/q_1) for selected field and laboratory data. 1-37

Figure 1-16. Percentile plots for the relative sediment size ($L/D50$) for selected field and laboratory data. 1-37

Figure 1-17. Percentile plots for the approach Froude number (Fr_1) for selected field and laboratory data. 1-38

Figure 1-18. Percentile plots for the ratio of the approach floodplain velocity to the critical velocity for selected data from the Coastal Plain and Piedmont of South Carolina (from Benedict and Caldwell, 2006). 1-38

Figure 1-19. Percentile plots for L/B_f for selected field and laboratory data. (Note: Vertical scale has been truncated to better display the trends for the majority of the data.) 1-39

Figure 1-20. Relation of the relative scour depth to relative flow depth for selected laboratory data and the U.S. Geological Survey field data. 1-42

Figure 1-21. Relation of the relative scour depth to relative abutment length for selected laboratory data and the U.S. Geological Survey field data. 1-42

Figure 1-22. Relation of abutment-scour depth to the geometric contraction ratio for selected field measurements in comparison to the South Carolina abutment-scour envelope curves. 1-45

Figure 1-23. Relation of relative scour depth (y_{sadj}/y_1) to the geometric contraction ratio for selected laboratory and field measurements. 1-45

Figure 1-24. Relation of the unit discharge ratio (q_2/q_1) to the geometric contraction ratio for selected laboratory and field measurements of abutment scour. 1-47

Figure 1-25. Relation of the unit discharge ratio (q_2/q_1) to the geometric contraction ratio for selected laboratory and field measurements of abutment scour. 1-47

Figure 2-1. Conceptual model of abutment scour where y_1 is the flow depth prior to scour, Y_C is the mean flow depth of the contraction scour, and Y_{MAX} is the maximum flow depth in the abutment-scour region (modified from Ettema et al. 2010). 1-4

Figure 2-2. Schematic showing selected hydraulic variables and the regions they represent at the approach and bridge cross sections. 2-7

Figure 2-3. Design curve for scour-amplification factor, α, for spill-through abutments subject to Scour Condition A ($L/B_f \geq 0.75$) (from Ettema et al. 2010). 2-8

Figure 2-4. Design curve for scour-amplification factor, α, for wing-wall abutments subject to Scour Condition A ($L/B_f \geq 0.75$) (from Ettema et al. 2010). 2-9

Figure 2-5. Design curve for scour-amplification factor, α, for spill-through abutments subject to Scour Condition B ($L/B_f < 0.75$) (from Ettema et al. 2010). 2-10

Figure 2-6. Design curve for scour-amplification factor, α, for wing-wall abutments subject to Scour Condition B ($L/B_f < 0.75$) (from Ettema et al. 2010). 2-11

Figure 2-7. General schematic for setback ratio ≤ 5 (modified from Arneson et al., 2012). 2-17

Figure 2-8. General schematic for setback ratio > 5 (modified from Arneson et al., 2012). 2-20

Figure 2-9. General schematic for setback ratio > 5 and ≤ 5 (modified from Arneson et al., 2012). 2-22

Figure 3-1. Relation of predicted and measured abutment-scour depth for selected laboratory data, using the NCHRP 24-20 scour prediction method for (*A*) only non-cohesive sediments and (*B*) cohesive and non-cohesive sediments. 3-5

Figure 3-2. Relation of predicted and measured abutment-scour depth for selected laboratory data with vertical-wall abutments, using the NCHRP 24-20 scour prediction method. 3-6

Figure 3-3. Relation of predicted and measured abutment-scour depth for selected laboratory data with spill-through abutments, using the NCHRP 24-20 scour prediction method. 3-6

Figure 3-4. Relation of predicted and measured abutment-scour depth for selected laboratory data with wing-wall abutments, using the NCHRP 24-20 scour prediction method. 3-7

Figure 3-5. Relation of prediction residuals and the median grain size, q_2, for (*A*) all of selected laboratory data and (*B*) only clear-water laboratory data applied to the NCHRP 24-20 scour prediction method..... 3-9

Figure 3-6. Relation of prediction residuals and the unit discharge ratio, q_2/q_1, for selected laboratory data applied to the NCHRP 24-20 scour prediction method..... 3-10

Figure 3-7. Relation of prediction residuals and the median grain size, *D50*, for (*A*) all of selected laboratory data and (*B*) only clear-water

laboratory data applied to the NCHRP 24-20 scour prediction method..... 3-12

Figure 3-8. Relation of prediction residuals and relative abutment length, L/y_1, for (*A*) all of selected laboratory data and (*B*) only clear-water laboratory data applied to the NCHRP 24-20 scour prediction method. 3-13

Figure 3-9. Relation of prediction residuals and y_1, for (*A*) all of selected laboratory data and (*B*) only clear-water laboratory data applied to the NCHRP 24-20 scour prediction method. 3-15

Figure 3-10. Relation of prediction residuals and the amplification factor (α), for (*A*) all of selected laboratory data and (*B*) only clear-water laboratory data applied to the NCHRP 24-20 scour prediction method..... 3-16

Figure 3-11. Relation of measured and predicted abutment-scour depth for selected field data using the NCHRP 24-20 scour prediction method..... 3-19

Figure 3-12. Relation of measured and predicted abutment-scour depth for selected field data using the NCHRP 24-20 scour prediction method for the (*A*) South Carolina Relief/Swamp Bridge, (*B*) South Carolina Coastal Plain, (*C*) South Carolina Piedmont, (*D*) Maine, (*E*) Alabama, and (*F*) National Bridge Scour Database (NBSD) data..... 3-21

Figure 3-13. Relation of prediction residuals and the unit discharge, q_2, for selected field data applied to the NCHRP 24-20 scour prediction method..... 3-24

Figure 3-14. Relation of prediction residuals and the unit discharge ratio, q_2/q_1, for selected field data applied to the NCHRP 24-20 scour prediction method. 3-25

Figure 3-15. Relation of prediction residuals and the median grain size, *D50*, for selected field data applied to the NCHRP 24-20 scour prediction method. 3-26

Figure 3-16. Relation of prediction residuals and the relative abutment length, L/y_1, for selected field data applied to the NCHRP 24-20 scour prediction method. 3-28

Figure 3-17. Relation of prediction residuals and the flow depth, y_1, for selected field data applied to the NCHRP 24-20 scour prediction method..... 3-28

Figure 3-18. Relation of prediction residuals and the amplification, α, for selected field data applied to the NCHRP 24-20 scour prediction method..... 3-30

Figure 3-19. Relation of the amplification factor and the unit discharge ratio for wing-wall and spill-through abutments based on the Briaud et al. (2009) formula and the NCHRP 24-20 curve for Scour Condition B (from Sturm et al. 2011). (Note: The Briaud et al. (2009) curves reflect design curves with a factor of safety.)..... 3-33

Figure 3-20. Relation of the amplification factor and the unit discharge ratio based on data from Melville (1997), Melville and Coleman (2000), Sturm (2004, 2006), and the NCHRP 24-20 curve (from Sturm et al. 2011)..... 3-34

Figure 3-21. Conceptual model for (*A*) Scour Condition A - hydraulic scour of the main-channel bed causes bank failure, which causes a failure of the face of the abutment embankment, and (*B*) Scour Condition B - hydraulic scour of the floodplain causes failure of the face of the abutment embankment (from Ettema et al. 2010)..... 3-35

Figure 3-22. Relation of the required amplification factor and the unit discharge ratio for selected field data compared with the NCHRP 24-20 amplification-factor curves (from Ettema et al. 2010). 3-39

Figure 3-23. Relation of the required amplification factor and the unit discharge ratio for selected laboratory data compared with the NCHRP 24-20 amplification-factor curves. 3-39

Figure 3-24. Relation of the required amplification factor and the unit discharge ratio for selected field data with (*A*) Scour Condition A and (*B*) Scour Condition B, compared with the NCHRP 24-20 amplification curves..... 3-40

Figure 3-25. Relation of measured and predicted abutment-scour depth for cohesive and non-cohesive field data using the NCHRP 24-20 scour prediction method..... 3-42

Figure 3-26. Relation of prediction residuals and the median grain size (*D50*) for the application of the NCHRP 24-20 scour prediction method for cohesive and non-cohesive field data..... 3-42

Figure 3-27. Critical-velocity curves for cohesive and non-cohesive sediments developed from Fortier and Scobey (1926) maximum permissible velocity field data. (Modified from Benedict et al. 2006.)..... 3-47

Figure 3-28. Critical-velocity curves for non-cohesive sediment as presented in Neill (1973)..... 3-49

Figure 3-29. Modified Neill (1973) critical-velocity curves for non-cohesive sediment (modified from Benedict, 2010). 3-49

Figure 3-30. Vanoni (1975) critical-velocity curves for cohesive and non-cohesive sediments..... 3-51

Figure 3-31. Relation of measured and predicted abutment-scour depth for the NCHRP 24-20 scour prediction method using field data and selected critical-velocity methods. (Numbers in graphs refer to sites in table 3-1.)..... 3-54

Figure 3-32. Relation of the median grain size (*D50*) and the abutment-scour prediction residual for the NCHRP 24-20 scour prediction method using field data and selected critical-velocity methods. (Numbers in graphs refer to sites in table 3-1.) 3-55

Figure 3-33. Relation of measured and predicted abutment-scour depth for Maryland abutment-scour equation (Chang and Davis, 1998, 1999) using field data and selected critical-velocity methods (from Benedict, 2010). 3-56

Figure 4-1. Definition of selected abutment-scour variables associated with the NCHRP 24-15(2) method (from Briaud et al. 2011). 4-5

Figure 4-2. Definition of variables associated with pressure flow (from Briaud et al. 2011)..... 4-6

Figure 4-3. Definition of short and long setback abutments (modified from Briaud et al. 2009)..... 4-11

Figure 4-4. Relation of median grain size and sediment critical velocity (from Briaud et al. 2011)..... 4-13

Figure 5-1. Relation of predicted and measured abutment-scour depth for (*A*) selected laboratory data, using the NCHRP 24-15(2) scour prediction method, and (*B*) the same data with a truncated scale. 5-5

Figure 5-2. Relation of predicted and measured abutment-scour depth for selected laboratory data with vertical-wall abutments, using the NCHRP 24-15(2) scour prediction method. 5-6

Figure 5-3. Relation of predicted and measured abutment-scour depth for selected laboratory data with spill-through abutments, using the NCHRP 24-15(2) scour prediction method. 5-6

Figure 5-4. Relation of predicted and measured abutment-scour depth for selected laboratory data with wing-wall abutments, using the NCHRP 24-15(2) scour prediction method. 5-7

Figure 5-5. Relation of predicted and measured abutment-scour depth for selected laboratory data under live-bed transport condition, using the NCHRP 24-15(2) scour prediction method. 5-7

Figure 5-6. Relation of predicted and measured abutment-scour depth for selected laboratory data under clear-water transport condition, using the NCHRP 24-15(2) scour prediction method. 5-8

Figure 5-7. Relation of predicted and measured abutment-scour depth based on the selected equation parameters, $7.94(1.65Fr_{f2} - Fr_c)$, for the NCHRP 24-15(2) scour prediction method. 5-10

Figure 5-8. Relation of predicted and measured abutment-scour depth based on the selected equation parameters, K_{Re} $7.94(1.65Fr_{f2} - Fr_c)$, for the NCHRP 24-15(2) scour prediction method. 5-10

Figure 5-9. Relation of predicted and measured abutment-scour depth based on the selected equation parameters, K_1 K_{Re} $7.94(1.65Fr_{f2} - Fr_c)$, for the NCHRP 24-15(2) scour prediction method. 5-11

Figure 5-10. Relation of predicted and measured abutment-scour depth based on the selected equation parameters, K_G K_1 K_{Re} $7.94(1.65Fr_{f2} - Fr_c)$, for the NCHRP 24-15(2) scour prediction method. 5-11

Figure 5-11. Relation of predicted and measured abutment-scour depth based on the selected equation parameters, K_L K_G K_1 K_{Re} $7.94(1.65Fr_{f2} - Fr_c)$, for the NCHRP 24-15(2) scour prediction method. 5-12

Figure 5-12. Relation of prediction residuals and the median sediment size (*D50*) for selected laboratory data, using the NCHRP 24-15(2) scour prediction method. 5-14

Figure 5-13. Relation of prediction residuals and the Briaud et al. (2009) sediment critical velocity (V_c) for selected laboratory data, using the NCHRP 24-15(2) scour prediction method, including (*A*) all of the data and (*B*) only clear-water scour data. 5-15

Figure 5- 14. Relation of prediction residuals and the sediment critical-velocity Froude number (Fr_c) for selected laboratory data, using the NCHRP 24-15(2) scour prediction method. 5-16

Figure 5-15. Comparison of the Briaud et al. (2009) and the Laursen (1963) sediment critical velocity (V_c) for selected laboratory data. 5-16

Figure 5-16. Relation of prediction residuals and the Laursen (1963) sediment critical velocity (V_c) for selected laboratory data, using the NCHRP 24-15(2) scour prediction method in conjunction with the Laursen (1963) V_c. 5-17

Figure 5-17. Relation of prediction residuals and the Froude number (Fr_{f2}) at the abutment for selected laboratory data, using the NCHRP 24-15(2) scour prediction method. 5-19

Figure 5-18. Relation of prediction residuals and the Froude number parameter, $7.94(1.65Fr_{f2} - Fr_c)$, for selected laboratory data, using the NCHRP 24-15(2) scour prediction method. 5-19

Figure 5-19. Relation of prediction residuals and the Reynolds number at the abutment (Re_{f2}) for selected laboratory data, using the NCHRP 24-15(2) scour prediction method, including (*A*) all of the data, and (*B*) without the Sturm (2004) data. 5-22

Figure 5-20 Relation of the Reynolds number at the abutment (Re_{f2}) and the Reynolds number correction factor, K_{Re}, for the NCHRP 24-15(2) scour prediction method. 5-23

Figure 5-21. Relation of prediction residuals and the Reynolds number correction factor, K_{Re}, for selected laboratory data, using the NCHRP 24-15(2) scour prediction method. 5-23

Figure 5-22. Relation of prediction residuals and the abutment-shape correction factor, K_1, for selected laboratory data, using the NCHRP 24-15(2) scour prediction method. 5-25

Figure 5-23. Relation of prediction residuals and the channel-geometry correction factor, K_G, using the NCHRP 24-15(2) scour prediction method for (*A*) vertical-wall abutments, (*B*) wing-wall abutments, and (*C*) spill-through abutments. 5-30

Figure 5-24. Relation of prediction residuals and the channel-geometry correction factor, K_G, using the NCHRP 24-15(2) scour prediction method for vertical-wall abutments and K_G for all data arbitrarily set to a value of 1.0. 5-31

Figure 5-25. Relation of relative scour to the parameter, $7.94(1.65Fr_{f2} - Fr_c)$, used to develop the channel-geometry correction factor, K_G (from Briaud et al. 2009). (Note: The term "WW in Rec." refers to wing-wall abutment in a rectangular channel. The term "WW" refers to wing-wall abutment in a compound channel. 5-31

Figure 5-26. Relation of relative scour to flow for the rectangular- and compound-channel data used to evaluate the channel-correction factor, K_G for rectangular channels in the NCHRP 24-25(2) method. 5-32

Figure 5-27. Relation of predicted and measured scour for selected laboratory data using the NCHRP 24-15(2) scour prediction method with all channel-geometry correction factors, K_G, arbitrarily set to a value of 1.0. 5-32

Figure 5-28. Relation of prediction residuals and the Froude number parameter, $7.94(1.65Fr_{f2} - Fr_c)$, using the NCHRP 24-15(2) scour prediction method and K_G for all data arbitrarily set to a value of 1.0..... 5-33

Figure 5-29. Relation of prediction residuals and the abutment-location correction factor, K_L, using the NCHRP 24-15(2) scour prediction method for (*A*) vertical-wall abutments and (*B*) spill-through abutments..... 5-36

Figure 5-30. Relation of predicted and measured scour for selected laboratory data using the NCHRP 24-15(2) scour prediction method with (*A*) K_L equal to 1.35 and (*B*) K_L equal to 1.0 and using the main-channel hydraulics. 5-37

Figure 5-31. Relation of predicted and measured abutment-scour depth for selected field data using the NCHRP 24-15(2) scour prediction method..... 5-41

Figure 5-32. Relation of measured and predicted abutment-scour depth for selected field data using the NCHRP 24-15(2) scour prediction method for the (A) South Carolina Relief/Swamp Bridge, (B) South Carolina Coastal Plain, (C) South Carolina Piedmont, (D) Maine, (E) Alabama, and (F) NBSD data..... 5-42

Figure 5-33. Relation of predicted and measured abutment-scour depth based on the selected equation parameter, $7.94(1.65Fr_{f2} - Fr_c)$, for the NCHRP 24-15(2) scour prediction method. 5-46

Figure 5-34. Relation of predicted and measured abutment-scour depth based on the selected equation parameters, K_{Re} $7.94(1.65Fr_{f2} - Fr_c)$, for the NCHRP 24-15(2) scour prediction method. 5-47

Figure 5-35. Relation of predicted and measured abutment-scour depth based on the selected equation parameters, K_1 K_{Re} $7.94(1.65Fr_{f2} - Fr_c)$, for the NCHRP 24-15(2) scour prediction method..... 5-47

Figure 5-36. Relation of predicted and measured abutment-scour depth based on the selected equation parameters, K_1 K_2 K_{Re} $7.94(1.65Fr_{f2} - Fr_c)$, for the NCHRP 24-15(2) scour prediction method. 5-48

Figure 5-37. Relation of predicted and measured abutment-scour depth based on the selected equation parameters, K_1 K_2 K_G K_{Re} $7.94(1.65Fr_{f2} - Fr_c)$, for the NCHRP 24-15(2) scour prediction method..... 5-48

Figure 5-38. Relation of predicted and measured abutment-scour depth based on the selected equation parameters, K_1 K_2 K_G K_L K_{Re} $7.94(1.65Fr_{f2} - Fr_c)$, for the NCHRP 24-15(2) scour prediction method..... 5-49

Figure 5-39. Relation of predicted and measured abutment-scour depth based on the selected equation parameters, $K_1\ K_2\ K_G\ K_L\ K_P\ K_{Re}\ 7.94(1.65Fr_{f2} - Fr_c)$, for the NCHRP 24-15(2) scour prediction method..... 5-49

Figure 5-40. Relation of prediction residuals and the median sediment size (*D50*) for selected field data, using the NCHRP 24-15(2) scour prediction method, including (*A*) all of the data, and (*B*) selected data from the South Carolina Piedmont and Maine data. 5-52

Figure 5-41. Relation of prediction residuals and the critical velocity (V_c) for selected field data, using the NCHRP 24-15(2) scour prediction method..... 5-53

Figure 5-42. Relation of prediction residuals and the sediment critical-velocity Froude number (Fr_c) for selected field data, using the NCHRP 24-15(2) scour prediction method..... 5-53

Figure 5-43. Relation of prediction residuals and the Froude number (Fr_{f2}) at the abutment for selected field data, using the NCHRP 24-15(2) scour prediction method..... 5-55

Figure 5-44. Relation of prediction residuals and the Froude number parameter, $7.94(1.65Fr_{f2} - Fr_c)$, for selected field data, using the NCHRP 24-15(2) scour prediction method. 5-55

Figure 5-45. Relation of prediction residuals and the Froude number (Fr_{f2}) at the abutment for selected field data, using the NCHRP 24-15(2) scour prediction method and setting K_G and K_L to a value of 1.0. 5-56

Figure 5-46. Relation of prediction residuals and the Froude number parameter, $7.94(1.65Fr_{f2} - Fr_c)$, for selected field data, using the NCHRP 24-15(2) scour prediction method and setting K_G and K_L to a value of 1.0..... 5-56

Figure 5-47. Relation of prediction residuals and the Reynolds number at the abutment (Re_{f2}) for selected field data, using the NCHRP 24-15(2) scour prediction method. 5-58

Figure 5-48. Relation of prediction residuals and the Reynolds number correction factor, K_{Re}, for selected field data, using the NCHRP 24-15(2) scour prediction method..... 5-58

Figure 5-49. Relation of the Froude number parameter, $7.94(1.65Fr_{f2} - Fr_c)$, and the Reynolds number correction factor, K_{Re}, for selected field data..... 5-59

Figure 5-50. Relation of predicted and measured abutment-scour depth for selected field data using the NCHRP 24-15(2) scour prediction

method, with the channel-geometry correction factor, K_G, set to a value of 1.0 for rectangular channels. 5-61

Figure 5-51. Relation of predicted and measured abutment-scour depth for selected field data using the NCHRP 24-15(2) scour prediction method, with (A) K_L equal to 1.35 and (B) K_L equal to 1.0 and using the main-channel hydraulics..... 5-63

Figure 5-52. Relation of prediction residuals and the relative abutment length (L/y_{f1}) for selected field data, using the NCHRP 24-15(2) scour prediction method. 5-65

Figure 5-53. Relation of predicted and measured abutment-scour depth for selected field data using the NCHRP 24-15(2) scour prediction method, with K_G and K_L set to a value of 1.0, and K_1 set to a value of 1.22 for the South Carolina Coastal Plain and Relief/Swamp Bridge data if the relative abutment length was greater than or equal to 25. 5-66

Figure 5-54. Relation of predicted and measured abutment-scour depth for selected field data grouped by cohesive and non-cohesive sediments, using the NCHRP 24-15(2) scour prediction method..... 5-67

Figure 5- 55. Relation of prediction residuals and the median sediment size (*D50*) for selected field data grouped by cohesive and non-cohesive sediments, using the NCHRP 24-15(2) scour prediction method..... 5-68

Figure 5- 56. Relation of predicted and measured abutment-scour depth for the NCHRP 24-15(2) scour prediction method using field data and selected critical-velocity methods..... 5-70

Figure 5- 57. Relation of the median grain size (*D50*) and the abutment-scour prediction residual for the NCHRP 24-15(2) scour prediction method using field data and selected critical-velocity methods. 5-71

Figure 6-1. Boxplots for the laboratory-data prediction residuals for the NCHRP 24-20 and 24-15(2) scour prediction methods. (Note: The terms “LB” and “CW” refer to live-bed and clear-water scour, respectively.) 6-6

Figure 6-2. Boxplots for the field-data prediction residuals for the NCHRP 24-20 and 24-15(2) scour prediction methods..... 6-7

Figure 6-3. Boxplots for the field-data prediction residuals for the NCHRP 24-20 and 24-15(2) scour prediction methods, grouped by cohesive and non-cohesive sediments, and by measured scour depth less than (LT) or greater than (GT) 10 feet..... 6-11

LIST OF TABLES

Table 1-1. Range of selected variables for abutment-scour measurements in the South Carolina, Maine, Alabama, and National Bridge Scour Databases. (Refer to figure 1-5 for schematic showing selected variable definitions.) 1-17

Table 1-2. Range of selected dimensionless variables for abutment-scour measurements in the South Carolina, Maine, Alabama, and National Bridge Scour Databases. (Refer to figure 1-5 for schematic showing selected variable definitions.)..... 1-18

Table 1-3. Range of selected variables for laboratory measurements of abutment scour. (Refer to figure 1-5 for schematic showing selected variable definitions.) 1-24

Table 1-4. Range of dimensionless variables for laboratory measurements of abutment scour. (Refer to figure 1-5 for schematic showing selected variable definitions.) 1-25

Table 1-5. Shape factors for shorter abutments (from Melville and Coleman (2000))..... 1-27

Table 2-1. Description of selected field data used in the application of the NCHRP 24-20 abutment-scour prediction method..... 2-13

Table 3-1. Sites with unique characteristics that may influence scour depth. 3-20

Table 3-2. Maximum Permissible Velocities from Fortier and Scobey (1926)..... 3-47

Table 6-1. Summary statistics for the laboratory-data prediction residuals for the NCHRP 24-20 and 24-15(2) scour prediction methods..... 6-5

Table 6-2. Summary statistics for the field-data prediction residuals for the NCHRP 24-20 and 24-15(2) scour prediction methods..... 6-5

Table 6-3. Summary statistics for the field-data prediction residuals for the NCHRP 24-20 and 24-15(2) scour prediction methods, grouped by cohesive and non-cohesive sediments, and by measured scour depth less than (LT) or greater than (GT) 10 feet..... 6-12

LIST OF SYMBOLS

a	amplification factor
A_2	flow area for the overbank of interest and half the main channel at the contracted section
A_{f2}	flow area on the overbank of interest at the contracted section
A_{mc2}	flow area in the main channel at the bridge
b	top width of the bridge opening
B	top width of the upstream approach cross section
B_f	left or right floodplain width
B_{f1}	top width of the left or right approach floodplain
B_{mc1}	top width of the approach main channel
d_1	distance from water surface to the low chord of the bridge at the upstream face of the bridge
$D50$	median grain size
d_{deck}	distance from high steel to the low chord of the bridge deck blocking flow
Fr_1	approach Froude number
Fr_{f2}	Froude number around the toe of the abutment
Fr_{fc}	critical Froude number around the toe of the abutment
g	acceleration due to gravity
K_1	correction factor for the abutment shape
K_2	correction factor for the abutment skew
K_{depth}	flow depth adjustment factor for the threshold velocity
K_G	correction factor for the channel geometry

K_L	correction factor for the abutment location
K_p	correction factor for pressure flow
K_s	abutment-shape factor (Melville and Coleman, 2000)
K_s^*	abutment-shape factor adjusted for abutment length (Melville and Coleman, 2000)
K_u	units conversion factor
L	abutment length
m	geometric contraction ratio defined as 1 – b/B
q_1	approach unit discharge
q_2	unit discharge at abutment
q_{f1}	unit discharge on the left or right approach floodplain
Q_{f1}	flow on the left or right approach floodplain
q_{f2}	unit discharge in the left or right overbank at the bridge
Q_{f1}	flow in the left or right approach floodplain
Q_{mc1}	flow in the approach main channel
$0.5Q$	flow associated with the approach floodplain of interest and half the approach main channel
q_{mc1}	unit discharge in the approach main channel
q_{mc2}	unit discharge in the main channel at the bridge
Re_{f2}	Reynolds number around the toe of the abutment
V_1	approach flow velocity
V_c	sediment critical velocity
V_{f2}	velocity around the toe of the abutment

V_{mpv}	Fortier and Scobey (1926) maximum permissible velocity
V_{Vanoni}	Vanoni (1975) critical velocity
y	average flow depth
y_1	approach flow depth
Y_C	mean flow depth of the contraction scour associated with a long contraction
y_f	floodplain flow depth
y_{f1}	floodplain flow depth upstream of the abutment (for NCHRP 24-15(2) method; comparable to approach flow depth, y_1)
y_{f2}	average flow depth in the left or right overbank at the bridge
Y_{MAX}	maximum flow depth in the abutment scour area
y_{mc}	channel flow depth
y_{mc1}	flow depth in the approach main channel
y_{mc2}	average flow depth in the main channel at the bridge
y_s	abutment-scour depth
y_{sadj}	abutment-scour depth adjusted for abutment shape
ν	kinematic viscosity
θ	angle of abutment skew

CHAPTER 1

INTRODUCTION AND OVERVIEW OF ABUTMENT-SCOUR DATA

1.1 Introduction

> *Scant situations of hydraulic engineering are more complex than those associated with scour in the vicinity of a bridge abutment, especially one located in a compound channel. Accordingly, few situations of scour depth estimation are as difficult (Ettema et al. 2005).*

The complexity of abutment-scour processes has made it difficult to formulate prediction methods, and few would dispute the above assessment by Ettema et al. (2005). In order to advance the state-of-the knowledge and practice for predicting abutment scour, the National Cooperative Highway Research Program (NCHRP) recently sponsored several projects for the development of new abutment-scour prediction methods in cohesive and non-cohesive sediments. These projects include:

NCHRP Project 24-15(2): Abutment Scour in Cohesive Materials (Briaud et al. 2009)
(Note: This project was expanded to include prediction of abutment scour in non-cohesive sediments as well.)
http://www.trb.org/TRBNet/ProjectDisplay.asp?ProjectID=712

NCHRP Project 24-20 Prediction of Scour at Bridge Abutments (Ettema et al. 2010)
http://www.trb.org/TRBNet/ProjectDisplay.asp?ProjectID=719

The NCHRP 24-15(2) (Briaud et al. 2009) and NCHRP 24-20 (Ettema et al. 2010) investigations (hereinafter noted as NCHRP 24-15(2) and NCHRP 24-20, without the reference citations) represent extensive efforts to develop conceptual models for abutment scour in cohesive and non-cohesive sediments, collect and evaluate laboratory data, and develop new methods for predicting abutment scour. The conceptual models, along with the data collected in these investigations, provide a valuable resource for current and future investigations of abutment

scour. Additionally, the resulting prediction methods provide tools to assist the engineer in evaluating abutment scour. With the completion of these investigations, there is a need to evaluate the performance of these new abutment-scour prediction methods under field conditions. With this need in mind, the current investigation, NCHRP Project 24-20(2), was initiated.

1.1.1 Project Objective

The primary objective of this investigation is to evaluate the performance of the abutment-scour prediction methods developed in the NCHRP 24-15(2) and 24-20 Projects using U.S. Geological Survey (USGS) field data, and based on this evaluation, note strengths and weakness of the methods, potential ways to improve performance, and provide limited guidance to the practitioner for application of these methods. While the NCHRP 24-20(02) investigation makes some general observations regarding the formulations of the NCHRP 24-15(02) and 24-20 methods, the focus is not on a rigorous critique of those formulations, but rather their performance when applied to selected field and laboratory data.

1.1.2 Approach

The USGS, in cooperation with various highway agencies, collected 375 field measurements of abutment scour with the objective to better understand abutment-scour trends in the field setting. Subsets of the USGS data have been used in previous investigations to evaluate the performance of selected abutment-scour prediction equations (Benedict, 2003; 2010; Benedict et al. 2006; 2007; Wagner et al. 2006; Lee and Hedgcock, 2008; Lombard and Hodgkins, 2008), and analysis similar to these investigations was used to evaluate the performance of the NCHRP Projects 24-15(2) and 24-20 abutment-scour prediction methods. The analysis primarily consisted of (1) application of the field data to the scour prediction methods, (2) development of selected scatter plots showing the relations of predicted and measured scour, as well as prediction residuals with respect to selected explanatory variables, and (3) reviewing those relations to evaluate method performance, identify potential ways to improve performance, and identify limited guidance to assist practitioners in applying the methods. The USGS field data have limitations and larger measurement uncertainty than that associated with laboratory data. Therefore, to provide some

confirmation of the prediction trends displayed in the field data, the prediction methods also were applied to 516 laboratory measurements from previous investigations and compared to prediction trends of the field data.

To assure appropriate application of the field and laboratory data to the NCHRP 24-15(2) and 24-20 prediction methods, the principal investigators for each method, Dr. Jean-Louis Briaud and Dr. Robert Ettema, respectively, along with Mr. Bart Bergendahl of the Federal Highway Administration were consulted during the development of the application procedures documented in report chapters 2 and 4, and were provided opportunity to review and comment on those chapters. Additionally, preliminary results of the analysis were reviewed with these individuals, and information exchanged during those reviews helped refine the analysis. Opportunity for review and comment on the draft final report also was provided.

1.1.3 Report Organization

This report presents (1) an overview of the field and laboratory data, (2) an overview of the NCHRP 24-20 prediction method and application procedure, (3) the results of applying the laboratory and field data to the NCHRP 24-20 prediction method along with comments on the strengths and weaknesses of the method, (4) an overview of the NCHRP 24-15(2) prediction method and application procedure, (5) the results of applying the laboratory and field data to the NCHRP 24-15(2) prediction method along with comments on the strengths and weaknesses of the method, and (6) a comparison of the two methods with concluding remarks.

1.2 Field Data

In the late 1990s, the USGS, in cooperation with various highway agencies, began to collect field measurements of abutment scour in order to better understand abutment-scour trends in the field setting and to evaluate laboratory-derived abutment-scour prediction equations. Currently, available USGS abutment-scour data include 209 measurements in South Carolina (Benedict, 2003), 29 measurements in the USGS National Bridge Scour Database (NBSD; http://water.usgs.gov/osw/techniques/bs/BSDMS/index.html, accessed March 2, 2013; U.S. Geological Survey, 2001), 100 measurements in Maine (Lombard and Hodgkins, 2008), and 37 measurements in Alabama (Lee and Hedgecock, 2008). A literature review conducted for this

investigation was unsuccessful in identifying additional field data that could be used in the analysis. During the literature review, some field measurements associated with case studies were found (Culbertson et al. 1967; Brice et al. 1978; Mueller et al. 1993; Conaway, 2006; Conaway and Brabets, 2011), but the supporting hydraulic data were insufficient for inclusion in the investigation. The findings of the literature review highlight the limited number of field observations of abutment scour beyond that of the USGS field data and indicate that these data are currently (2015) the primary data source for the evaluation of laboratory-derived prediction equations for field applications. While there are limitations associated with the USGS data, the number of measurements (375; approximately 60 percent non-cohesive and 40 percent cohesive) is sufficient to (1) evaluate the range of the dimensionless parameters used in the laboratory with those of the range found in the field, (2) provide an assessment of the general performance trends of an equation, (3) identify selected strengths and weaknesses of an equation, (4) identify selected strengths and weaknesses of prescribed methods for applying an equation in design manuals, and (5) potentially identify ways to improve equation performance. (Note: Only 329 of the field measurements were used in the analysis, because some of the data had incomplete information.)

Investigations of scour in the controlled environment of the laboratory allow the accurate and precise measurement of selected parameters, such as flow depth, flow velocity, grain size, and scour depth. However, in the field setting, measuring these parameters can be a difficult task that often cannot be accomplished to the same degree of accuracy and thoroughness. Parameters, such as hydraulic and sediment characteristics, typically must be approximated, introducing some error into the data. When using field data to evaluate laboratory-derived equations, it is important to understand field data characteristics and limitations. Therefore, a brief summary of the characteristics of the USGS field data used in this investigation is provided below.

1.2.1 South Carolina Data

The South Carolina data include 209 measurements of clear-water abutment scour collected at 144 bridges in the Piedmont and Coastal Plain of South Carolina (Benedict, 2003) with scour depths ranging from 0 to 23.6 feet (ft). The bridge lengths associated with the abutment-scour measurements range from 45 to 1,273 ft with a median length of 240 ft. Figure 1-1 provides a

percentile plot of bridge length for the 6,865 bridges in South Carolina identified in the National Bridge Inventory Database (NBI, 2012) as crossing water (excluding culverts). This figure shows that the range of the sampled bridges falls within the 20th to 98th percentiles for bridge lengths in South Carolina, indicating that the bridges in the South Carolina abutment-scour database provide a good representation of the bridge lengths found in South Carolina. The dominant abutment geometry at these bridges was the spill-through abutment, which was observed at 141 bridges. The remaining 3 bridges had wing-wall abutments. These scour measurements represent the maximum clear-water abutment-scour depth that has occurred on the bridge overbanks since construction. All observations were located on the floodplain, and the reference surface used to determine the scour depth was the average undisturbed floodplain elevation in the vicinity of the observed scour. Because of clear-water scour conditions, infill sediments within the scour holes were, in general, negligible. A grab sample of sediment in the approach floodplain was obtained at each site and was analyzed to estimate the median grain size. Because sediment characteristics in the field setting can vary substantially in the vertical and horizontal direction, the grab sample taken at a point may not fully represent the sediment characteristics at a given site.

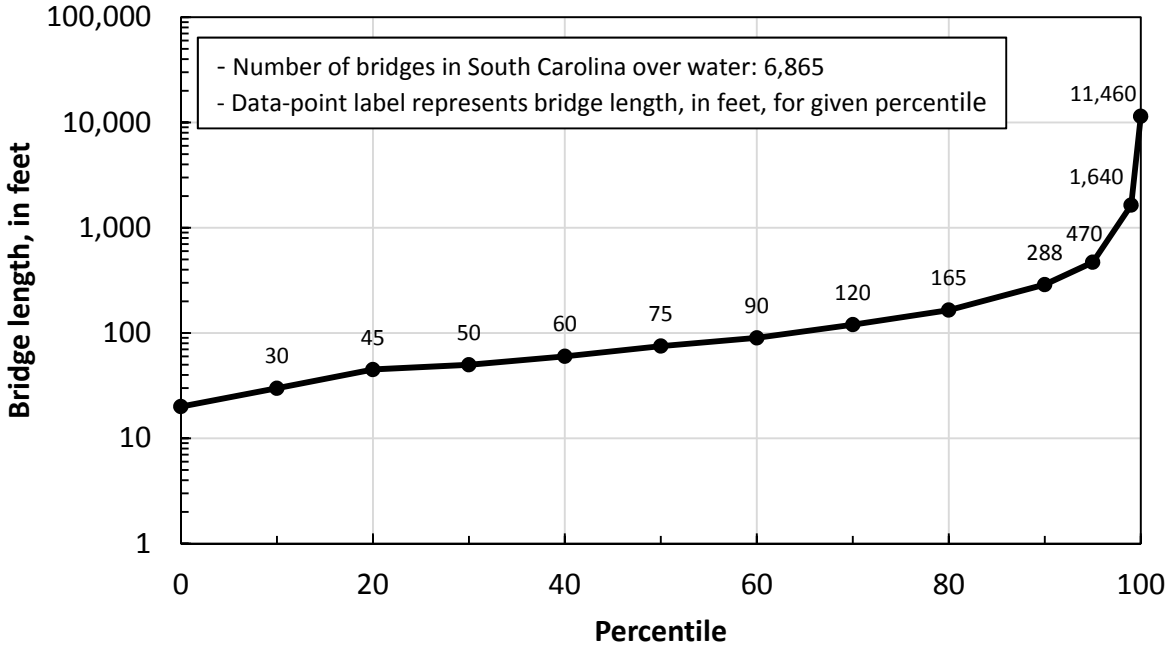

Figure 1-1. Percentile plot of bridge lengths for bridges in South Carolina crossing water.

The South Carolina abutment-scour depths represent historical post-flood measurements that were made during low-flow conditions, and the hydraulic conditions that created the scour are not known. To gain insights into hydraulic conditions that may have created the observed scour, numerical models were developed for each site using the one-dimensional step-backwater model, WSPRO (Shearman, 1990). A review of streamgage records and the general flood history of South Carolina indicated that 127 of the 144 bridges in the study likely had experienced flows equaling or exceeding 70 percent of the 100-year flow magnitude (Benedict, 2003). Therefore, the 100-year flow was assumed to be representative of a common flow that may have occurred at all sites and was used in the WSPRO model for all of the bridges. All hydraulic variables associated with the South Carolina data were derived from the WSPRO model and should be viewed as approximate rather than measured data. The approximated hydraulic data will introduce error into predicted scour computations, making the comparison of predicted and observed abutment scour less than ideal. However, the large number of field observations (209) in the database will allow trends to be assessed, providing insights into the strengths and weaknesses of a particular equation.

The data collected in South Carolina have been grouped into two databases based on regional location within the State. One database contains data collected in the Piedmont Physiographic Province, and the other contains data collected in the Coastal Plain Physiographic Province. (Sites in the Coastal Plain were not tidally influenced.) This division is justified due to the distinct regional characteristics of the Piedmont and Coastal Plain Provinces. The Piedmont generally has cohesive soils, moderate stream gradients with well-defined channels, relatively narrow floodplains, and relatively short flood-flow durations. Setback abutments are common in the Piedmont region, and figure 1-2 shows a typical bridge cross section for such sites, defining the regions of clear-water scour on the bridge overbanks. Figure 1-3 shows a typical bridge plan and profile for setback abutments. (Note: Relatively small piers are assumed to have negligible influence on abutment-scour depth and are not shown in the bridge cross sections for figures 1-3 through 1-5. Findings from Benedict (2003) and Ettema et al. (2010) support this assumption.)

In contrast, the Coastal Plain generally has sandy soils, low gradient streams, relatively wide floodplains, and relatively long flood-flow durations. While rivers with large drainage areas typically have well-defined channels, many Coastal Plain streams are characterized by small,

poorly-defined channels on swampy floodplains and tend to approximate a rectangular channel similar to a laboratory flume. A typical bridge opening at such sites is shown in figure 1-4. Additionally, the sandy alluvium sediments that form the floodplains are more representative of sediment conditions used in the laboratory, and relatively large abutment-scour holes can occur. However, these sandy sediments are typically underlain by older marine deposits that are more scour resistant, and when encountered, will modify the scour processes. To provide some understanding of the differences between these regions, tables 1-1 and 1-2 list the median and range of selected dimensional and dimensionless variables, respectively, for the abutment-scour field data collected in the Piedmont and Coastal Plain. A schematic that defines selected variables in tables 1-1 and 1-2 is provided as figure 1-5. (Note: Eleven of the 209 measurements were excluded from this investigation because the measurements had insufficient hydraulic data or were questionable. Tables 1-1 and 1-2 present values associated with data used in this study.) Additional details regarding the South Carolina data can be found in Benedict (2003).

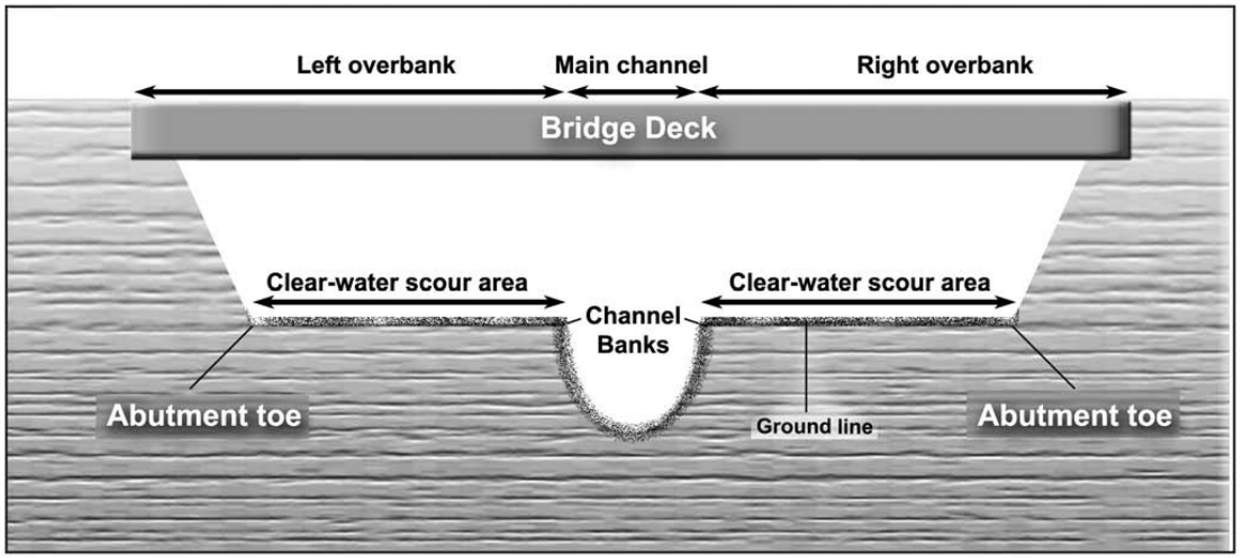

Figure 1-2. Typical cross section for bridges with setback abutments (from Benedict, 2003).

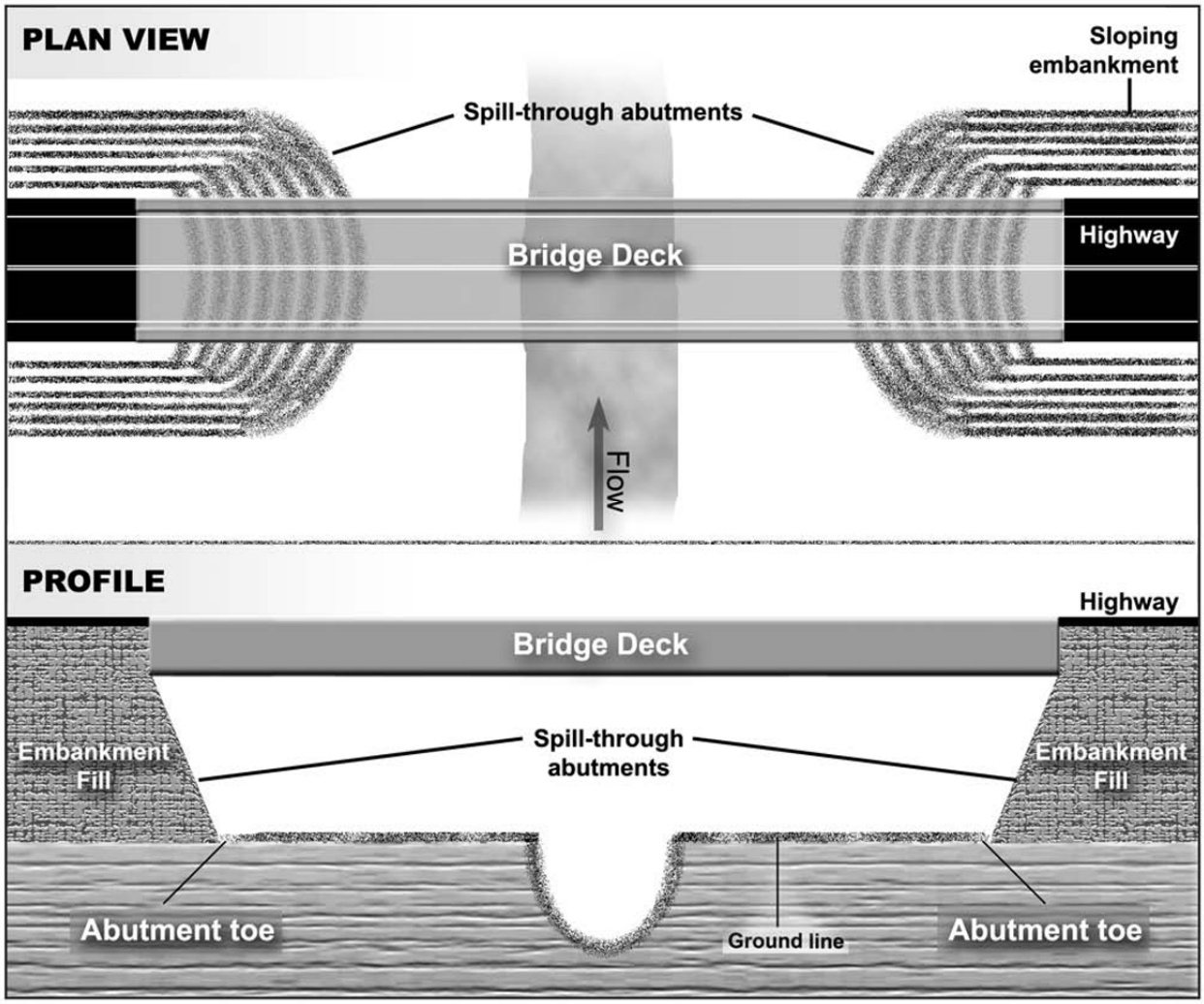

Figure 1-3. General plan and profile for bridges with setback abutments (from Benedict, 2003).

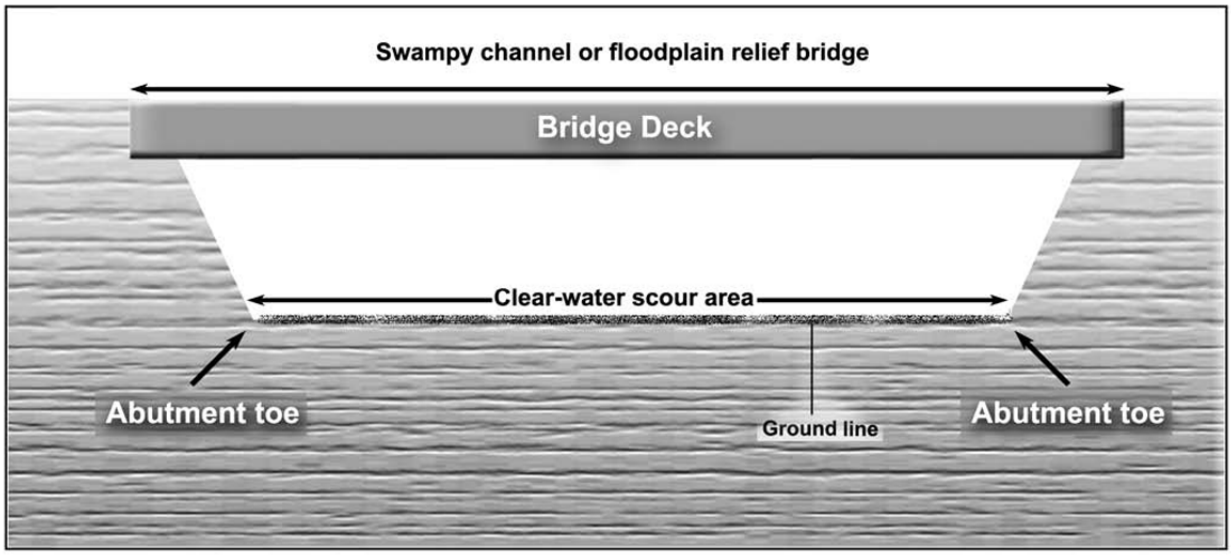

Figure 1-4. Typical cross section for bridges crossing swampy channels or for floodplain relief bridges (from Benedict, 2003).

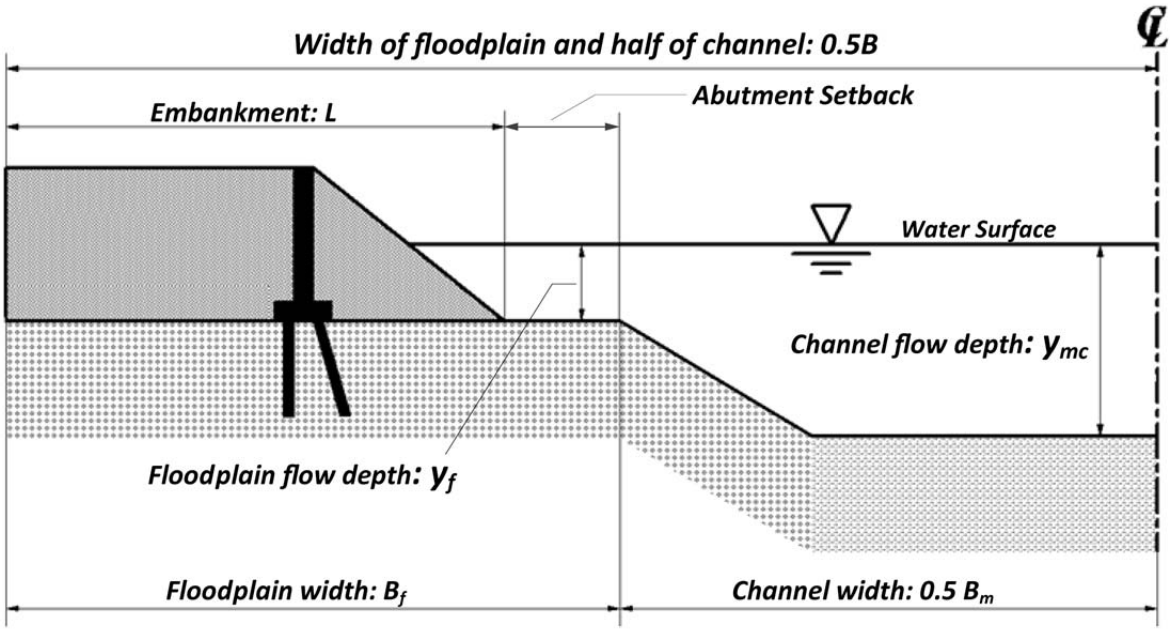

Figure 1-5. Typical cross section for bridge abutment/embankment with definition of selected variables from tables 1-1 through 1-4 (modified from Ettema et al., 2010).

1.2.2 Maine Data

The Maine data include 100 measurements of abutment scour collected at 50 bridges throughout the State of Maine (Lombard and Hodgkins, 2008). The bridge spans were relatively small, with bridge lengths ranging from 12.7 to 126 ft and a median length of 25 ft; most bridges have lengths between 15 and 65 ft. Figure 1-6 provides a percentile plot of bridge length for the 1,580 bridges in Maine identified in the NBI (2012) as crossing water (excluding culverts). This figure shows that the range of the sampled bridges falls within the 0 to 72nd percentile for bridge lengths in the State, indicating that the bridges in the Maine abutment-scour database provide a good representation of the bridge lengths found in Maine. The abutment geometry was wing wall, and measured scour depths ranged from 0 to 6.8 ft. Ninety percent of the bridges had abutments that protruded into the channel (figures 1-7 and 1-8); therefore, most of the scour measurements are in the streambed. These scour measurements represent the maximum abutment-scour depth that has occurred at the bridge since construction, and the streambed-surface elevation just outside a scour hole was used as a reference surface to determine the scour depth. A representative sample of bed material was obtained by grid sampling for beds with predominantly coarse-grained sediments (greater than 2 millimeters (mm)), and bulk sampling for beds with predominantly fine-grained sediments (less than 2 mm). Based on a theoretical analysis, approximately 30 percent of the sites had live-bed scour conditions, and the remaining sites had clear-water scour conditions. When compared with the South Carolina, Alabama, and NBSD data (table 1-1), the Maine data represent scour associated with substantially steeper streams and larger sediment sizes. Therefore, the Maine data will provide a good contrast with the moderate- to low-gradient streams and fine sediments of the South Carolina, Alabama, and NBSD data.

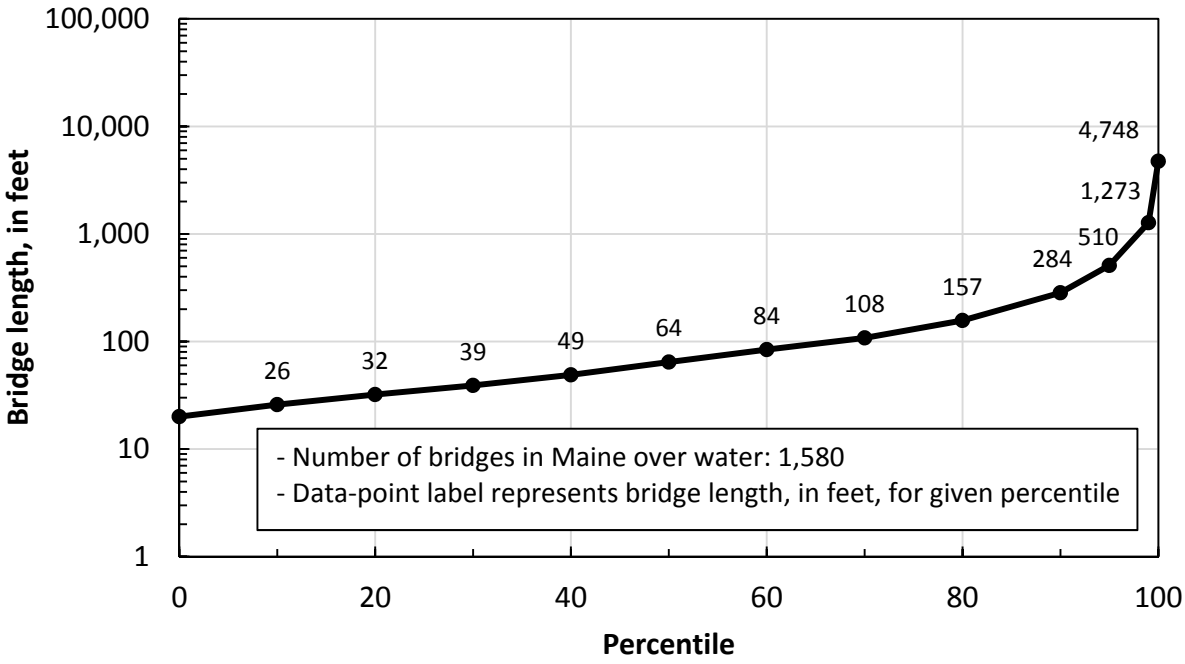

Figure 1-6. Percentile plot of bridge lengths for bridges in Maine crossing water.

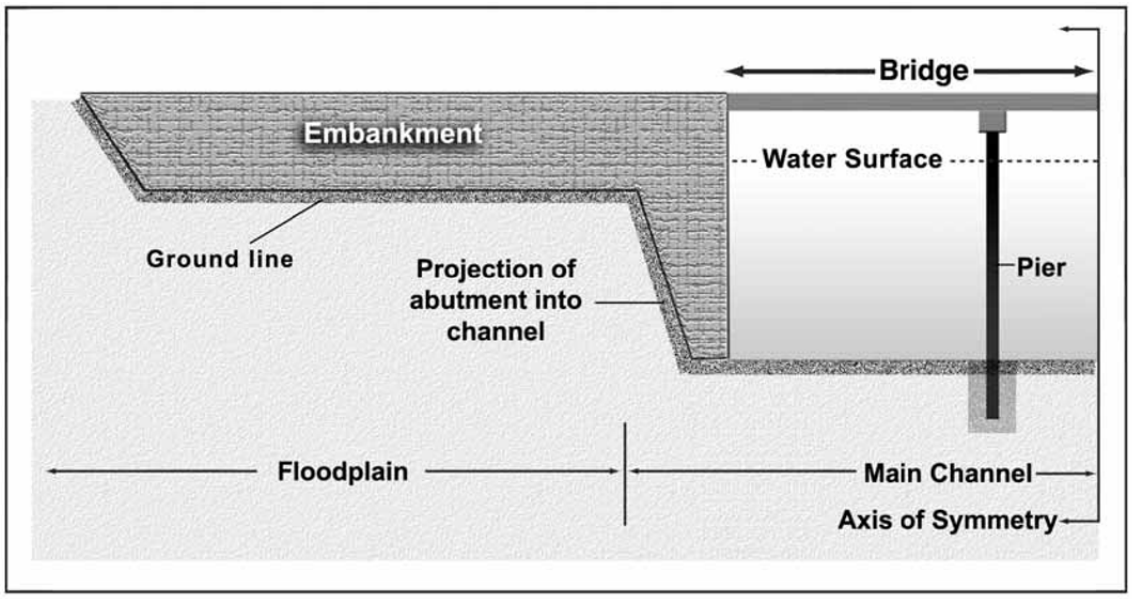

Figure 1- 7. Typical cross section for abutment protruding into main channel (from Benedict, 2003).

Figure 1- 8. Example of abutments protruding into main channel at East Branch of the Wesserunsett Stream at Athens, Maine (from Lombard and Hodgkins, 2008).

Similar to the South Carolina data, the Maine abutment-scour depths represent historical post-flood measurements that were made during low flows, and the flow conditions that created the scour are not known. To gain insights into hydraulic conditions that may have created the observed scour, hydraulic models were developed for each site using the one-dimensional step-backwater model, HEC-RAS (U.S. Army Corps of Engineers, 2001). The flows used in the models were estimated by determining the peak flow associated with a 50-percent chance of exceedance based on the bridge age. Recurrence intervals for the 50 bridges ranged from 40 to 125 years. All hydraulic variables associated with the Maine data were derived from the HEC-RAS model and should be viewed as approximate rather than measured data. The approximated hydraulic data will introduce error into predicted scour computations, making the comparison of predicted and observed abutment scour less than ideal. However, the large number of field observations (100) in the database will allow trends to be assessed, providing insights into the strengths and weaknesses of a particular equation. Tables 1-1 and 1-2 list the median and range of selected dimensional and dimensionless variables, respectively, for the Maine field data. (Note: Seven of the 100 measurements were excluded from this investigation because the

measurements had insufficient hydraulic data or were questionable. Table 1-1 lists values associated with data used in this study.) Additional details regarding the Maine data can be found in Lombard and Hodgkins (2008).

1.2.3 Alabama Data

The Alabama data include 37 measurements of clear-water abutment and (or) contraction scour collected at 37 bridges in the Black Prairie Belt of the Coastal Plain of Alabama, with scour depths ranging from 1.4 to 10.4 ft (Lee and Hedgecock, 2008). The bridge lengths associated with the scour measurements range from 46 to 894 ft, with a median length of 144 ft. Figure 1-9 provides a percentile plot of bridge length for the 9,632 bridges in Alabama identified in the NBI (2012) as crossing water (excluding culverts). This figure shows that the range of the sampled bridges falls within the 20th to 96th percentile for bridge lengths in Alabama, indicating that the bridges in the Alabama database provide a good representation of the bridge lengths found in the State. The abutment geometry consisted of wing wall at 28 of the bridges and spill through at 9 of the bridges. Additionally, 24 of the 37 bridges are floodplain relief bridges (figure 1-4). These scour measurements represent the maximum clear-water scour depth that has occurred on the bridge overbanks since construction. All observations were located on the floodplain, and the reference surface used to determine the scour depth was the average undisturbed floodplain elevation in the vicinity of the observed scour. The floodplains of the Black Prairie Belt of Alabama are noted for their highly cohesive clays (Lee and Hedgecock, 2008), and the sediments at all of the scour measurements were classified as cohesive. The floodplain clays, along with low flow velocities, help create clear-water scour conditions. Therefore, infill sediments within the scour holes were considered negligible. A grab sample of sediment was obtained at each site and was analyzed to estimate the median grain size. Because sediment characteristics in the field setting can vary substantially in the vertical and horizontal direction, the grab sample taken at a point may not fully represent the sediment characteristics at a given site.

Benedict (2003) observed that relief bridges and bridges crossing swampy areas, 240 ft or less in length with large contractions of flow, tend to create a single scour hole that extends across the entire bridge opening, with the deepest scour occurring near the center of the bridge. While it is

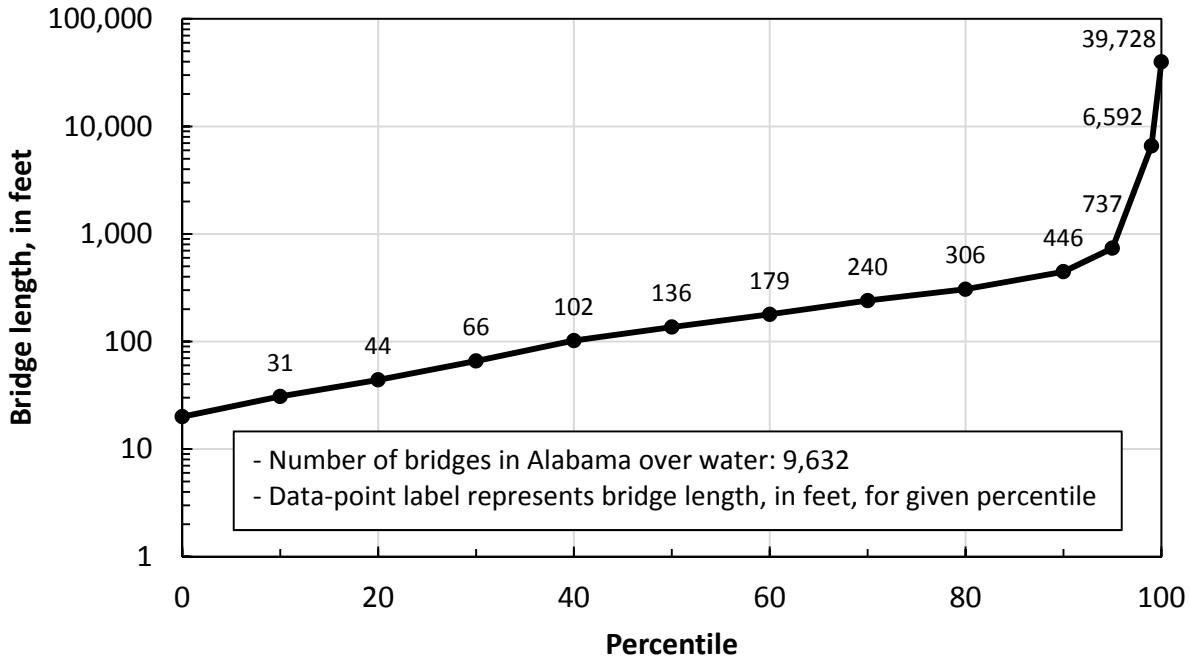

Figure 1-9. Percentile plot of bridge lengths for bridges in Alabama crossing water.

possible to classify such scour as contraction scour, Benedict (2003) noted that it also could be classified as a special case of abutment scour where the left and right abutment scour holes merge to form the single scour hole near the center of the bridge. This classification is consistent with the findings of Ettema et al. (2010) where contraction- and abutment-scour depths approach equality as the severity of the contraction increases. Twenty-two of the Alabama measurements were associated with floodplain relief bridges less than 250 ft in length (figure 1-10). One additional bridge, less than 250 ft in length, was associated with a swamp with a poorly defined channel. Lee and Hedgecock (2008) noted that it was common to find the deepest scour holes near the center of these bridges similar to the pattern noted by Benedict (2003). Lee and Hedgecock (2008) originally classified the Alabama scour measurements as contraction scour. However, for the purposes of the current (2015) report, it was considered appropriate to classify these 23 noted measurements as abutment scour. Table 1-1 presents values of the 23 sites associated with the selected data used in this study.

Similar to the South Carolina and Maine data, the Alabama abutment-scour depths represent historical post-flood measurements that were made during low flows, and the flow conditions

that created the scour are not known. To gain insights into hydraulic conditions that may have created the observed scour, numerical models were developed for each site by using the one-dimensional step-backwater model, WSPRO (Shearman, 1990). Based on a review of streamgage records and the general flood history of Alabama, a 50-year flow magnitude was assumed to be representative of a common flow that may have occurred at all sites and was used in the WSPRO model for all of the bridges. All hydraulic variables associated with the Alabama data were derived from the WSPRO model and should be viewed as approximate rather than measured data. Tables 1-1 and 1-2 list the median and range of selected dimensional and dimensionless variables, respectively, for the Alabama field data. Additional details regarding the Alabama data can be found in Lee and Hedgecock (2008).

1.2.4 National Bridge Scour Database

The National Bridge Scour Database (USGS, 2001) contains 29 measurements of abutment scour taken in Minnesota (18), Missouri (1), Montana (9), and South Dakota (1). Four of the measurements had limited hydraulic data and were removed from the analysis. Multiple

Figure 1- 10. A floodplain relief bridge at Cottonwood Creek crossing of County Road 12, Hale County, Alabama (from Lee and Hedgecock, 2008).

measurements at several small bridges were considered redundant, and 2 measurements were removed. Additionally, 16 of the measurements were associated with time-series measurements or concurrent measurements at the upstream and downstream bridge faces. At these sites, the largest scour measurement was included in the investigation, with 8 smaller measurements excluded. The 15 measurements included in the NCHRP 24-20(2) analysis included 8 measurements in Minnesota, 6 in Montana, and 1 in South Dakota. The scour measurements at the Minnesota sites were obtained during flood conditions along with concurrent flow measurement data at or near the sites. The other measurements are post-flood measurements (similar to those in the South Carolina, Maine, and Alabama data) with estimates of the flow conditions from indirect flow measurements or gage data. For the 15 measurements included in the NCHRP 24-20(2) analysis, bridge lengths ranged from 88 to 450 ft with a median length of 121 ft, and abutment-scour depths ranged from 0 to 18 ft. The abutment geometry at 13 of the measurements was the spill-through abutment, with the remaining measurements associated with wing-wall abutments.

While all of the NBSD data have supporting flow measurements, one-dimensional flow models (HEC-RAS or WSPRO), with the associated flow data, were required to estimate the hydraulic properties at the approach and bridge sections. Some of the hydraulic data required for application to the scour prediction methods were not published in the NBSD, and these data were obtained for the current investigation (2015) by referring to the unpublished models. Seven of the scour measurements are associated with meandering streams that are challenging to model with a one-dimensional flow model. The one-dimensional flow models associated with the NBSD data were reviewed and in some cases modified to better represent the unconstricted approach section. The models provide estimates of the hydraulic conditions that likely created the scour, but the site complexities and limitations of one-dimensional models will likely introduce some error in estimates and the hydraulic data should be viewed as approximate rather than measured data. Tables 1-1 and 1-2 list the median and range of selected dimensional and dimensionless variables, respectively, for the NBSD field data. Additional details associated with the data can be found at the NBSD Web page (http://water.usgs.gov/osw/techniques/bs/BSDMS/) as well as in Wagner et al. (2006).

Table 1-1. Range of selected variables for abutment-scour measurements in the South Carolina, Maine, Alabama, and National Bridge Scour Databases. (Refer to figure 1-5 for schematic showing selected variable definitions.)

[miles^2, square miles; ft, feet; ft/s, feet per second; mm, millimeters]

Range value	Drainage area (miles^2)	Channel slope (ft/ft)	Average abutment approach velocity (ft/s)	Average abutment approach depth (y_1) (ft)	Embankment length (L) blocking flow (ft)	Median grain size (mm)	Observed abutment-scour depth (ft)
South Carolina Piedmont (92 observations)							
Minimum	10.7	0.00015	0.17	2.19	18.4	0.003	0.0
Median	76	0.00120	0.96	5.90	268	0.029	1.2
Maximum	1,620	0.00240	3.57	15.60	1,669	0.447	18.0
South Carolina Coastal Plain (106 observations)							
Minimum	6.1	0.00007	0.05	2.00	86.7	0.005	0.0
Median	120	0.00054	0.48	4.91	610	0.179	7.0
Maximum	8,830	0.00240	0.96	16.04	7,440	0.782	23.6
Maine (93 observations)							
Minimum	4.1	0.00041	0.18	1.11	0.0	0.25	0.0
Median	20.1	0.00275	1.04	7.06	40.1	45	0.0
Maximum	95.1	0.04446	5.62	15.25	808	109	6.8
Alabama (23 observations)							
Minimum	10.0	0.00040	0.18	3.21	43.0	0.001	1.4
Median	80.2	0.00080	0.62	5.00	400	0.009	4.7
Maximum	607	0.00160	1.31	9.34	1,141	0.170	10.4
National Bridge Scour Database (15 observations)							
Minimum	836	0.00050	0.49	3.95	15.0	0.001	0.0
Median	970	0.00060	0.71	8.81	560	0.150	4.5
Maximum	16,010	0.00060	3.37	36.56	3,522	35	18.0

Table 1-2. Range of selected dimensionless variables for abutment-scour measurements in the South Carolina, Maine, Alabama, and National Bridge Scour Databases. (Refer to figure 1-5 for schematic showing selected variable definitions.)

[y_f, floodplain flow depth; y_{mc}, channel flow depth; L, abutment length; B_f, floodplain width; $0.5B$, channel width including floodplain width associated with abutment and half of the main-channel width; y_1, approach flow depth; y_s, abutment-scour depth; y_{sadj}, abutment-scour depth adjusted for abutment shape; q_1, approach unit discharge; q_2, unit discharge at abutment; $D50$, median grain size; Fr_1, approach Froude number]

Range value	[a] y_f / y_{mc}	[b] L/B_f	[a] $B_f/0.5B$	L/y_1	[c] y_s/y_1	[d] y_{sadj}/y_1	q_2/q_1	$L/D50$	Fr_1
South Carolina Piedmont (92 observations)									
Minimum	0.17	0.15	0.68	2.51	0.00	0.00	0.44	98,067	0.02
Median	0.47	0.80	0.92	36.70	0.16	0.17	4.22	1,535,454	0.07
Maximum	1.00	1.00	1.00	228.56	2.99	2.99	24.63	72,939,527	0.23
South Carolina Coastal Plain (106 observations)									
Minimum	0.17	0.29	0.90	20.45	0.00	0.00	0.65	140,566	0.00
Median	1.00	0.88	1.00	125.60	1.51	1.51	6.56	876,321	0.04
Maximum	1.00	1.03	1.00	760.46	4.21	4.21	47.53	62,277,493	0.12
Maine (93 observations)									
Minimum	0.07	1.00	0.03	0.00	0.00	0.00	0.19	12	0.01
Median	0.30	1.22	0.52	5.35	0.00	0.00	2.01	363	0.07
Maximum	0.70	10.33	0.97	96.49	2.52	3.36	9.16	265,789	0.39
Alabama (23 observations)									
Minimum	1.00	0.54	1.00	9.84	0.15	0.15	2.91	77,097	0.01
Median	1.00	0.86	1.00	74.89	1.00	1.01	6.52	11,554,187	0.05
Maximum	1.00	0.97	1.00	204.28	2.11	2.11	16.86	154,535,479	0.11
National Bridge Scour Database (15 observations)									
Minimum	0.19	1.00	0.17	2.01	0.00	0.00	0.94	131	0.02
Median	0.41	1.00	0.92	56.30	0.49	0.59	1.95	872,077	0.04
Maximum	1.00	1.67	1.00	143.68	1.25	1.25	13.09	187,149,476	0.22

[a] A value of 1.00 represents a floodplain relief bridge or a swampy site with a poorly defined channel.

[b] A value of 1.00 or greater represents an abutment located at the channel bank or protruding into the channel.

[c] Scour depth is not adjusted for abutment shape.

[d] Scour depth is adjusted for abutment shape. Because a large percentage of the field data is associated with long abutments, there is little change from the y_s/y_1 and y_{sadj}/y_1 values.

1.2.5 Limitations

Laboratory investigations have been essential in advancing the understanding of abutment scour and undoubtedly will continue to play a prominent role in future investigations. However, field conditions will often differ from the idealized conditions of the laboratory, and it is important to understand some of these differences. Laboratory models typically consist of simple river plans that include uniform channel geometry, straight approach channels, uniform floodplain and channel roughness, uniform non-cohesive sediments, approach flow velocities near threshold conditions, and constant flow of sufficient duration to create equilibrium scour depths (Melville and Coleman, 2000). These characteristics rarely exist concurrently in the field, and the equilibrium abutment-scour depth associated with the laboratory studies is likely unattainable at most field sites. As will be shown later in this chapter, the upper bound of the relative scour depth (scour depth divided by approach flow depth) for the laboratory data is about 11 for rigid abutment/embankment models and about 4 for erodible abutment/embankment models as used in the NCHRP 24-20 investigations. In comparison, the maximum relative scour depth is 4.2 for the USGS field data. The upper bound within the USGS field data has some confirmation from the large abutment-scour measurement at the Interstate 70 (I-70) crossing of the Missouri River (Parola et al. 1998). The I-70 abutment scour was caused by the 1993 flood with high-flow durations lasting nearly 7 days. The scour was strongly influenced by an upstream levee breach in close proximity to the abutment, and the largest scour depth (56 ft) was located just downstream from the breach. As flows moved around the embankment and into the bridge opening, the deepest scour depth at the bridge was 30 ft. These scour depths were not created by the typical flow patterns associated with abutment scour, but rather by adverse conditions that tend to promote large scour depths. The I-70 scour depths are presented here for perspective. The relative abutment-scour depth for the 56-ft deep measurement is 4.0 indicating that the upper bound of abutment scour in the USGS data is not unreasonable for the field, even under severe flood conditions, such as the I-70 measurements.

The NCHRP 24-20 investigation demonstrates how laboratory models with erodible embankments and abutment substructures, comparable to conditions often found in the field, will tend to reduce the magnitude of abutment scour in comparison to laboratory models with rigid abutments/embankments that have vertical-wall substructures that extend fully into the bed

sediments. It is of interest that the largest relative scour depth for the NCHRP 24-20 data, about 4, conforms well to that of the field, about 4.2. The similarity in the largest relative scour depths could indicate that erodible abutment substructures produced the smaller scour depths in the USGS field data, similar to those of the NCHRP 24-20 data. While this may contribute in some measure to this pattern, the evidence indicates that abutments/embankments associated with the USGS field data largely remained intact; therefore, the smaller relative scour depths cannot be attributed solely to this type of scour process. While many factors likely contribute to the smaller relative abutment-scour depths in the field data, non-uniform sediments, short flow durations, and approach flow velocities below critical-velocity conditions are thought to be prominent reasons for the discrepancies between the laboratory data associated with rigid abutment models and the field data.

Sediment characteristics can play a prominent role in preventing the attainment of equilibrium abutment-scour depths in the field. Sediments in the field are non-uniform in grain size and often have varying degrees of cohesion. This is particularly the case for floodplain sediments where clear-water abutment scour occurs at setback abutments. Additionally, natural streams with alluvium floodplain sediments often have subsurface strata that are more resistant to scour than the surface sediments. In the South Carolina data, it was common for abutment-scour holes, exceeding approximately 5 ft in depth, to cut down to a scour-resistant layer that likely impeded scour (Benedict, 2003). Of the South Carolina abutment-scour measurements, 124 resulted in scour depths less than 5 ft. For these smaller scour depths, only one measurement had a subsurface scour-resistant layer at the bottom of the scour hole that was distinctly different from the surface sediments. In contrast, of the 85 abutment-scour measurements in South Carolina that had scour depths exceeding 5 ft, 48 measurements had a subsurface scour-resistant sediment layer at the bottom of the scour hole. Similarly, Parola et al. (1998) note that the 56-ft-deep abutment-scour hole at the I-70 crossing of the Missouri River likely was limited by a subsurface layer of relatively resistant material. These sediment characteristics, commonly found in the field, will tend to reduce the magnitude of relative scour in comparison to the uniform non-cohesive sediments of the laboratory, and these sediment characteristics are thought to be a prominent reason for the smaller relative scour depths in the field.

Another factor that could limit the attainment of equilibrium abutment-scour depths in the field comparable to those of the laboratory is insufficient flow duration. Flow durations must often last for days in laboratory experiments in order to achieve equilibrium abutment-scour depths (Sturm, 2004). In contrast, small to moderate drainage areas, commonly associated with many bridges, will have peak-flow durations substantially smaller than those of the laboratory, thus limiting the potential to attain equilibrium abutment-scour depths. This is particularly the case for clear-water abutment scour on the floodplain, because it takes longer flow durations to attain equilibrium clear-water scour depths (Melville and Coleman, 2000).

The largest potential for abutment-scour depth generally occurs when approach flow velocities are near the sediment critical velocity (Melville and Coleman, 2000), which is the threshold velocity that transitions from clear-water to live-bed scour conditions. Laboratory experiments are often conducted near threshold velocity in order to assess the worst-case conditions for abutment scour. As approach flow velocities decrease below threshold velocities, scour depth decreases (Melville and Coleman, 2000). As will be shown later in report section 1.4.1, flow velocities on the approach floodplain are often below threshold velocities and will likely contribute to the smaller relative-scour depths observed in the field. Because abutment-scour field data tend to have relative scour depths smaller than the laboratory, it is logical to assume that laboratory-derived equations applied to field data should consistently overpredict the field measurements. If underprediction frequently occurs, additional consideration should be given to assess why this is the case.

All of the hydraulic properties used in this investigation are based on one-dimensional flow models. As such, they must be viewed as approximate rather than measured data, and such data will likely introduce error in the predicted scour. The South Carolina, Alabama, and Maine investigations assumed various flow conditions for use in the hydraulic models. Based on a review of historical flow records, the South Carolina and Alabama studies assumed that the 100-year and 50-year peak flows, respectively, would represent approximate flow conditions that created the measured scour. For the Maine investigation, the peak flow associated with a 50-percent chance of exceedance based on the bridge age was used to represent the hydraulic conditions that may have created the scour. It is likely that these flow magnitudes will provide overestimates of hydraulic conditions, especially for the South Carolina data. The NCHRP 24-

20 and 24-15(2) methods require estimates of the flow velocity at the abutment. One-dimensional flow models often do not simulate well the increased flow velocities at large flow contractions at an abutment and, therefore, will tend to underestimate this value. Underestimates of the velocity at the abutment will tend to produce underestimates of abutment-scour depth. To compensate for this limitation in one-dimensional flow models, the NCHRP 24-20 and 24-15(2) methods use algorithms, described later in the report, that provide conservative estimates of the flow velocity at the abutment. These algorithms likely perform well at sites with a well-defined channel. However, at sites with poorly defined channels, such as a swamp or floodplain relief bridge, the algorithms may underestimate the increased flow velocity at the abutment.

The uncertainty and limitations associated with the USGS field data, as noted above, will introduce some error into any analysis in which these data are used. Therefore, relations in the field data and comparisons of predicted and measured field data will generally have more scatter than that associated with laboratory data. While the limitations of the USGS field data are acknowledged, it is currently (2015) the best available set of field data for the evaluation of abutment-scour prediction equations. The error and limitations make these data less than ideal; however, the large number of field observations used in the analysis (329) and the wide range of regional characteristics associated with the data allow trends for selected scour prediction methods to be assessed. Such an assessment will provide insights into the strengths, weaknesses, and limitations of a particular scour prediction method.

1.3 Laboratory Data

The harsh and uncontrolled environment of the field makes it challenging to measure abutment scour and the associated hydraulic characteristics creating the scour. In contrast, the controlled environment of the laboratory allows for more accurate measurement of these values. While the objective of this investigation is to evaluate the performance of the NCHRP 24-15(2) and NCHRP 24-20 methods with field data, the use of the more precise laboratory data can help confirm the trends observed in the field data assessment. Selected data from Palaviccini (1993) and Sturm (2004) were compiled and used to compare with the dimensionless trends of the laboratory data for NCHRP 24-15(2) and NCHRP 24-20. Additionally, these data were applied to the NCHRP 24-15(2) and NCHRP 24-20 equations to assist in evaluating the performance of

these equations. The Palaviccini (1993) data consist of 404 measurements of live-bed and clear-water abutment scour compiled from selected investigations prior to 1990. The measurements were collected in rectangular flumes and included 57 spill-through, 56 wing-wall, 246 vertical-wall, and 45 other types of abutments. The Palaviccini (1993) data associated with spill-through, wing-wall, and vertical-wall abutments were used in this investigation. The Sturm (2004) data consist of 74 measurements of clear-water abutment scour collected in compound channels, more closely reflecting the laboratory conditions associated with the NCHRP 24-15(2) and NCHRP 24-20. These data represent longer abutment lengths than those associated with Palaviccini (1993) and the NCHRP 24-15(2) and NCHRP 24-20 investigations and include spill-through and vertical-wall abutments. Additionally, the Sturm (2004) data include point measurements of velocity and depth at the approach floodplain, as well as measurements of the maximum velocity and associated depth at the abutment. These data provide a means to determine the unit discharges at the approach and bridge, which are the primary variables used in the NCHRP 24-20 method.

Some notable differences in the Palaviccini (1993) and Sturm (2004) data from the NCHRP 24-15(2) and NCHRP 24-20 data include the following. The NCHRP 24-15(2) method was originally developed for scour in cohesive sediments, but was expanded to include scour in non-cohesive sediments (Briaud et al. 2009; 2011), as is described later in the report. The Palaviccini (1993) and Sturm (2004) data represent scour in non-cohesive sediments, making it difficult to assess the performance of the NCHRP 24-15(2) method for scour in cohesive sediments, but useful for assessing equation performance in non-cohesive sediments. The NCHRP 24-20 laboratory investigation evaluated scour for various combinations of erodible and non-erodible floodplains, embankments, and abutment substructures. In contrast, the other laboratory investigations evaluated scour for solid-form (rigid) abutments typically having a vertical wall at the abutment toe, similar to a sheet-pile skirt, extending into the bed. The erodible abutment/embankment models will tend to reduce abutment-scour depth in contrast to the rigid abutment/embankment models. The Palaviccini (1993) and Sturm (2004) data represent rigid abutments/embankments, and some underprediction is likely when these data are applied to the NCHRP 24-20 method. Tables 1-3 and 1-4 list the median and range of selected dimensional and dimensionless variables, respectively, for the Palaviccini (1993) and Sturm (2004) data. Figure 1-5 provides a schematic that defines selected variables in tables 1-3 and 1-4. Data

ranges for the NCHRP 24-15(2) and NCHRP 24-20 laboratory data also are included. Additional details associated with the data can be found in Palaviccini (1993) and Sturm (2004).

Table 1-3. Range of selected variables for laboratory measurements of abutment scour. (Refer to figure 1-5 for schematic showing selected variable definitions.)

[ft/s, feet per second; ft, feet; mm, millimeters]

Range value	Average approach velocity (ft/s)	Average approach depth (y_1) (ft)	Embank-ment length (L) blocking flow (ft)	Flume width (0.5B) (ft)	Median grain size ($D50$) (mm)	Observed abutment-scour depth (y_s) (ft)	[a]Abutment/ embank-ment model (Rigid or Erodible)	Channel shape (Rectangular or Compound)
Palaviccini (1993) (359 observations)								
Minimum	0.31	0.09	0.0	2.0	0.29	0.0	Rigid	Rectangular
Median	1.07	0.33	1.0	4.0	0.82	0.5		
Maximum	4.03	1.64	3.7	8.0	3.30	1.9		
Sturm (2004) (74 observations)								
Minimum	0.34	0.09	2.6	13.8	1.10	0.0	Rigid	Compound
Median	0.76	0.19	7.1	13.8	3.30	0.6		
Maximum	1.18	0.38	12.0	13.8	3.30	1.0		
Briaud et al. (2009) (19 observations)								
Minimum	0.68	0.60	3.3	12.0	[b] 0.004	0.2	Rigid	Compound and Rectangular
Median	1.35	0.96	6.0	12.0	[b] 0.004	1.4		
Maximum	1.90	1.31	9.0	12.0	[b] 0.004	4.7		
[c] Ettema et al. (2010) (62 observations)								
Minimum	1.07	0.49	1.1	13.1	0.45	0.6	Erodible and Rigid	Compound and Rectangular
Median	1.07	0.49	4.3	13.1	0.45	1.0		
Maximum	1.38	0.98	9.9	13.1	0.45	1.4		

[a] Rigid abutment/embankment models are not susceptible to erosion during the scouring process. Erodible abutment/embankment models simulate earthfill embankments similar to field conditions. Scour depths associated with erodible abutments/embankments models are typically less than those associated with rigid abutment/embankment models (Sturm et al. 2011).

[b] The Briaud et al. (2009) investigation used clay sediments.

[c] Some of these data (22 measurements) were excluded from the analysis because they represented baseline conditions without abutments or test runs for evaluating the influence of erodible and non-erodible floodplains on scour in the main channel.

Table 1-4. Range of dimensionless variables for laboratory measurements of abutment scour. (Refer to figure 1-5 for schematic showing selected variable definitions.)

[y_f, floodplain flow depth; y_{mc}, channel flow depth; L, abutment length; $\boldsymbol{B_f}$, floodplain width; $0.5B$, channel width including floodplain width associated with abutment and half of the main-channel width; $\boldsymbol{y_1}$, approach flow depth which could be y_f or y_{mc} depending on location of abutment toe; y_s, abutment-scour depth; y_{sadj}, abutment-scour depth adjusted for abutment shape; q_1, approach unit discharge; q_2, unit discharge at abutment; $D50$, median grain size; Fr_1, approach Froude number]

Range value	[a] y_f / y_{mc}	[b] L/B_f	[a] $B_f/0.5B$	L/y_1	[c] y_s/y_1	[d] y_{sadj}/y_1	q_2/q_1	$L/D50$	Fr_1
Palaviccini (1993) (359 observations)									
Minimum	1.00	0.05	1.00	0.38	0.01	0.01	1.05	45	0.06
Median	1.00	0.27	1.00	3.10	1.65	2.09	1.37	378	0.36
Maximum	1.00	0.63	1.00	13.00	5.62	8.89	2.67	2,014	1.28
Sturm (2004) (74 observations)									
Minimum	0.11	0.22	0.87	13.68	0.36	0.36	0.96	242	0.47
Median	0.18	0.59	0.87	57.09	5.20	5.20	1.53	727	0.58
Maximum	0.28	1.00	0.87	161.95	10.96	10.96	5.84	2,182	0.93
Briaud et al. (2009) (19 observations)									
Minimum	0.48	0.28	0.67	2.77	0.18	0.24	1.32	253,746	0.11
Median	0.59	0.75	0.67	6.23	1.43	3.16	1.56	457,200	0.24
Maximum	1.00	1.00	1.00	10.01	4.86	9.09	4.00	685,800	0.34
[e] Ettema et al. (2010) (62 observations)									
Minimum	0.50	0.14	0.23	2.15	0.61	1.02	1.01	716	0.24
Median	0.50	0.75	0.43	6.65	1.34	2.52	1.31	2,944	0.24
Maximum	1.00	2.13	1.00	18.40	2.79	5.93	3.18	6,720	0.26

[a] Rectangular channels have a value of 1.00.
[b] A value of 1.00 or greater represents an abutment located at the channel bank or protruding into the channel.
[c] Scour depth is not adjusted for abutment shape.
[d] Scour depth is adjusted for abutment shape.
[e] Some of these data (22 measurements) were excluded from the analysis because they represented baseline conditions without abutments or test runs for evaluating the influence of erodible and non-erodible floodplains on scour in the main channel.

1.3.1 Adjustment for Abutment Shape

The following sections of this report will present some simple comparisons of the laboratory and field data. When making such comparisons, it is useful to adjust the data to a common abutment shape, and a brief description of this adjustment procedure follows. Abutment shape can have a strong influence on abutment-scour depth, with blunt abutment shapes, such as vertical walls, creating larger scour depths than streamlined shapes, such as spill-through abutments. As the abutment length increases, the benefits of a streamlined shape diminish and scour depths approach those of the blunt-faced abutments (Melville and Coleman, 2000). In order to review and compare the relations in the laboratory data (table 1-3), it is necessary to convert scour depths associated with various abutment shapes to a common reference shape. This conversion is accomplished by dividing the measured scour depth by the associated abutment-shape factor (table 1-5). To account for the change in the abutment-shape factor as abutment length increases, Melville and Coleman (2000) recommend the following equations. By using equation 1-1, the laboratory data (table 1-3) were converted to a common reference shape prior to investigating selected relations by dividing the measured scour depth by the associated abutment-shape factor.

$$K_s^* = K_s, \quad \text{for } L/y_1 \leq 10 \qquad \text{(1-1a)}$$

$$K_s^* = K_s + 0.667(1 - K_s)\left(0.1\,{}^{L}/_{y_1} - 1\right), \quad \text{for } 10 < L/y_1 < 25 \qquad \text{(1-1b)}$$

$$K_s^* = 1 \quad \text{for } L/y_1 \geq 25 \qquad \text{(1-1c)}$$

where

K_s^* is the abutment-shape factor adjusted for abutment length;

K_s is the abutment-shape factor for shorter abutments (table 1-5);

L is the abutment length in ft; and

y_1 is the approach flow depth in ft.

Table 1-5. Shape factors for shorter abutments (from Melville and Coleman (2000)).

Abutment shape	Abutment-shape factor (K_s)
Vertical wall	1
Wing wall	0.75
Spill through (horizontal to vertical slope: 0.5:1)	0.6
Spill through (horizontal to vertical slope: 1:1)	0.5
Spill through (horizontal to vertical slope: 1.5:1)	0.45

1.3.2 Upper Bound of Laboratory Data

Melville (1992) developed upper-bound envelope curves for relative abutment-scour depth based on dimensionless plots of selected laboratory data. Figures 1-11 and 1-12 present the laboratory data listed in table 1-3 along with Melville's upper-bound envelopes. Figure 1-11 represents a modified version of the Melville (1992) envelope curve as presented in Melville and Coleman (2000) and describes the influence of the flow shallowness with respect to the abutment length (y_1/L) on the upper bound of relative scour depth (y_{sadj}/L). The trend in figure 1-11 indicates that the upper bound of y_{sadj}/L generally increases as y_1/L increases and becomes a constant of 2 when y_1/L equals or exceeds 1. Figure 1-12 describes the influence of the relative abutment length (L/y_1) on the upper bound of relative scour depth (y_{sadj}/y_1) and indicates that the upper bound of y_{sadj}/y_1 generally increases as L/y_1 increases and becomes a constant of 10 when L/y_1 equals or exceeds 25. The Melville (1992) curve was developed with data from rectangular channels, and the Palaviccini (1993) data, all associated with rectangular channels, generally conform to the Melville (1992) envelope curves with occasional exceedance. In contrast, the Sturm (2004), Briaud et al. (2009), and Ettema et al. (2010) data, primarily associated with compound channels, generally plot below the envelope curves. This pattern possibly could be caused by the differing flow patterns associated with compound channels. Additionally, the erodible abutments/embankments, along with the differing abutment substructures associated with the Ettema et al. (2010) data, likely contribute to the smaller relative scour depths for those data. It is notable that the Briaud et al. (2009) data in cohesive sediments have similar values of relative scour depth to those of the non-cohesive sediments, indicating that maximum relative-scour depths in cohesive sediments will be comparable to those of non-cohesive sediments, given sufficient time to scour. Both figures display Melville's (1992) abutment-length categories of

short, intermediate, and long abutments, and indicate that the Palaviccini (1993) data consist of short and intermediate abutments; the Briaud et al. (2009) and Ettema et al. (2010) data consist of intermediate abutments; and the Sturm (2004) data consists primarily of long abutments with a few intermediate abutments. The diversity of the Palaviccini (1993) and Sturm (2004) data with respect to the Briaud et al. (2009) and Ettema et al. (2010) data indicates that applying these data to the NCHRP 24-15(2) and NCHRP 24-20 methods will likely provide good insights to the performance of those methods.

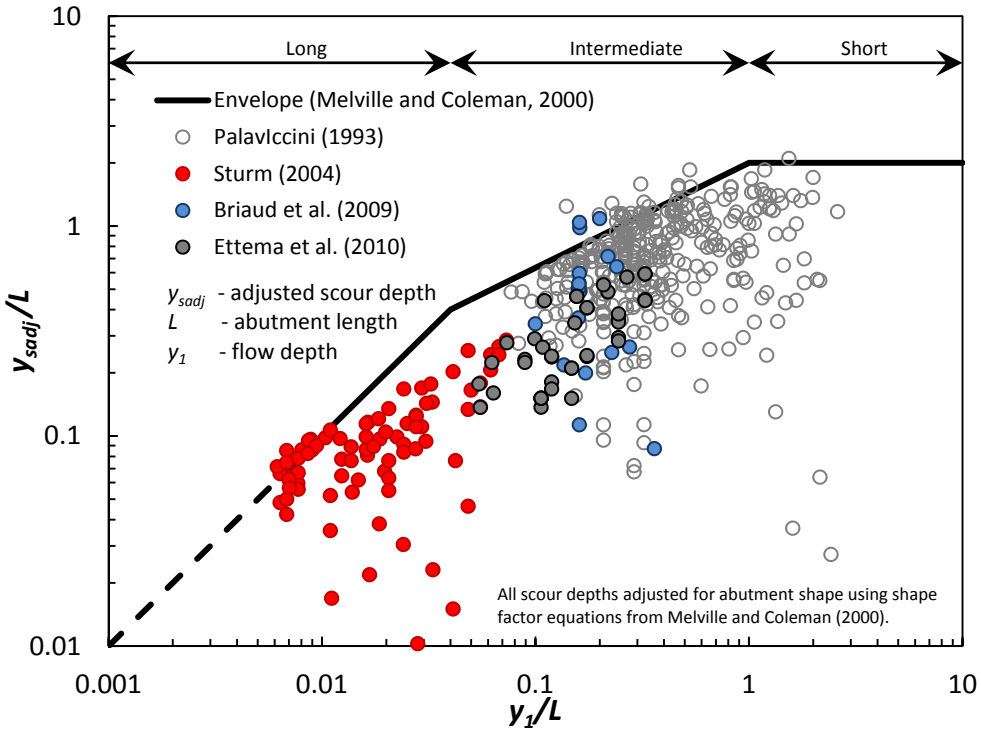

Figure 1- 11. Relation of the relative scour depth to relative flow depth, with respect to abutment length, for selected laboratory data.

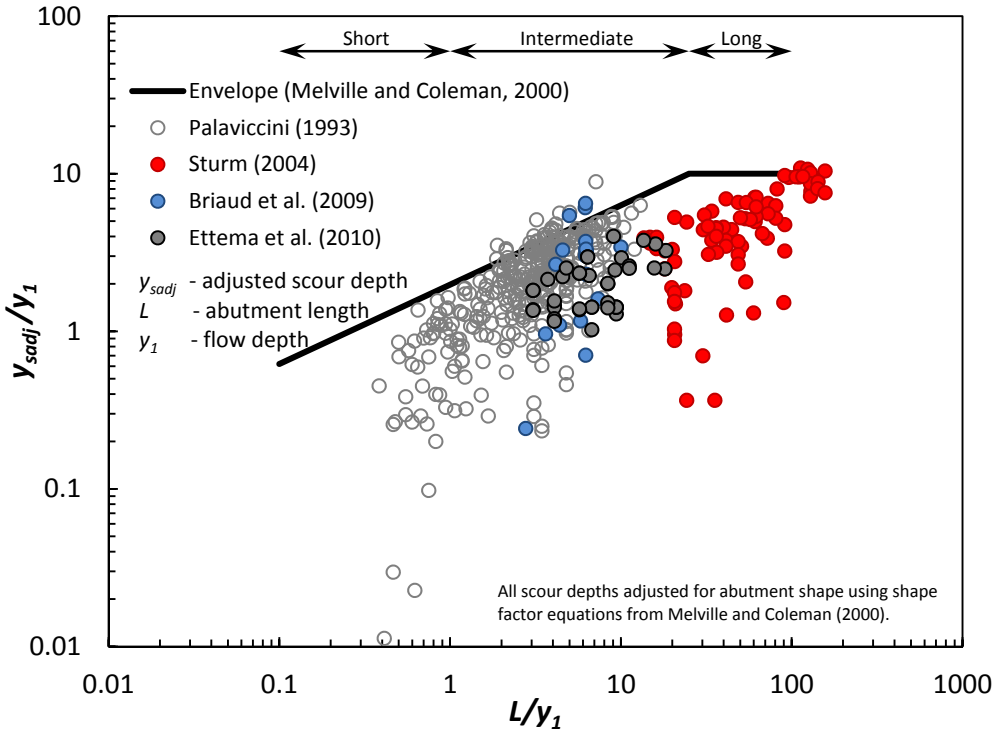

Figure 1- 12. Relation of the relative scour depth to relative abutment length, with respect to flow depth, for selected laboratory data.

1.4 Comparison of Field and Laboratory Data

Scour prediction equations developed from small-scale laboratory investigations are scaled to the field through the development of equations associated with dimensionless variables. To assure the success of a laboratory-derived equation, the range of the dimensionless variables associated with the laboratory data should approximate the typical range found in the field. When the dimensionless variables in the field extend substantially beyond the range of the dimensionless variables associated with a laboratory equation, it is possible that the laboratory equation may perform differently than expected (Sturm et al. 2011). Because the values of dimensionless variables can have a wide range in the field, designing laboratory experiments to adequately encompass the range of the dimensionless variables found in the field can be challenging. The range of dimensionless variables for the field and laboratory data (tables 1-2 and 1-4, respectively) along with selected plots of these data is briefly reviewed.

1.4.1 Percentile Plots of Selected Dimensionless Variables

The following figures (1-13 through 1-19) show percentile plots for selected dimensionless variables that are commonly used in the analysis of abutment scour, including relative abutment length (L/y_1), relative scour depth (y_{sadj}/y_1) adjusted for abutment shape, unit discharge ratio (q_2/q_1), relative sediment size ($L/D50$), the approach Froude number (Fr_1), and the ratio of embankment length blocking flow to the floodplain width (L/B_f) for the field and laboratory data. Each percentile plot includes separate curves for the field and laboratory data as grouped in tables 1-2 and 1-4. It should be kept in mind when assessing the data that some of these plots have logarithmic scales on the vertical axis in order to better display the data.

Abutment-scour depth tends to increase at a decreasing rate as the relative abutment length, L/y_1, increases (Melville, 1992; figure 1-12), where L is the length of the embankment blocking flow and y_1 is the approach flow depth. Figure 1-13 shows the percentile plots for L/y_1 indicating that the field data generally have larger relative abutment lengths in contrast to the laboratory data. The lower gradient streams of the South Carolina Coastal Plain, with their wide flat floodplains, have the largest relative abutment lengths as well as some of the largest abutment-scour depths within the USGS field data (tables 1-1 and 1-2). In contrast, the steeper gradient streams of

Maine have the smallest relative abutment lengths and smaller scour depths (tables 1-1 and 1-2). While L/y_1 undoubtedly influences the difference in scour magnitude for the Coastal Plain and Maine data, the differing sediment characteristics (table 1-1) also contribute to this pattern. The Palaviccini (1993), Briaud et al. (2009), and Ettema et al. (2010) data have smaller relative abutment lengths than the Maine data. In contrast, the longer abutment lengths associated with the Sturm (2004) data fall within the range of the Alabama, NBSD, and South Carolina Piedmont data. The fact that most of the laboratory data have L/y_1 values substantially smaller than those of the field is indicative of the difficulty of modeling the long abutments in the laboratory similar to those associated with the field.

The relative scour depth is the ratio of abutment-scour depth to the approach flow depth (y_{sadj}/y_1). This is a common way to express abutment-scour depth as a dimensionless variable and is frequently the dependent variable used in the development of abutment-scour prediction equations. Figure 1-14 shows the percentile plots for y_{sadj}/y_1. With respect to the field data, the lower gradient, sandy streams of the South Carolina Coastal Plain have the largest relative scour depths, with the steeper gradient, coarse sediment streams of Maine having the lowest values. Coarse sediments generally yield smaller scour depths than those for sandy sediments (Melville and Coleman, 2000), and therefore, the smaller scour depths for the Maine data are reasonable. The cohesive-sediment data of the Piedmont and Alabama generally have smaller values of y_{sadj}/y_1 than the non-cohesive sediments of the Coastal Plain, providing some perspective on the influence of cohesive sediments on scour depth in the field. The relative scour depths for the cohesive sediments of the Briaud et al. (2009) laboratory data exceed those of the Piedmont and Alabama field data and can be attributed to the long flow durations used in the laboratory to reach maximum scour depths. It is instructive to note that the largest relative scour depths are associated with the Coastal Plain data, indicating that low gradient streams with non-cohesive sediments and relatively long abutments (figure 1-13) will have the largest potential for scour. The relative scour depths for the laboratory data generally exceed the values associated with the field data, with the largest value of 11 being associated with the Sturm (2004) data, in contrast to a maximum value of 4.2 for the field. The Ettema et al. (2010) data generally have the smallest values of y_{sadj}/y_1 within the laboratory data and conform well to the South Carolina Coastal Plain data that represent the largest values of y_{sadj}/y_1 within the field data. The similar percentile plots for the Ettema et al. (2010) and the South Carolina Coastal Plain data could lead one to conclude

that erodible abutments/embankments could be a primary reason why the field data have lower values of y_{sadj}/y_1 in contrast to the rigid abutment models of the other laboratory data. (Note: Rigid abutments have solid substructures, similar to piers that extend into the bed sediments. Such abutments generally create flow fields that produce deeper scour at the abutment structure than the erodible abutments/embankments that are seated on, rather than into, the bed.) While erodible abutments/embankments may contribute to this pattern, report section 1.2.5 describes other factors that likely contribute to the smaller values of y_{sadj}/y_1 in the field data, including non-uniform sediments, short flow durations, and approach velocities below threshold conditions. Additional details regarding the possible reasons for the smaller values of y_{sadj}/y_1 in the field data can be found in report section 1.2.5. Because values of y_{sadj}/y_1 for the field data are generally smaller than those for the laboratory, it is reasonable to assume that laboratory-derived equations applied to field data should overpredict the field measurements. If underprediction frequently occurs, additional consideration should be given to assess why this is the case.

The unit discharge ratio, q_2/q_1, is the ratio of the contracted unit discharge at the abutment to the uncontracted unit discharge at the approach. This dimensionless variable expresses the severity of the flow contraction created by the abutment, and the potential for abutment-scour depth generally increases as q_2/q_1 increases. Figure 1-15 shows the percentile plots for q_2/q_1. With respect to the field data, the lower gradient streams of the South Carolina Coastal Plain have the largest unit discharge ratios and, therefore, the largest potential for scour, as is indicated in figure 1-14, where the South Carolina Coastal Plain data have the largest values of relative-scour depth within the field data. In contrast, the steeper gradient streams of Maine have the smallest unit discharge ratios (figure 1-15) and smaller relative scour depths (figure 1-14). The laboratory data have small unit discharge ratios comparable to the small, steep-gradient streams of the Maine data. Severe contractions of flow, such as those associated with the low-gradient streams of the South Carolina Coastal Plain, can create large water-surface differentials (or backwater) across a bridge, which can create severe hydraulic conditions that produce excessive scour. For example, the one-dimensional flow model for the Interstate 95 crossing of the Pee Dee River in South Carolina indicates that the backwater for the 100-year flow exceeds 2 ft. This site had the largest measured scour depth, 23.6 ft, in the USGS field data. Similarly, the I-70 crossing of the Missouri River, as described in report section 1.2.5, had a backwater of about 2.5 ft during the 1993 flood (Missouri Department of Transportation, I-70 Second Tier Draft Environmental

Impact Statement) with a corresponding scour depth of 56 ft. While other factors likely contributed to the scour at these sites, the large flow contraction and backwater undoubtedly contributed in some measure. The largest value of q_2/q_1 for the laboratory data (about 6) is much smaller than that for the field data (about 48), indicating that the laboratory data may not be adequately capturing the severe flow contractions more commonly found in the field. Therefore, laboratory-derived prediction equations may tend to underpredict scour at such sites. As previously noted, modeling long abutments in a laboratory flume presents challenges because of scaling issues. Likewise, modeling the severe flow contractions as found in the field will present challenges because such contractions are typically associated with long abutments.

The relative sediment size, *L*/*D50*, was used by Melville and Coleman (2000) to define the influence of sediment size on abutment-scour depth, noting that for values greater than 25, the influence is negligible. Sturm et al. (2011) notes that there is some uncertainty regarding the influence of this variable, and therefore, *L*/*D50* is often not used in abutment-scour prediction formulas. Figure 1-16 shows the percentile plots for *L*/*D50*. Most of the field data have very large relative sediment-size values that greatly exceed the laboratory data, indicating that these field data are associated with smaller sediment sizes, typically less than 1 mm, and long abutments (table 1-1). The exception to this is the Maine data where the coarser sediments and shorter abutments (table 1-1) produce *L*/*D50* values that are much smaller than the other field data. The Palaviccini (1993), Sturm (2004), and Ettema et al. (2010) data have percentile plots similar to the Maine data, indicating, from a relative perspective, that the sediments are coarser than much of the field data. The Briaud et al. (2009) data have larger *L*/*D50* values because of the small *D50* associated with the cohesive clay used in the experiments. The *L*/*D50* parameter is intended for evaluation of non-cohesive sediments and, therefore, is not applicable to the cohesive sediments of the Briaud et al. (2009) data. However, the Briaud et al. (2009) data are shown in figure 1-16 for information. Generally, the values for the *L*/*D50* parameter tend to be less than 25 for almost all of the field and laboratory data and, therefore, will likely have negligible influence on scour depths.

Figure 1-17 shows the percentile plots for the approach Fr_1, with most of these values representing conditions on the approach floodplain. With respect to the field data, the lower gradient streams of the South Carolina Coastal Plain tend to have the smallest approach Froude

numbers, with the steeper gradient streams of Maine generally having the largest values. Interestingly, the range of the approach Froude numbers for the field data is relatively small, with about 80 percent of the data having values less than 0.1. In contrast, the laboratory data have approach Froude numbers that often are an order of magnitude larger than those of the field data, with the majority having values of about 0.25 or greater. The larger Froude numbers associated with the laboratory data can probably be attributed to the low floodplain roughness in the laboratory models, which will produce relatively larger flow velocities and thus larger Froude numbers. Additionally, many laboratory investigations conduct flume experiments near threshold (or critical) velocity conditions where sediment transport conditions transition from clear water to live bed and the potential for scour is considered to be greatest. In contrast, the floodplains associated with the field data are typically densely vegetated, producing lower velocities and thus lower Froude numbers. The small Froude numbers in the field data also are indicative that approach flow velocities for field conditions are typically below the critical velocity. Figure 1-18 shows a percentile plot of the approach floodplain flow velocity normalized by the sediment critical velocity (V_1/V_c) for a sample of 116 bridges, with 63 bridges in the South Carolina Coastal Plain and 53 in the Piedmont (Benedict and Caldwell, 2006). (Note: Many of the bridges in the South Carolina abutment-scour database were included in figure 1-18.) Values equal to 1 represent conditions where the approach flow velocity is at critical flow. Figure 1-18 demonstrates how floodplain flow velocities can be considerably below the critical velocity, which, according to Melville and Coleman (2000), will tend to reduce scour depths.

The ratio of embankment length blocking flow (L) to the floodplain width (B_f) is a geometric measure of the portion of the floodplain flow being blocked by the embankment, and the potential for abutment-scour depth generally increases as L/B_f increases. Figure 1-19 shows the percentile plots for L/B_f, with values of 1 or greater representing abutments at the channel bank or protruding into the channel. With respect to the field data, the Maine and NBSD data have a large number of abutments located at the channel bank or protruding into the channel and, therefore, have a high percentage of L/B_f values equal to or greater than 1. The Alabama and South Carolina Coastal Plain data tend to have wide swampy floodplains with embankments that block a large portion of the floodplain. This is highlighted in figure 1-19 where about 80 percent of the embankments for Alabama and the South Carolina Coastal Plain are shown to block 80

percent or more of the floodplain. The South Carolina Piedmont data generally have more narrow floodplains; therefore, the values of L/B_f tend to be lower than the other field data. The values of L/B_f for the laboratory data tend to approximate the range of the field data with the exception of the Palaviccini (1993) data that tend to have smaller abutment lengths.

The percentile plots in figures 1-13 through 1-19 provide perspective on the range of selected explanatory variables for the laboratory and field data. They particularly highlight some of the challenges of modeling the more severe scour conditions associated with long embankments (figure 1-13) that produce large contractions of flow (figure 1-15) and yield some of the largest abutment-scour depths (figure 1-14) in the field setting. Additionally, they show how approach flow velocities in the field are typically below threshold velocity conditions (figures 1-17 and 1-18), which may diminish the potential for scour. In contrast, many laboratory experiments are run at or near threshold conditions. They also show how relative scour depths for the field are generally smaller than those for the laboratory (figure 1-14), especially for the laboratory data with rigid abutment/embankment models.

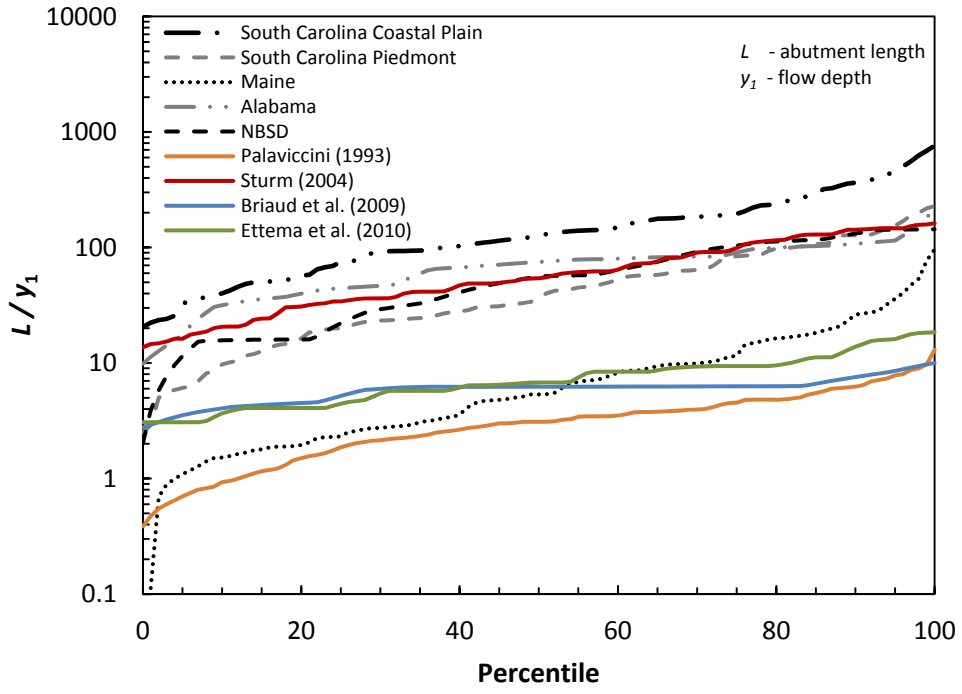

Figure 1-13. Percentile plots for the relative abutment length (L/y_1) for selected field and laboratory data.

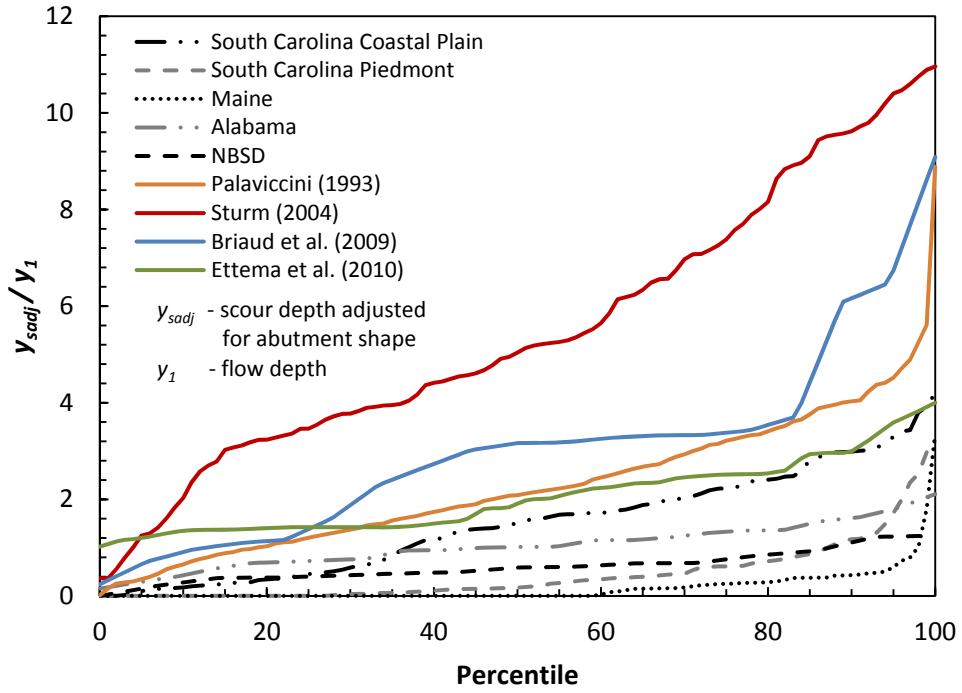

Figure 1-14. Percentile plots for the relative abutment scour (y_{sadj}/ y_1) for selected field and laboratory data.

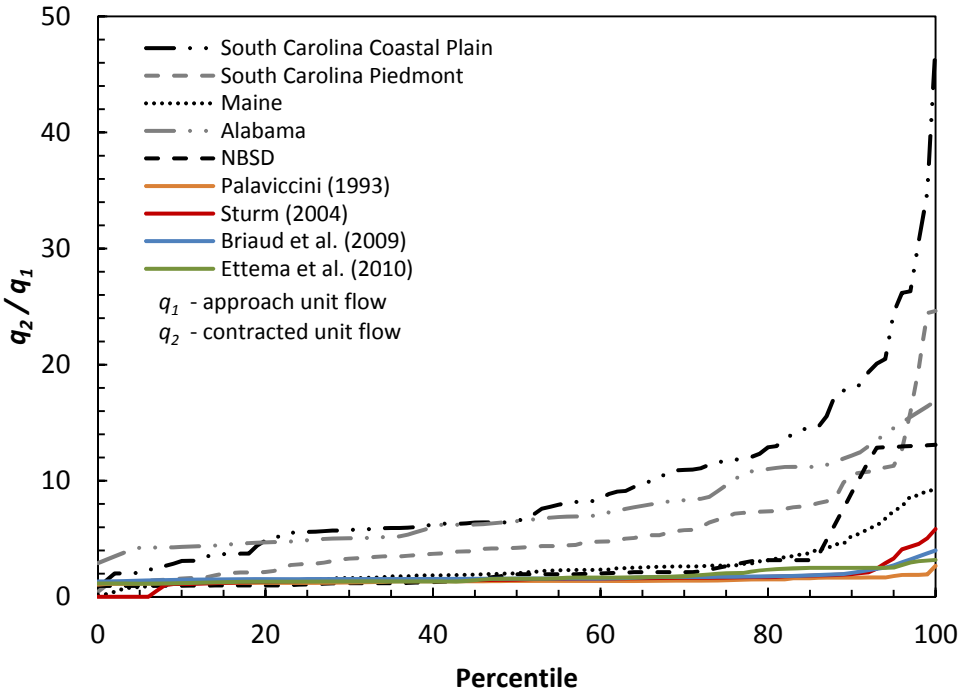

Figure 1-15. Percentile plots for the unit discharge ratio (q_2/q_1) for selected field and laboratory data.

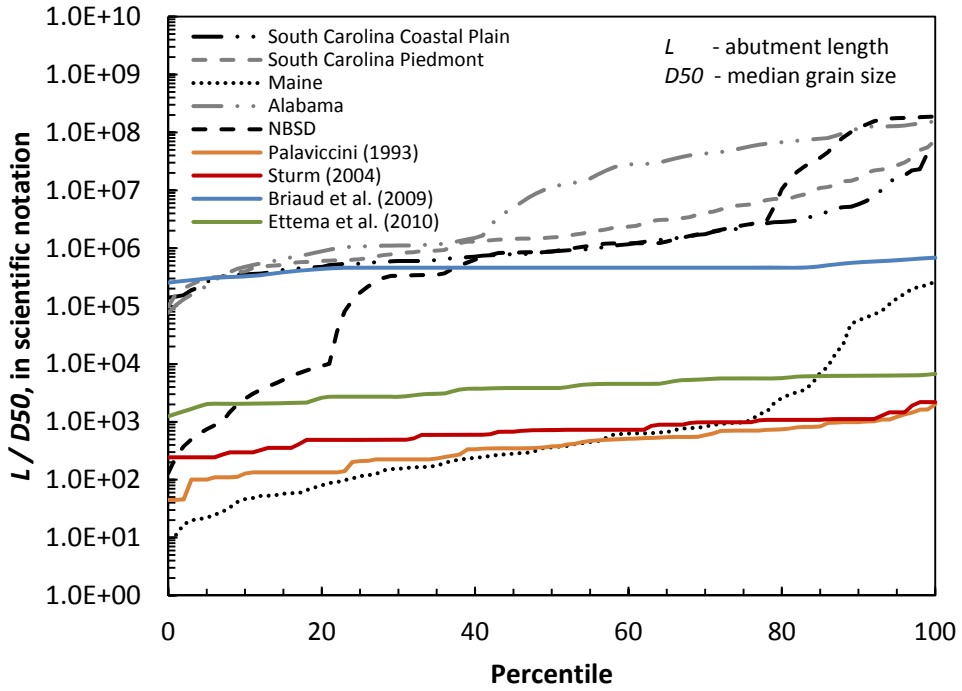

Figure 1-16. Percentile plots for the relative sediment size (*L*/*D50*) for selected field and laboratory data.

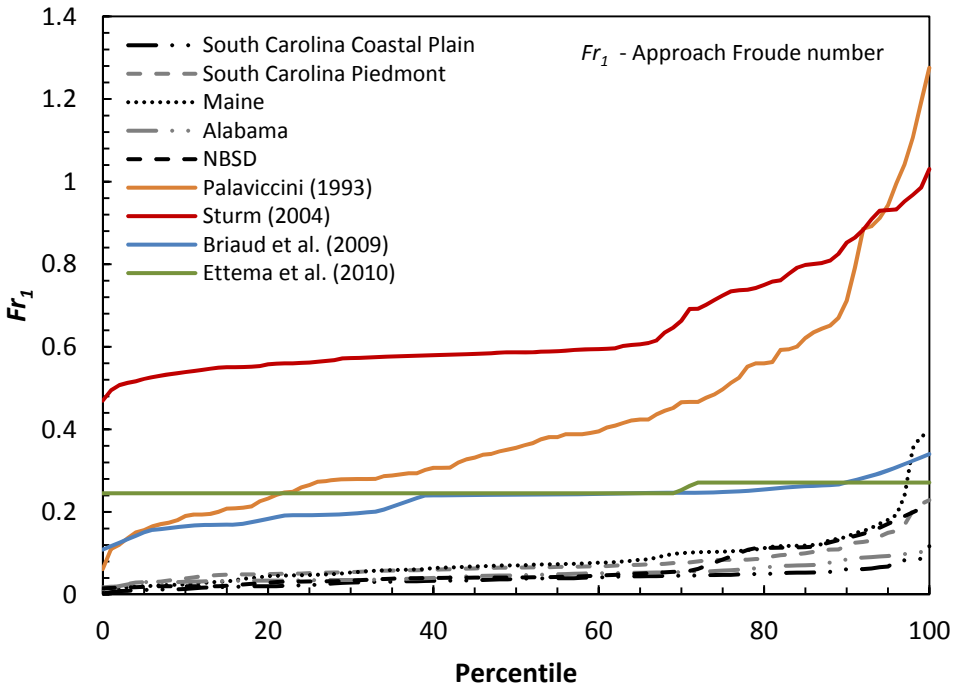

Figure 1-17. Percentile plots for the approach Froude number (Fr_1) for selected field and laboratory data.

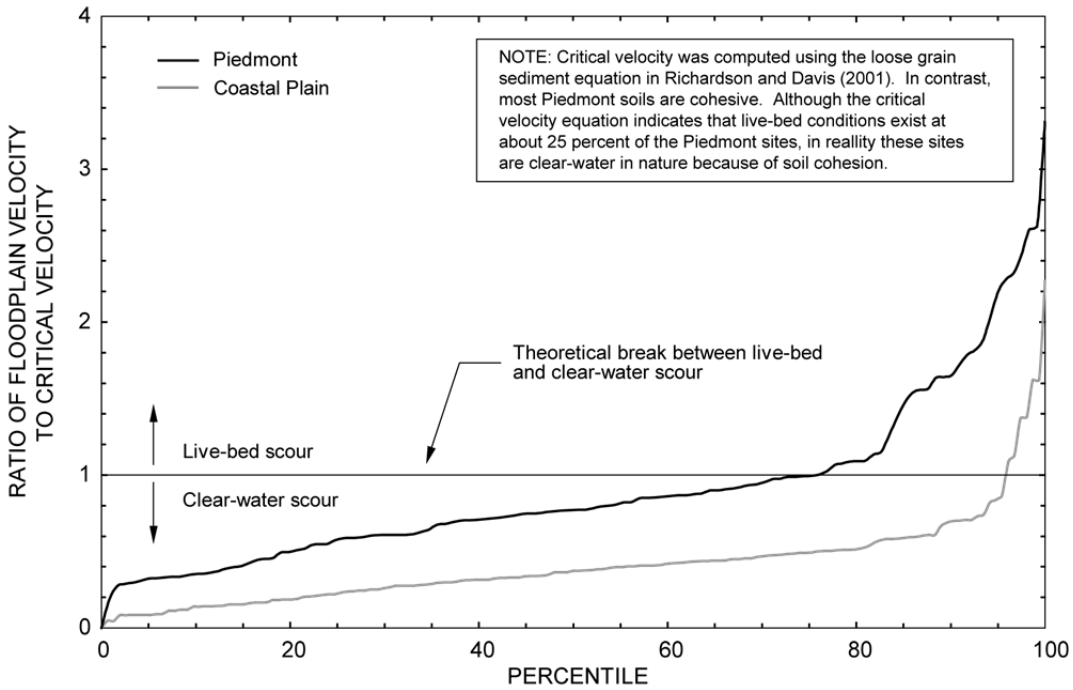

Figure 1-18. Percentile plots for the ratio of the approach floodplain velocity to the critical velocity for selected data from the Coastal Plain and Piedmont of South Carolina (from Benedict and Caldwell, 2006).

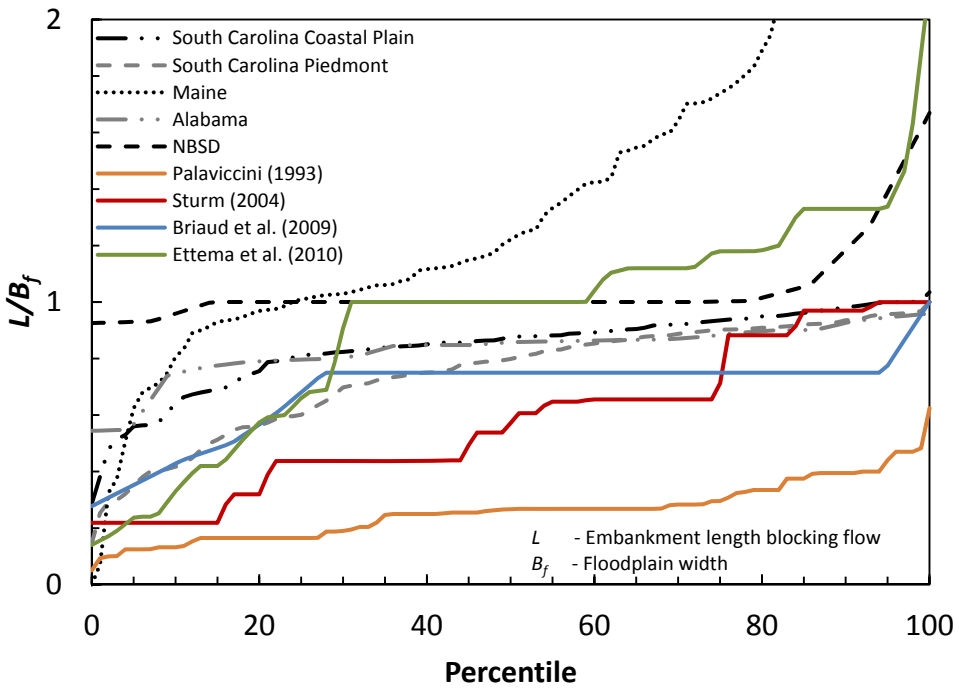

Figure 1-19. Percentile plots for L/B_f for selected field and laboratory data. (Note: Vertical scale has been truncated to better display the trends for the majority of the data.)

1.4.2 Upper Bound of Abutment Scour

Using the Melville (1992) upper-bound envelope curves, figures 1-20 and 1-21 present the laboratory data (table 1-4) and the USGS field data (table 1-2) in dimensionless plots similar to those in figures 1-11 and 1-12, respectively. The Palaviccini (1993) laboratory data were not included in these figures to provide better visibility of the other laboratory and field data. The field data in these figures are grouped as presented in table 1-1, with the exception that a subset of 41 South Carolina measurements associated with floodplain relief bridges and swampy sites, with poorly defined channels (similar to a floodplain) were plotted as an additional group. These sites are associated with bridge lengths less than 240 ft and tended to have a single scour hole that encompassed most of the bridge opening. Thirty-nine of these relief/swamp bridges were taken from the 106 Coastal Plain measurements in South Carolina, with the remaining 2 sites taken from the Piedmont data. These data were grouped separately to show the potential for scour at such sites. Because of the single scour hole at these sites, it was not possible to determine which abutment created the scour. Therefore, the longest of the left or right abutment and its associated hydraulic data was assumed to have produced the scour hole. Based on Melville's (1992) abutment-length categories, 3 of the field measurements are short, 125 are intermediate, and 201 are long abutments. (Note: Measured scour depths with a value of 0 ft are not displayed in figures 1-20 and 1-21 because of the logarithmic scale.) Of the 125 intermediate abutment lengths, 107 are located close to the breakpoint for long abutments, highlighting that the field data are weighted strongly towards long abutments. As noted previously, the reduction in scour depths associated with streamlined abutments (spill through and wing wall) is likely minimized for long abutments (Melville, 1992; Melville and Coleman, 2000). Therefore, in order to properly predict abutment scour at long abutments under field conditions, it may be important that laboratory prediction equations include some mechanism, similar to equation 1-1, to account for the effects of abutment length on scour depth. The current forms of the NCHRP 24-15(2) and NCHRP 24-20 methods do not have a mechanism similar to equation 1-1 to account for the changing influence of abutment shape on scour depth as abutment length increases. Incorporating a mechanism such as this into these methods may be a matter for further consideration.

Figures 1-20 and 1-21 clearly show that the upper bound of the field data is below that of the laboratory data. For the case of long abutments, figure 1-21 indicates that the upper bound for the laboratory data is approximately 11 times the flow depth. In contrast, the upper bound for the field data is 4.2 times the flow depth. As noted previously (report section 1.2.5), field conditions such as non-uniform sediments, approach velocities below threshold conditions, and short flow durations will tend to limit the ability to develop equilibrium-scour depths in the field that are comparable to those of the laboratory. This is part of the reason why the upper bound of the field data is less than the upper bound of the laboratory data.

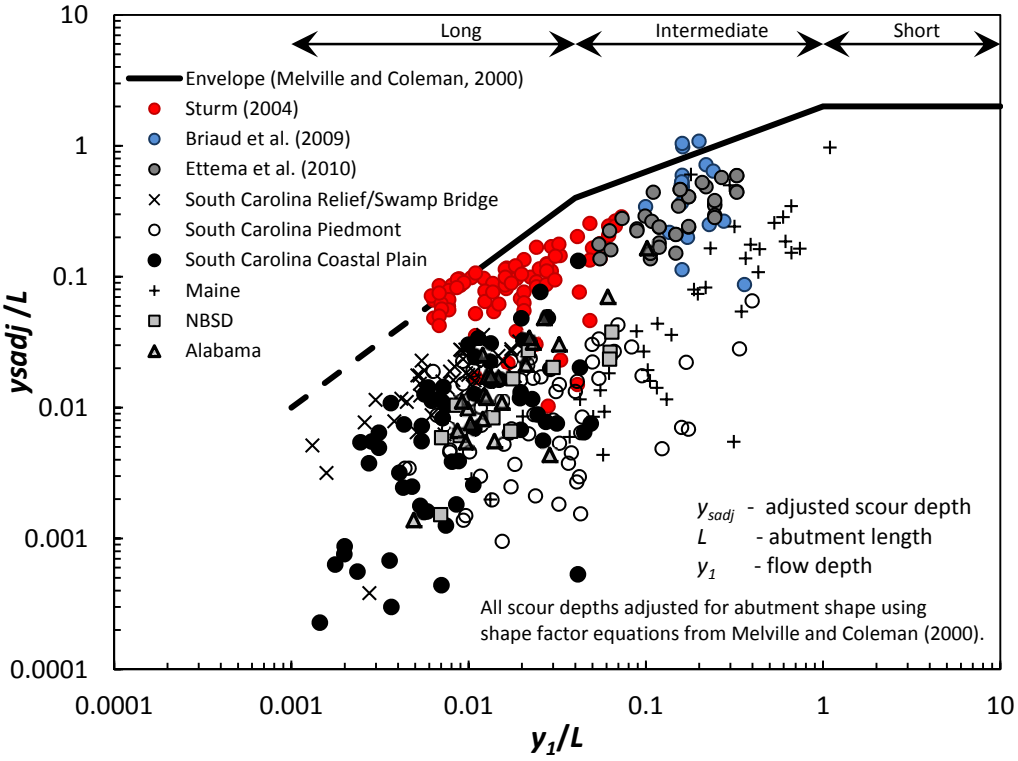

Figure 1-20. Relation of the relative scour depth to relative flow depth for selected laboratory data and the U.S. Geological Survey field data.

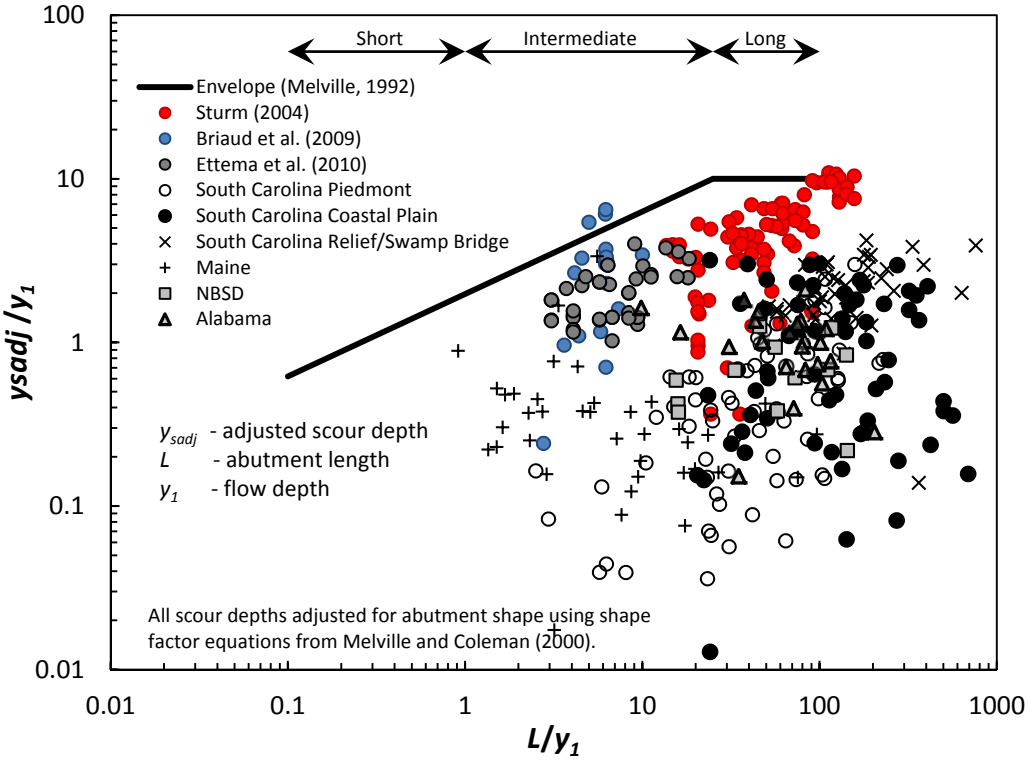

Figure 1-21. Relation of the relative scour depth to relative abutment length for selected laboratory data and the U.S. Geological Survey field data.

1.4.3 Abutment Scour with Respect to the Geometric Contraction Ratio

The geometric contraction ratio (m) is a common dimensionless variable used in bridge hydraulics to evaluate the severity of contraction created by a bridge. The geometric contraction ratio is defined as $m = 1 - b/B$, where B is the flow top width of the upstream approach cross section and b is the flow top width of the bridge opening. The range of m is from 0 to 1, with a value of 0 representing no contraction and a value of 1 representing a complete blockage of flow. Because abutment scour is considered a function of the contraction, it would be reasonable to anticipate that larger abutment-scour depths be associated with larger values of m. Figure 1-22 shows the relation of the abutment-scour field data to the geometric contraction ratio, indicating that the larger abutment-scour depths are associated with larger contraction ratios. For m ranging from 0 to approximately 0.6, scour depths are approximately 5 ft or less, which are depths that will likely be inconsequential for most bridges. However, beyond a value of 0.6, the upper bound of abutment scour sharply increases to values approximately 3 to 5 times the magnitude of the scour depths for values of m less than 0.6. The upper bound of abutment-scour depth associated with values of m greater than 0.6 is sufficiently large (approximately 15 to 25 ft) to have potential adverse effects at a bridge. This trend indicates that the largest potential for abutment scour will be associated with bridges having values of m approximately 0.6 or greater; therefore, laboratory investigations of abutment scour need to encompass m values in this range.

Based on the data trends shown in figure 1-22, Benedict (2003) developed abutment-scour envelope curves for the Piedmont and Coastal Plain of South Carolina (figure 1-22). The Maine, Alabama, and NBSD data fall within these envelope curves with only one exception, indicating that the general trend of the curves is reasonable. While the envelope curves shown in figure 1-22 must be limited to sites with similar conditions to those that form the curves, the large number of data that fall within the curves indicates that the envelope curves potentially could serve as useful supplementary tools in assisting in the evaluation of abutment scour.

In order to compare the upper-bound trends of scour for the field and laboratory data with respect to m, the relation of the dimensionless scour depth (y_{sadj}/y_1) and the geometric contraction ratio for the laboratory and field data are presented in figure 1-23. The increase in the upper bound of scour as m increases is evident in the laboratory and field data. This trend is most prominent in

the Sturm (2004) data. The Sturm (2004) data are associated with rigid abutments models and relatively long abutments that have potential to produce large scour depths. The Ettema et al. (2010) data, associated with erodible abutment/embankment models, produce lower values of relative scour than the rigid models of the Sturm (2004) data. Beyond an m of approximately 0.4, the upper bound of the Ettema et al. (2010) data decreases. These data are associated with bankline or protruding abutments where the approach flow depth in the main channel was used to determine the relative scour depth. The flow depths in the main channel will produce smaller relative scour values in comparison with those based on the smaller floodplain flow depths. This also is the case for the one bankline abutment in the Briaud et al. (2009) data at an m of 0.67. The relative-scour depths for the Briaud et al. (2009) data are lower than for the Sturm (2004) data, and can be attributed, in part, to the cohesive sediments. The upper bound of the field data is distinctly lower than that of the laboratory data and can be attributed, in part, to non-uniform sediments, short flow durations, and approach flow velocities below critical-velocity conditions (see report section 1.2.5). The largest values for m in the Briaud et al. (2009) and Ettema et al. (2010) data are 0.75 and 0.76, respectively, with the majority of the data being associated with m values of 0.7 or less. In contrast, approximately 73 percent of the field data have values of m exceeding 0.7, with a maximum value of 0.98, and this is where the largest relative scour depths occur. The laboratory data do not encompass the larger values of m associated with the field data, indicating a potential need for laboratory investigations that model the more extreme contractions present in the field. As noted previously, the percentile plot of the unit discharge ratio (q_2/q_1; figure 1-15), a measure of the flow contraction, highlights this observations as well.

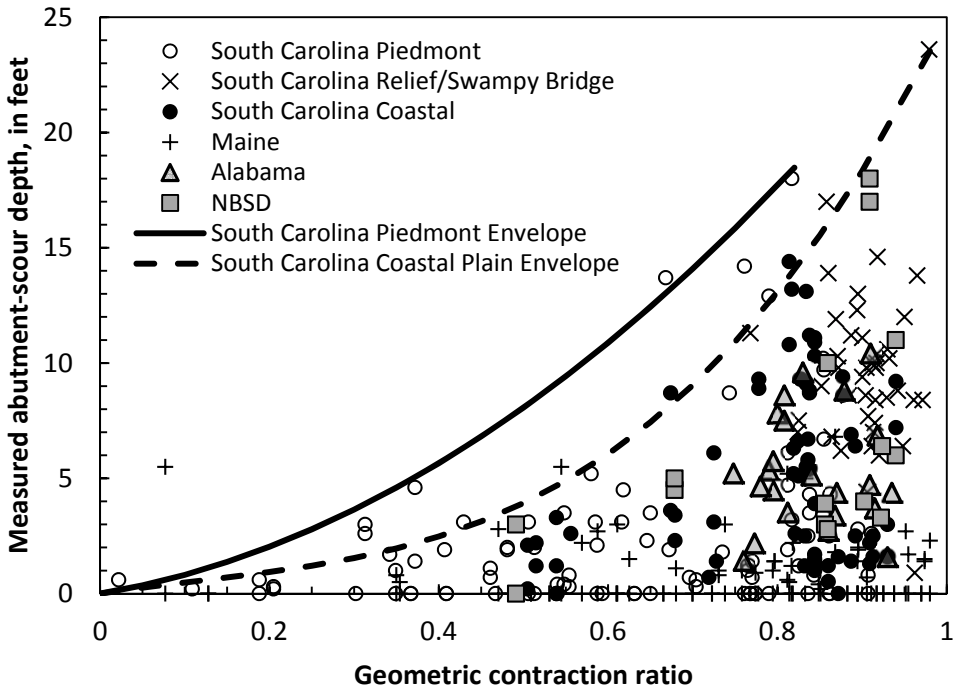

Figure 1-22. Relation of abutment-scour depth to the geometric contraction ratio for selected field measurements in comparison to the South Carolina abutment-scour envelope curves.

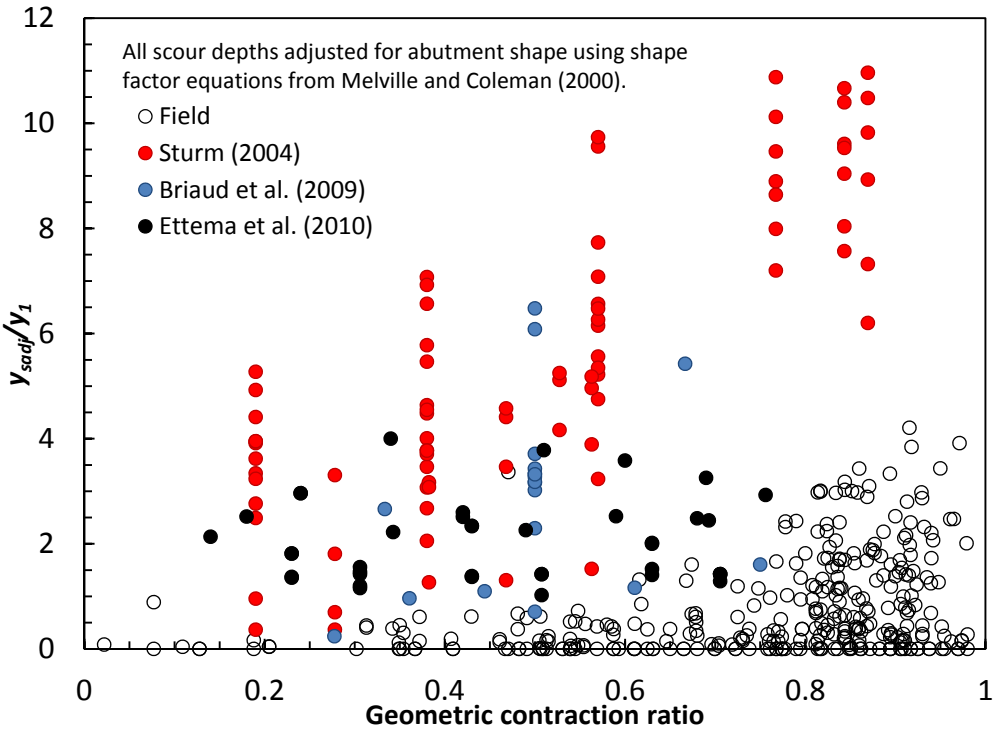

Figure 1-23. Relation of relative scour depth (y_{sadj}/y_1) to the geometric contraction ratio for selected laboratory and field measurements.

1.4.4 Unit Discharge Ratio

The NCHRP 24-20 prediction method uses the ratio of the constricted unit discharge at the bridge abutment (q_2) to the unconstricted unit discharge at the approach section (q_1). This dimensionless variable, q_2/q_1, is a measure of the flow contraction created by the abutment, and as m increases it would be expected that the value of q_2/q_1 also would increase. Figure 1-24 shows the relation of q_2/q_1 for the field and laboratory data to m, indicating that q_2/q_1 increases as the geometric contraction ratio increases. Over the range of m from 0 to 0.7, the approximate range of the NCHRP 24-20 data, the field and laboratory data show similar patterns with an approximate linear increase in q_2/q_1 with increasing m. As m exceeds 0.7, the rate of increase in q_2/q_1 begins to increase and the field data indicate a sharp increase beyond an m of approximately 0.85, the approximate upper limit of the Sturm (2004) data. The patterns in figure 1-24 indicate that the Sturm (2004), Briaud et al. (2009), and Ettema et al. (2010) data are capturing the range and trend of q_2/q_1, associated with the field data, for values of m less than approximately 0.75. However, for values of m greater than 0.75, where scour potential is greatest (figure 1-23), the laboratory data are limited, indicating a need for laboratory data with values of m closer to 1 to ensure that the worst-case conditions for abutment scour can be modeled. Figure 1-25 shows the same data as that shown in figure 1-24, with an approximate upper-bound curve for q_2/q_1 drawn through the laboratory data and extended with guidance from the field data. This curve provides some perspective on the upper-bound values of q_2/q_1 with respect to m, providing some guidance for future laboratory investigations and to practitioners applying scour prediction methods that employ q_2/q_1.

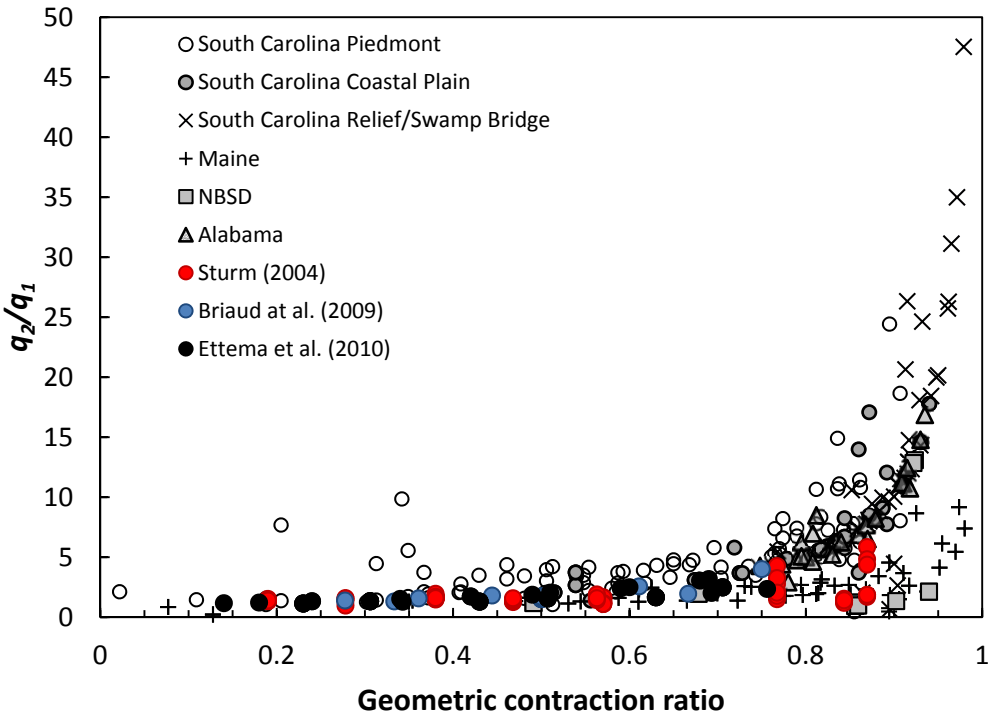

Figure 1-24. Relation of the unit discharge ratio (q_2/q_1) to the geometric contraction ratio for selected laboratory and field measurements of abutment scour.

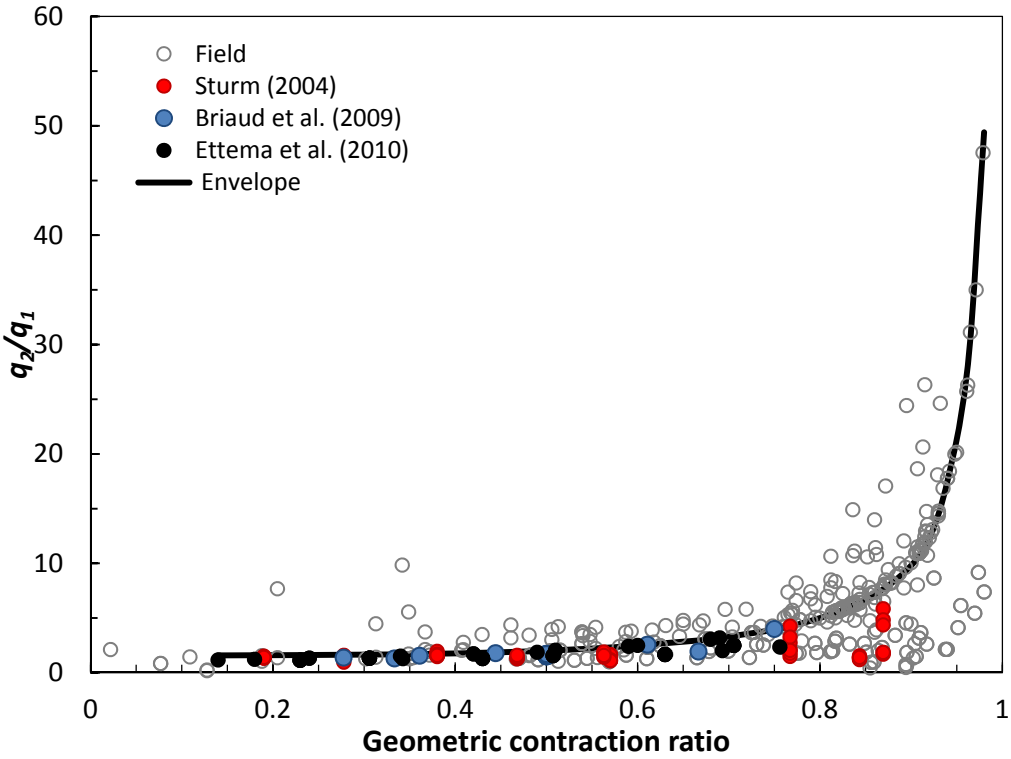

Figure 1-25. Relation of the unit discharge ratio (q_2/q_1) to the geometric contraction ratio for selected laboratory and field measurements of abutment scour.

CHAPTER 2

APPLICATION PROCEDURE FOR THE NCHRP 24-20 PREDICTION METHOD

2.1 Introduction

The NCHRP 24-20 report provides general guidance for applying the abutment-scour prediction method at a selected bridge site. Hydraulic Engineering Circular No. 18 (Arneson et al. 2012; for remainder of this section will be noted as HEC-18 without the reference) provides additional application guidance. These two sources were used to develop the procedure for applying the NCHRP 24-20 method to the laboratory and USGS field data. Additionally, Dr. Robert Ettema, the Principal Investigator for NCHRP 24-20, and Mr. Bart Bergendahl of the Federal Highway Administration were consulted in the development of the this procedure and were provided opportunity for review and comment. A brief description of the application steps follows.

2.2 Summary of NCHRP 24-20 Scour Prediction Method

The NCHRP Project 24-20 was an extensive laboratory investigation of abutment scour that produced new insight into the mechanics of abutment scour and led to a method for estimating abutment-scour depth in compound channels. The method encompasses a range of abutment-scour conditions including (A) abutments set near or in the main channel, (B) abutments on the floodplain set well back from the main channel, (C) abutments with breached embankments and exposed abutment column, and (D) abutment-scour associated with geotechnical failure at a location at some distance from the end of the abutment. Scour conditions C and D were not evaluated in this investigation. A unique feature about the NCHRP 24-20 laboratory investigation was the use of abutment models having various combinations of erodible and non-erodible floodplains, embankments, and abutment substructures. Such characteristics are thought to better represent the range of conditions frequently found in the field, where embankment and abutment substructures can be susceptible to scour and possible failure. Previous investigations of abutment scour typically used non-erodible, rigid abutment models

having an abutment substructure consisting of a vertical wall at the abutment toe extending into the bed, similar to a sheet-pile skirt. These rigid abutment models with the vertical wall substructures tend to strengthen flow turbulence near the abutment, increasing the potential for scour. In contrast, the NCHRP 24-20 abutment models used a variety of erodible and non-erodible embankment and abutment substructures that primarily excluded the vertical wall substructure associated with many previous laboratory investigations. These models better represent embankments and abutment substructures for many field sites and will tend to reduce the potential for scour in contrast to the rigid abutment models. Additionally, the erodible embankments/abutments will provide some measure of hydraulic relief in the cases where the embankment/abutment breaches under high-flow conditions, further reducing the potential for scour. For Scour Condition A, where the abutment is set near the main channel, the NCHRP 24-20 laboratory tests consisted of non-erodible (fixed) floodplains and abutments, as well as erodible floodplains and abutments, with the embankment and abutment armored with riprap. For the fixed conditions, scour was forced to occur in the main channel under live-bed scour conditions and produced larger scour depths than the erodible conditions produced. Because of the complexity of flow and scour patterns for Scour Condition A, NCHRP 24-20 developed scour prediction methods based on data from the fixed floodplain and abutment model, providing a more conservative estimate of abutment scour. For Scour Condition B, where the abutment is well set back from the main channel, the laboratory model used in developing the design procedure primarily consisted of an erodible floodplain and abutment, with the embankment and abutment armored with rip rap. Under these conditions, the abutment and embankment could erode, providing some hydraulic relief that tended to reduce abutment scour. Additionally, the abutment substructure for these models typically did not consist of a rigid wall below the bed, further reducing the potential for scour.

The laboratory models used to develop the NCHRP 24-20 method are distinctly different from the models used to develop other abutment-scour prediction equations, such as the Froehlich (1989) equation and the NCHRP 24-15(2) method (Briaud et al. 2009) that used rigid abutments/embankments. As such, it is likely that the NCHRP 24-20 method will produce smaller values of predicted scour than prediction equations developed from rigid abutment models. This will most likely be evident for the case of Scour Condition B, where erodible embankments were used, but less so for Scour Condition A where fixed embankments/abutments

were used. Additionally, when the NCHRP 24-20 method is applied to laboratory or field data that is more representative of a rigid abutment model, it is likely that the NCHRP 24-20 will produce some underprediction of scour for such conditions. Again, this will likely be more evident for Scour Condition B than for A. With the exception of the NCHRP 24-20 data, the majority of laboratory data used in the current (2015) investigation [NCHRP Project 24-20(2)] represents scour at non-erodible rigid abutments, and therefore, application of the NCHRP 24-20 method to these data will likely produce some underprediction. Additionally, the field data are thought to largely represent abutment scour where the road embankment and abutment substructures did not appreciably erode. While not identical, this field condition is similar to a rigid laboratory model, and therefore, application of the NCHRP 24-20 method to these field data may produce some underprediction. These differing scour conditions associated with the NCHRP 24-20 prediction method and the laboratory and field data should be kept in mind when reviewing results of this investigation.

When using the NCHRP 24-20 method it is important to apply the procedure to the correct scour condition. For abutments with Scour Conditions A and B, the NCHRP 24-20 abutment-scour method assumes that abutment scour is a function of contraction scour at a long contraction as represented by the following equation:

$$Y_{MAX} = \alpha Y_C \qquad (2\text{-}1)$$

where

Y_{MAX} is the maximum flow depth in the abutment scour area, in feet (figure 2-1);

Y_C is the mean flow depth of the contraction scour associated with a long contraction, in feet (figure 2-1); and

α is an amplification factor that accounts for additional scour (beyond the contraction scour) at the abutment associated with the non-uniform flow distribution and macro-turbulence structures in the vicinity of the abutment.

The conceptual model represented in equation 2-1 has been used by other researchers (Laursen, 1963; Chang and Davis, 1998 and 1999; Sturm, 2004); however, Ettema et al. (2010) developed

a unique application of the model by using erodible abutments/embankments with non-rigid abutment substructures. Having determined Y_{MAX} with equation 2-1, the depth of scour at the abutment, y_s, can be estimated by equation 2-2.

$$y_s = Y_{MAX} - y_1 \tag{2-2}$$

where

y_s is the abutment-scour depth, in feet, and

y_1 is the upstream flow depth prior to scour, in feet (figure 2-1),

with Y_{MAX} previously defined. Figure 2-1 provides a general schematic of selected variables in equations 2-1 and 2-2.

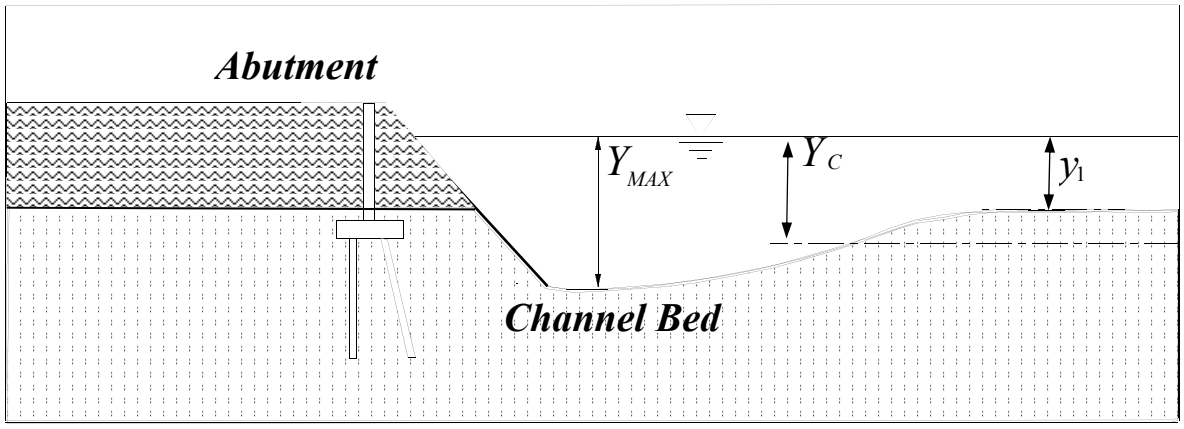

Figure 2-1. Conceptual model of abutment scour where y_1 is the flow depth prior to scour, Y_C is the mean flow depth of the contraction scour, and Y_{MAX} is the maximum flow depth in the abutment-scour region (modified from Ettema et al. 2010).

The conceptual model for the NCHRP 24-20 method, as presented in equations 2-1 and 2-2, can be applied to cohesive and non-cohesive sediments by incorporating an appropriate equation for predicting contraction scour, Y_C, for those respective types of sediments. However, the current formulation of the NCHRP 24-20 method uses the live-bed and clear-water contraction-scour equations developed by Laursen (1960; 1963, respectively) that were originally developed for non-cohesive sediments. The Laursen (1960; 1963) equations are shown in equations 2-3 and 2-4, respectively. (Note: Equation 2-3 is a simplified version of the original equation.)

$$Y_c = y_1 \left(\frac{q_2}{q_1}\right)^{6/7} \quad (2\text{-}3)$$

$$Y_c = \left(\frac{q_2}{K_u D50^{1/3}}\right)^{6/7} \quad (2\text{-}4)$$

where

q_1 is the unconstricted unit discharge at the approach section, in square feet per second ; (Note: The unit discharge, also called unit flow, represents the unit width flow at the approach floodplain (q_{f1}) or the main channel (q_{mc1}) as shown in figure 2-2, and can be estimated in several ways: (1) by dividing the flow through the selected section by the corresponding flow top width, or (2) multiplying the flow depth and velocity at a given location in the cross section.);

q_2 is the contracted unit discharge at the bridge abutment (figure 2-2) accounting for non-uniform flow distribution at the abutment, in square feet per second;

K_u is a units conversion factor equal to 11.17 for English units;

D50 is the median particle size of the bed sediment, in feet; and

other variables are as previously defined.

Equation 2-4 is intended for non-cohesive sediments; therefore, HEC-18 recommends limiting the *D50* to a value of 0.000656 ft [0.2 millimeter (mm)].

For setback abutments located on the floodplain, the unit discharges q_1 and q_2 will generally reflect flows on the upstream approach floodplain (q_{f1}) and the associated overbank at the bridge (q_{f2}), respectively, as shown in figure 2-2. For abutments located at the channel banks or protruding into the channel, the unit discharges q_1 and q_2 will generally reflect flows in the upstream approach main channel (q_{mc1}) and the main channel at the bridge (q_{mc2}), respectively (figure 2-2). Guidance for estimating q_1 and q_2 is provided in NCHRP 24-20 and HEC-18 and is reviewed later. Upon obtaining an estimate of Y_C, the maximum flow depth in the abutment scour area, Y_{MAX}, can be estimated by applying the amplification factor, α, as shown in equation 2-1.

The amplification factor, α, accounts for the additional scour at the abutment, beyond the average contraction scour, that is associated with the non-uniform flow distribution and macro-turbulence structures in the vicinity of the abutment. It is assumed that abutment scour will always exceed contraction scour, and therefore, the amplification factor always has a value greater than 1. The amplification factor is a function of the abutment shape (spill through or wing wall), the configuration of the embankment length (L, in feet; figure 1-5 and 2-2) with respect to the floodplain width (B_f, in ft; figure 1-5 and 2-2) as defined by the ratio L/B_f, and the degree of flow contraction created by the bridge as defined by the unit discharge ratio, q_2/q_1. The graphs that display the relation of the amplification factor with respect to these variables are shown in figures 2-3 through 2-6. For design purposes, HEC-18 recommends that only the solid curves in these figures be used, and this was the approach implemented in this investigation.

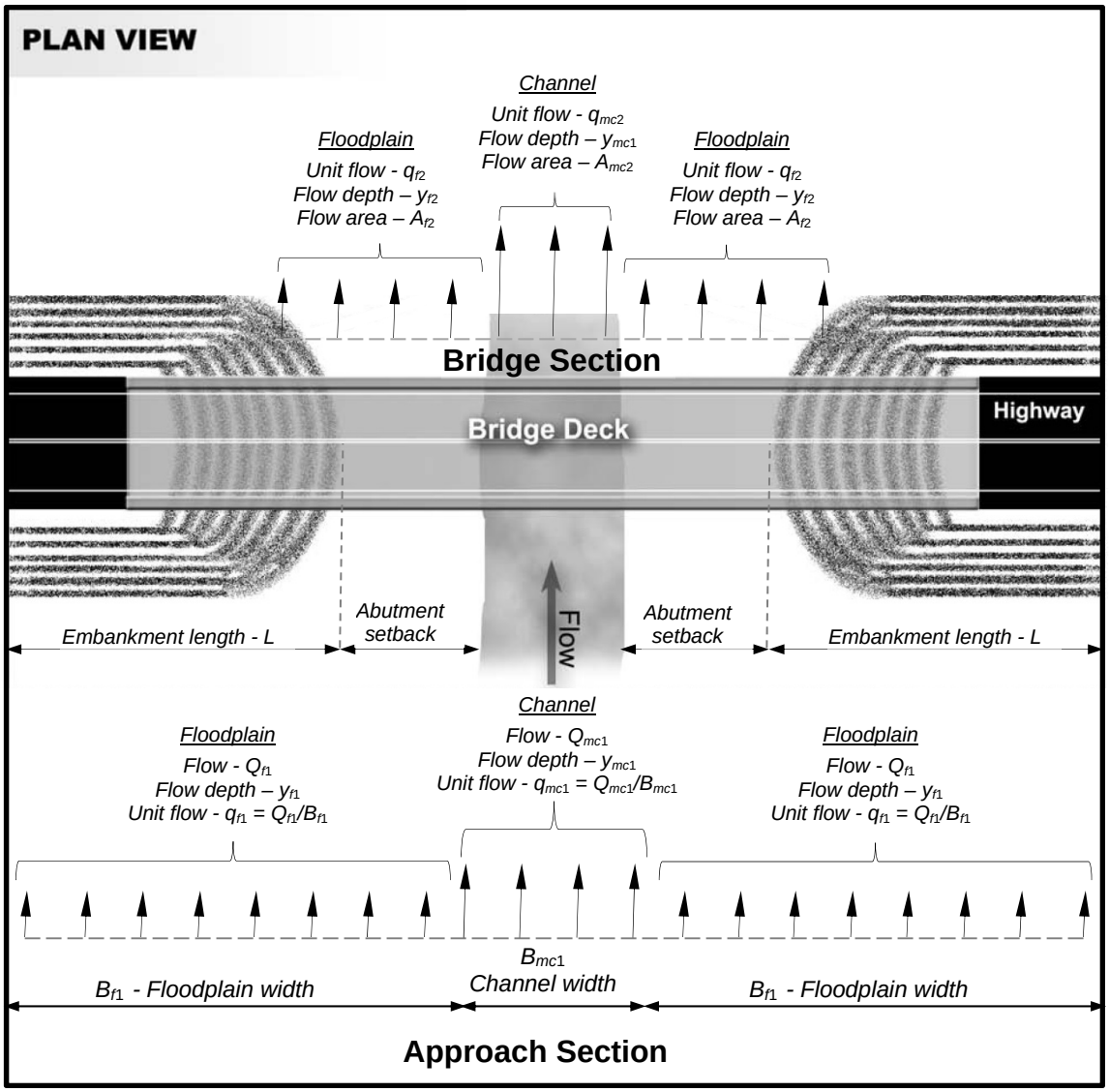

Figure 2-2. Schematic showing selected hydraulic variables and the regions they represent at the approach and bridge cross sections.

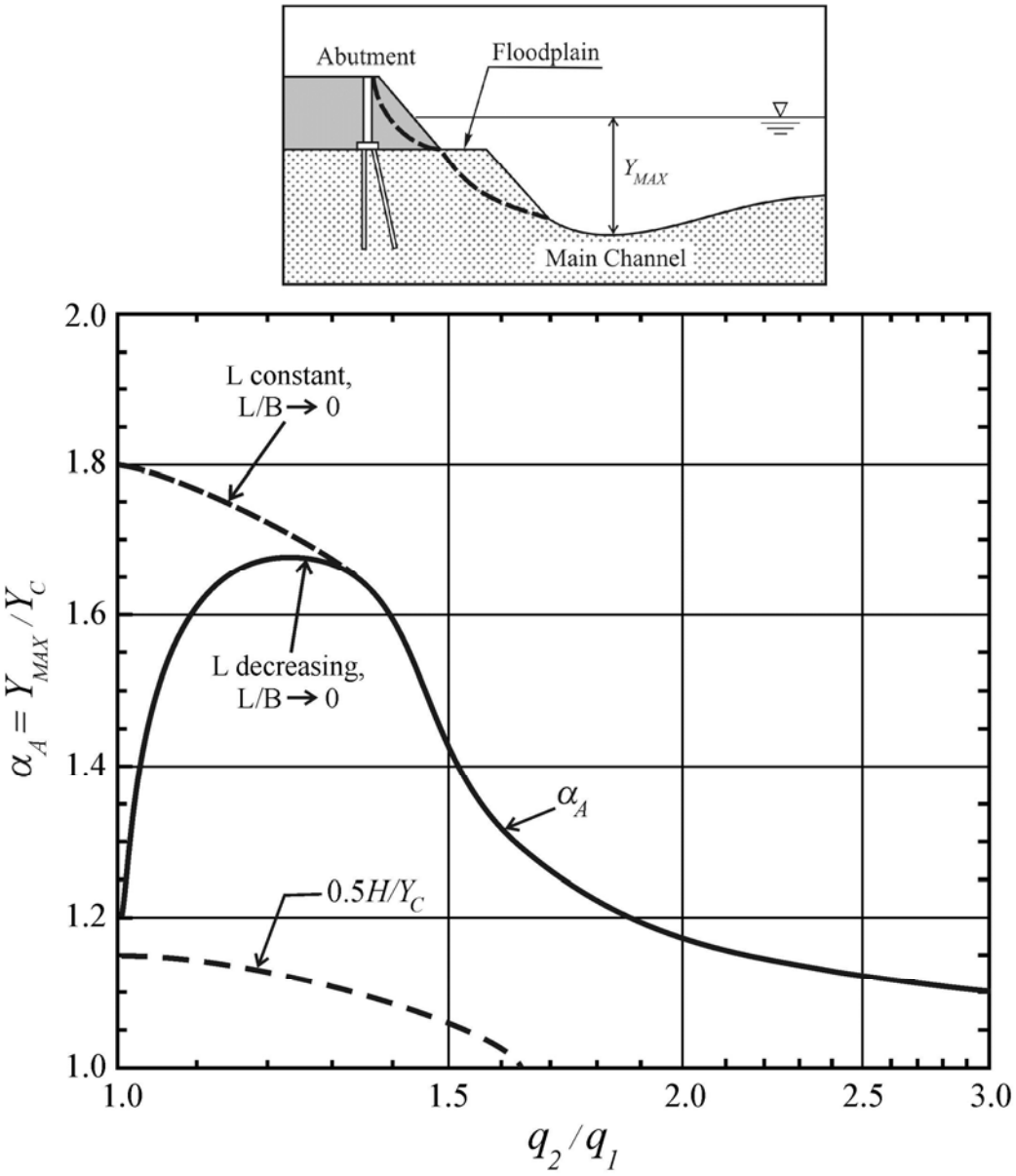

Figure 2-3. Design curve for scour-amplification factor, α, for spill-through abutments subject to Scour Condition A ($L/B_f \geq 0.75$) (from Ettema et al. 2010).

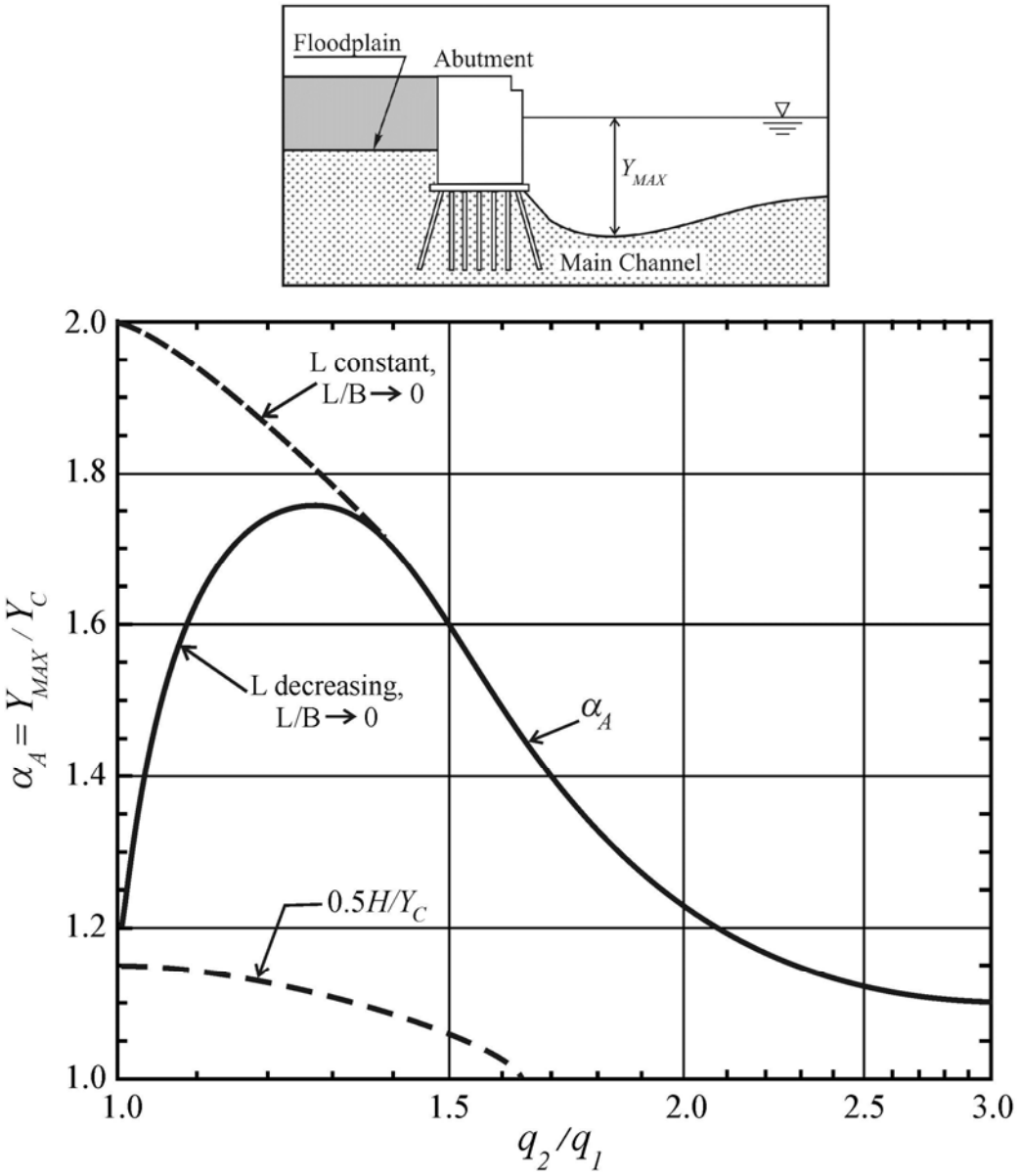

Figure 2-4. Design curve for scour-amplification factor, α, for wing-wall abutments subject to Scour Condition A ($L/B_f \geq 0.75$) (from Ettema et al. 2010).

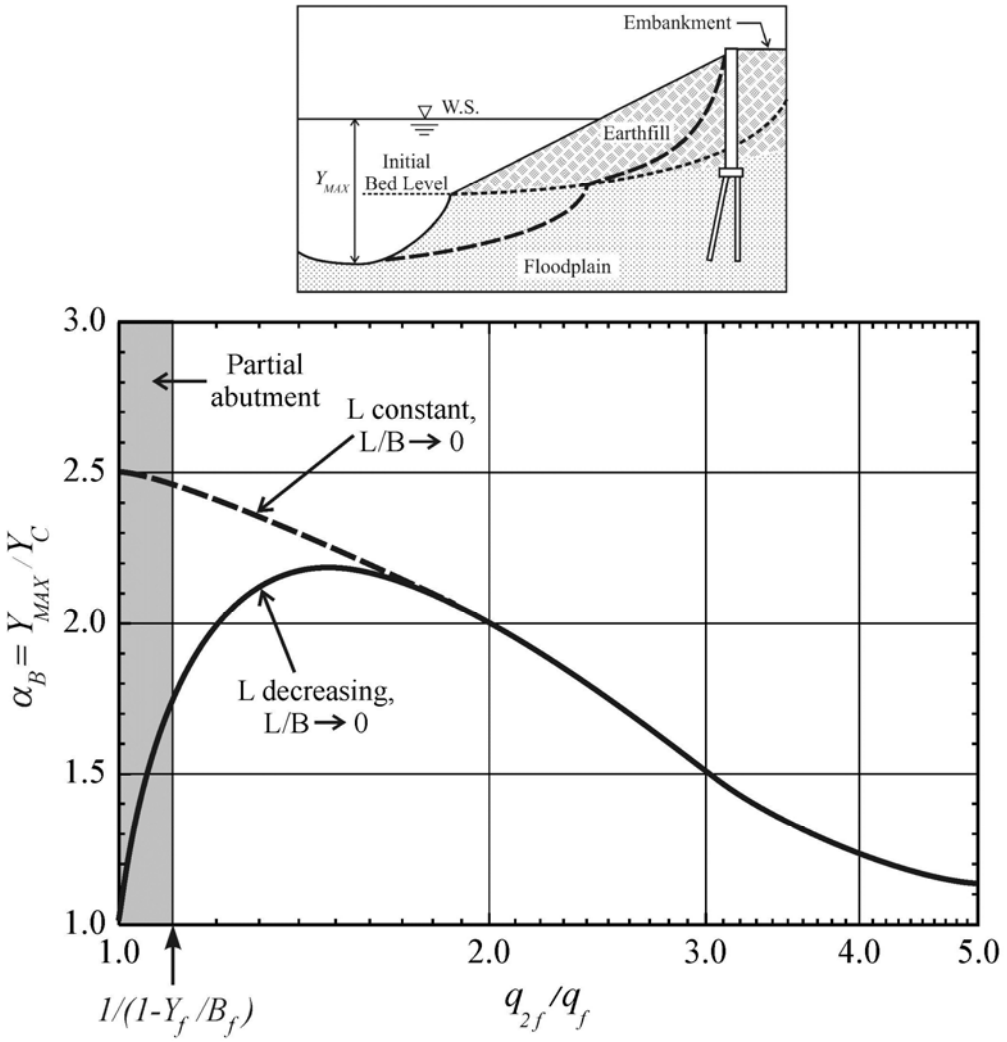

Figure 2-5. Design curve for scour-amplification factor, α, for spill-through abutments subject to Scour Condition B ($L/B_f < 0.75$) (from Ettema et al. 2010).

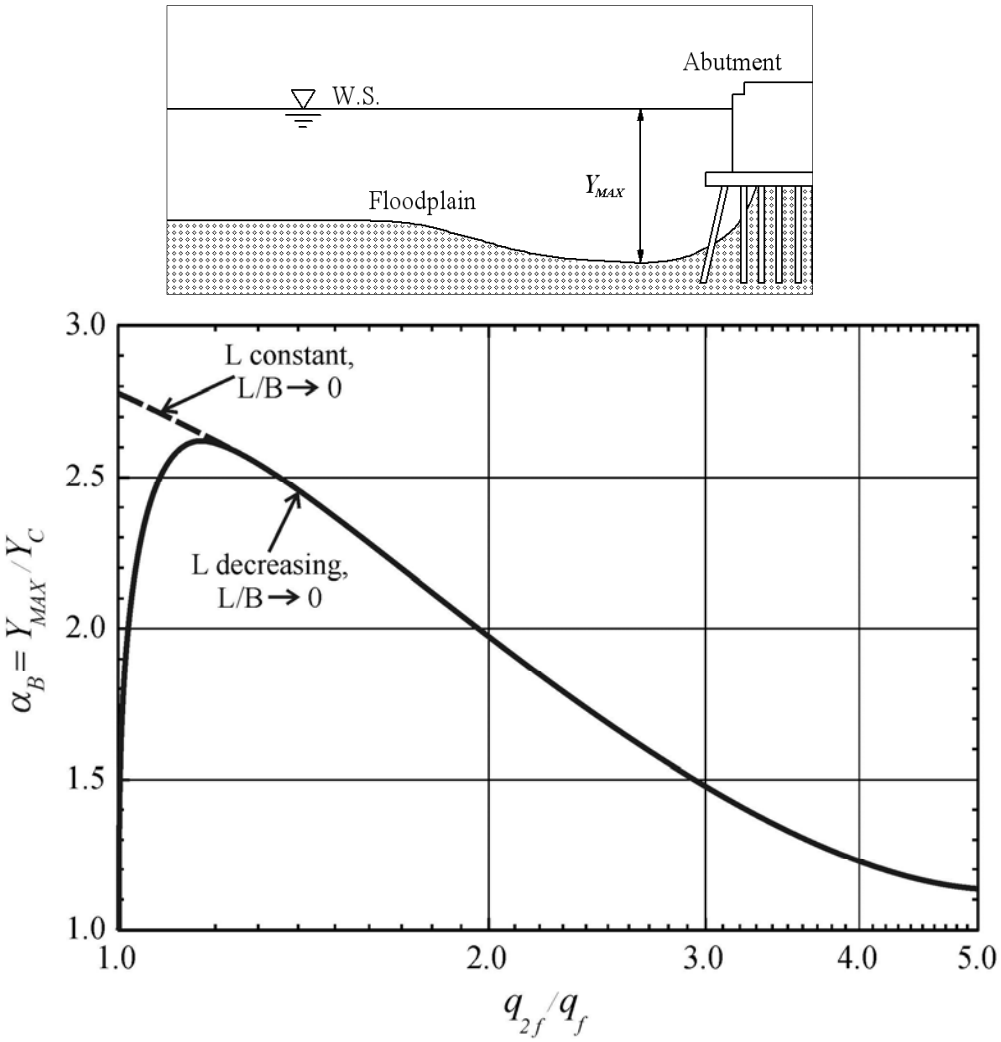

Figure 2-6. Design curve for scour-amplification factor, α, for wing-wall abutments subject to Scour Condition B ($L/B_f < 0.75$) (from Ettema et al. 2010).

2.3 General Procedure for Application of NCHRP 24-20 to the Laboratory and the USGS Field Data

Field conditions associated with the riverine environment are typically more complex than those of the laboratory. Channel geometry, surface roughness, sediment characteristics, and flow distributions can be highly variable in the field in contrast to the controlled and idealized environment of the laboratory. The disparity between laboratory and field conditions can present challenges for selecting appropriate field values for application to laboratory-derived scour prediction methods. To assist the practitioner, NCHRP 24-20 and HEC-18 present procedures for applying the NCHRP 24-20 method to field sites. The procedures described in HEC-18 were given preference in this investigation, and additional details can be found in HEC-18. A brief review of the steps used in applying the NCHRP 24-20 method to the USGS field data follows. These same general procedures were used in the application of the NCHRP 24-20 method to the laboratory data.

1. **Compile laboratory and USGS field data**

   The previously described laboratory and USGS field data (tables 1-1 and 1-3) were reviewed, and data pertinent for application to the NCHRP 24-20 method were entered into a spreadsheet. These data included selected hydraulic, sediment, and bridge-geometry characteristics as described in table 2-1.

2. **Determine the Scour Condition (A or B) for the abutment of interest**

   The following criteria were used to determine the Scour Condition (A or B) for the abutment of interest:

   - Scour condition A was assumed when

     -$L/B_f \geq 0.75$;

   - Scour condition B was assumed when

     -$L/B_f < 0.75$.

Variables are as previously defined.

Table 2-1. Description of selected field data used in the application of the NCHRP 24-20 abutment-scour prediction method.

<table>
<tr><td colspan="2">Hydraulic characteristics at upstream approach cross section</td></tr>
<tr><td>Left floodplain</td><td rowspan="3">- Flow
- Flow area
- Average flow depth
- Top width</td></tr>
<tr><td>Channel</td></tr>
<tr><td>Right floodplain</td></tr>
<tr><td colspan="2">Hydraulics characteristics at bridge cross section</td></tr>
<tr><td>Left floodplain</td><td rowspan="3">- Flow
- Flow area
- Average flow depth
- Channel top width or width of the floodplain</td></tr>
<tr><td>Channel</td></tr>
<tr><td>Right floodplain</td></tr>
<tr><td colspan="2">Abutment</td></tr>
<tr><td>Left</td><td rowspan="2">- Measured scour depth
- Abutment type (spill through or wing wall)
- Embankment length blocking flow
- Blocked flow
- Blocked area
- Blocked flow depth (average)
- Blocked flow velocity (average)
- Embankment skew
- Abutment toe to top-of-bank set back distance
- Median grain size of sediment
- General classification of sediment at the abutments as cohesive or non-cohesive</td></tr>
<tr><td>Right</td></tr>
</table>

3. Determine the unconstricted unit discharge in the upstream approach cross section

When available, a two-dimensional flow model can be used to estimate the unconstricted unit discharge, q_1, at the approach cross section. However, for unconstricted cross sections, such as an upstream approach cross section, a one-dimensional flow model can provide reasonable estimates of this unit discharge. When a one-dimensional flow model is used at a bridge site, NCHRP 24-20 and HEC-18 recommend the following procedure for estimating the unconstricted unit discharge. In the current investigation, the bridge sites associated with the field data had only one-dimensional flow models; therefore, this was the method used. This approach also was used with the laboratory data.

- **Approach floodplain (left or right; see figure 2-2):**

$$q_{f1} = Q_{f1}/B_{f1} \quad (2\text{-}5)$$

where

q_{f1} is the unit discharge on the left or right approach floodplain, in square feet per second;

Q_{f1} is the flow in the left or right approach floodplain, in cubic feet per second; and

B_{f1} is the top width of the left or right approach floodplain, in feet.

- **Approach main channel (see figure 2-2):**

$$q_{mc1} = Q_{mc1}/B_{mc1} \quad (2\text{-}6)$$

where

q_{mc1} is the unit discharge in the approach main channel, in square feet per second;

Q_{mc1} is the flow in the approach main channel, in cubic feet per second; and

B_{mc1} is the top width of the approach main channel, in feet.

4. Determine the unit discharge in the bridge cross section

Flow distributions at a contracted cross section, such as a bridge, are more complex than flow distributions associated with an unconstricted cross section. NCHRP 24-20 and

HEC-18 recommend, when possible, the use of a two-dimensional flow model to estimate contracted unit discharge at an abutment. A one-dimensional flow model does not capture well the increased velocities near the abutment of a contracted bridge opening; therefore, special consideration must be given to estimating the unit discharge at a bridge when a one-dimensional flow model is used. To assure conservative estimates of unit discharge at a bridge abutment when using a one-dimensional flow model, HEC-18 recommends use of the setback ratio (SBR) method as presented in HEC-23 (Lagasse et al. 2009) for estimating flow velocities at bridge abutments that, in turn, can be used to estimate the unit discharge. The SBR is the ratio of the abutment setback length (distance from the abutment toe to the top of bank at the main channel; figures 1-5 and 2-2), for the respective abutment, to the average flow depth in the main channel (y_{mc2}) at the bridge. Lagasse et al. (2006) investigated the SBR method by using two-dimensional flow models of hypothetical abutments and concluded that the SBR method is well suited for determining velocity at an abutment if the estimated velocity does not exceed the maximum velocity in the main channel. The SBR method assumes that for relatively short bridges with small abutment setbacks (SBR $\leq$ 5) the average velocity through the full bridge (overbanks and channel) will provide a reasonable estimate of the increased velocities at an abutment as well as velocities in the main channel. For relatively long bridges with abutments set back some distance from the main-channel banks (SBR > 5), the SBR method assumes that all of the flow on the left or right upstream approach floodplain will pass through the corresponding overbank flow area at the bridge, providing estimates of the increased velocity at the abutment. Because the bridge sites associated with the USGS field data only have one-dimensional flow models, the SBR method was used in the current investigation. A brief description of the steps used to apply the SBR method to the USGS field sites follows. Additional details are presented in HEC-18.

The SBR was calculated for the left and right abutments at a site of interest by dividing the setback length (distance from the abutment toe to the top of bank at the main channel; figures 1-5 and 2-2), for the respective abutment, by the average flow depth in the main channel at the bridge. Based on the SBR values, the following procedures were used to

estimate the flow velocity and unit discharge in the overbanks and main channel at the bridge.

- **SBR ≤ 5 at the left and right abutments**

  A general schematic for the SBR ≤ 5 is shown in figure 2-7. The left and right abutment configurations can have several combinations for this case, including (1) the abutment is located near the channel bank and the setback length is relatively small, as shown in figure 2-7; (2) the abutment is located at the main-channel bank; or (3) the abutment protrudes into the channel. In all of these abutment combinations, it was assumed that the average flow velocity through the bridge opening (V_{Br}; figure 2-7) provides a reasonable estimate of the flow velocity in the left and right bridge overbanks as well as the main channel. When the abutment is located at the channel bank or protrudes into the channel, no flow is in the bridge overbank, and the overbank flow velocity and flow depth were set to zero. For the various abutment configurations described above, the unit discharge for the left and right bridge overbank and main channel were estimated with the following equations:

  $$q_{f2} = V_{Br} y_{f2} \quad (2\text{-}7)$$

  $$q_{mc2} = V_{Br} y_{mc2} \quad (2\text{-}8)$$

  where

  q_{f2} and q_{mc2} are the unit discharges in the left or right overbank and main channel at the bridge, respectively, in square feet per second;

  y_{f2} and y_{mc2} are the average flow depths in the left or right overbank and main channel at the bridge, respectively, in feet; and

  V_{Br} is the average flow velocity through the bridge opening (overbanks and main channel; figure 2-7), in feet per second.

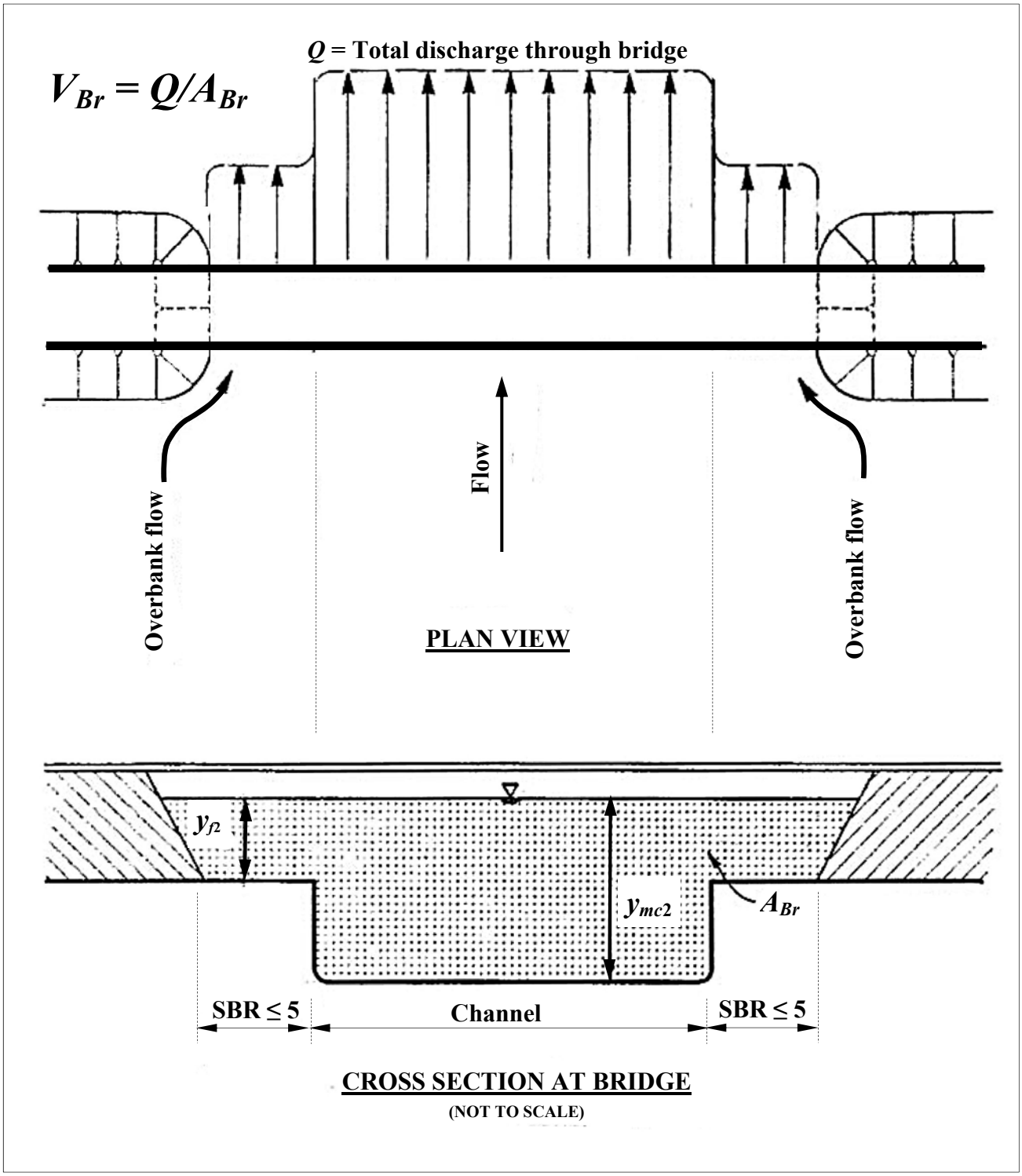

Figure 2-7. General schematic for setback ratio ≤ 5 (modified from Arneson et al., 2012).

Most of the Maine and NBSD data are represented by the case where both the left and right abutments are at the channel bank or protrude into the channel so that there is neither a left or right overbank at the bridge. For this case, the average flow velocity in the bridge, V_{Br}, was used in equation 2-8 to determine q_{mc2}. Additionally, for this case, the approach unit discharge determined by equation 2-6 was used to represent the unit discharge, q_{mc1}, in the approach channel. In some cases, the channel at the bridge is larger than the approach channel, such that q_{mc2} is smaller than q_{mc1}, and the unit discharge ratio, q_{mc2}/q_{mc1}, is less than a value of 1. This scenario can potentially lead to underprediction of contraction scour and the amplification coefficient, producing underprediction of abutment scour. To address this concern, the unit discharge at the bridge, q_{mc2}, was arbitrarily increased to force the unit discharge ratio, q_{mc2}/q_{mc1}, to have a value of 1.1. There were 10 scour measurements in the USGS database (6 in Maine and 4 in the NBSD) where both abutments were at the channel bank or protruded into the channel, and the unit discharge ratio was less than 1. Tests on these data verified that a unit discharge ratio set to a value of 1.1 eliminated underprediction for all but one measurement. Therefore, this procedure was used for these 10 measurements.

An additional application adjustment was made to 3 measurements in the NBSD data where the bridge length exceeded 350 ft and both abutments were at the channel bank or protruded into the channel. For small bridge lengths, use of the average flow velocity through the bridge is a reasonable value to estimate the flow velocity near the abutment. However, as the bridge length increases, it is probable that this average flow velocity begins to underestimate the larger flow velocity near the abutment. Therefore, to minimize the risk of underestimating the flow velocity at the abutment, a factor of 1.2 was applied to V_{Br} in equation 2-8 for the case where both abutments are at the bank or protrude into the channel and the bridge length equals or exceeds 240 ft. The factor of 1.2 is based on research by Hayes (1996), Briaud et al. (2009), and Ettema et al. (2010) and is described in more detail in the following report section on relief bridges and bridges over swamps. The bridge length of 240 ft is based on field observations

from Benedict (2003) and also is discussed in the report section on relief bridges and bridges over swamps. This adjustment was tested with the 3 NBSD measurements in the NCHRP 24-20 method, and performance at these types of bridges was found to be improved.

- **SBR > 5 at a selected abutment**

A general schematic for the SBR > 5 is shown in figure 2-8. For this case, the abutment of interest is located a considerable distance from the channel banks, and the setback length is relatively large. It was assumed that this abutment functions similar to an abutment in a rectangular channel with all of the flow on the upstream approach floodplain passing through the corresponding overbank at the bridge. The unit discharge for the bridge overbank of interest was estimated with the following equations:

$$q_{f2} = V_{f2}\, y_{f2} \qquad (2\text{-}9)$$

$$V_{f2} = Q_{f1}/A_{f2} \qquad (2\text{-}10)$$

where

V_{f2} is the flow velocity at the left or right overbank of interest at the bridge (figure 2-8), in feet per second;

Q_{f1} is the flow on the left or right approach floodplain corresponding to the left or right overbank of interest at the bridge, in cubic feet per second;

A_{f2} is the flow area at the left or right overbank of interest at the bridge, in square feet; and other variables are as previously defined.

If the estimated overbank flow velocity, V_{f2}, in equation 2-9 exceeds the maximum flow velocity in the main channel at the bridge, then HEC-18 recommends that the main-channel flow velocity should be used in place of V_{f2}. Some of the sites in the USGS field data did not have an estimate of the maximum flow velocity in the main channel; therefore, this recommendation could not be evaluated.

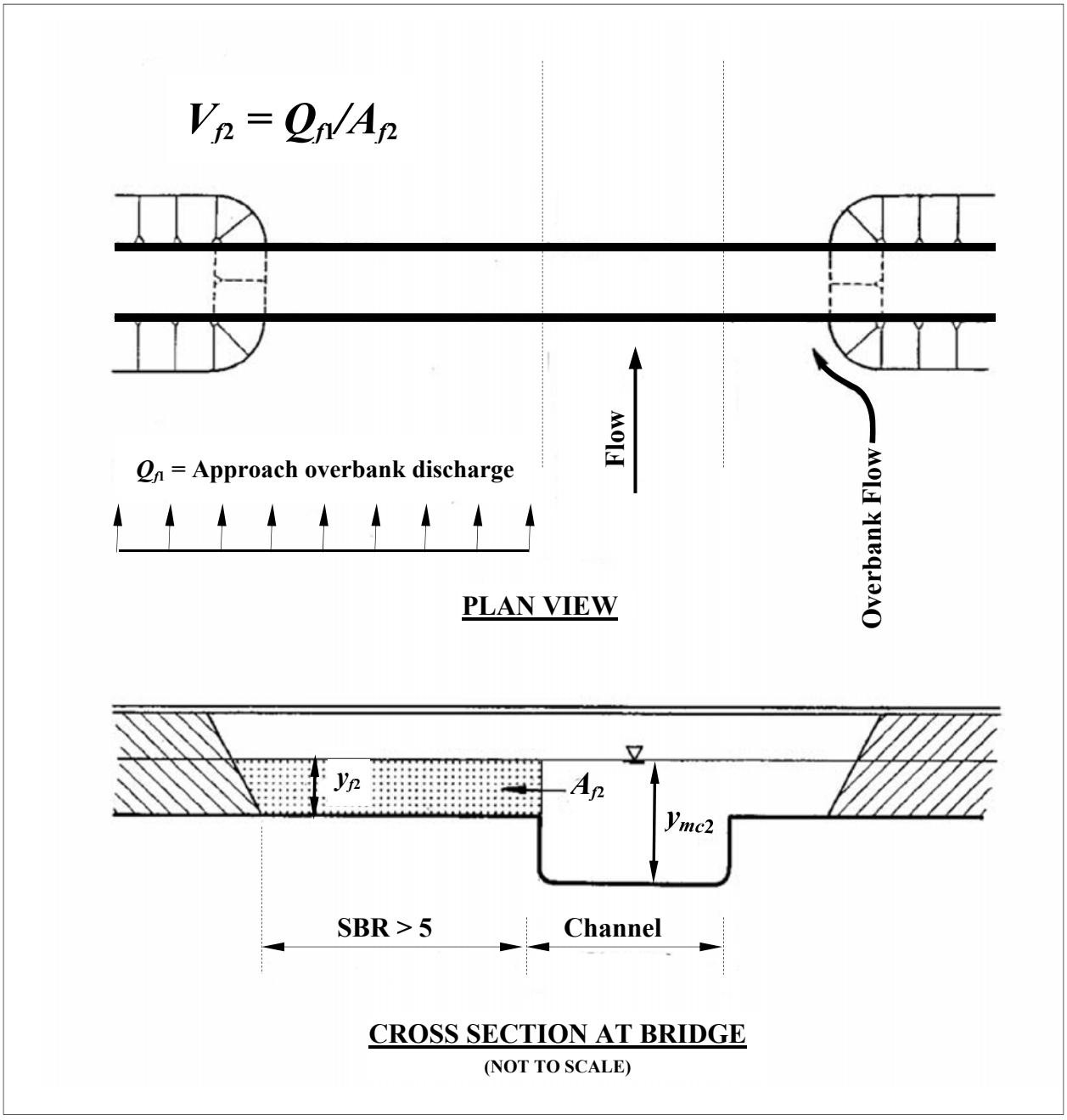

Figure 2-8. General schematic for setback ratio > 5 (modified from Arneson et al., 2012).

SBR ≤ 5 at abutment of interest and SBR > 5 at other abutment

A general schematic for the SBR > 5 is shown in figure 2-9. For this case, the setback length for the abutment of interest is relatively small, but relatively large at the other abutment. The average flow velocity for the abutment with an SBR ≤ 5 is determined by assuming the flow on the upstream approach floodplain associated with the abutment and flow in the approach main channel pass through the corresponding overbank and main-channel flow area at the bridge. The unit discharge for the abutment of interest (SBR ≤ 5) and main channel can be determined with the following equations:

$$q_{f2} = [(Q_{f1}+Q_{mc1})/(A_{f2}+A_{mc2})]\, y_{f2} \qquad (2\text{-}11)$$

$$q_{mc2} = [(Q_{f1}+Q_{mc1})/(A_{f2}+A_{mc2})]y_{mc2} \qquad (2\text{-}12)$$

where

A_{mc2} is the flow area in the main channel at the bridge, in square feet,

with other variables as previously defined.

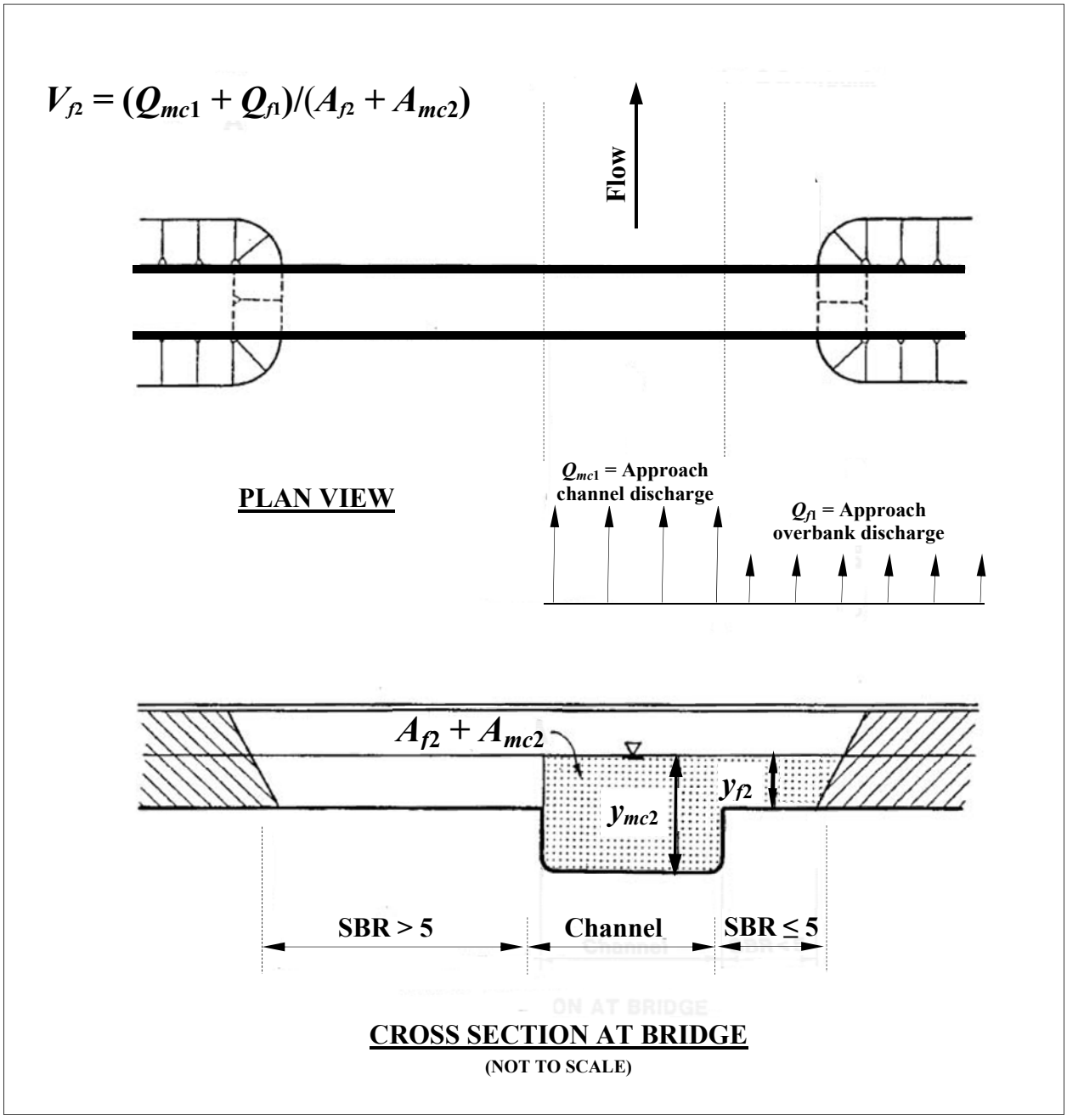

Figure 2-9. General schematic for setback ratio > 5 and ≤ 5 (modified from Arneson et al., 2012).

- **Relief bridge and bridge over a swamp**

  Special consideration must be given for application of the SBR method to a relief bridge on a floodplain or a bridge crossing a swamp with a poorly defined channel. In general, it was assumed that the contracted unit discharge for abutments at relief or swamp bridges could be estimated with equation 2-7, which assumes the average flow velocity through the bridge approximates the flow velocity near the abutments. Based on observations by Benedict (2003), relief and swamp bridges that are approximately 240 ft or less in length tend to form a single scour hole across the bridge opening. This phenomenon is indicative of a more uniform flow velocity distribution across these smaller-length bridges, providing some support for the use of equation 2-7. However, as bridge length increases, the assumption that the average flow velocity through the bridge approximates the flow velocity near the abutments will become less valid. One way to address this concern is to apply a multiplier to the average bridge velocity, V_{Br}, in equation 2-7 that will approximate the increased flow velocity near the abutment. Hayes (1996) analyzed 579 streamflow measurements at gages located at bridges in Delaware, Maryland, and Virginia and found that the maximum point flow velocity in the bridge opening, on average, was 1.19 times the mean flow velocity at the bridge. The Hayes (1996) relation is limited to average flow velocities at the bridge of 10 feet per second (ft/s) or less. [Note: Hayes (1996) added a value of 2.64 ft/s to the relation to form an envelope of the data. For purposes of this study, the average value was considered most appropriate, rather than the envelope values.] In support of the Hayes (1996) observation, Briaud et al. (2009) found in laboratory data that the maximum flow velocity near the abutment ranged from 1.04 to 1.17 times the average flow velocity through the bridge opening. Similarly, Ettema et al. (2010) found in two-dimensional flow models that the maximum flow velocity near the abutment ranged from slightly greater than 1 to approximately 1.2 times the average flow velocity through the bridge opening. (Note: The work of Morales and Ettema (2013) provides relations for estimating the maximum flow velocity and unit discharge at spill-through abutments with respect to selected abutment and

channel configurations, and these relations may be useful for assessing the velocity near an abutment.) Based on these findings, it would seem reasonable to add a multiplier of 1.2 to V_{Br} in equation 2-7, to conservatively approximate the increased velocity at an abutment for relief and swamp bridges. This procedure was used at all relief and swamp bridges, with bridge lengths equaling or exceeding 240 ft. This procedure was tested with the USGS field data in the NCHRP 24-20 method, and performance at such bridges was improved. (Note: This adjustment method only was applied to the field data because of its dependence on bridge length.)

- **Laboratory data**

  For Palaviccini (1993) laboratory data with rectangular channels, the contraction was treated like a relief bridge, as described previously, and equation 2-7 was used to determine unit discharge through the contraction, with no adjustments. The flow depth at the contraction, y_{f2}, was not published in the Palaviccini (1993) data; therefore, the approach flow depth was used to represent this value. Sturm (2004) published the flow velocity and depth at the abutment, and these values were used in equation 2-9 to determine unit discharge at the abutment. Ettema et al. (2010) published the unit discharge at the abutment, and no computation was required.

5. Calculate contraction-scour flow depth (Y_C)

Generally, there are two cases for contraction-scour computations: (1) abutments located on the floodplain (setback abutments and swamps or relief bridges), and (2) abutments located at the channel bank or protruding into the channel. A brief description of each case follows. This approach was used in the analysis for the laboratory and field data.

- **Abutments located on the floodplain (setback abutments and swamp or relief bridges)**

  As a general rule, NCHRP 24-20 assumes that clear-water scour conditions will prevail on the floodplain. This is a reasonable assumption for the USGS field data where the floodplains typically have lower velocities and are covered with vegetation. Therefore, for setback abutments and relief and swamp bridges, equation 2-4 was used to estimate the clear-water contraction-scour flow depth, Y_C, at the abutment. For this case, the overbank unit discharge, q_{f2} as determined in step 4, was used to represent the contracted unit discharge, q_2, in equation 2-4. Because the South Carolina and Alabama data primarily consist of setback abutments or relief and swamp bridges located on vegetated floodplains, clear-water contraction scour was assumed at all these sites.

- **Abutments located at the channel bank or protruding into the channel**

  When an abutment was located at the channel bank or protruded into the channel, it was assumed that the prevailing sediment transport conditions within the channel would determine the type of scour at the abutment. To determine if clear-water or live-bed contraction-scour conditions prevailed, the average velocity in the channel was compared with the critical velocity of the median grain size. When live-bed scour conditions prevailed, equation 2-3 was used to estimate the contraction-scour flow depth, Y_C. For this case, the unit discharge in the approach channel, q_{mc1} as determined in step 3, was used to represent the unconstricted unit discharge, q_1. Similarly, the unit discharge in the bridge channel, q_{mc2} as determined in step 4, was used to represent the contracted unit discharge, q_2. When clear-water scour conditions prevailed, equation 2-4 was used to estimate the contraction-scour flow depth, Y_C. For this case, the unit discharge in the bridge channel, q_{mc2} as determined in step 4, was used to represent the contracted unit discharge, q_2. For channels with coarse sediments in which a critical-velocity analysis indicates that live-bed conditions prevail, HEC-18 recommends that both live-bed and clear-water contraction-scour flow depths

be computed and the smaller of these values used as the estimate for contraction scour. (Note: It was assumed that sediments with a *D50* greater than 2 mm were coarse sediments.) Because the USGS Maine data primarily consist of protruding abutments into channels with coarse sediments, the smaller of the live-bed and clear-water contraction-scour estimates was used at these sites when live-bed scour conditions exist.

6. Determination of the amplification coefficient

Using the Scour Condition A or B as determined in step 2, the unit discharge ratio (q_2/q_1), and the general abutment shape (spill through or wing wall), the appropriate graph from figures 2-3 through 2-6 was selected, and the amplification factor, α, was determined. In order to incorporate the selection of α into a spreadsheet algorithm, the solid curves for each figure were discretized and broken into segments, and polynomial trend lines were developed for each segment. At field sites where the unit discharge ratio, q_2/q_1, exceeded the maximum value of the curves (3 for Scour Condition A and 5 for Scour Condition B), α was set to the value associated with the maximum value of q_2/q_1 for the given curve.

7. Calculation of abutment-scour flow depth (Y_{MAX}) and scour-hole depth (y_s)

The values Y_C and α, as determined in steps 5 and 6, respectively, were applied to equation 2-1 to estimate the maximum flow depth in the abutment scour area (Y_{MAX}). Equation 2-2 was then used to estimate the scour-hole depth (y_s). The upstream flow depth prior to scour, y_1, as used in equation 2-2 was determined in the following manner as for the same abutment configurations in step 5. This approach was used for laboratory and field data.

- **Abutments located on the floodplain (setback abutments and swamp or relief bridges)**

  The upstream flow depth prior to scour, y_1, was determined from the average flow depth on the left or right upstream approach floodplain associated with the abutment of interest.

- **Abutments located at the channel bank or protruding into the channel**

  The upstream flow depth prior to scour, y_1, was determined from the average flow depth in the upstream approach channel.

CHAPTER 3

APPLICATION OF THE NCHRP 24-20 PREDICTION METHOD TO LABORATORY AND FIELD DATA

3.1 Introduction

The conceptual model for the NCHRP 24-20 abutment-scour prediction method assumes that abutment scour is a function of contraction scour. This conceptual model can be applied to cohesive and non-cohesive sediments by incorporating an appropriate equation for predicting contraction scour for those respective sediments. However, the current formulation of the NCHRP 24-20 method uses the Laursen (1960; 1963) live-bed and clear-water contraction-scour equations, which are primarily applicable to scour in non-cohesive sediments (Ettema et al. 2010; Arneson et al. 2012). A unique feature of the NCHRP 24-20 investigation was the incorporation of laboratory data reflecting a variety of erodible and non-erodible embankments and abutment substructures, rather than the more common fixed (or rigid) embankments and abutments having vertical wall substructures at the abutment toe. These models better represent embankments and abutment substructures for many field sites and will tend to reduce the potential for abutment scour in contrast to the rigid embankment and abutment substructures used in previous studies. The current (2015) investigation will only evaluate the NCHRP 24-20 method for Scour Condition A, where an abutment is set near the main channel, and Scour Condition B, where the abutment is well set back from the main channel. Because of the complexity of flow and scour patterns for Scour Condition A, NCHRP 24-20 developed scour prediction methods based on data from the fixed floodplain and abutment models, providing a more conservative estimate of abutment scour. For Scour Condition B, NCHRP 24-20 developed scour prediction methods based on data from erodible floodplain and abutment substructures, with the embankment and abutment armored with rip rap. (See report section 2.2 for more details regarding the abutment models used in the NCHRP 24-20 investigation.)

With the exception of the NCHRP 24-20 laboratory data, the laboratory data used in evaluating the performance of the NCHRP 24-20 prediction method represent scour at non-erodible rigid

embankments, abutments, and abutment substructures. Additionally, the conditions of the embankments/abutments for the USGS field data are thought to represent abutment scour where the road embankment and abutments did not appreciably erode (see report section 1.2.5 for details). These characteristics of the laboratory and field data differ in some measure from the abutment models used in the NCHRP 24-20 investigation (see report section 2.2). These differences should be kept in mind when reviewing the results of the NCHRP 24-20 prediction method presented in this report.

The procedure described in chapter 2 was used to apply the NCHRP 24-20 abutment-scour prediction method to the selected laboratory (table 1-3) and field (table 1-1) abutment-scour data. The results from this application were incorporated into selected scatter plots to display the relations of predicted and measured scour, as well as prediction residuals with respect to selected explanatory variables. If a prediction equation is capturing the trends of the data, then the relation of the predicted and measured scour will tend to follow the line of agreement, with predicted scour increasing as measured scour increases. The relation of prediction residuals with respect to an explanatory variable will help identify prediction bias associated with that variable. If prediction residuals display a sloped trend with respect to a given explanatory variable, some prediction bias with respect to that variable is likely. Boxplots of the prediction residuals for the laboratory and field data are presented in chapter 6 and compared with the prediction residuals of the NCHRP 24-15(2) method. The boxplots display the distribution of the prediction residuals by quartiles, providing a simple but useful tool for evaluating the performance of each method and comparing their performance. A table of summary statistics for these boxplots also is provided in chapter 6 in order to quantify the trends in the boxplots.

The performance of the NCHRP 24-20 prediction method presented in the following sections of this report represents the combined influence of the equation, the prescribed application procedure, and the data, each having inherent limitations. These limitations will undoubtedly introduce uncertainty into the results; however, the large number of laboratory (table 1-3) and field (table 1-1) data should be adequate to provide valuable insights into the general performance of the equation. The results associated with the laboratory data will be presented first followed by the results of the field data.

3.2 Analysis of the Laboratory Data

The NCHRP 24-20 method was initially evaluated with the laboratory measurements of abutment scour listed in table 1-3. The analysis included a comparison of predicted and measured scour and an evaluation of prediction residuals with respect to selected variables. The analysis of the laboratory data is presented in the following report sections.

3.2.1 Relation of Measured and Predicted Scour

The data in figure 3-1 show the relation of predicted and measured abutment scour for the application of the laboratory data (table 1-3) to the NCHRP 24-20 abutment-scour prediction method using the procedure described in chapter 2. The data in figure 3-1 are grouped by data source, abutment shape, and bed transport condition. Live-bed scour conditions are represented by the solid symbols, with hollow symbols representing clear-water scour conditions. Figure 3-1A shows the relation for the data in non-cohesive sediments, while figure 3-1B shows the same data, but includes the cohesive sediment data from Briaud et al. (2009). Figures 3-2 through 3-4 present the data in figure 3-1 grouped by abutment shape, including vertical-wall, spill-through, and wing-wall abutments, respectively. The laboratory data in these figures represent abutment scour from a variety of experimental conditions, and therefore, the scatter displayed in the data is not unreasonable. As expected, the Ettema et al. (2010) data all plot approximately at or above the line of agreement. Excluding the Sturm (2004) data, the other data in figure 3-1A generally show an approximate symmetric scatter of the predicted values around the line of agreement, with the frequency and magnitude of overprediction being larger than that of underprediction. The data patterns indicate that the NCHRP 24-20 prediction method is tending to follow the measured data, with predicted scour depth increasing as measured scour depth increases; this is most notable in the wing-wall data in figure 3-4. However, the patterns in the Palaviccini (1993) vertical-wall and spill-through data, as well as the Briaud et al. (2009) data, indicate that the frequency and magnitude of underprediction increase with increasing scour depth. While the theory of the NCHRP 24-20 method is applicable to both non-cohesive and cohesive sediments, the formulation has yet to be adapted to cohesive sediments. Therefore, its current formulation is not applicable to cohesive sediments, and the Briaud et al. (2009) data are presented in figure 3-1B only for information. Most of the laboratory data reflect scour at non-erodible rigid abutments/embankments with abutment setbacks classified as Scour Condition B (approximately

87 percent of the data). In contrast, the NCHRP 24-20 investigation used erodible abutments/embankments for Scour Condition B, and this model difference likely contributes, in part, to the underprediction. These differing embankment models will be noted at selected locations in the following review, but should be kept in mind as a factor that likely contributes to underprediction. The patterns in figures 3-1 through 3-4 indicate that some underprediction likely will occur when the NCHRP 24-20 method is applied to the field data. The Sturm (2004) data display substantial underprediction that is likely caused by a combination of factors, including rigid abutments substructures, small flow depths at the abutment, long abutments that tend to produce larger scour depths, and large sediment sizes that reduce the estimate of contraction scour. These factors are noted later in the report.

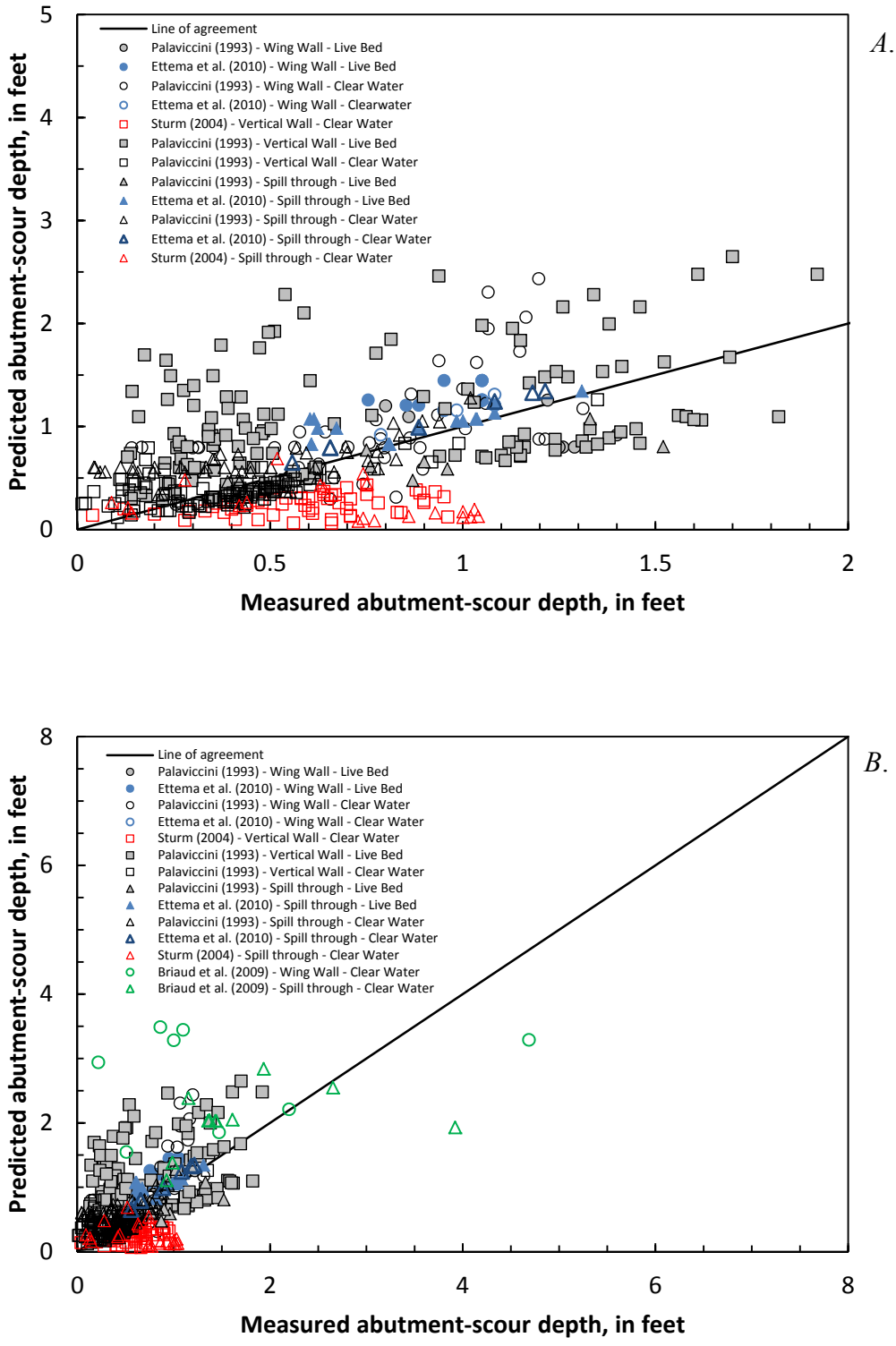

Figure 3-1. Relation of predicted and measured abutment-scour depth for selected laboratory data, using the NCHRP 24-20 scour prediction method for (*A*) only non-cohesive sediments and (*B*) cohesive and non-cohesive sediments.

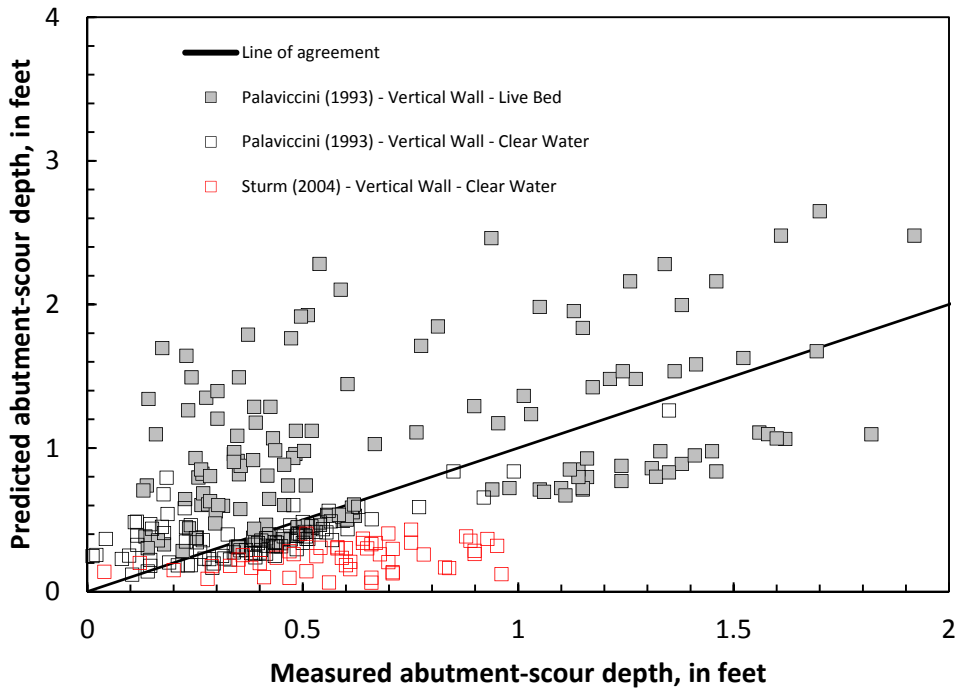

Figure 3-2. Relation of predicted and measured abutment-scour depth for selected laboratory data with vertical-wall abutments, using the NCHRP 24-20 scour prediction method.

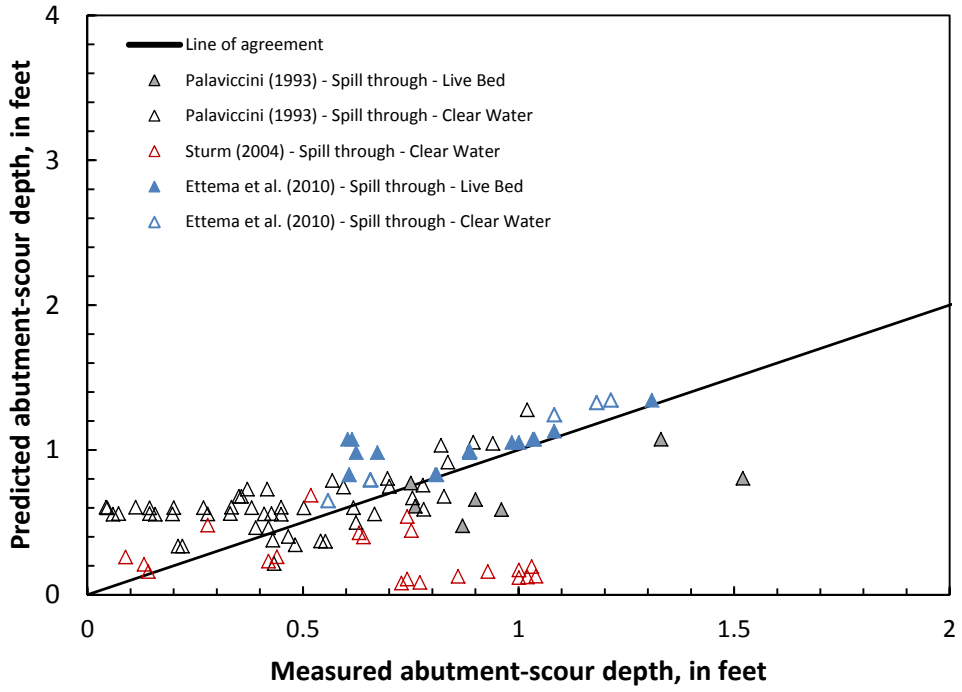

Figure 3-3. Relation of predicted and measured abutment-scour depth for selected laboratory data with spill-through abutments, using the NCHRP 24-20 scour prediction method.

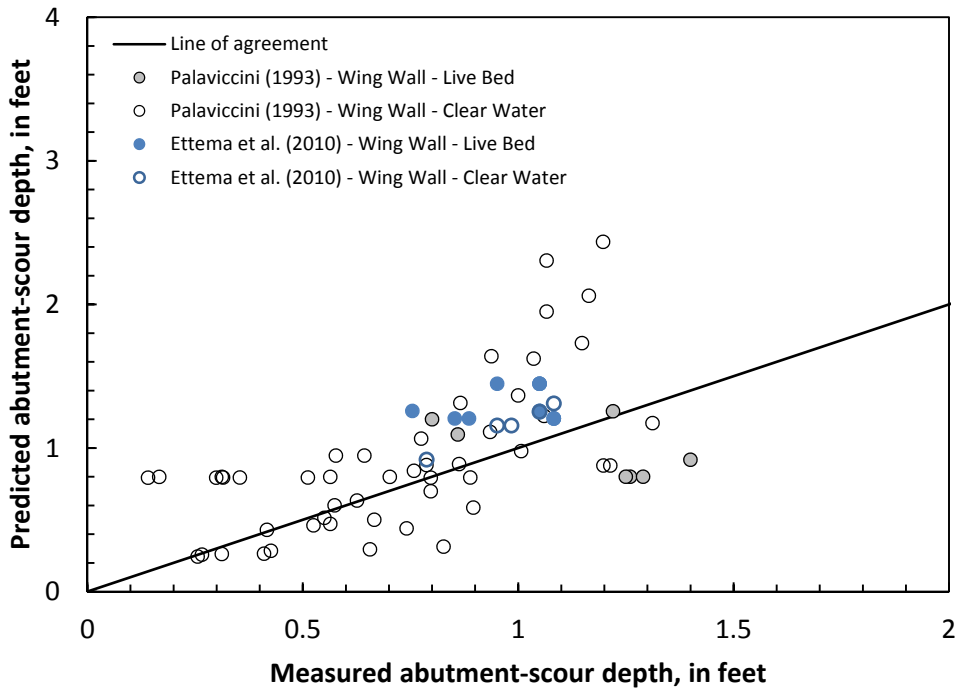

Figure 3-4. Relation of predicted and measured abutment-scour depth for selected laboratory data with wing-wall abutments, using the NCHRP 24-20 scour prediction method.

3.2.2 Prediction Residuals with Respect to Selected Explanatory Variables

The following figures (figures 3-5 through 3-10) show the prediction residuals in relation to selected explanatory variables, including q_2, q_2/q_1, *D50*, L/y_1, y_1, and the amplification factor (α), respectively. The data symbols used in these plots are identical to those used in figure 3-1. These plots were reviewed to identify potential trends regarding under- and overprediction, and a discussion of these plots follows.

i. Prediction Residuals with Respect to q_2

The NCHRP 24-20 method uses the unit discharge at the abutment, q_2, for estimating the live-bed and clear-water contraction-scour depth (equations 2-3 and 2-4, respectively). Figure 3-5 displays the prediction residuals with respect to q_2 for (A) the live-bed scour data and (B) the clear-water scour data. These data display a trend, with overprediction increasing as q_2 increases, and this trend is more distinct in the clear-water scour data.

The underprediction in the Sturm (2004) data is likely caused by multiple factors, including small flow depths, large sediment sizes, relatively long abutments, and rigid abutments/embankments; these factors provide some explanation for the performance of the Sturm (2004) data in the NCHRP 24-20 method. A review of table 1-3 indicates that the Sturm (2004) data have flow depths that are much smaller than the other laboratory data and tend to yield smaller values of q_2 for comparable flow velocities. These small values of q_2, when applied to equation 2-4, will produce smaller estimates of clear-water contraction scour, potentially leading to underprediction. The Sturm (2004) data also have the largest *D50*s in the laboratory data, which will further reduce the estimate of clear-water contraction scour when applied to equation 2-4. Some of the Palaviccini (1993) data, which have smaller *D50*s, have values of q_2 in the same range as the Sturm (2004) data, yet underprediction is not as severe, further indicating that sediment size may play some role in the underprediction of the Sturm (2004) data. The Sturm (2004) data are associated with relatively long abutments that tend to produce the largest relative abutment-scour depths (figure 1-12). In contrast, the NCHRP 24-20 data used to develop the prediction method were primarily associated with intermediate abutment lengths (figure 1-12) and therefore, may tend to underpredict scour at longer abutments. Adjustments for abutment length, as described in report section 1.3.1, were applied to the Sturm (2004) data shown in figure 3-5 to account for the longer abutments, but underprediction is still substantial. The possible influence of long abutments on scour depth will be described in more detail later in the report. The rigid embankment and abutment substructure associated with the Sturm (2004) data tend to produce larger scour depths than those associated with the abutment models used to develop the NCHRP 24-20 method and will contribute to the underprediction in the Sturm (2004) data. In particular, as the scour hole develops, the rigid abutment substructure below the bed will tend to strengthen the local flow field at the modeled abutment, thereby increasing the potential for scour.

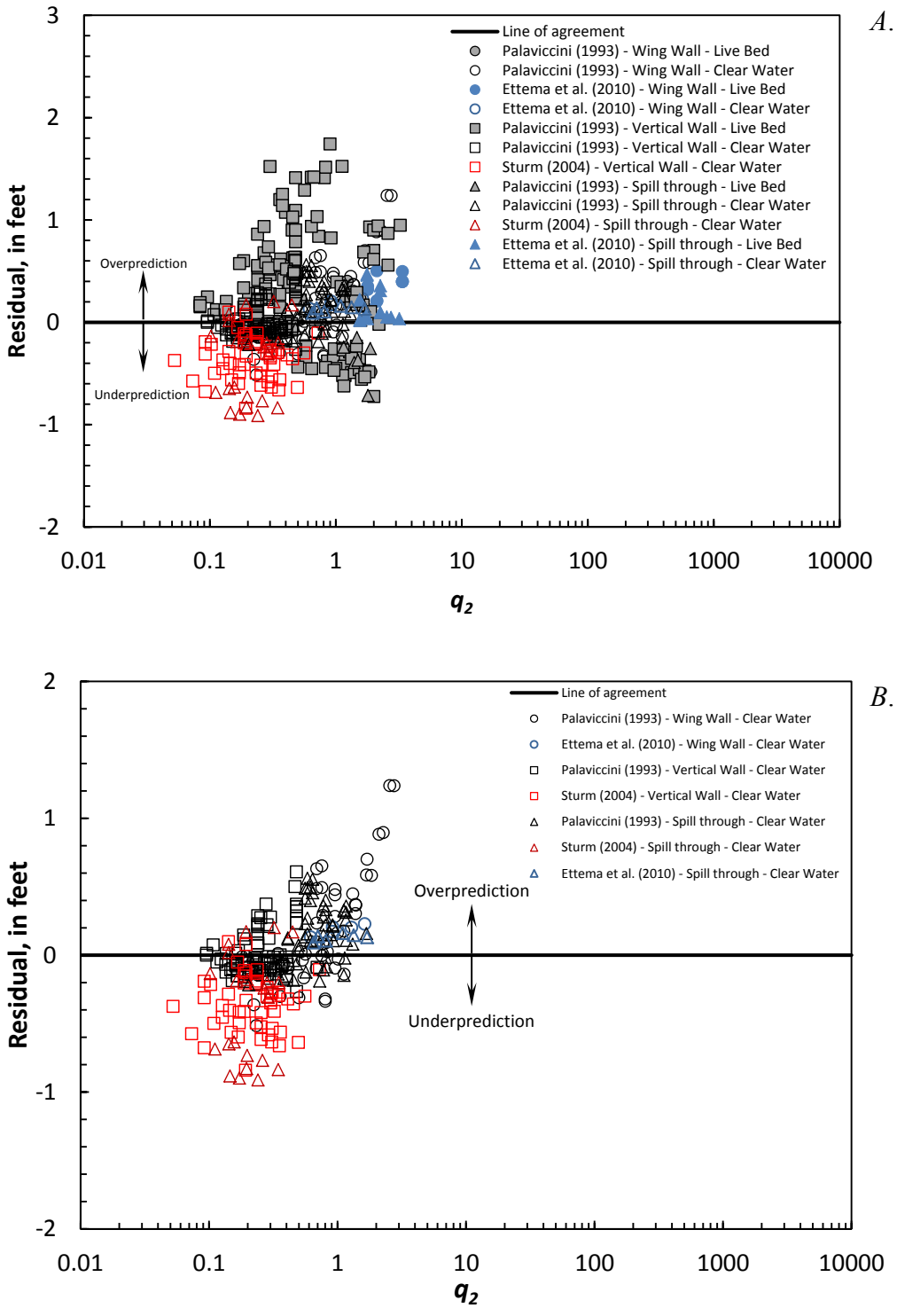

Figure 3-5. Relation of prediction residuals and the median grain size, q_2, for (*A*) all of selected laboratory data and (*B*) only clear-water laboratory data applied to the NCHRP 24-20 scour prediction method.

ii. Prediction Residuals with Respect to q_2/q_1

The NCHRP 24-20 method uses the unit discharge ratio (q_2/q_1) to determine the amplification factor for application to equation 2-1 and for the prediction of live-bed contraction scour in equation 2-3. Figure 3-6 displays the prediction residuals with respect to q_2/q_1. Excluding the Sturm (2004) data, the patterns display the larger frequency and magnitude of overprediction, but generally do not display a strong trend towards under- or overprediction with respect to q_2/q_1. While the Sturm (2004) data have substantial underprediction, the residuals for these data do not display a strong trend with respect to q_2/q_1.

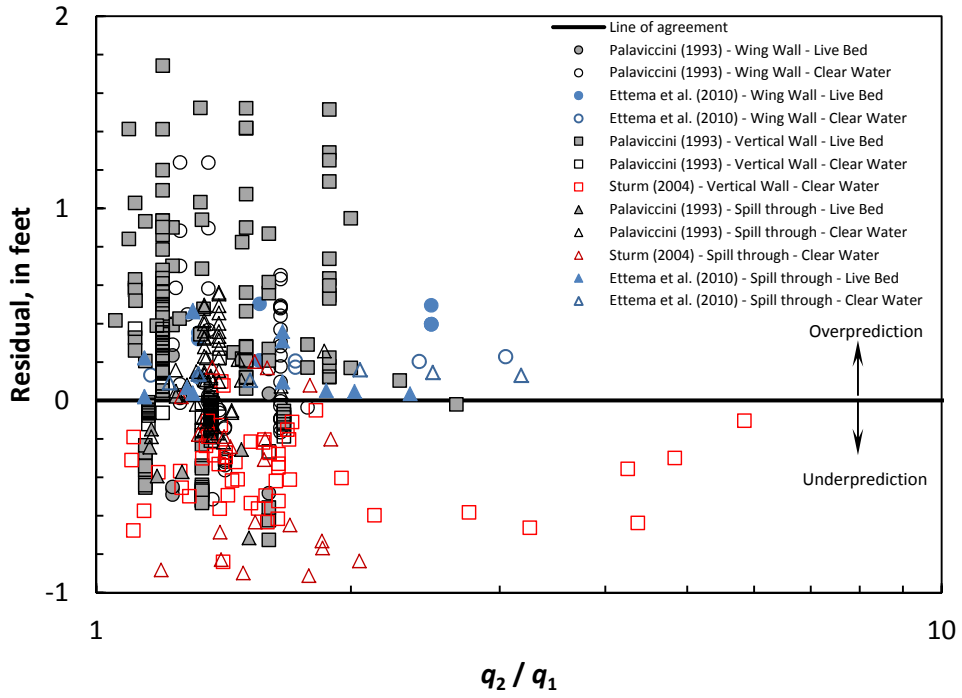

Figure 3-6. Relation of prediction residuals and the unit discharge ratio, q_2/q_1, for selected laboratory data applied to the NCHRP 24-20 scour prediction method.

iii. Prediction Residuals with Respect to *D50*

The median grain size of the sediment, *D50*, is used in equation 2-4 to estimate the clear-water contraction-scour depth. Figure 3-7 shows the relation of the prediction residuals with respect to *D50* for (A) all of the laboratory data and (B) the clear-water scour data. The trend in figure 3-7A indicates that the magnitude of overprediction diminishes with more frequent underprediction as *D50* increases. The data for clear-water scour (figure 3-7B) display a similar, but less prominent relation. The Sturm (2004) data strongly influence the patterns in figure 3-7B, and if they are neglected, the trend is not as prominent. As noted previously, multiple factors likely contribute to the underprediction associated with the Sturm (2004) data, with sediment size being one of these factors.

iv. Prediction Residuals with Respect to L/y_1

The relative abutment length, L/y_1, is a variable used by Melville and Coleman (2000) to classify abutments into categories of short, intermediate, and long abutments, with the potential for abutment-scour increasing as the abutment length increases (report section 1.3.2 and figure 1-12). The relation of the prediction residuals with respect to L/y_1 is shown in figure 3-8 for (A) all of the laboratory data and (B) the clear-water scour data. The figure identifies the range for short, intermediate, and long abutments as classified by Melville and Coleman (2000). The data indicate a trend of overprediction associated with shorter abutments and underprediction associated with longer abutments. If the Sturm (2004) data are neglected, the trend is still prominent, indicating that L/y_1 likely has some influence on residual patterns and that underprediction will tend to be associated with clear-water scour at relatively long abutments. Because a large number of the USGS field data are classified as clear-water scour with relatively long abutments, figure 3-8B provides some insight on how such field data may perform with the NCHRP 24-20 method.

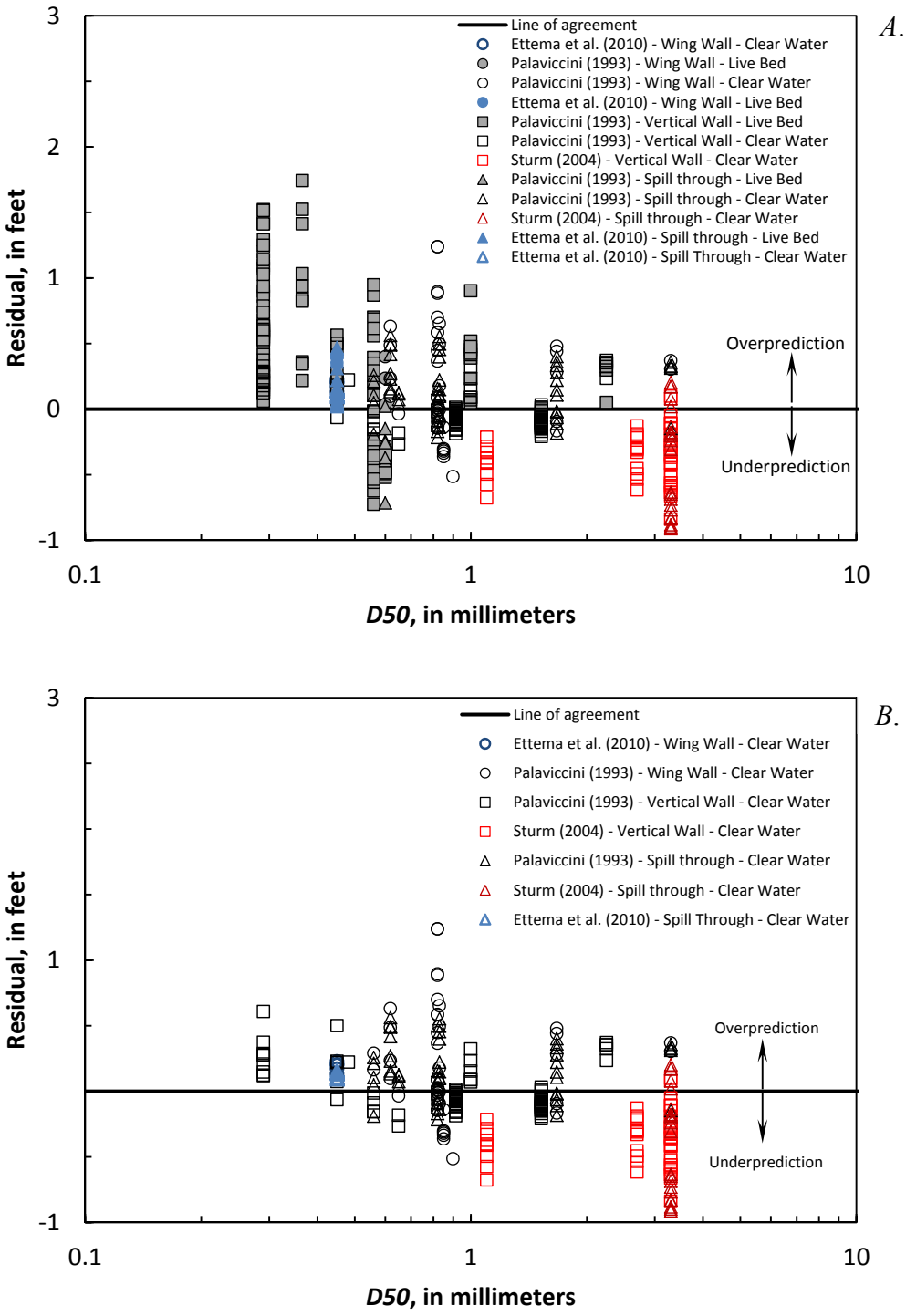

Figure 3-7. Relation of prediction residuals and the median grain size, *D50*, for (*A*) all of selected laboratory data and (*B*) only clear-water laboratory data applied to the NCHRP 24-20 scour prediction method.

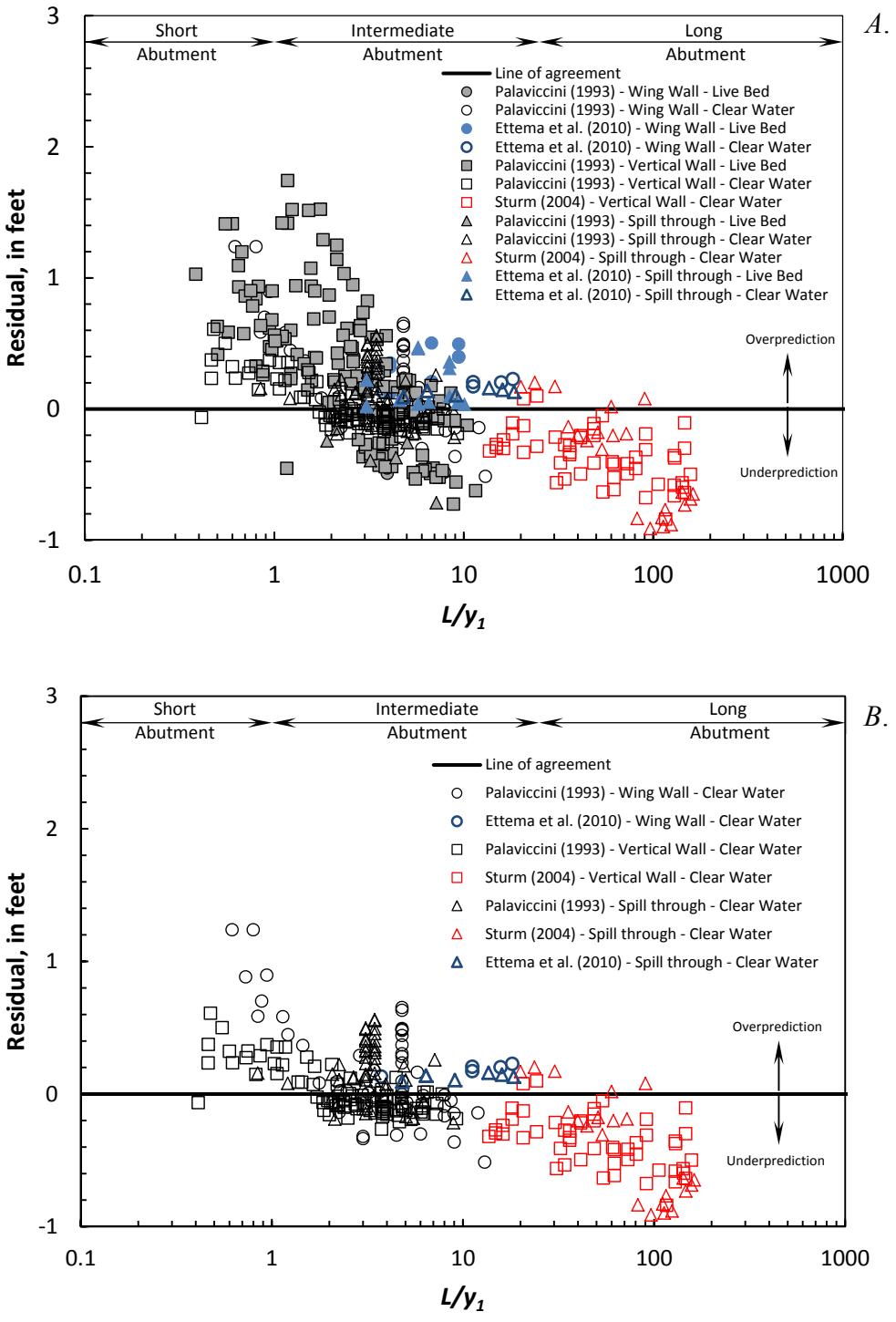

Figure 3-8. Relation of prediction residuals and relative abutment length, L/y_1, for (*A*) all of selected laboratory data and (*B*) only clear-water laboratory data applied to the NCHRP 24-20 scour prediction method.

v. Prediction Residuals with Respect to y_1

The approach flow depth, y_1, is a variable used directly or indirectly in equations 2-2 through 2-4 for predicting abutment scour. The relation of the prediction residuals with respect to y_1 is shown in figure 3-9 for (A) all of the laboratory data and (B) the clear-water scour data. There is a relation associated with these data, with the frequency and magnitude of overprediction increasing as y_1 increases. Underprediction is associated with small flow depths and provides some explanation for the differing performance of the Sturm (2004) data, which have the smallest values of y_1 within the laboratory data.

vi. Prediction Residuals with Respect to α

The amplification factor, which is used in equation 2-1, accounts for the additional scour at an abutment that is above and beyond the contraction scour. The relation of the prediction residuals with respect to the amplification factor is shown in figure 3-10 for (A) all of the laboratory data and (B) the clear-water scour data without the Sturm (2004) data. For amplification factors greater than 2, there is more frequent overprediction, but no strong trend in the residuals. The Sturm (2004) data indicate a tendency for increased underprediction as the amplification factor decreases, but the trend is not strong and is likely influenced by other factors as noted previously.

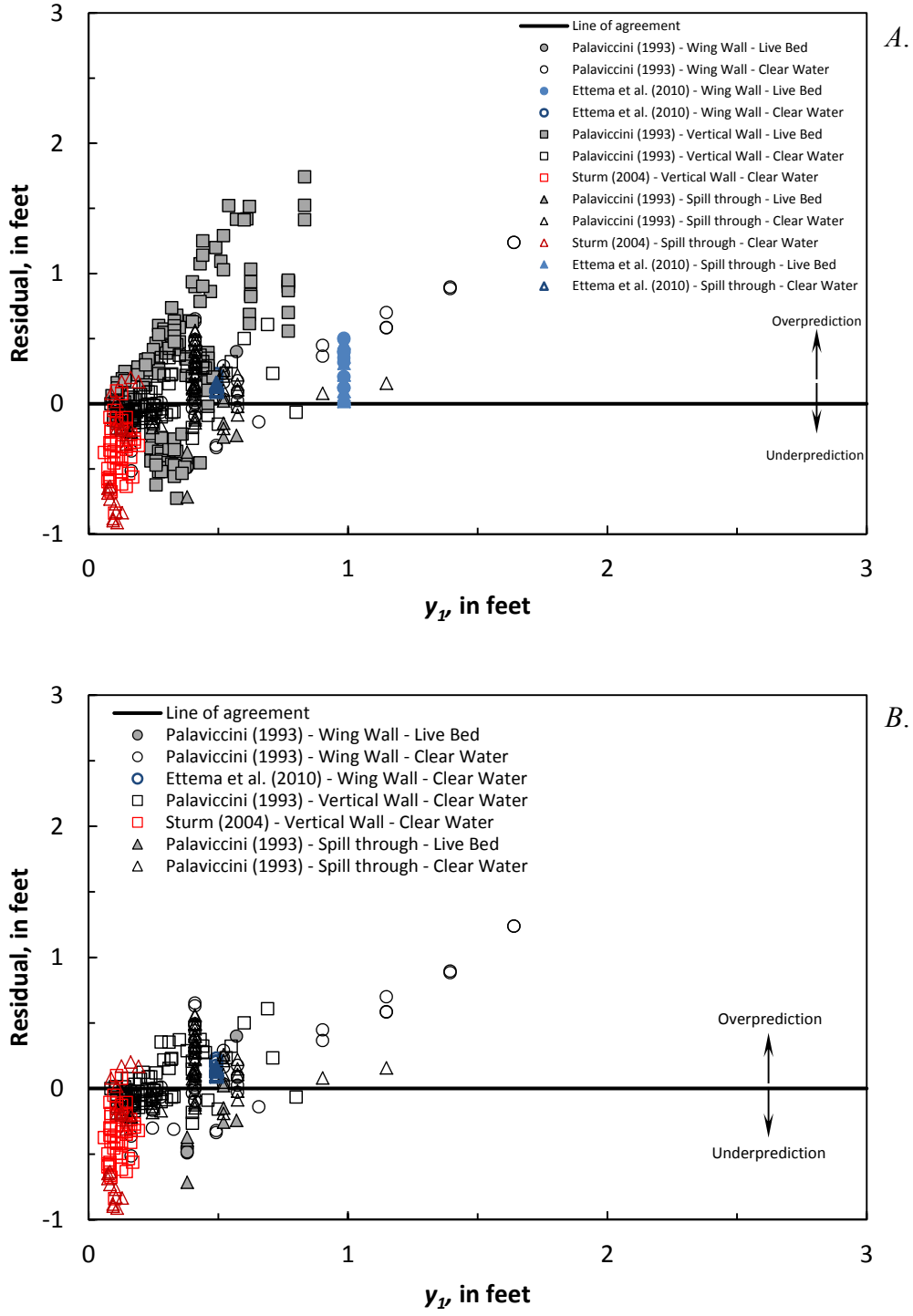

Figure 3-9. Relation of prediction residuals and y_1, for (*A*) all of selected laboratory data and (*B*) only clear-water laboratory data applied to the NCHRP 24-20 scour prediction method.

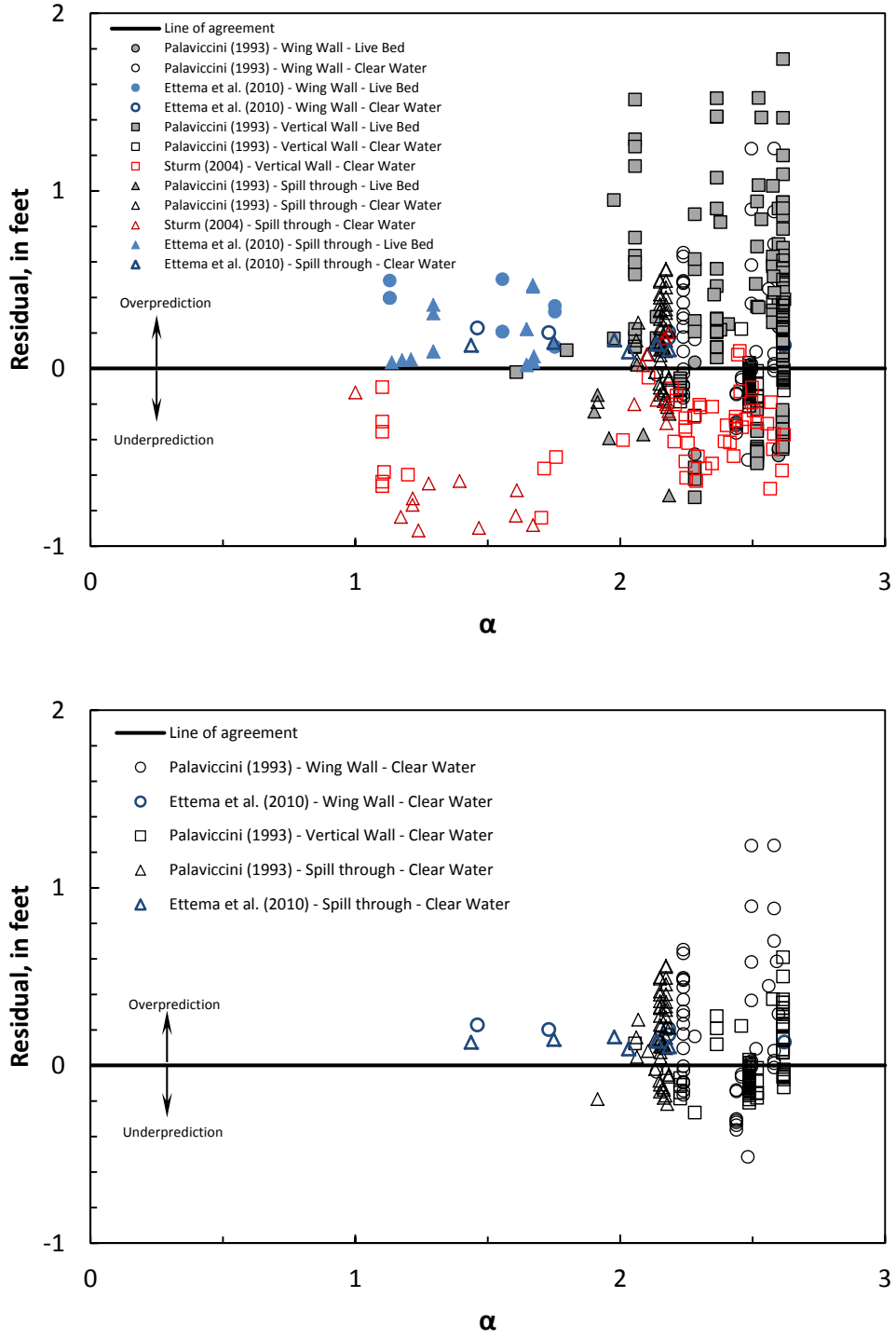

Figure 3-10. Relation of prediction residuals and the amplification factor (α), for (*A*) all of selected laboratory data and (*B*) only clear-water laboratory data applied to the NCHRP 24-20 scour prediction method.

3.3 Analysis of the USGS Field Data

The NCHRP 24-20 method was evaluated with the field measurements of abutment scour listed in table 1-1. The analysis included a comparison of predicted and measured scour and an evaluation of prediction residuals with respect to selected variables. The analysis of the field data is presented in the following report sections.

3.3.1 Measured and Predicted Scour for the USGS Field Data

Figure 3-11 shows the relation of measured abutment-scour depth to predicted scour for the application of the NCHRP 24-20 method to the USGS field data listed in table 1-1. The application method is described in chapter 2 of this report. The field data in this figure are grouped as presented in table 1-1, with the exception that a subset of 41 South Carolina measurements associated with floodplain relief bridges and swampy sites with poorly defined channels (similar to a floodplain) were plotted as an additional group. These data are described in more detail in report section 1.4.2. In the controlled environment of the laboratory, many of the variables that influence scour, such as flow and sediment characteristics and abutment geometry, can be modeled in a relatively consistent and repeatable manner. In a laboratory dataset, measurements outside the range of the majority of the data (i.e., outliers) often can be associated with some model inconsistency and appropriately excluded from the data analysis. In contrast, the field environment includes many site conditions that deviate from the ideal setting of the laboratory, and such deviations can be frequent. Therefore, outliers associated with field data are not necessarily indicative of poor data, but are likely highlighting some unique feature at the site of interest. As such, their inclusion in any analysis offers an opportunity to gain insights into equation performance under various field conditions. In the analysis of the NCHRP 24-20 scour prediction method, data that performed as outliers were included in the analysis, and an attempt was made to identify reasons for their performance. Table 3-1 provides a list of selected sites that had larger under- or overpredictions in the application of the NCHRP 24-20 prediction method and provides a description of site features that could possibly cause such performance. These sites are identified in figure 3-11 with the associated site number as listed in table 3-1. Other figures in this analysis identify these sites in a similar manner. The largest measured scour depth (23.6 ft) in the USGS abutment-scour database occurs at a floodplain relief bridge for the Interstate 95 multiple-bridge crossing of the Pee Dee River (site 3 in table 3-1) that is associated

with an approximately 8-mile-wide floodplain. The one-dimensional model for this site indicates a large water-surface differential (backwater) of approximately 2 ft across the bridge, which creates hydraulic conditions that can have a large potential for scour. Because of these adverse hydraulic conditions, this site likely will perform poorly with most laboratory-derived scour prediction equations that typically would not include data for such severe hydraulic conditions. Additionally, the one-dimensional flow model for this site will not fully capture the hydraulics, introducing some error in any scour analysis. This data point was included in the analysis to provide perspective of how the selected equation will perform under more severe scour conditions.

To better visualize the trends in figure 3-11, the data points associated with each data group are shown in figure 3-12 as a series of plots. All of the field data are shown as hollow circles, with the selected data group identified with solid circles. The lower gradient and wide floodplain streams associated with the South Carolina Relief/Swamp Bridges and the Coastal Plain are shown in figures 3-12A and B, respectively. The larger outliers associated with these data groups have site features that provide some explanation for their performance (table 3-1). Excluding the data in table 3-1, the data generally show an approximate symmetric scatter of the predicted values around the line of agreement, with the frequency and magnitude of overprediction being larger than that for underprediction. However, as with the laboratory data (figure 3-1), there is a trend of more frequent underprediction as the scour depth increases. In particular, there is more frequent underprediction of scour for measured abutment-scour depths of approximately 10 ft and larger. The underprediction in these data likely is caused by multiple factors, some of which include (1) relatively long abutments that tend to produce larger scour depths in contrast to the intermediate abutments used to develop the NCHRP 24-20 method (see report section 1.3.1), (2) the less accurate estimates of flow velocity from the one-dimensional flow models, and (3) relatively non-erodible abutments/embankments in contrast to the erodible abutments/embankments used to develop the NCHRP 24-20 prediction method (see report section 1.2.5). Note that 23 of the 29 underpredictions from these two data groups are associated with Scour Condition B, where the NCHRP 24-20 method assumes erodible embankments and abutments, giving some support to item 3 in the previous sentence. For the cohesive sediments of the South Carolina Piedmont and Alabama (figures 3-12C and E), the data pattern indicates a higher occurrence of overprediction with infrequent underprediction. Because the current

formulation of the NCHRP 24-20 method is primarily for non-cohesive sediments, this pattern is reasonable. The excessive overprediction in figure 3-12C (number 9) is associated with excessive overprediction of the unit discharge at the bridge based on the SBR method. The Maine data are shown in figure 3-12D. Most of the underprediction in the Maine data is associated with grain sizes of 64 mm, and the values of the underprediction are small. In contrast, large overpredictions in the Maine data are associated with sand grain sizes. Excluding the large overpredictions, much of the Maine data has an approximate symmetric scatter about the line of agreement with a smaller prediction scatter than that of the other field data. The NBSD data are shown in figure 3-12F. The two largest overpredictions are associated with cohesive sediments (site number 8). The other data have an approximate symmetric scatter about the line of agreement with minimal underprediction.

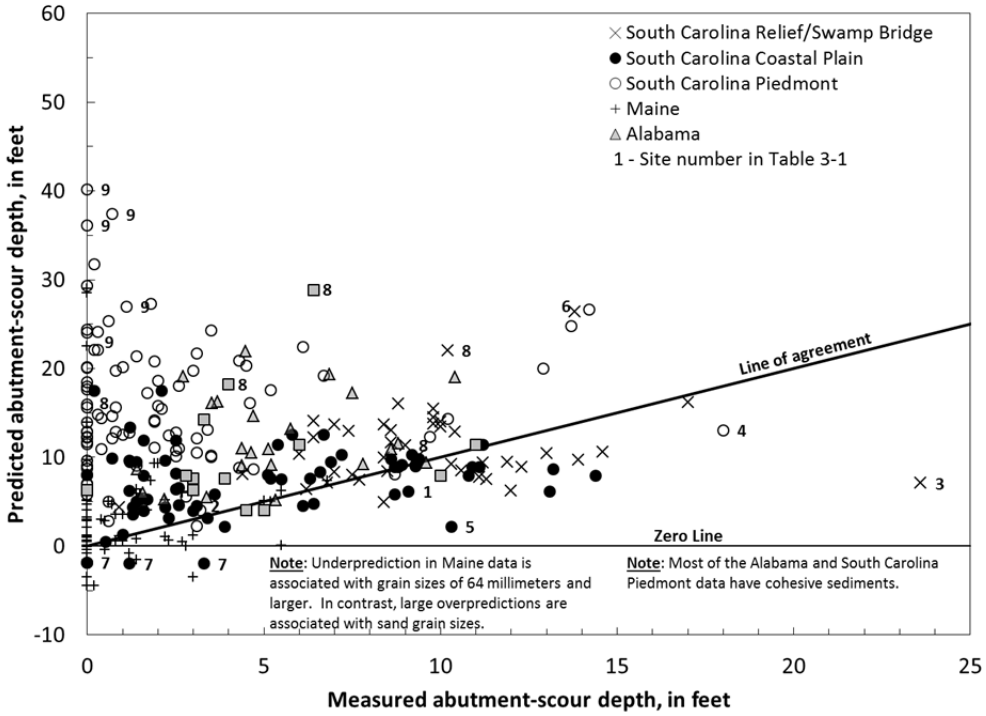

Figure 3-11. Relation of measured and predicted abutment-scour depth for selected field data using the NCHRP 24-20 scour prediction method.

The prediction patterns in figures 3-11 and 3-12 indicate that the NCHRP 24-20 method is approximating the general trend of the non-cohesive field data, with an approximate scatter about the line of agreement and predicted scour depth increasing as measured scour depth increases. As measured scour increases, however, underprediction increases, which is of concern. The prediction patterns for cohesive sediments indicate infrequent underprediction and overprediction that at times is excessive.

Table 3-1. Sites with unique characteristics that may influence scour depth.

[US, U.S. Route; SC, S.C. Route; I, Interstate; S, Secondary Road; NBSD, U.S. Geological Survey National Bridge Scour Database]

Site Number	Database	Site Name	Scour Depth, in feet	Comments
1	South Carolina Coastal Plain	Coosawhatchie River at US 601	13.1	Previous smaller bridge may have contributed to scour depth.
2	South Carolina Coastal Plain	Four Hole Swamp at SC 453	13.2	Bridge near floodplain edge that may create unique flow distribution influencing scour depth.
3	South Carolina Relief/Swamp Bridge	Great Pee Dee River at I-95	23.6	Severe contraction of flow with large head differential across the bridge; upstream guide banks may influence scour depth. See description of site in report section 3.3.1.
4	South Carolina Piedmont	Indian Creek at US 176	18.0	Beaver dam directs flow into abutment region that may influence scour depth.
5	South Carolina Coastal Plain	Little Pee Dee River at US 501	10.3	Large ditch along upstream embankment may influence scour depth.
6	South Carolina Relief/Swamp Bridge	Maiden Down Swamp at SC 41	13.8	Riprap from abutment slopes has slumped into channel, likely limiting scour depth.
7	South Carolina Coastal Plain	[a]Waccamaw River at SC 22	Less than 4.0	Very low stream gradient produces small velocities and thus small scour depths.
8	NBSD, South Carolina Coastal Plain, and South Carolina Relief/Swamp Bridge	Beaver Creek Overflow, US 2 Great Pee Dee River, US 76 South Saluda River S-40	From 0.2 to 10.2	These sites have cohesive sediments that produce substantial overprediction, beyond that of the other data associated with the respective databases.
9	South Carolina Piedmont	Enoree River, SC 49 Enoree River, SC 146 Enoree River, SC 296 South Tyger River S-62	From 0 to 1.4	For these measurements, the setback ratio method produces large unit discharges at the bridge because of low Manning's n-value on the approach floodplain or small overbank at the bridge.

[a]Three abutment-scour measurements are associated with this site, all of which are less than 4 feet.

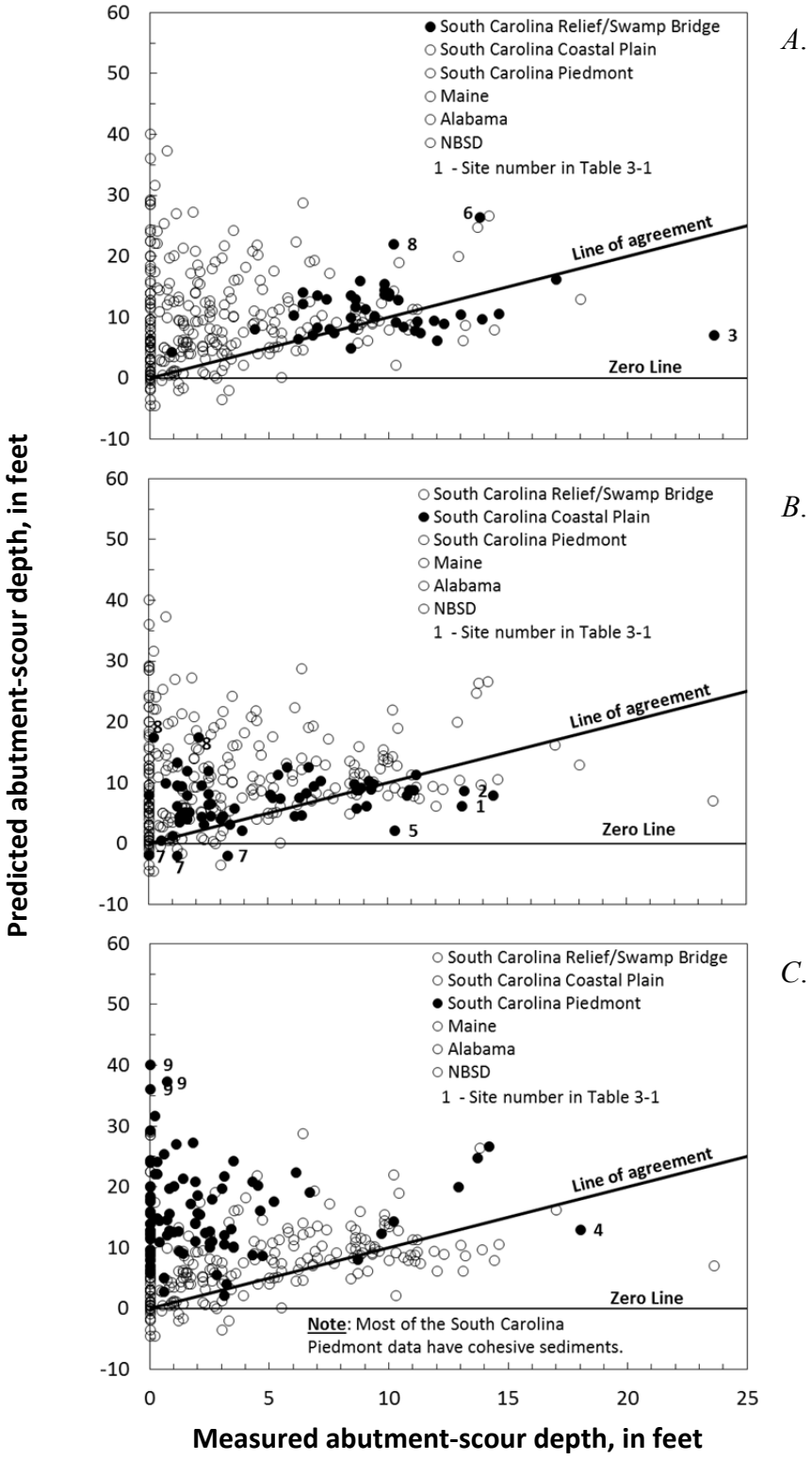

Figure 3-12. Relation of measured and predicted abutment-scour depth for selected field data using the NCHRP 24-20 scour prediction method for the (*A*) South Carolina Relief/Swamp Bridge, (*B*) South Carolina Coastal Plain, (*C*) South Carolina Piedmont, (*D*) Maine, (*E*) Alabama, and (*F*) National Bridge Scour Database (NBSD) data.

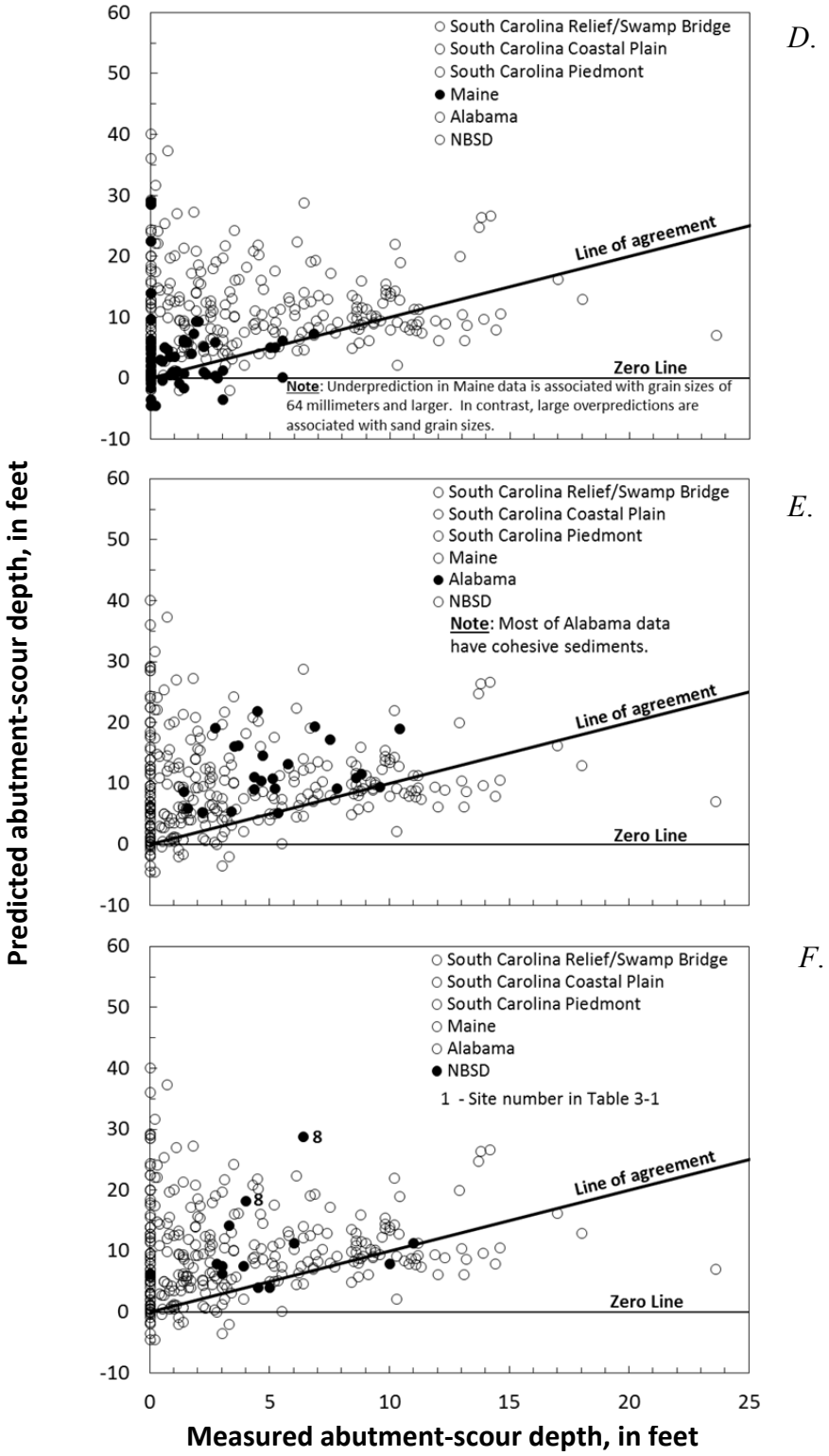

Figure 3-12. Continued --Relation of measured and predicted abutment-scour depth for selected field data using the NCHRP 24-20 scour prediction method for the (*A*) South Carolina Relief/Swamp Bridge, (*B*) South Carolina Coastal Plain, (*C*) South Carolina Piedmont, (*D*) Maine, (*E*) Alabama, and (*F*) National Bridge Scour Database (NBSD) data.

3.3.2 Prediction Residuals with Respect to Selected Variables

The following figures show the prediction residuals in relation to selected variables, including q_2, q_2/q_1, $D50$, L/y_1, y_1, and α, respectively. The data symbols used in these plots are identical to those used in figure 3-11. These plots were reviewed to identify potential relations regarding under- and overprediction, and a discussion of these plots follows.

i. Prediction Residuals with Respect to q_2

The NCHRP 24-20 method uses the unit discharge at the abutment, q_2, for estimating the live-bed and clear-water contraction-scour depth (equations 2-3 and 2-4, respectively). Figure 3-13 displays the prediction residuals with respect to q_2. The cohesive data for the South Carolina Piedmont and Alabama have large, and at times excessive, overprediction and display a relation of increasing overprediction with increasing values of q_2. Because the NCHRP 24-20 method, in its current formulation, is not applicable to cohesive sediments, this pattern is reasonable. The majority of the prediction residuals associated with the steep-gradient streams of Maine have an approximate symmetric scatter about the zero line, indicating no trend. The few exceptions to this are 3 data points that have small grain sizes in the sand range (about 0.4 mm or less) and relatively large values of q_2 that likely contribute to the large overpredictions. Neglecting the cohesive data, the Maine data with sandy sediments, and the data in table 3-1, the pattern of the prediction residuals shows that much of the non-cohesive data for the South Carolina Relief/Swamp Bridges, the Coastal Plain, the NBSD, and Maine have an approximate symmetric scatter about the zero line, with the frequency and magnitude of overprediction being moderately larger than that for underprediction. This pattern indicates no strong trend towards under- or overprediction associated with q_2 for non-cohesive sediments.

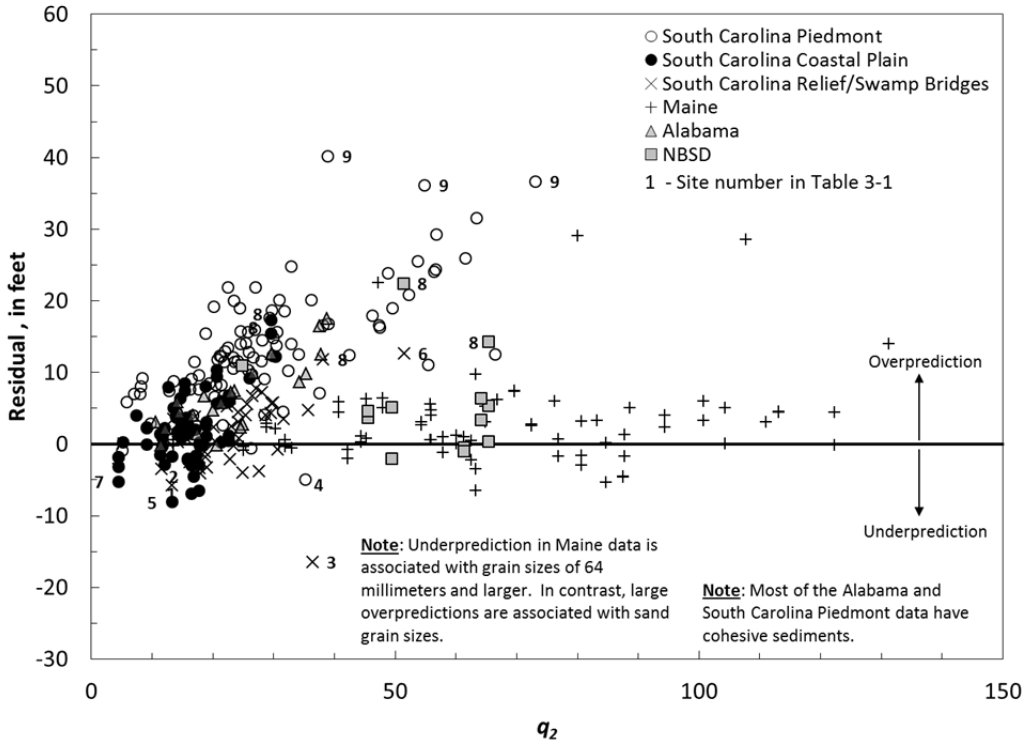

Figure 3-13. Relation of prediction residuals and the unit discharge, q_2, for selected field data applied to the NCHRP 24-20 scour prediction method.

ii. Prediction Residuals with Respect to q_2/q_1

The unit discharge ratio (q_2/q_1) is used in the NCHRP 24-20 method to determine the amplification factor (equation 2-1), and for the prediction of live-bed contraction scour (equation 2-3). The relation of the prediction residuals with respect to q_2/q_1 are shown in figure 3-14. As noted previously, there is large overprediction for the cohesive data because the NCHRP 24-20 method, in its current formulation, is intended for non-cohesive sediments. However, when excluding the data in table 3-1, much of the non-cohesive data have an approximate symmetric scatter about the zero line, with the frequency and magnitude of overprediction being moderately larger than that for underprediction. This pattern indicates no strong trend towards under- or overprediction associated with q_2/q_1 for non-cohesive sediments. While there is more scatter in the prediction residuals for the laboratory data (figure 3-6), the residual patterns of the laboratory data confirm the patterns in the field data.

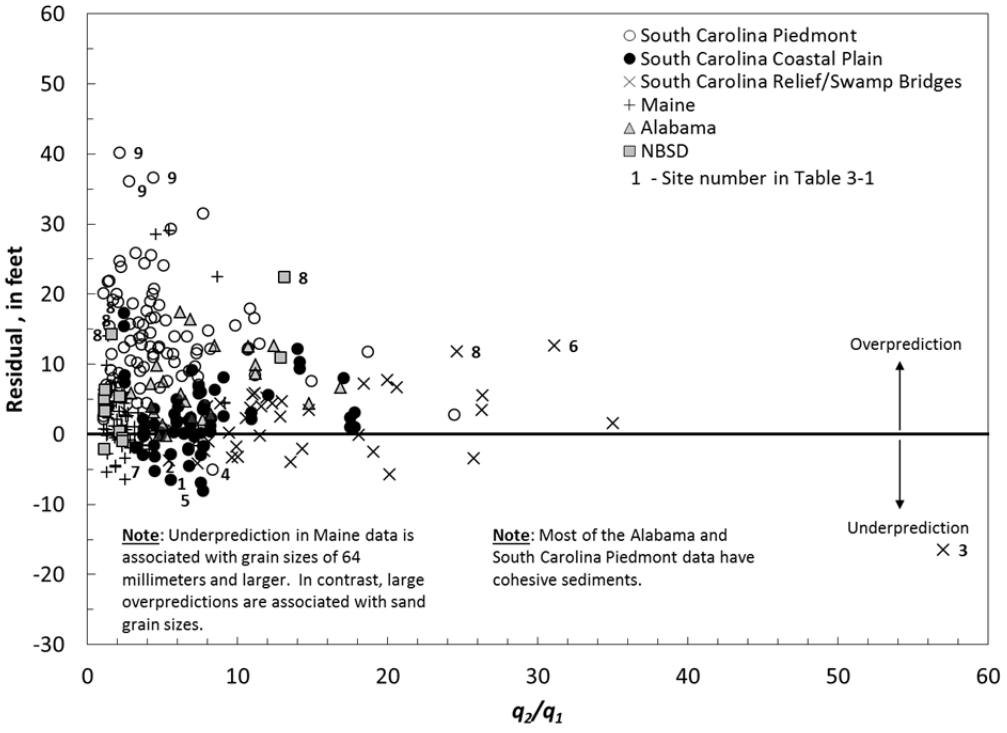

Figure 3-14. Relation of prediction residuals and the unit discharge ratio, q_2/q_1, for selected field data applied to the NCHRP 24-20 scour prediction method.

iii. Prediction Residuals with Respect to *D50*

The median grain size of the sediment, *D50*, is used in equation 2-4 to estimate the clear-water contraction-scour depth, which is the prominent type of scour in the USGS field data. The relation of the prediction residuals with respect to *D50* (figure 3-15) indicates frequent and larger overprediction for *D50* less than about 0.2 mm. In general, these data are associated with cohesive sediments, providing a reasonable explanation for this pattern. More frequent underprediction begins to occur at a *D50* of about 0.1 mm where the non-cohesive data become dominant. When excluding the data from table 3-1, much of the non-cohesive data have an approximate symmetric scatter about the zero line, with the frequency and magnitude of overprediction being larger than that for underprediction. This pattern indicates no strong trend towards under- or overprediction associated with *D50* for non-cohesive sediments. Excluding the Sturm (2004) data, a comparison of the laboratory (figure 3-7B) and field residuals (figure 3-15) shows some similarity in the scatter about the zero line for non-cohesive sediments for clear-water scour conditions, confirming the patterns in the field data.

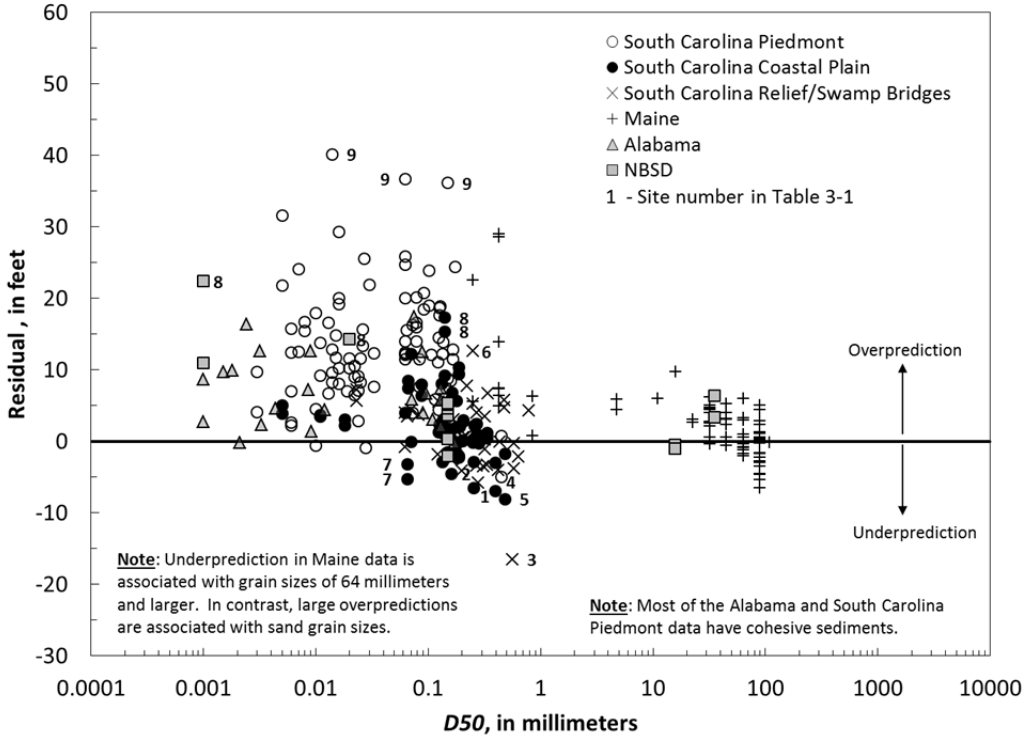

Figure 3-15. Relation of prediction residuals and the median grain size, *D50*, for selected field data applied to the NCHRP 24-20 scour prediction method.

iv. Prediction Residuals with Respect to L/y_1

Melville and Coleman (2000) used the relative abutment length, L/y_1, to classify abutments as short, intermediate, and long and demonstrate that the potential for abutment-scour increases as the abutment length increases (report section 1.3.2 and figure 1-12). The relation of the prediction residuals with respect to relative abutment length, L/y_1, is shown in figure 3-16. The figure identifies the range for short, intermediate, and long abutments as defined by Melville and Coleman (2000) and indicates how the field data are heavily weighted towards relatively long abutments. As noted previously, the large overprediction for the cohesive data is to be expected from the NCHRP 24-20 method, which is intended for non-cohesive sediments in its current formulation. When excluding the data from table 3-1, much of the non-cohesive data have an approximate symmetric scatter about the zero line, with the frequency and magnitude of overprediction being moderately larger than that for underprediction. This pattern indicates no strong trend towards under- or overprediction associated with L/y_1 for non-cohesive sediments. However, if the data from table 3-1 are considered, the magnitude of underprediction increases with increasing L/y_1, indicating the potential for increased underprediction at relatively long abutments. This is similar to the pattern in the laboratory data (figure 3-8) but not as pronounced. While the 3 largest underpredictions (site numbers 1, 5, and 3) have unique features that likely promote larger scour depths, it is possible that other factors, such as relatively long abutments, contribute to this pattern. Improved estimates of the flow velocity at the abutment from a two-dimensional flow model would likely diminish the underprediction at these sites. However, the uncertainty in the data in figure 3-16, in conjunction with the trends of the laboratory data (figure 3-8), indicates a need for caution and conservatism at such sites when assessing abutment scour with the NCHRP 24-20 prediction method.

v. Prediction Residuals with Respect to y_1

The approach flow depth, y_1, is used directly or indirectly in equations 2-2 through 2-4 for predicting abutment scour, and the relation of the prediction residuals with respect to y_1 is shown in figure 3-17. When excluding the data from table 3-1, much of the non-cohesive data for the South Carolina Relief/Swamp Bridges, the Coastal Plain, the NBSD, and Maine have an

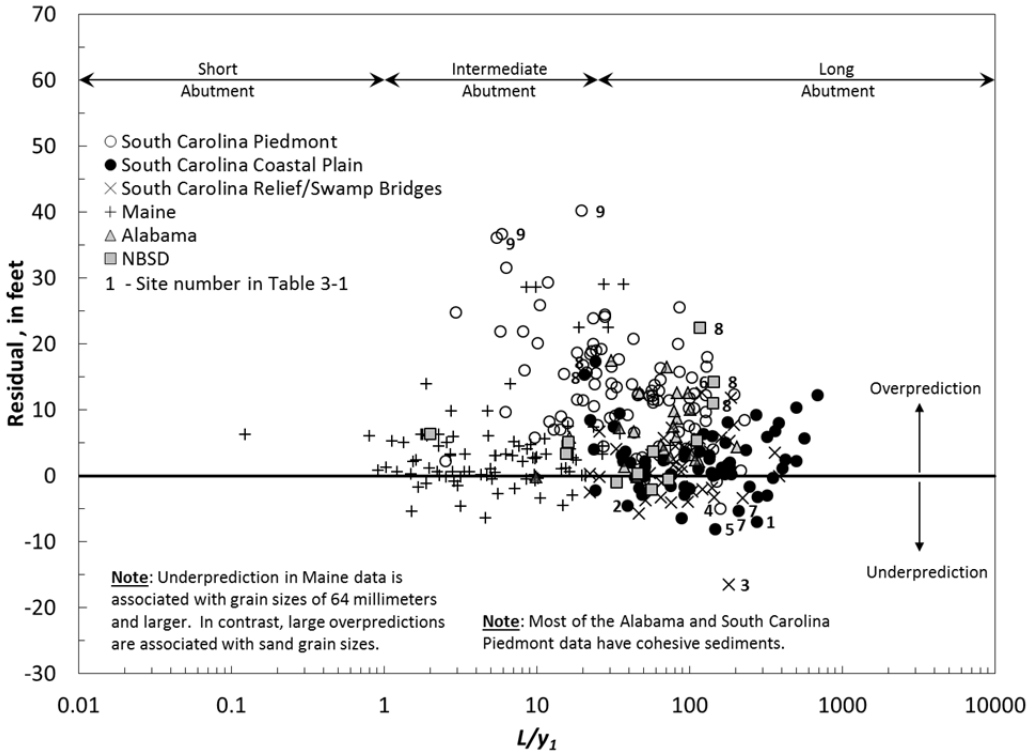

Figure 3-16. Relation of prediction residuals and the relative abutment length, L/y_1, for selected field data applied to the NCHRP 24-20 scour prediction method.

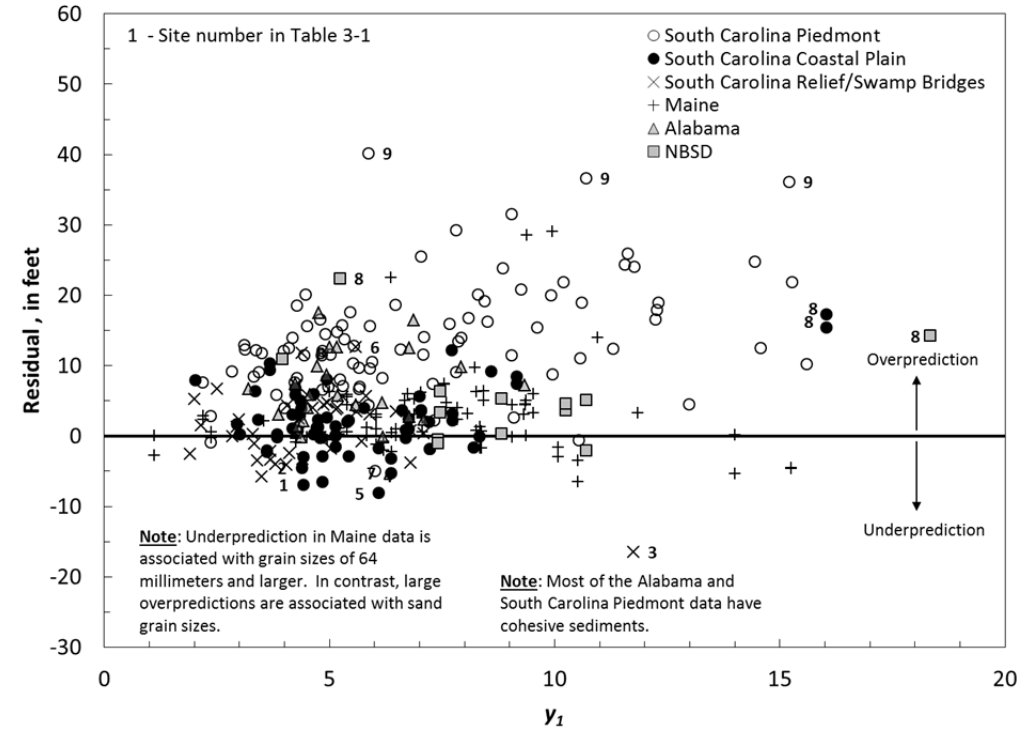

Figure 3-17. Relation of prediction residuals and the flow depth, y_1, for selected field data applied to the NCHRP 24-20 scour prediction method.

approximate symmetric scatter about the zero line, with the frequency and magnitude of overprediction being moderately larger than that for underprediction. In the coarse sediments of Maine, there is more frequent underprediction for flow depths greater than about 10 ft, indicating a possible small trend towards underprediction with increasing flow depth. Overall, the residual patterns for the non-cohesive sediments in the sand range indicate no strong trend towards under- or overprediction associated with y_1, while there is likely a small trend in the coarse sediments of the Maine data. In the cohesive sediments of the South Carolina Piedmont, the magnitude of overprediction is large and increases with increasing flow depth. The residual patterns in the non-cohesive laboratory data (figure 3-9) differ from those of the non-cohesive field data (figure 3-17), showing an increase in overprediction with increasing flow depth, similar to the cohesive sediments in the field data. The reason for the difference between the laboratory and field data is unclear.

vi. Prediction Residuals with Respect to α

The amplification factor accounts for the additional scour at an abutment above and beyond the contraction scour (equation 2-1), and the relation of the prediction residuals with respect to the amplification factor, α, is shown in figure 3-18. The trend in the data indicates that the potential for underprediction increases as α decreases, with the largest underprediction associated with values of α near 1.1. This pattern is particularly evident in the long abutments associated with South Carolina Relief/Swamp Bridge and the Coastal Plain data. If the data in table 3-1 are excluded, the pattern is less pronounced, though still evident. While not as prominent, the longer abutments in the laboratory data (figure 3-10) have a similar trend, with the magnitude of underprediction increasing slightly with decreasing α. A number of field data have common amplification factors with values of 1.1 and 1.13. These data have large values of q_2/q_1 that exceed the upper bound of the amplification-factor curves (figures 2-3 through 2-6); therefore, α was arbitrarily set to values of 1.1 or 1.13, representing the α associated with the maximum value of q_2/q_1 in the curves. The South Carolina Piedmont and Alabama data have infrequent underprediction and larger overprediction values in comparison to the other field data and is attributed to the cohesive sediments associated with those data. A more detailed evaluation of α is presented in the next report section.

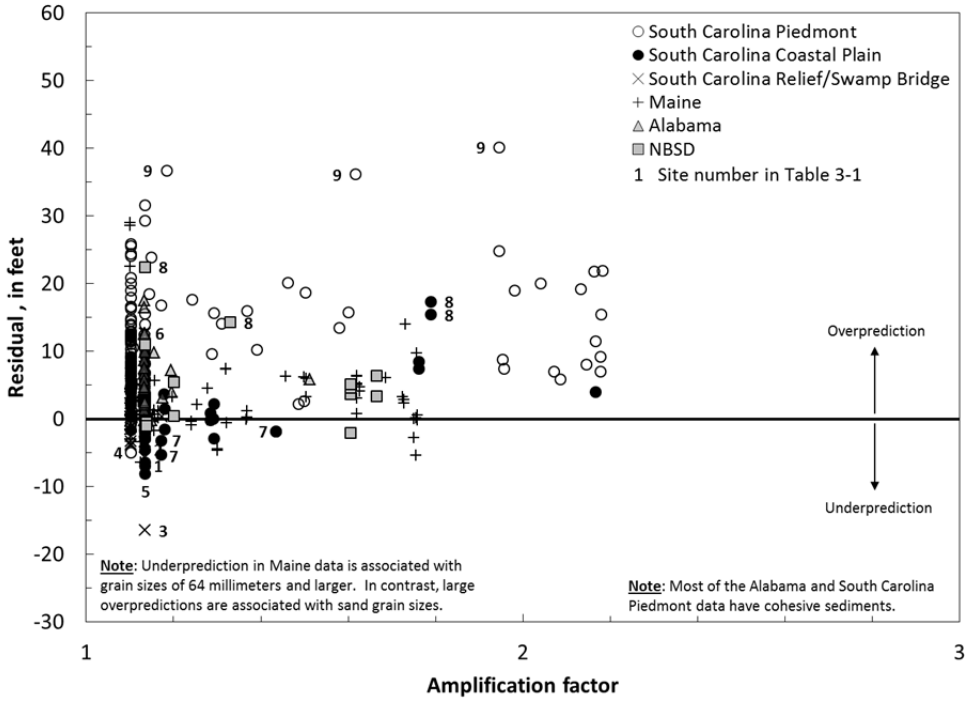

Figure 3-18. Relation of prediction residuals and the amplification, α, for selected field data applied to the NCHRP 24-20 scour prediction method.

3.4 Evaluation of the Amplification Factor

The amplification factor is an important explanatory variable in the NCHRP 24-20 method as can be deduced by a review of equation 2-1. The amplification-factor curves (figures 2-3 through 2-6) represent hand-drawn envelope curves of the laboratory data, where α was determined by equation 3-1:

$$\alpha = Y_{MAX} / Y_C \qquad (3\text{-}1)$$

where

Y_{MAX} is the measured flow depth in the abutment-scour hole, in feet, and

Y_C is the reference contraction-scour flow depth, in feet, determined by equation 2-3 or 2-4.

In a review of abutment-scour research and prediction equations, Sturm et al. (2011) made a limited comparison of amplification factors from selected laboratory data. The relation of α and the unit discharge ratio for wing-wall and spill-through abutments associated with the Briaud et al. (2009) abutment-scour equation can be compared to the NCHRP 24-20 curves for Scour Condition B (figures 2-5, 2-6, and 3-19). (Note: The Briaud et al. (2009) curves reflect design curves with a factor of safety.) Sturm et al. (2011) notes that the peaks of the Briaud et al. (2009) curves are higher than the NCHRP 24-20 curves and have a more gradual decrease in α as the unit discharge increases. Sturm et al. (2011) also compares the NCHRP 24-20 α curve for wing walls under Scour Condition B with selected data from Melville (1997), Melville and Coleman (2000), and Sturm (2004, 2006; figure 3-20). The trends in the other laboratory data in figure 3-20 exceed that of the NCHRP 24-20 curve. Sturm et al. (2011) attributes the difference in the NCHRP 24-20 curves and the other laboratory data curves in figures 3-19 and 3-20 to the differing laboratory models. The NCHRP 24-20 experiments for Scour Condition B used erodible abutments/embankments (and not rigid abutments that extended to depth in the model bed or floodplain) that could erode to varying degrees. Sketches of this conceptual model are shown in figure 3-21. The erodible abutments create flow fields that tend to reduce scour depth in comparison to rigid abutments. Data associated with erodible abutments/embankments were used to develop the NCHRP 24-20 amplification curves for Scour Condition B, with selected data from that investigation shown in figure 3-20. In contrast, the other laboratory data shown in figure 3-20 represent scour associated with rigid abutment/embankment models that had rigid substructures below the bed. These types of models tend to produce larger scour depths than the erodible abutments in the NCHRP 24-20 experiments and provide a reasonable explanation for the differing amplification factors in figure 3-20.

The NCHRP 24-20 study is the most extensive laboratory investigation to date of scour at erodible abutments/embankments and provides valuable insights on abutment-scour processes at eroded abutments and breached embankments. Additionally, Ettema et al. (2010) provide anecdotal evidence that these types of scour processes are common occurrences in the field. (Note: The author has seen these types of scour processes and would concur that they are common.) While it seems appropriate to say that such scour processes are common, it would seem incorrect to assume that they are the solitary mode of abutment scour in the field. Evidence indicates that many abutments in the field can sustain high flows with minimal erosion and no

embankment failure. Perhaps the best example of this can be found in the USGS abutment-scour field data where there is little indication of appreciable erosion of the abutments or embankment breaches. As such, the USGS data represent abutment scour resulting from abutments/embankments that remained intact during the scour process and, therefore, would possibly have larger scour depths than those associated with eroded abutments as modeled in the NCHRP 24-20 investigation. (Note: Vegetation growth on the embankment/abutment and varying degrees of cohesion in the embankment fill material are a likely cause of the embankments/abutments in the USGS data remaining intact.) This implies that the amplification curves for the NCHRP 24-20 may be too low for intact abutments and therefore, may underpredict scour at sites such as those in the USGS abutment-scour database. If the objective is to design a bridge that can sustain a large flood with the abutments and embankments remaining intact, the practitioner will need to evaluate the appropriateness of using the NCHRP 24-20 prediction method in its current formulation for the study's design objectives. A way to address this concern would be the inclusion of an appropriate abutment-scour countermeasure, which is recommended as a standard design procedure by Sturm et al. (2011) for all new abutment designs.

The trends in figures 3-19 and 3-20 indicate how amplification factors can vary substantially for various laboratory datasets and highlight the challenge in defining this explanatory variable. It could be argued that the amplification curves associated with the rigid-abutment models, such as the upper curve shown in figure 3-20, is too excessive for field conditions and will produce unrealistically large estimates of abutment scour. Some support for this argument can be found in figure 1-21 where the upper bound of the relative scour depth for the field data (4.2) is much smaller than that for the rigid abutment models of the Sturm (2004) data (11). However, as previously noted, the NCHRP 24-20 amplification curves based on the erodible abutment/embankment models may be too low for some field conditions and may produce underprediction at abutments with minimal erosion that remain intact during a flood. To gain insight on the range and trend of the amplification factor in the field, field data can be used to back-calculate the required amplification factor, which is described in the following report section.

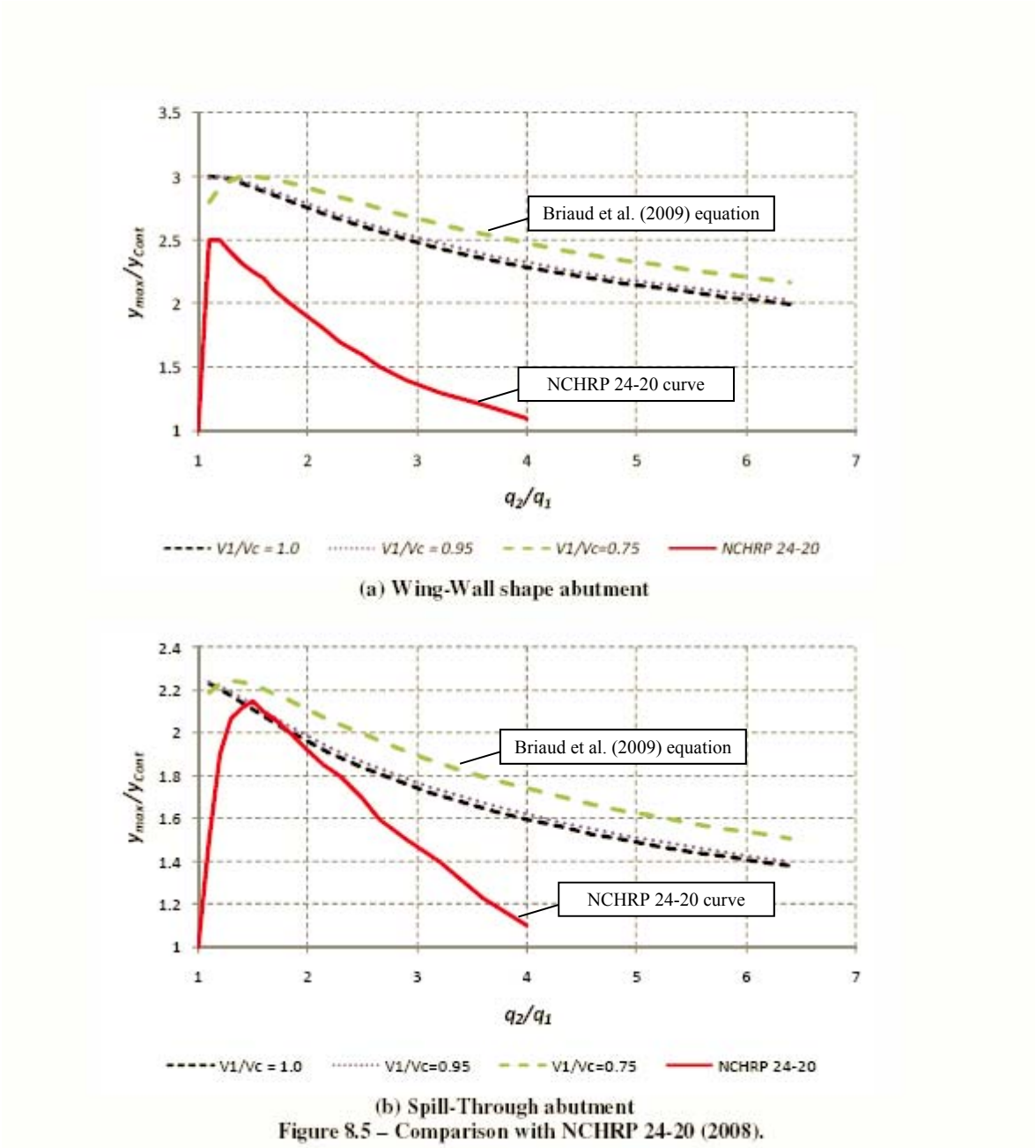

Figure 3-19. Relation of the amplification factor and the unit discharge ratio for wing-wall and spill-through abutments based on the Briaud et al. (2009) formula and the NCHRP 24-20 curve for Scour Condition B (from Sturm et al. 2011). (Note: The Briaud et al. (2009) curves reflect design curves with a factor of safety.)

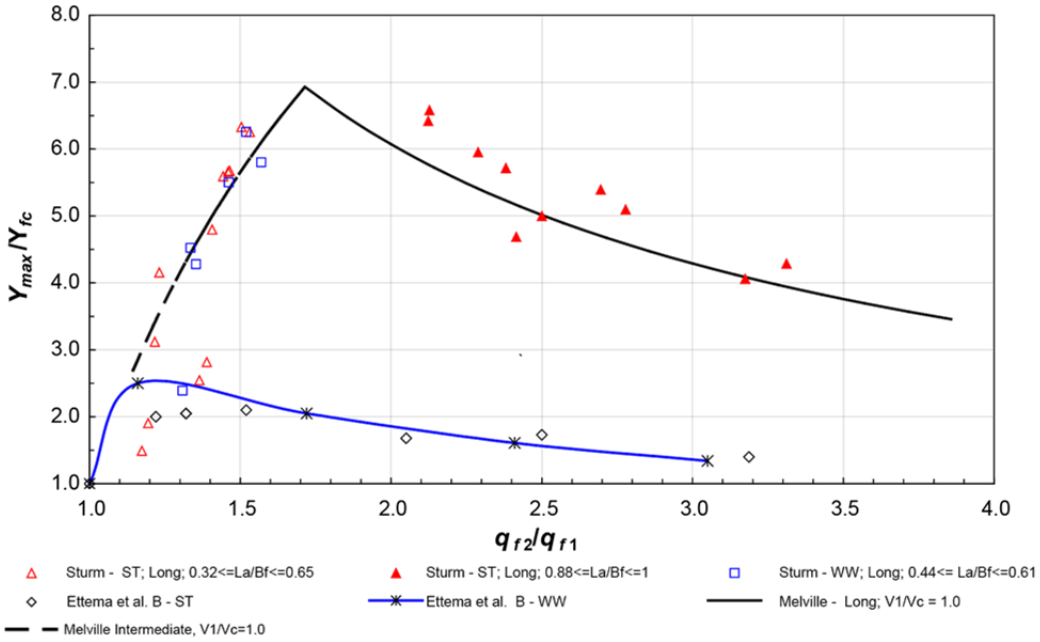

Figure 3-20. Relation of the amplification factor and the unit discharge ratio based on data from Melville (1997), Melville and Coleman (2000), Sturm (2004, 2006), and the NCHRP 24-20 curve (from Sturm et al. 2011).

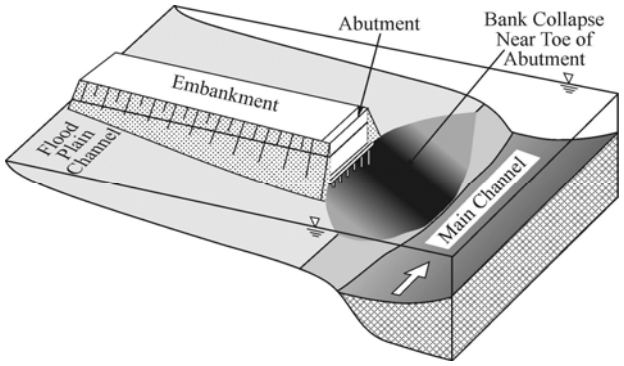

(*A*)

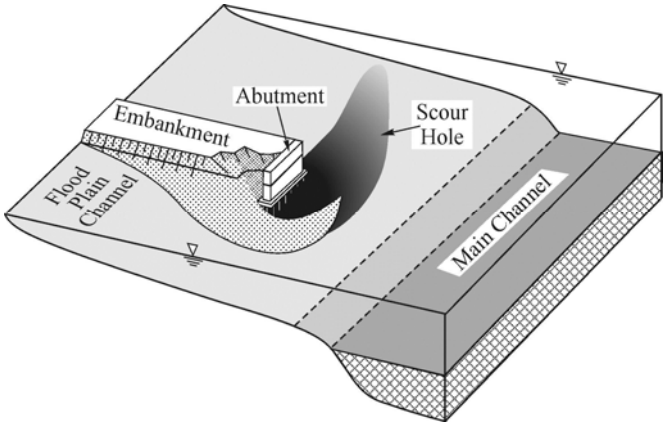

(*B*)

Figure 3-21. Conceptual model for (*A*) Scour Condition A - hydraulic scour of the main-channel bed causes bank failure, which causes a failure of the face of the abutment embankment, and (*B*) Scour Condition B - hydraulic scour of the floodplain causes failure of the face of the abutment embankment (from Ettema et al. 2010).

3.4.1 Determination of the Required Amplification Factor

Ettema et al. (2006) made a limited comparison of amplification factors derived from selected field data with the NCHRP 24-20 amplification curves (figure 3-22). The selected field data in figure 3-22 were taken from Mueller and Wagner (2005) and Benedict (2003). Ettema et al. (2010) concluded that the limited comparison indicated that the NCHRP 24-20 amplification curves produced scour-depth estimates that reasonably concur with those observed in the field, but that further evaluation was needed. To gain further insights regarding the range of amplification factors associated with field data, equation 3-1 can be used to back-calculate the required amplification factor that would force the NCHRP 24-20 method to match the field measurement of abutment scour. Applying equation 3-1 in this manner would require using the field measurement to represent Y_{MAX}. The value of Y_C would be determined from equations 2-3 or 2-4 for the site of interest. This technique was first applied to the laboratory data (table 1-3), and results are shown in figure 3-23. Because the NCHRP 24-20 amplification-factor curves include only spill-through and wing-wall abutments, the laboratory data in figure 3-23 were limited to these types of abutments. Additionally, the Sturm (2004) data associated with Scour Condition A were excluded because of the uncertainty regarding the hydraulic conditions near the channel. A review of figure 3-23 indicates that a substantial number of data exceed the NCHRP 24-20 amplification-factor curves. The large amplification factors associated with the Sturm (2004) data can be attributed, in part, to the longer relative abutment lengths associated with those data. Neglecting the Sturm (2004) data and the 2 outliers from the Palaviccini (1993) data, the largest required amplification factor is about 3.7. As noted by Sturm et al. (2011), the larger amplification factors are likely created, in part, by the rigid abutments used in the other laboratory models in contrast to the erodible abutments/embankments used in the NCHRP 24-20 models. In particular, as the scour hole develops, the rigid abutment substructure below the bed will tend to strengthen the local flow field at the modeled abutment, thereby increasing the potential for scour.

The required amplification factors associated with the USGS field data for Scour Conditions A and B are shown in figure 3-24. The large scatter in this figure (3-24) is not atypical for field data and can be attributed, in part, to the complex field conditions that diverge from those of the laboratory, as well as the uncertainty of the field data. A large percentage of the required

amplification factors for the field data fall within the range of the NCHRP 24-20 amplification-factor curves, providing a measure of support for the curves. The smallest required amplification factors on figure 3-24 are primarily associated with the cohesive sediments of the Piedmont. Because the current formulation of the NCHRP 24-20 method is primarily for non-cohesive sediments, these small required amplification factors for the cohesive sediments is to be expected. For Scour Condition A (figure 3-24A), the required amplification factors for the Maine data that exceed the curves have sediment sizes greater than about 64 mm, and the prediction error is relatively small, with all but one value of underprediction being less than 3 ft. A few required amplification factors from the other data groups exceed the curves in figure 3-24A, but not excessively. While the exceedance of the amplification curves in figure 3-24A is not excessive, it still is of some concern and may indicate a need to adjust the curves higher. If an offset of 0.4 is added to the spill-through amplification curve, as shown in figure 3-24A, the majority of the data is included within the offset curve. Other factors may contribute to the required amplification factors exceeding the NCHRP 24-20 curve, making it difficult to conclude that the offset curve is an appropriate adjustment. However, the data trends do suggest that some adjustment may be appropriate.

All of the required amplification factors exceeding the curves for Scour Condition B (figure 3-24B) are from the South Carolina Coastal Plain and Relief/Swamp Bridge data. If the data in table 3-1 are excluded from figure 3-24B, most of the other data exceeding the line are in close proximity to the amplification curve, indicating that the curve is approximating the trend of the field data. Better estimates of the flow velocity at the abutment, such as from a two-dimensional model, would likely reduce the magnitude and frequency of data exceeding the amplification factor curves. While the data patterns in figure 3-24B provide some support for the NCHRP 24-20 amplification curves, the exceedance still is of some concern, and as noted previously, may indicate a need to adjust the curves higher, especially to account for scour at intact abutments in the field. Following the pattern in figure 3-24A, a curve with an offset of 0.4 added to the spill-through amplification curve is shown in figure 3-24B, and the number of the required amplification factors exceeding the offset curve is smaller. The offset curves in figure 3-24 provide some perspective on how an offset applied to the NCHRP 24-20 amplification curves could be used to reduce the frequency of underprediction.

The patterns of the required amplification factors in figure 3-24 provide some measure of support for the validity of the NCHRP 24-20 amplification curves. However, additional verification and modification of these curves may be needed because the NCHRP 24-20 amplification curve for Scour Condition B is for erodible abutments and (or) embankments and because there is some exceedance. In particular, some additional thought and consideration should be given to the amplification curves with respect to intact abutments in the field. Because other factors are likely contributing to the exceedance patterns in figure 3-24, it is difficult to modify the amplification curves with confidence only based on the results in figure 3-24. A possible way to refine the analysis of the required amplification factors as shown in figure 3-24 would be to redo the analysis at a strategically selected sample of sites by using a two-dimensional flow model. This second analysis would reduce the potential error associated with the less accurate estimates of flow velocity from one-dimensional flow models, providing better estimates of the required amplification factors. For the current amplification curves, figure 3-24 indicates the need for conservative estimates of the maximum velocity at the abutment and perhaps some offset applied to the amplification factor to reduce the potential for underprediction.

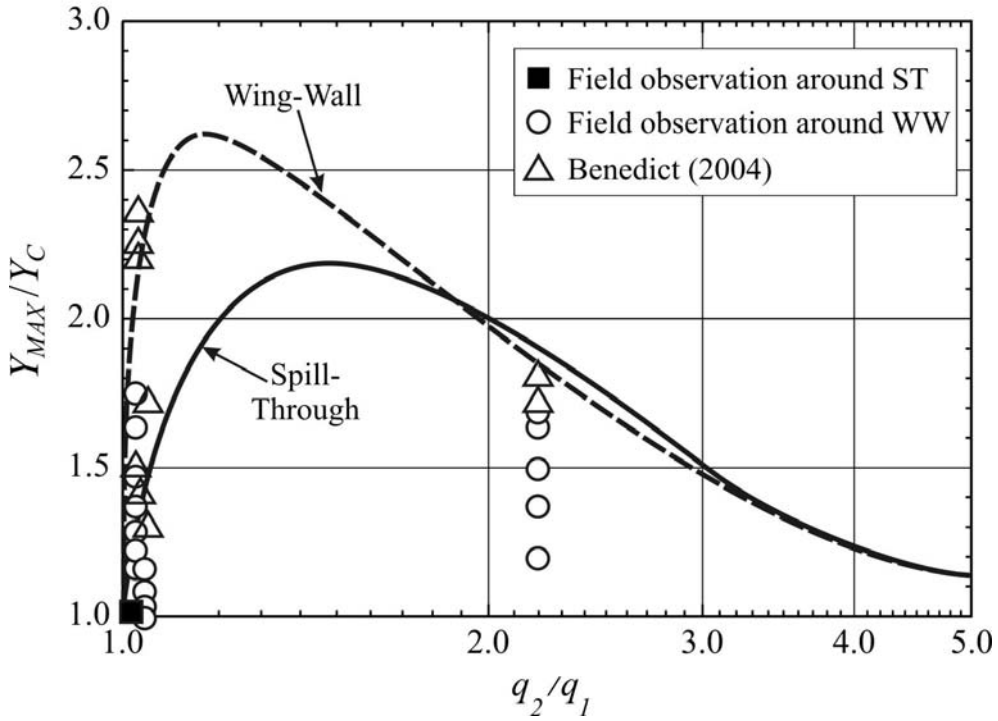

Figure 3-22. Relation of the required amplification factor and the unit discharge ratio for selected field data compared with the NCHRP 24-20 amplification-factor curves (from Ettema et al. 2010).

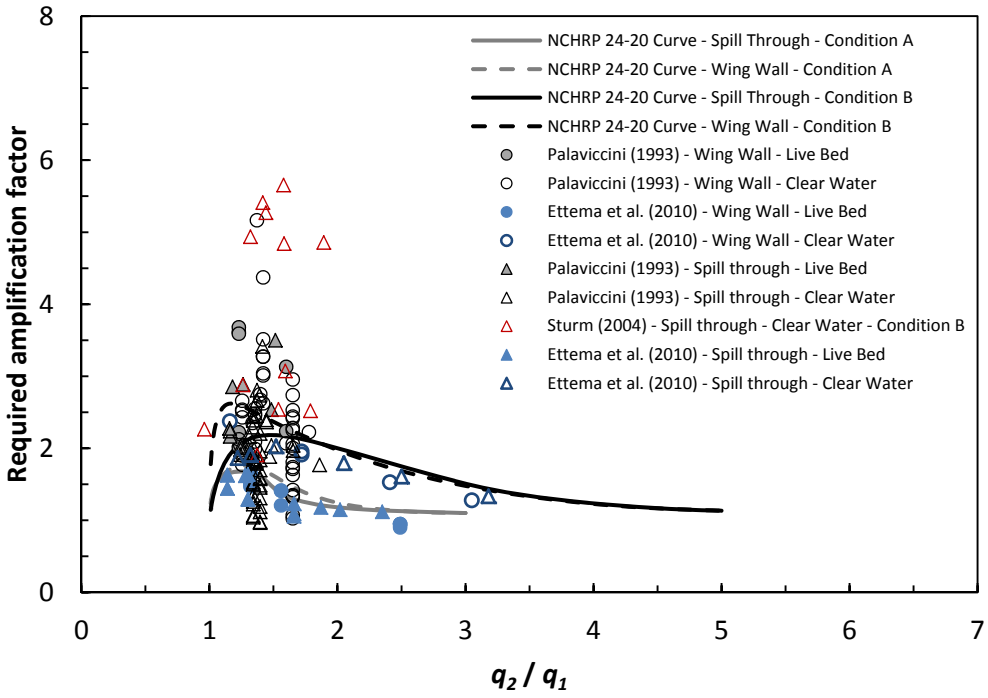

Figure 3-23. Relation of the required amplification factor and the unit discharge ratio for selected laboratory data compared with the NCHRP 24-20 amplification-factor curves.

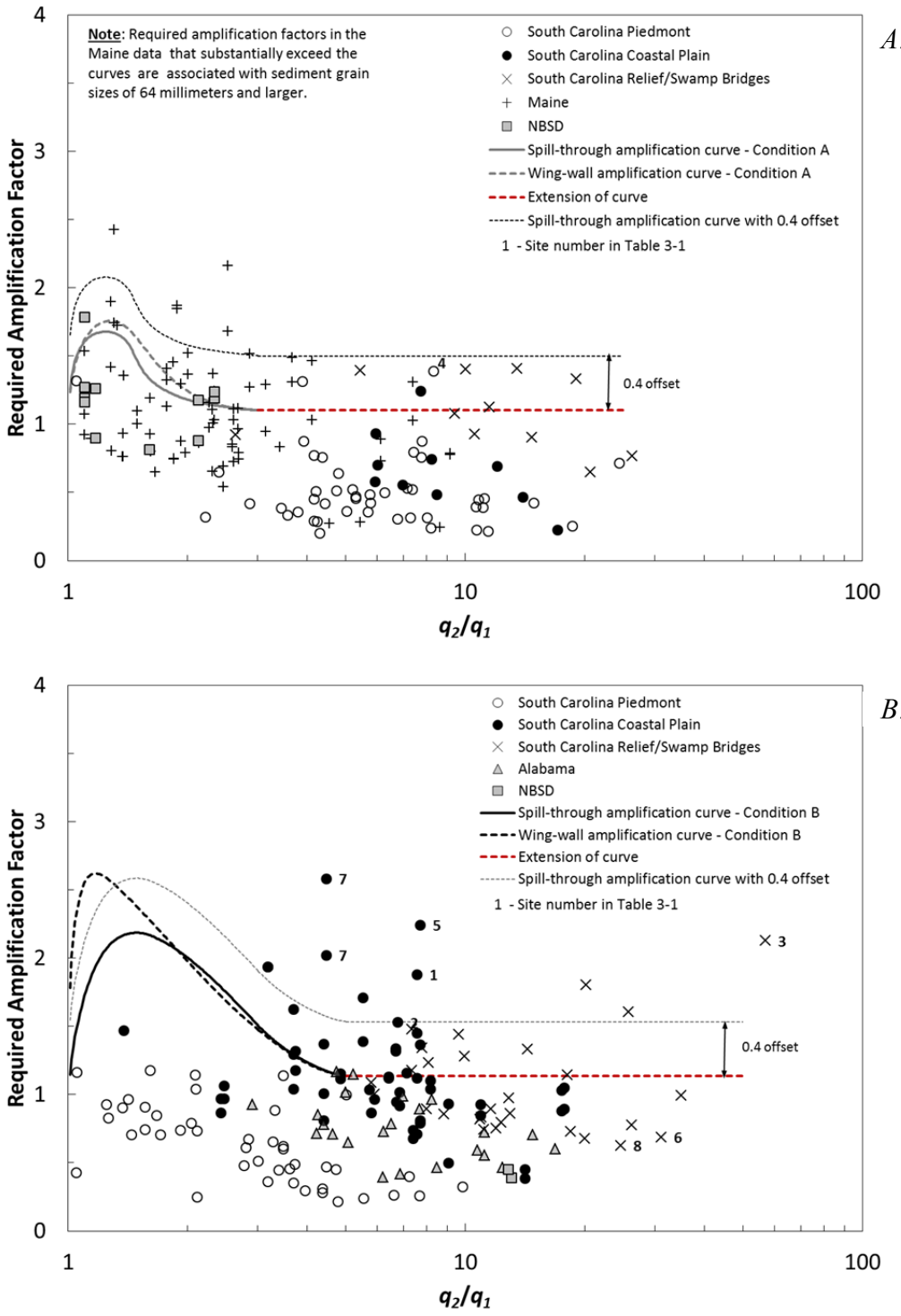

Figure 3-24. Relation of the required amplification factor and the unit discharge ratio for selected field data with (*A*) Scour Condition A and (*B*) Scour Condition B, compared with the NCHRP 24-20 amplification curves.

3.5 Prediction Trends for Cohesive and Non-Cohesive Sediments

Figures 3-25 and 3-26 are the same data shown in figures 3-11 and 3-15, respectively, with the data grouped by the categories of cohesive and non-cohesive sediments. The trends in figures 3-25 and 3-26 indicate that cohesive sediments have the largest overpredictions. The NCHRP 24-20 method was developed for non-cohesive sediments, and therefore, the overprediction associated with cohesive sediments is to be expected. The NCHRP 24-20 method can be modified to include a contraction-scour prediction method that accommodates cohesive as well as non-cohesive sediments, thus reducing the excessive overprediction for cohesive sediments. Modifications of the NCHRP 24-20 method for cohesive sediments are examined later in report section 3.6. With regard to non-cohesive sediments, the relations in figure 3-25 display an approximate symmetric scatter about the line of agreement, with more frequent overprediction than underprediction. This pattern indicates that the NCHRP 24-20 prediction method, on average, is reflecting the general trend of the non-cohesive field data, with predicted scour depth increasing as measured scour depth increases. When measured abutment-scour depths are about 10 ft or larger, however, scour is frequently underpredicted. The linear trend line through the non-cohesive data (figure 3-25) indicates that the frequency and magnitude of underprediction increases with measured scour depth. (Note: If the non-cohesive sites in table 3-1 are excluded, the trend line is essentially the same as that in figure 3-25, indicating that these data do not strongly influence the average trend.) A more desirable pattern would be to have the trend line in figure 3-25 parallel the line of agreement indicating that the NCHRP 24-20 method is capturing the overall data trend for small and large measurements of scour. The current pattern indicates that underprediction will more likely occur for the larger measured scour depths. As noted previously, the underprediction can likely be attributed, in part, to less accurate estimates of the flow velocity at the abutment from one-dimensional flow models, and better estimates of the flow velocity, such as from a two-dimensional model, would likely reduce the number of underpredictions and improve the trend line. Overall, the relation in the non-cohesive data indicates that the NCHRP 24-20 method is approximating the trends of abutment scour in the field and that additional improvement could be obtained with better estimates of flow velocity. However, other factors besides low estimates of flow velocity are likely contributing to the underprediction in figure 3-25. The larger underpredictions in figure 3-25 are associated with

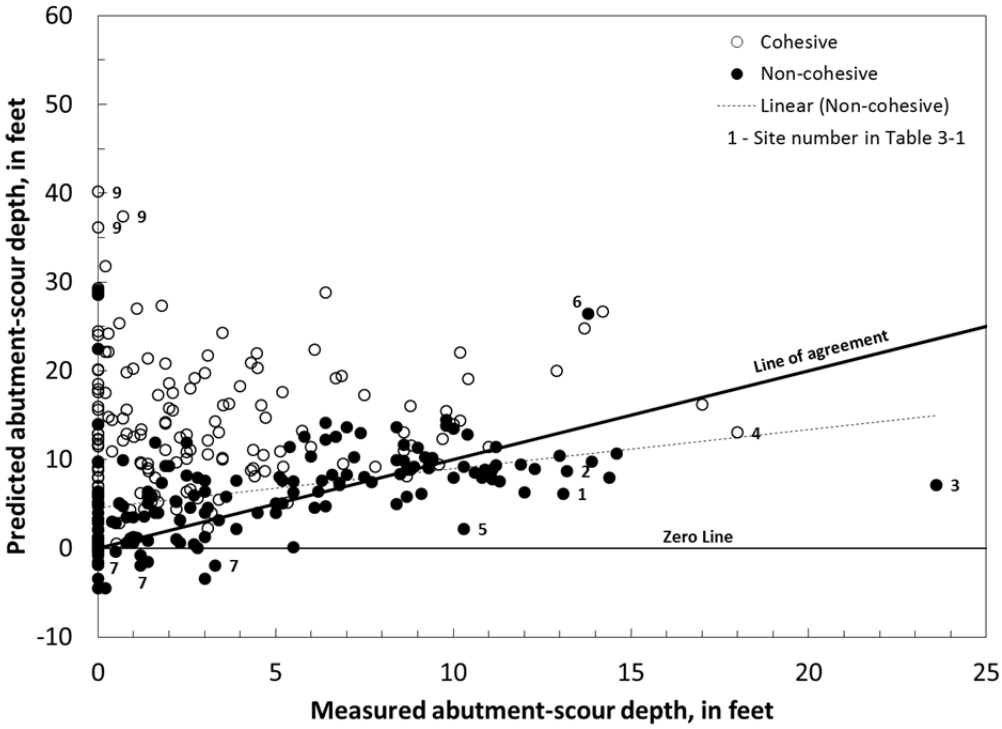

Figure 3-25. Relation of measured and predicted abutment-scour depth for cohesive and non-cohesive field data using the NCHRP 24-20 scour prediction method.

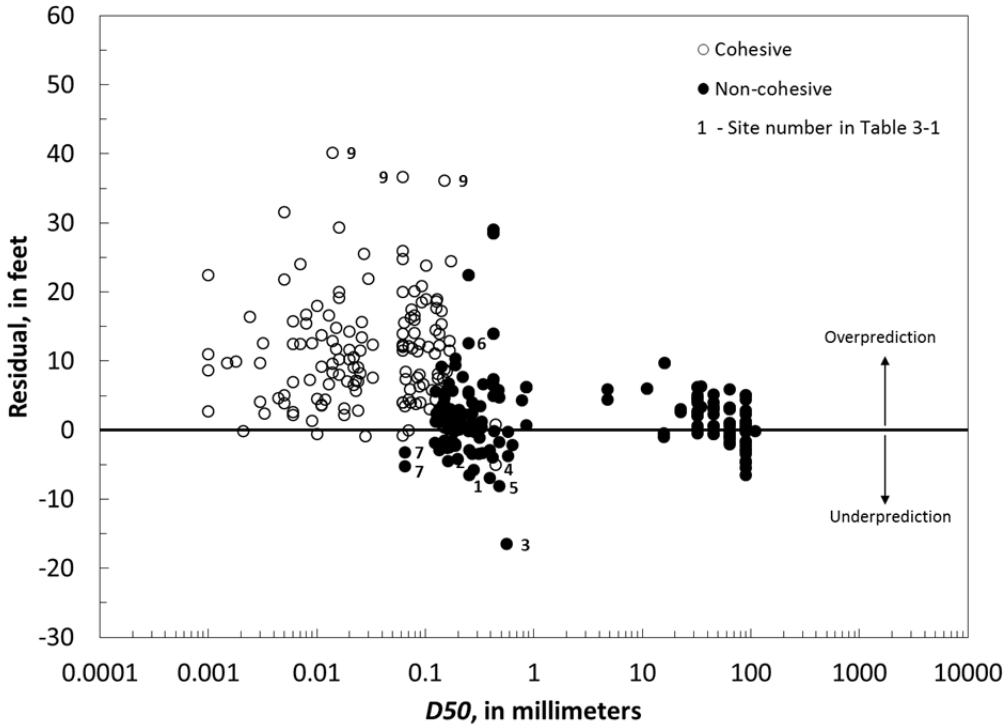

Figure 3-26. Relation of prediction residuals and the median grain size (*D50*) for the application of the NCHRP 24-20 scour prediction method for cohesive and non-cohesive field data.

relatively long abutments (figure 3-16) that likely have a larger potential for scour. The laboratory data also show a pattern of larger underprediction at relatively long abutments (figure 3-8), indicating that some adjustment for longer abutments as presented in Melville and Coleman (2000) may be a matter for consideration. While there is some uncertainty in the data in figure 3-25, the patterns indicate a need for caution and conservatism when using the NCHRP 24-20 prediction method at sites with relatively long abutments.

3.6 Alternate Critical-Velocity Methods for Estimating Clear-Water Contraction Scour

Approximately 93 percent of the USGS field data are classified as clear-water scour and therefore, use the clear-water contraction-scour equation (eq. 2-4) as part of the abutment-scour computation. Equation 2-4 can be expressed in simplified form as the following:

$$Y_c = {}^{q_2}/_{V_c} \qquad (3\text{-}2)$$

where

V_c is the sediment critical velocity at which a given sediment begins to erode, in feet per second,

and other variables are as previously defined.

The contracted unit discharge, q_2, in equation 3-2 can be determined by using the SBR method as described in chapter 2. Various methods can be used to estimate V_c. However, HEC-18 (Arneson et al. 2012) recommends using the Laursen (1963) critical-velocity equation for non-cohesive sediments as shown in the following equation:

$$V_c = K_u y^{1/6} {D_{50}}^{1/3} \qquad (3\text{-}3)$$

where

y is the average flow depth, in feet;

K_u is a unit conversion factor equal to 11.17 for English units;

and V_c and *D50* are as previously defined.

Substituting equation 3-3 into 3-2 leads to equation 3-4:

$$Y_c = {q_2}/{K_u y^{1/6} {D_{50}}^{1/3}} \quad (3\text{-}4)$$

To be physically consistent, the flow depth, *y*, in equation 3-4 must be equal to the flow depth in the contraction-scour hole, Y_C, which yields equation 3-5:

$$Y_c = {q_2}/{K_u {Y_c}^{1/6} {D_{50}}^{1/3}} \quad (3\text{-}5)$$

Simplifying equation 3-5 yields the same clear-water contraction-scour equation presented in chapter 2 (equation 2-4). Equation 2-4 is a useful tool for assessing clear-water contraction-scour flow depth. However, its application is limited to non-cohesive sediments; therefore, HEC-18 recommends limiting the *D50* to a value of 0.2 mm or greater. As can be seen in figures 3-25 and 3-26, the application of equation 2-4 to the USGS field data associated with cohesive sediments (all of which are clear-water scour) produce substantial overprediction. This pattern indicates that improved equation performance possibly could be achieved at sites with cohesive sediments (median grain sizes less than 0.2 mm) by using alternate methods for estimating the critical velocity in equation 3-2 that include critical velocities for cohesive sediments. Some methods for consideration include Fortier and Scobey (1926), Neill (1973), and Vanoni (1975). These alternate methods were used by Benedict (2010) in evaluating the performance of the Maryland abutment-scour equation (Chang and Davis, 1998, 1999). A brief description of these alternate critical-velocity methods (largely taken from Benedict, 2010) and their incorporation into the NCHRP 24-20 method, by use of equation 3-2, follows.

3.6.1 Fortier and Scobey Maximum Permissible Velocity

In the early 1900s, focus was given to the refinement of design criteria for earthen irrigation canals. An important component for the design criteria was the concept of the maximum permissible velocity. A notable investigation of this phenomenon was conducted by Fortier and Scobey (1926). This investigation was commissioned by the American Society of Civil Engineers (ASCE) Special Committee on Irrigation Hydraulics and involved an extensive survey

of the experienced irrigation engineers of that day. As Fortier and Scobey (1926) note, the weakness of these data is that they are based on the "personal deductions" of experienced engineers, "and not from experimental work." The data were tabulated into general soil groups for given flow conditions (table 3-2). The application of this table is simple in that it does not require the median grain size of the sediment. However, judgment is needed in selecting the appropriate soil category and flow condition, which introduces a measure of subjectivity into the method. As recommended in Yang (1996), critical velocities estimated by his method should be adjusted for flow depth by using the following adjustment factor:

$$K_{depth} = \left({}^{y}/_{3}\right)^{1/6} \qquad (3\text{-}6)$$

where

K_{depth} is the flow depth adjustment for the threshold velocity,

and y is as previously defined.

[Note: The denominator of equation 3-6 was set to 3 ft to represent the approximate flow depth in the canals associated with the permissible velocity estimates in Fortier and Scobey (1926).] Benedict et al. (2006) developed a graph that approximates the trends of the permissible velocity data presented in Fortier and Scobey (1926) (figure 3-27). Sediment sizes for this graph were estimated based on soil descriptions given in table 3-2, and curves for scour-resistant and less scour-resistant soils were developed. Using the appropriate curve from figure 3-27, the critical velocity, V_c, for the sediment of interest can be defined by the following equation:

$$V_c = \left({}^{y}/_{3}\right)^{1/6} V_{mpv} \qquad (3\text{-}7)$$

where

V_{mpv} is the Fortier and Scobey (1926) maximum permissible velocity determined from figure 3-27, in feet per second,

and y is as previously defined.

Substituting equation 3-7 into 3-2 leads to equation 3-8:

$$Y_c = {q_2}/{\left({y}/{3}\right)^{1/6} V_{mpv}} \quad (3\text{-}8)$$

To be physically consistent, the flow depth, *y*, in equation 3-8 must be equal to the flow depth in the contraction-scour hole, Y_C, which yields equation 3-9:

$$Y_c = {q_2}\Big/{\left({Y_c}/{3}\right)^{1/6} V_{mpv}} \quad (3\text{-}9)$$

Simplifying equation 3-9 yields equation 3-10:

$$Y_c = \left[1.2\left({q_2}/{V_{mpv}}\right)\right]^{6/7} \quad (3\text{-}10)$$

When applying equation 3-10 to the USGS field data, it was assumed that V_{mpv} for cohesive sediments would be best represented by the scour-resistant curve in figure 3-27 and non-cohesive sediments would be best represented by the less scour-resistant curve. (Note: The curves in figure 3-27 are approximate and should be used with caution.)

Table 3-2. Maximum permissible velocities from Fortier and Scobey (1926).

Original material excavated for canal	Velocity, in feet per second	
	For aged canal carrying clear water	For aged canal carrying water transporting silts
Fine sand (non-colloidal)	1.50	2.50
Sandy loam (non-colloidal)	1.75	2.50
Silt loam (non-colloidal)	2.00	3.00
Alluvial silts when non-colloidal	2.00	3.50
Ordinary firm loam	2.50	3.50
Volcanic ash	2.50	3.50
Fine gravel	2.50	5.00
Stiff clay (very colloidal)	3.75	5.00
Graded loam to cobbles, when non-colloidal	3.75	5.00
Alluvial silts when colloidal	3.75	5.00
Graded silt to cobble, when colloidal	4.00	5.50
Coarse gravel (non-colloidal)	4.00	6.00
Cobbles and shingles	5.00	5.50
Shales and hard pans	6.00	6.00

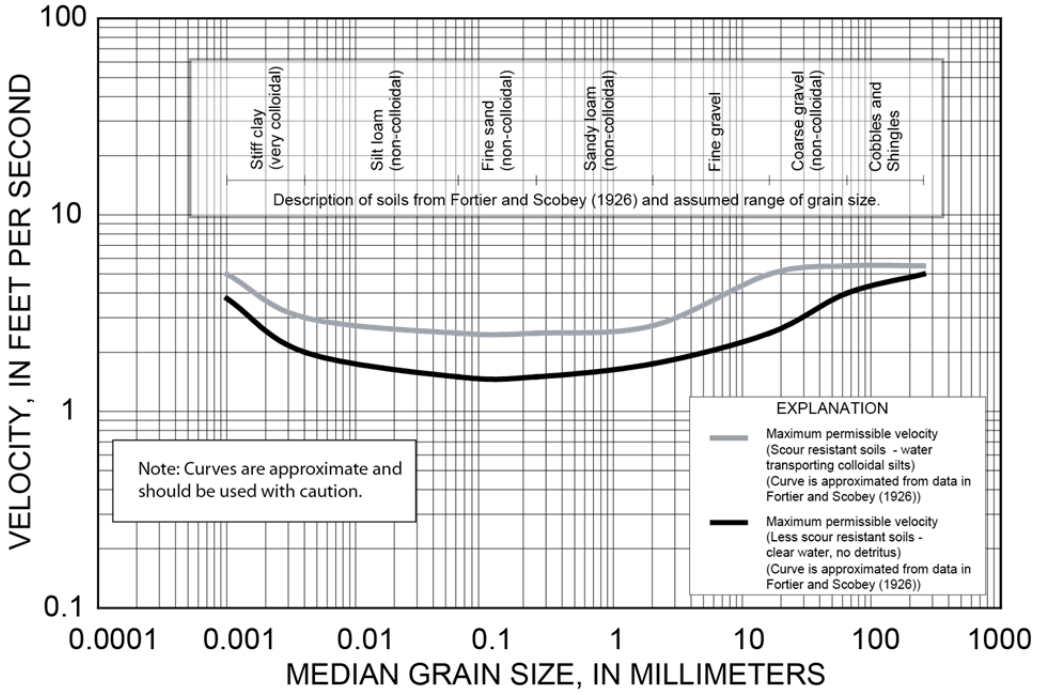

Figure 3-27. Critical-velocity curves for cohesive and non-cohesive sediments developed from Fortier and Scobey (1926) maximum permissible velocity field data. (Modified from Benedict et al. 2006.)

3.6.2 The Neill Critical-Velocity Curve

Using a combination of field and laboratory relations, Neill (1973) developed a family of curves (figure 3-28) for estimating critical velocities [called "the competent velocity" by Neill (1973)] for non-cohesive sediments for varying flow depths and grain sizes. Neill (1973) used a critical-velocity equation similar to the Laursen (1963) equation (eq. 3-3) to estimate the critical velocity for grain sizes greater than or equal to 0.1 ft (30 mm). For a grain size of 0.001 ft (0.3 mm), Neill (1973) used a field-derived regime equation for stable sand channels to estimate critical velocity. Having defined the critical velocities for a grain size of 0.001 ft (0.3 mm) and for grain sizes greater than or equal to 0.1 ft (30 mm), transition curves were hand-drawn for grain sizes between 0.001 ft (0.3 mm) and 0.1 ft (30 mm). Neill (1973) states that the transition curves "are not based on experimental data" and that "the entire diagram requires extensive testing in practice" and should be "treated with reservations." The Maryland abutment-scour equation (Maryland State Highway Administration, 2014) uses a modified version of Neill's (1973) curves (figure 3-29) presented in Benedict (2010), and equations for these curves are as follows:

$D50 \geq 0.1$ ft, $\quad V_c = 11.5 y^{0.167} D50^{0.33}$ (3-11)

$0.1 \text{ ft} > D50 \geq 0.0005$ ft, $\quad V_c = 11.5 y^{\left(0.123/D50^{0.2}\right)} D50^{0.35}$

$D50 < 0.0005$ ft, $\quad V_c = 0.8 y^{(0.562)}$

where variables are as previously defined. Substituting equation 3-11 into 3-2 and simplifying leads to equation 3-12:

$D50 \geq 0.1$ ft, $\quad Y_c = \left(q_2 / 11.5 D50^{1/3}\right)^{6/7}$ (3-12)

$0.1 \text{ ft} > D50 \geq 0.0005$ ft, $\quad Y_c = \left(q_2 / 11.5 D50^{0.35}\right)^{1/\left(1+0.123/D50^{0.2}\right)}$

$D50 < 0.0005$ ft, $\quad Y_c = \left(1.25 q_2\right)^{0.64}$.

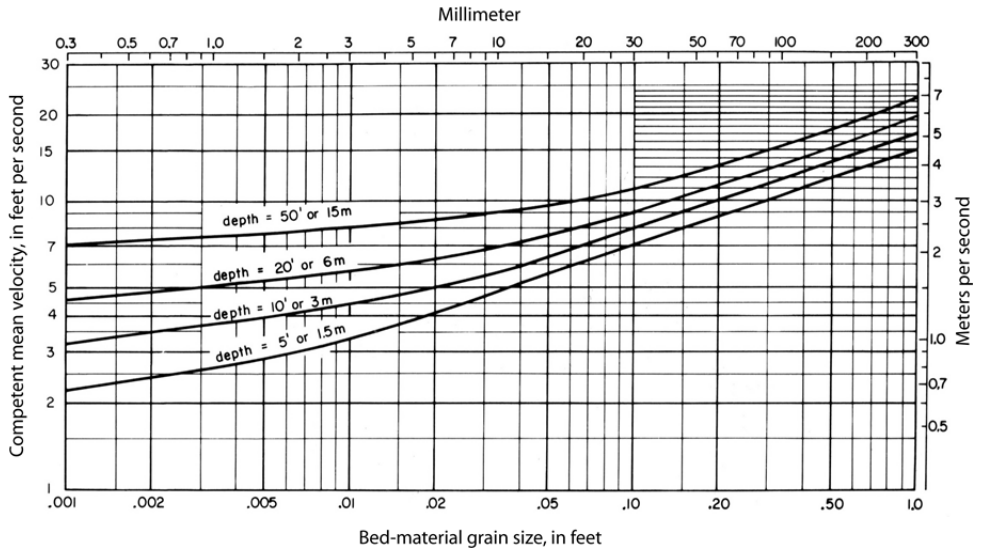

Figure 3-28. Critical-velocity curves for non-cohesive sediment as presented in Neill (1973).

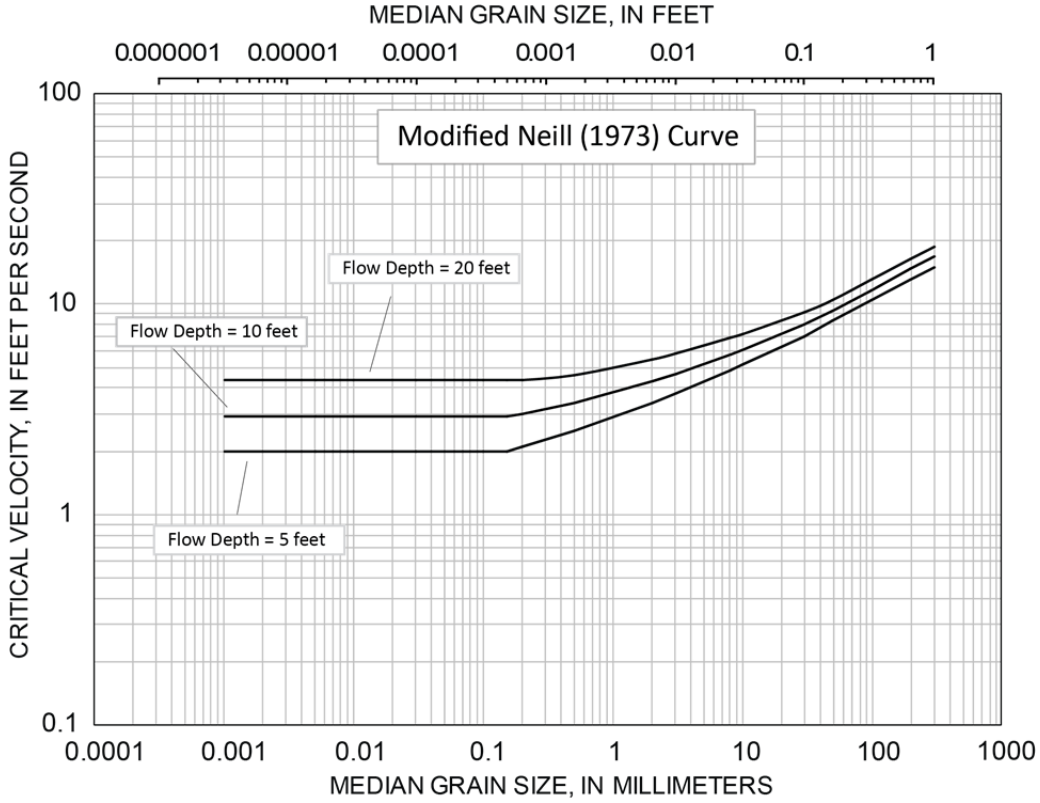

Figure 3-29. Modified Neill (1973) critical-velocity curves for non-cohesive sediment (modified from Benedict, 2010).

3.6.3 The Vanoni Critical-Velocity Curve

The ASCE Sedimentation Task Committee (Vanoni, 1975) reviewed and compiled laboratory data and limited field data to develop the critical-velocity curves shown in figure 3-30. For non-cohesive sediments greater than 0.01 mm, the curves include data from selected laboratory investigations. For grain sizes less than 0.01 mm (typically cohesive sediments), the ASCE committee relied upon maximum permissible velocity data presented in Fortier and Scobey (1926). Because of the scatter within the laboratory and field data, curves representing the lower limit, average, and upper limit of critical velocities were developed. Critical velocities determined with this method were adjusted for flow depth by using equation 3-6. By using the appropriate curve from figure 3-30, the critical velocity for the sediment of interest can be defined by the following equation:

$$V_c = \left({}^{y}/_{3}\right)^{1/6} V_{Vanoni} \qquad (3\text{-}12)$$

where

V_{Vanoni} is the Vanoni (1975) critical velocity unadjusted for flow depth, as determined from figure 3-30, in feet per second,

and other variables are as previously defined.

Following the same procedure used to develop equation 3-10 for the Fortier and Scobey (1926) maximum-permissible velocity, the following equation was developed:

$$Y_c = \left[1.2\left({}^{q_2}/_{V_{Vanoni}}\right)\right]^{6/7} \qquad (3\text{-}13)$$

For the current investigation, the upper and average curves were applied to the NCHRP 24-20 equation.

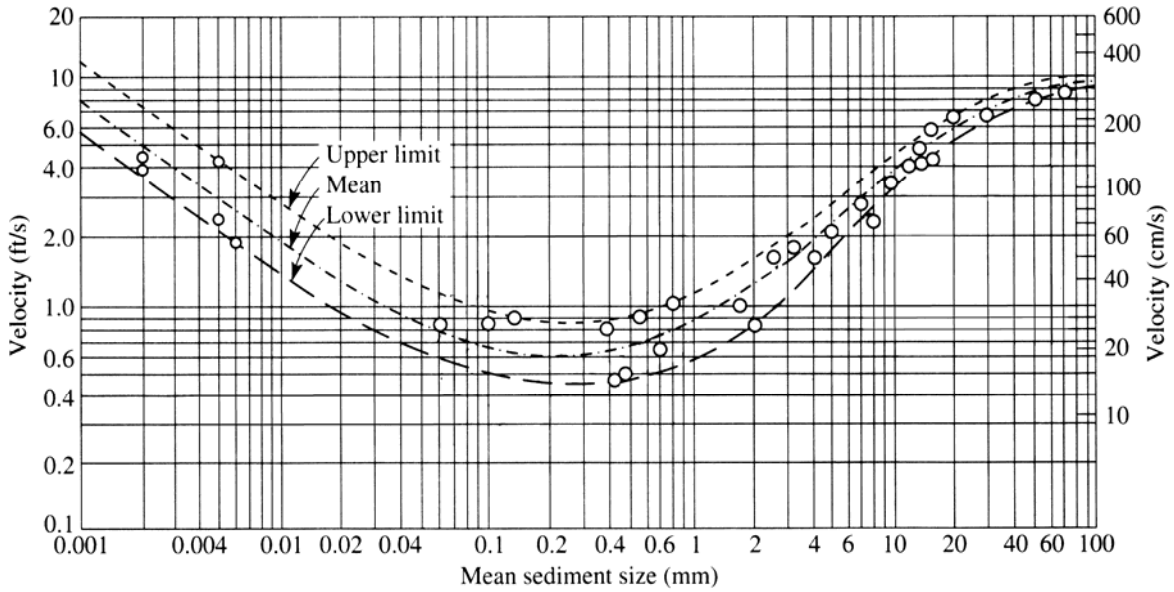

Figure 3-30. Vanoni (1975) critical-velocity curves for cohesive and non-cohesive sediments.

3.6.4 Application of Alternate Critical Velocities to the NCHRP 24-20 Method for Clear-Water Scour Sites

By using clear-water scour data (292 measurements) from the USGS field data, the alternate critical-velocity methods previously described were applied to the NCHRP 24-20 abutment-scour prediction method, and the results are presented below. Figure 3-31 shows the relation of predicted scour to measured scour for the data grouped by cohesive and non-cohesive sediments. Figure 3-32 shows the relation of prediction residuals (predicted minus measured scour) with respect to the median grain size. Results displayed in these figures show the sensitivity of the NCHRP 24-20 method to critical velocity for clear-water scour conditions. For cohesive sediments (primarily from the South Carolina Piedmont and Alabama), the Laursen (1963) equation and the upper Vanoni (1975) critical-velocity curve have frequent overprediction, which is sometimes excessive. There is only one underprediction for the cohesive sediments when using the Laursen (1963) equation. In contrast, there is frequent underprediction with the upper Vanoni (1975) curve for grain sizes less than about 0.03 mm. A review of the Vanoni (1975) upper curve (figure 3-30) indicates that the critical velocity substantially increases as *D50* decreases below about 0.03 mm, which in turn leads to more frequent underprediction. This indicates that limiting the *D50* value to about 0.03 mm when using the upper Vanoni (1975)

curve for cohesive sediments may yield better results for sites with a *D50* less than 0.03 mm. The Fortier and Scobey (1926) and modified Neill (1973) methods have similar prediction patterns for the cohesive data, with prediction residuals following more closely to the line of agreement (figure 3-31). The overpredictions are not as excessive as those for the Laursen (1963) and Vanoni (1975) methods. However, the underprediction for the Fortier and Scobey (1926) and modified Neill (1973) methods is of some concern.

With regard to the non-cohesive sediments, the Laursen (1963) and Fortier and Scobey (1926) methods have similar patterns with an approximate symmetry about the line of agreement (figure 3-31), with the Laursen (1963) method following the line of agreement more closely. However, underprediction tends to increase in magnitude as measured scour increases for both methods. The modified Neill (1973) method has the largest number of underpredictions for the non-cohesive sediments. The upper Vanoni (1975) curve has the smallest number of underpredictions for the non-cohesive sediments, and the underprediction for the largest observed scour (23.6 ft) is smaller than for the other critical-velocity methods.

The underprediction in figure 3-31 likely is caused, in part, by the less accurate estimates of flow velocity from the one-dimensional flow models, and performance could vary with better estimates of flow velocity. This should be kept in mind when evaluating the results. The patterns in figure 3-32 indicate that the Laursen (1963) method, currently used in the NCHRP 24-20 prediction method, is a reasonable method for non-cohesive sediments and underprediction possibly may be minimized with better estimates of flow velocity. For a more conservative estimate of abutment scour in non-cohesive sediments, the upper Vanoni (1975) curve may be appropriate. For cohesive sediments, the Fortier and Scobey (1926) and modified Neill (1973) methods minimize the excessive overprediction associated with the Laursen (1963) method. However, the frequent underprediction with these methods is of concern.

Benedict (2010) conducted a similar analysis with the Maryland abutment-scour equation (Chang and Davis, 1998, 1999) only using the South Carolina field data, and the results are shown in figure 3-33. The Maryland abutment-scour equation is similar in form to that of the NCHRP 24-20 method, with abutment scour being a function of contraction scour amplified by a series of amplification coefficients. A comparison of figures 3-31 and 3-33 shows similar prediction patterns between the two methods, highlighting the similarity of equation

performance. (Note: The different scales in figures 3-31 and 3-33 should be kept in mind when making comparisons.) The data applied to the Maryland equation in figure 3-33 are the South Carolina data grouped by the Piedmont and Coastal Plain regions. With only a few exceptions, these data correspond to cohesive and non-cohesive sediments, respectively, allowing a reasonable comparison to the cohesive and non-cohesive data in figure 3-31. Some application differences between the Maryland equation (figure 3-33) and the NCHRP 24-20 equation (figure 3-31) are as follows, and these should be kept in mind when making comparisons between the methods.

- The Maryland equation sets all negative scour prediction values to zero. In contrast, the application of the NCHRP 24-20 equation in figure 3-31 retains all negative values.

- The computation of the critical velocity in the Maryland equation (figure 3-31) used the actual *D50* and did not limit the *D50* to 0.2 mm. In contrast, the NCHRP 24-20 method (figure 3-31) set the *D50* to 0.2 mm if the actual *D50* was less than 0.2 mm. Therefore, sites having a *D50* less than 0.2 mm will tend to produce larger abutment-scour depths with the Maryland equation than with the NCHRP 24-20 method. A review of table 1-1 indicates that many of the USGS field data have *D50*s less than 0.2 mm, which will tend to produce more overprediction in the Maryland equation in contrast to the NCHRP 24-20 method. This trend is particularly noticeable in the cohesive sediments where *D50*s generally are less than 0.2 mm. The limiting of the *D50*s to a value of 0.2 mm in the NCHRP 24-20 method is likely a primary reason why that method produces less overprediction than the Maryland equation.

- A comparison of non-cohesive sediments in figure 3-31 with the Coastal Plain data (also non-cohesive) in figure 3-33 indicates that the Maryland and NCHRP 24-20 methods have similar patterns of prediction. However, the NCHRP 24-20 prediction method generally has smaller overpredictions and smaller scatter about the line of agreement. Table 1-1 indicates that many of the non-cohesive data have *D50*s less than 0.2 mm and, as described previously, this is likely a primary reason for the differing prediction patterns between the Maryland equation and the NCHRP 24-20 method.

- Based on the analysis of the Maryland equation by Benedict (2010; figure 3-33), the Maryland State Highway Administration (2014) recommends using the modified Neill (1973) critical-velocity curves (figure 3-29) in the Maryland equation for sites having characteristics similar to the Piedmont Physiographic Province of South Carolina. The Vanoni (1975) critical-velocity curves (figure 3-30) are recommended for sites having characteristics similar to the Coastal Plain Physiographic Province of South Carolina. Additionally, the Maryland State Highway Administration (2014) recommends safety factors be applied to the Maryland equation.

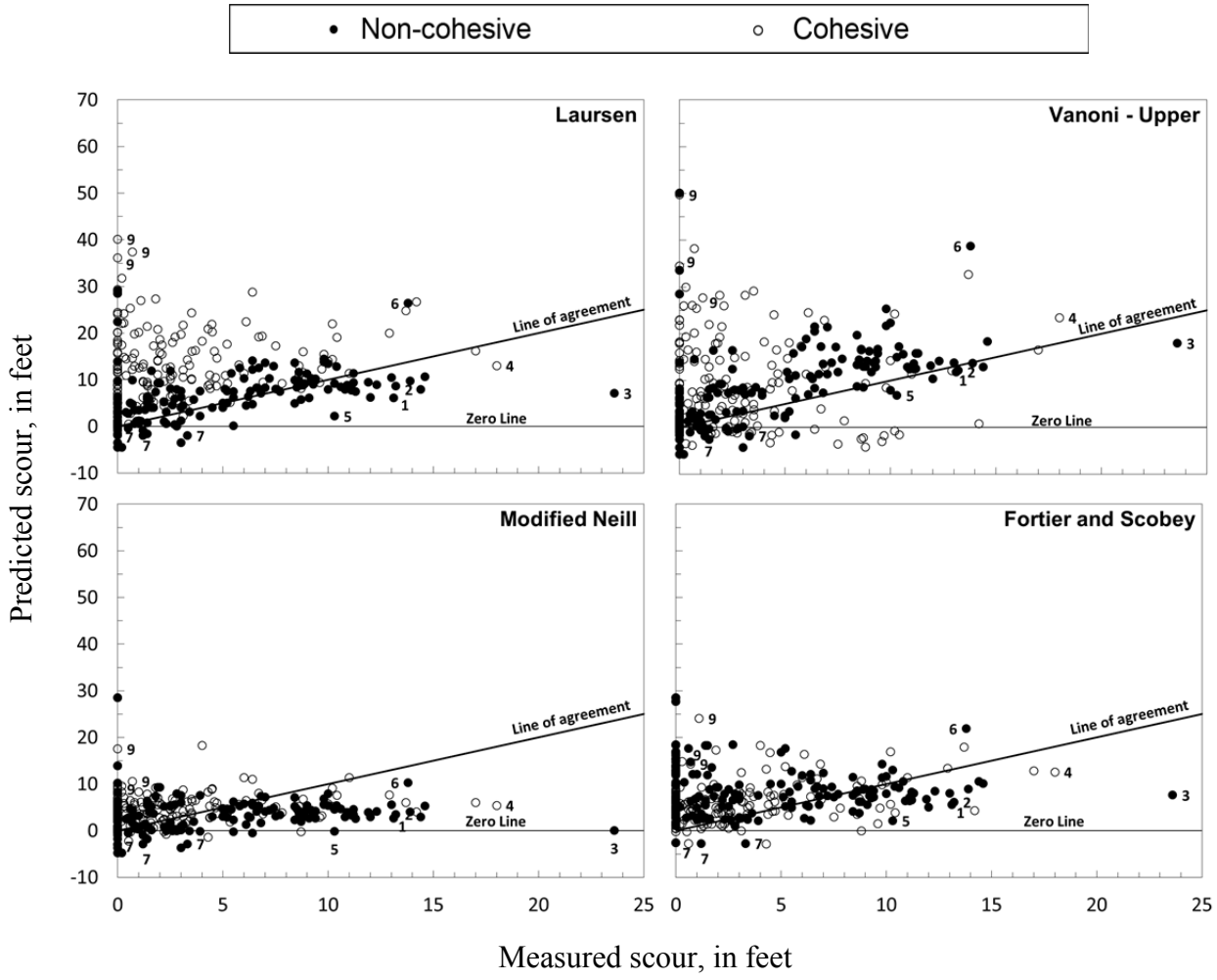

Figure 3-31. Relation of measured and predicted abutment-scour depth for the NCHRP 24-20 scour prediction method using field data and selected critical-velocity methods. (Numbers in graphs refer to sites in table 3-1.)

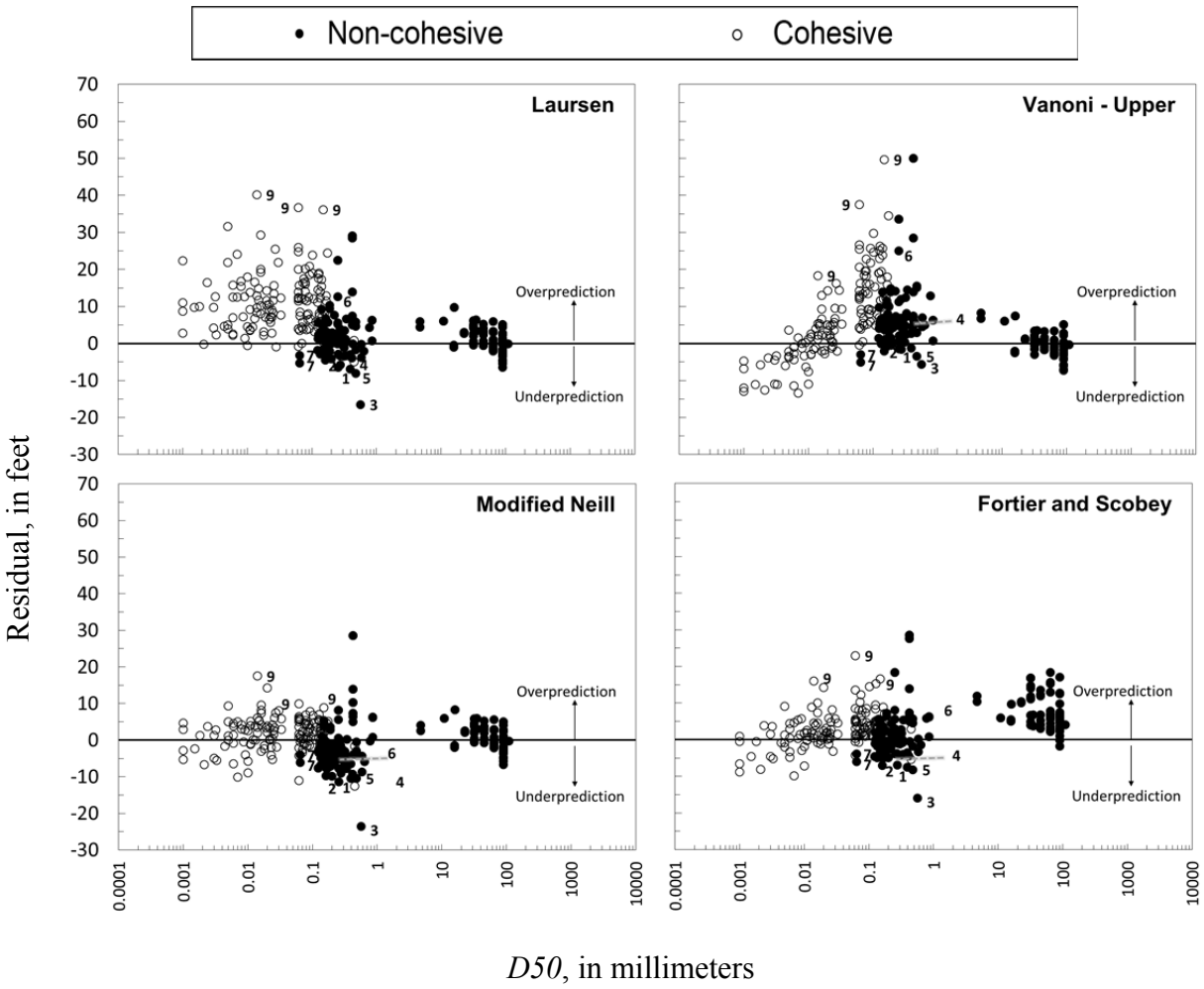

Figure 3-32. Relation of the median grain size (*D50*) and the abutment-scour prediction residual for the NCHRP 24-20 scour prediction method using field data and selected critical-velocity methods. (Numbers in graphs refer to sites in table 3-1.)

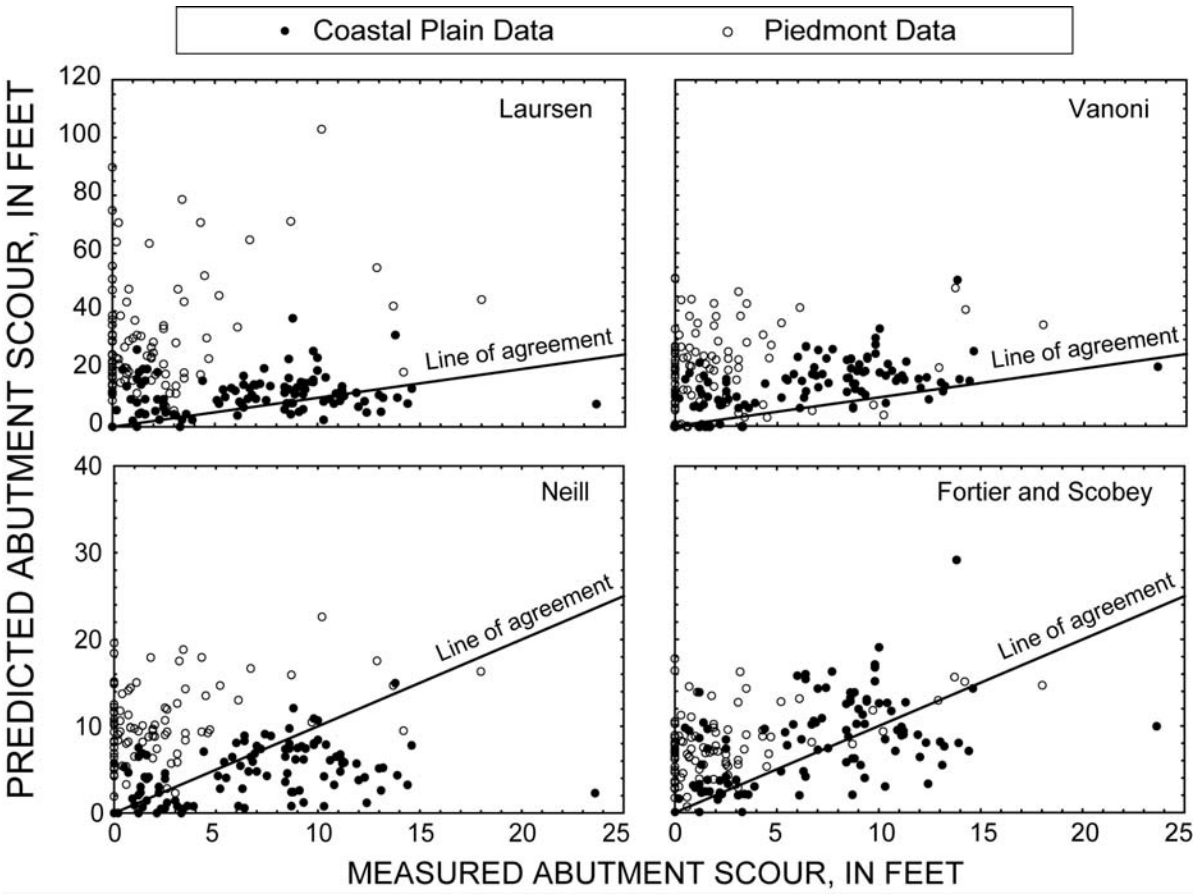

Figure 3-33. Relation of measured and predicted abutment-scour depth for Maryland abutment-scour equation (Chang and Davis, 1998, 1999) using field data and selected critical-velocity methods (from Benedict, 2010).

3.7 Assessment of the NCHRP 24-20 Prediction Method

Based on the review of the NCHRP 24-20 prediction method (Ettema et al. 2010; Arneson et al. 2012) and the analysis associated with the laboratory and USGS field data, a limited assessment of the method will be presented, including noted strengths and weaknesses, recommended analyses for further verification of the method's performance, and limited guidance for applying the method. The complexity of scour processes at abutments and the limitations of the data used in this analysis make it difficult to fully evaluate the performance of the NCHRP 24-20 prediction method. The following report sections should be viewed in light of this challenge.

3.7.1 Strengths

The strengths of the NCHRP 24-20 abutment-scour prediction method include the following:

1. **Simple conceptual model based on physical processes:**

   The method uses a simple conceptual model based on accepted physical processes associated with hydraulics and sediment transport, in which abutment scour is considered a function of contraction scour. The conceptual model provides a logical explanation of the relation between abutment and contraction scour helping clarify the long-standing question regarding the additive nature (or lack thereof) of these scour components. Additionally, its derivation from physical processes should allow the equation to have broad application to a variety of field conditions.

2. **Uses well-accepted and familiar equations:**

   The current formulation of the NCHRP 24-20 method uses the live-bed and clear-water contraction-scour equations developed by Laursen (1960; 1963). These equations are well accepted, have broad application, and should be familiar to the practitioner.

3. **Method potentially can be extended to include cohesive sediments:**

   The current formulation of the NCHRP 24-20 method is for non-cohesive sediments. However, the conceptual model is applicable to cohesive sediments, and with an

appropriate contraction-scour equation, the method could be adapted for the prediction of abutment scour in cohesive sediments.

4. **Has some underprediction, but tends to capture trend of non-cohesive data:**

   While there is some underprediction in the application of the non-cohesive field data to the NCHRP 24-20 method, the prediction patterns in figure 3-25 indicate that the method is reflecting the general trend of the non-cohesive field data, with predicted scour depth increasing as measured scour depth increases, particularly for measured scour depths less than about 10 ft. The underprediction is of concern, but could likely be reduced, in some measure, with better estimates of flow velocity at the abutment using a two-dimensional flow model.

3.7.2 Weaknesses

The weaknesses of the NCHRP 24-20 abutment-scour prediction method include the following:

1. **Erodible abutments/embankments for Scour Condition B yield smaller scour depths than intact abutments:**

   The conceptual model for Scour Condition B (relatively large abutment setbacks) assumes erodible abutments/embankments that can erode (figure 3-21). These conditions produce smaller abutment-scour depths than those of rigid abutment models (figure 3-20), which treat abutments as solid bodies extending to depth in a channel bed or floodplain. While scour processes associated with Scour Condition B are common in the field, it would be incorrect to assume that they are the only mode of abutment scour. Rather, these scour processes should be viewed as one of multiple modes. Many abutments remain intact during high flows, with minimal erosion and no embankment failure. For intact abutments in the field under Scour Condition B, the NCHRP 24-20 prediction method may underpredict scour. While multiple factors likely contribute to the underprediction in figure 3-25, the erodible abutment/embankment data for Scour Condition B in NCHRP 24-20 likely play some role. Because of the differing scour patterns between erodible and intact abutments, the practitioner will need to evaluate the appropriateness of using the NCHRP 24-20 prediction method for abutments with Scour

Condition B. (See report section 3.4 for additional details.) A way to address this concern would be the inclusion of an appropriate abutment-scour countermeasure, which is recommended as a standard design procedure by Sturm et al. (2011) for all new abutment designs.

2. **Laboratory data do not include the range of embankment lengths and flow contractions measured in the field where potential for scour is greatest:**

   The challenges of the laboratory make it difficult to develop models that reflect the full range of abutment lengths and flow contractions measured in the field. Therefore, the ranges of L/y_1 (figure 1-13) and q_2/q_1 (figure 1-15) for the field data are larger than that of the laboratory data, indicating that the field data represent more severe contractions of flow, where scour potential is greatest, than those represented by the laboratory data. Long abutments and large contractions can create large head differentials across a bridge, creating adverse conditions for scour. Because the NCHRP 24-20 laboratory data do not encompass the range of the field data, scour may be underpredicted at such sites. It is notable that the most severe flow contraction (q_2/q_1 equals about 50) in the USGS abutment-scour database (Pee Dee River at I-95) has the largest measured scour depth (23.6 ft), but also has the largest underprediction (figure 3-11) with the NCHRP 24-20 method. While other factors likely contribute to this underprediction, the severe flow contraction that greatly exceeds the range of the laboratory data likely plays some role. (For additional details, see the discussions about figures 1-15 and 1-24 in report sections 1.4.1 and 1.4.4, respectively.)

3. **Large overprediction for cohesive sediments:**

   Figure 3-25 shows the prediction patterns for cohesive and non-cohesive sediments and indicates infrequent underprediction for cohesive sediments and overprediction that at times is excessive. The current formulation for the NCHRP 24-20 method is for non-cohesive sediments; therefore, the method is expected to overpredict for cohesive sediments.

4. **Increasing underprediction with increasing measured scour for non-cohesive sediments:**

While the prediction patterns for non-cohesive sediments in figure 3-25 are capturing the general trend of the field data for measured scour depths less than 10 ft, there is a trend of increasing underprediction as measured scour increases beyond 10 ft. The laboratory data show a similar trend, although not as severe, with increased underprediction as measured scour increases (figures 3-2 through 3-4). This pattern is of concern and indicates that abutment scour at sites having the largest potential for scour will tend to be underpredicted. The exact cause of this underprediction is difficult to determine and, as noted previously, is likely caused by multiple factors. Better estimates of flow velocity at the abutment from a two-dimensional model would likely improve results. This underprediction is most notable in the low-gradient streams of the South Carolina Coastal Plain data that generally have wide densely-vegetated floodplains, severe contractions of flow, and some of the largest measured scour depths. This pattern of underprediction indicates a need for caution when assessing scour at such sites.

5. **Differing sediment characteristics between laboratory and field:**

Laboratory experiments typically use uniform non-cohesive sediments. In contrast, sediments in the field are non-uniform in grain size and often have varying degrees of cohesion. Additionally, natural streams typically have scour-resistant subsurface strata that impede or limit scour depths (see report section 1.2.5). These characteristics tend to reduce scour depths in the field below those associated with laboratory investigations (figure 1-21). The erodible abutments/embankments for the NCHRP 24-20 data (Scour Condition B) also tend to produce smaller scour depths than those associated with rigid abutment models (figure 1-12). It is interesting to note that the upper bounds of the field data and the NCHRP 24-20 data are approximately the same (figure 1-21). While the USGS field data and the NCHRP 24-20 laboratory data both have reduced scour depths in comparison to rigid abutment models, the mechanisms that produced the smaller scour depths may differ (see report section 1.2.5). If a field site has conditions where the depth of the erodible sediments was very large, allowing scour depths to exceed those of the USGS field data, the NCHRP 24-20 method may tend to have larger underprediction.

3.7.3 Recommendations for Additional Analysis

The analysis presented in this report indicates that the NCHRP 24-20 method is capturing the general trends of scour in the field for non-cohesive sediments, but still has some underprediction that is of concern. The following recommendations are made with the goal of identifying the cause of underprediction and minimizing it. Other factors likely contribute to underprediction, but they are not addressed here.

1. **Evaluating sensitivity to flow velocity:**

   The prediction patterns in the non-cohesive sediments of the USGS field data (figure 3-25) indicate that the NCHRP 24-20 method is reflecting the general trend of the field data, but with increasing magnitude and frequency of underprediction as measured scour increases. The uncertainty of the USGS field data makes it difficult to determine the exact cause of the underprediction pattern. Better estimates of flow velocity near the abutment may improve performance. This assumption could be evaluated by selecting a strategic sample of sites from the USGS field database, developing two-dimensional flow models for the sites, and applying the better estimates of flow velocity to the NCHRP 24-20 method. This analysis would help identify how sensitive the NCHRP 24-20 method is to the estimate of flow velocity at the abutment. If prediction is substantially improved, this would indicate that prediction error from other factors may be negligible, providing a direction for further improving performance.

2. **Evaluating the Scour Condition B amplification factor for field conditions where the abutment/embankment remain intact:**

   The current amplification curves for Scour Condition B represent abutment scour associated with eroded abutments/embankments that produce smaller abutment-scour depths than rigid abutments (see report section 3.4). While it can be argued that the rigid abutment models typically used in laboratory investigations will tend to produce larger relative scour depths than those found in the field, the erodible abutment/embankments models used in the NCHRP 24-20 investigation may produce smaller scour depths than those associated with abutments in the field that remain intact during a flood. The

required amplification factors shown in figure 3-24 indicate that there may be some justification in modifying the amplification curves. Using the results from the evaluation of the sensitivity of the NCHRP 24-20 method to flow velocity (see item 1 above), the required amplification factor could be reanalyzed (see report section 3.4.1) to gain insights about this factor. Also, consideration should be given on how to model intact abutments in the laboratory that better reflect field conditions that could be used to evaluate the amplification factor for intact abutments.

3. **Long abutments:**

Melville (1992) and Melville and Coleman (2000) note that the reduction in scour depth derived from streamlined abutment shapes, such as the spill-through and wing-wall abutments, diminishes as abutment length increases, and for longer abutments, scour depths approach those for a vertical wall regardless of abutment shape. This pattern was observed in laboratory data associated with rigid abutment models and will likely differ or be absent from scour patterns for erodible abutments/embankments such as those used in the NCHRP 24-20 investigation for Scour Condition B. Therefore, the exclusion of an adjustment factor for relatively long abutments from the NCHRP 24-20 method is reasonable. In the field setting, however, abutments/embankments can often remain largely intact during floods, as is the case for the field data used in this investigation. Under such conditions, it would be reasonable to expect scour patterns to be similar to those of rigid abutments, therefore having a larger potential for scour in general, but particularly at relatively long abutments with spill-through or wing-wall shapes. The largest underpredictions in the field data are associated with the relatively long spill-through abutments of the South Carolina Coastal Plain and Relief/Swamp Bridge data (figure 3-16), with most of these data representing Scour Condition B. This pattern of underprediction at relatively long abutments also is seen in the rigid abutment models in the laboratory data (figure 3-8), indicating that the phenomenon noted by Melville (1992) may contribute, in part, to this underprediction. The underprediction in the field data is likely caused by multiple factors. Because the limitations of the data do not allow for clear identification of these factors, the possible contribution of relatively long abutments to underprediction cannot be fully excluded. Based on the work of Melville (1992) and

Melville and Coleman (2000) and the fact that it is possible for abutments to remain intact during a flood, it may be appropriate to include an adjustment factor for long abutments under Scour Condition B to minimize the potential for underprediction for design purposes. Therefore, consideration should be given to incorporating an adjustment for long abutments to minimize the potential for underprediction at such abutments. Additional research may be required in order to determine an appropriate adjustment factor.

4. **Safety factor:**

The prediction patterns associated with the non-cohesive sediments of the USGS field data (figure 3-25) indicate that the frequency and magnitude of underprediction increase as measured scour increases. Therefore, consideration should be given to the incorporation of a safety factor to minimize underprediction.

5. **Cohesive sediments:**

While the theory of the NCHRP 24-20 method is applicable to both non-cohesive and cohesive sediments, its current formulation has yet to be adapted to cohesive sediments. Therefore, consideration should be given to developing a formulation appropriate for cohesive sediments.

6. **Evaluation of current contraction-scour prediction equations:**

The NCHRP 24-20 method uses an estimate of contraction scour to predict abutment scour. Current methods for predicting contraction scour are based on simplified equations that do not capture the complexity of the field. Therefore, it would be beneficial to conduct research to advance the understanding of, and methods for estimating contraction scour. Such research should evaluate contraction geometry (including abutment length and asymmetry of abutment lengths), and channel and floodplain roughness characteristics commonly found in the field. The Laursen method does not fully account for these conditions.

3.7.4 General Application Guidance

This section contains some general guidance for application of the NCHRP 24-20 method. This guidance is not exhaustive and is not intended to supersede the guidance in HEC-18 or NCHRP 24-20. Additionally, the practitioner will need to evaluate the appropriateness of using the NCHRP 24-20 method for the given design criteria and site conditions.

1. **Estimate of the maximum flow velocity near the abutment:**

   The maximum flow velocity at the abutment is a critical variable in the NCHRP 24-20 prediction method. A two-dimensional flow model will provide the most accurate assessment of this variable. When a one-dimensional model is being used to evaluate hydraulic characteristics, HEC-18 recommends the use of the SBR method (chapter 2). The SBR method is most applicable to bridge sites with a well-defined main channel. However, the SBR method is not as applicable to swamps and floodplain relief bridges, and a two-dimensional flow model is the better tool for making this assessment. If a one-dimensional flow model is used at such a site, engineering judgment must be used to estimate the larger velocity associated with contracted flow at an abutment. The work of Morales and Ettema (2013) provides relations for estimating the maximum flow velocity and unit discharge at spill-through abutments with respect to selected abutment and channel configurations, and these relations may be useful for assessing the velocity near an abutment. In general, conservative, but reasonable, estimates of the velocity should be used.

2. **Evaluation of sediments:**

   The surface and subsurface sediments at a site will influence the potential for abutment-scour depth, and it is important to give consideration to this matter when evaluating scour at a bridge site. Scour depth is often limited by cohesive sediments or by subsurface scour-resistant layers (see report section 1.2.5). However, the depth of the erodible sediments could be very large, allowing for large scour depths to develop beyond those measured in the USGS field data. Because of the complexity of soil conditions in the

field, using a multidisciplinary team including geotechnical, structural, and hydraulic engineers to assess the potential influence of soil conditions on scour is advised.

3. **Long abutments and large contractions:**

Long abutments and large flow contractions have high potential for scour, and the underprediction in the USGS field data is often associated with these types of site characteristics. When such sites are being analyzed with the NCHRP 24-20 method, it is important to use judgment and a strong measure of conservatism in the assessment. Conservative estimates of flow velocity near the abutment, along with some type of safety factor, would be advisable. Additionally, because long abutments tend to have a larger potential for scour (Melville, 1992; Melville and Coleman, 2000), it may be appropriate to include an adjustment factor for long abutments to minimize the potential for underprediction at such bridges (see item 2 in report section 3.7.3).

4. **Application to cohesive sediments:**

While the conceptual model for the NCHRP 24-20 method is applicable to cohesive and non-cohesive sediments, the current formulation of the NCHRP 24-20 method is primarily applicable to non-cohesive sediments rather than cohesive sediments. The performance of the cohesive sediments of the South Carolina Piedmont and Alabama data (figures 3-11 and 3-12) indicate that the current formulation of the NCHRP 24-20 method will have infrequent underprediction and also overpredictions that at times are excessive when applied to cohesive sediments. For clear-water scour conditions, alternate critical-velocity methods can be applied to the NCHRP 24-20 method (report section 3.5). However, the alternate methods produced frequent underprediction, which is of concern. Performance of the NCHRP 24-20 method in cohesive sediments may vary for sites that have characteristics beyond the range of the South Carolina Piedmont and Alabama data. Table 1-1 provides a summary of site characteristics associated with the South Carolina and Alabama data, and the table can be used to evaluate if a site of interest has characteristics similar to those data. Additionally, the reports associated with these data can be reviewed for more information (Benedict, 2003; Lee and Hedgecock, 2008).

5. **Application to coarse sediments in small, steep-gradient streams:**

   The prediction patterns in the small streams of Maine with steep gradients and coarse sediments have an approximate symmetric scatter about the line of agreement, indicating that the NCHRP 24-20 prediction method, on average, is reflecting the general trend of the measured data (figures 3-11 and 3-12). However, there is underprediction in this pattern, and a safety factor would be advisable. The analysis of steep-gradient and coarse-sediment streams presented in this report primarily reflects the characteristics associated with the Maine data. Performance of the NCHRP 24-20 method for steep-gradient and coarse-sediment streams may vary for sites that have characteristics beyond the range of the Maine data. Table 1-1 provides a summary of site characteristics associated with the Maine data, and the table can be used to evaluate if a site of interest has characteristics similar to those data. Additionally, the report associated with these data can be referred to for more information (Lombard and Hodgkins, 2008).

6. **Application to non-cohesive sediments in low-gradient streams:**

   The prediction patterns in the non-cohesive sediments of low-gradient streams of the South Carolina Coastal Plain and Relief/Swamp Bridge data have an approximate symmetric scatter about the line of agreement, indicating that the NCHRP 24-20 prediction method, on average, is reflecting the general trend of the measured data. However, there is more frequent underprediction of scour for measured abutment-scour depths of approximately 10 ft and larger. The underprediction in these data likely is caused by multiple factors, including relatively long abutments that tend to produce larger scour depths and the less accurate estimates of flow velocity from the one-dimensional flow models. As noted in item 1, to minimize underprediction at these sites, obtaining a conservative, reasonable estimate of the maximum flow velocity at the abutment is critical. Additionally, as noted in item 2, including an adjustment factor for long abutments may be appropriate to minimize the potential for underprediction. Performance of the NCHRP 24-20 method in sandy, non-cohesive sediments may vary for sites that have characteristics beyond the range of the South Carolina Coastal Plain data. Table 1-1 provides a summary of site characteristics associated with the South Carolina data; the table can be used to evaluate if a site of interest has characteristics similar to those data and Benedict (2003) can be referred to for additional information.

CHAPTER 4

APPLICATION PROCEDURE FOR THE NCHRP 24-15(2) PREDICTION METHOD

4.1 Introduction

The NCHRP 24-15(2) report (Briaud et al. 2009) and the Summary Report (Briaud et al. 2011) provide general guidance for applying the NCHRP 24-15(2) abutment-scour prediction method. The Summary Report (Briaud et al. 2011) is recommended as the primary guidance manual (J.-L. Briaud, written commun., February 2014) and was used in this investigation to develop the procedure for applying the NCHRP 24-15(2) method to the laboratory and USGS field data. Additionally, Dr. Jean-Louis Briaud, the Principal Investigator for NCHRP 24-15(2), and Mr. Bart Bergendahl of the Federal Highway Administration were consulted in the development of this procedure and were provided opportunity for review and comment. A brief description of the application steps follows.

4.2 Summary of NCHRP 24-15(2) Scour Prediction Method

The rate of scour development can be rapid in non-cohesive sediments such that maximum (also called equilibrium) scour depths can be reached within hours to a few days and often within a single flood (Briaud et al. 2011; Arneson et al. 2012). Therefore, scour prediction equations for non-cohesive sediments have typically neglected the influence of time, assuming that the maximum scour depth will occur for a given flood. However, for cohesive sediments, the rate of scour development can be much smaller than for non-cohesive sediments, requiring many floods before the maximum scour depth can occur (Briaud et al. 2011; Arneson et al. 2012). Time dependency for scour in cohesive sediments therefore becomes a prominent influence on scour depth. To address this issue, Briaud et al. (1999a and b) developed a time-dependent method for estimating scour in cohesive soils known as the Scour Rate in Cohesive Soils method (SRICOS). The SRICOS method was originally developed for estimating scour at bridge piers, and later was

extended to include contraction (Briaud et al. 2004; NCHRP Project 24-15) and abutment (Briaud et al. 2009; NCHRP Project 24-15(2)) scour. The method generally evaluates the time-dependent scour by determining the cumulative scour depth occurring over the duration of a hydrograph. To apply the SRICOS method requires (1) hydraulic data, including velocity and flow rating curves at the bridge, (2) approach and bridge cross-section data, (3) a flow hydrograph, and (4) sediment data, including the critical shear stress for the sediment, and a sediment-erosion function curve determined from an Erosion Function Apparatus (EFA) test (Briaud et al. 2011). The SRICOS method incorporates an equation for estimating the maximum abutment-scour depth for constant flows, independent of time, and can be used to obtain a less refined, but conservative estimate of abutment-scour depth. The data required for application of the maximum scour-depth equation are less detailed, comparable to the data used in other non-cohesive scour prediction equations such as Froehlich (1989).

No laboratory or field abutment-scour databases include the detailed data required for application of the time-dependent SRICOS method (Briaud et al. 2009; 2011). Therefore, any performance evaluation of the NCHRP 24-15(2) abutment-scour prediction method with existing laboratory and field data must be limited to use of the maximum scour-depth equation. The equation was originally developed for predicting abutment scour in cohesive sediments by using an empirical relation for evaluating the sediment critical velocity for cohesive sediments. (The empirical relation is described later in report.) This empirical relation for sediment critical velocity was later expanded for non-cohesive sediments, thus extending the applicability of the NCHRP 24-15(2) method to cohesive and non-cohesive sediments. Therefore, cohesive and non-cohesive laboratory and field data were used to evaluate the equation performance. Use of the maximum abutment-scour depth equation for evaluation of the NCHRP 24-15(2) abutment-scour prediction method is less than ideal, and the equation cannot be used to fully evaluate the time-dependent component of the SRICOS method for abutment scour in cohesive sediments. However, the evaluation does provide a good assessment of the maximum scour-depth equation, which is an integral part of the SRICOS method, giving insights on the method performance. This limitation should be kept in mind when reviewing the results of this investigation. A summary of the maximum abutment-scour depth equation follows.

Briaud et al. (2009) used regression analysis of laboratory data to develop the following equation to predict the maximum abutment-scour depth:

$$y_s/y_{f1} = K_1K_2K_LK_GK_pK_{Re}7.94\left(1.65Fr_{f2} - Fr_{fc}\right) \quad (4\text{-}1)$$

where

y_s is the abutment-scour depth (figure 4-1), in feet,

y_{f1} is the floodplain flow depth upstream of the abutment (figure 4-1), in feet,

K_1 is the correction factor for the abutment shape defined by the following values:

$$\begin{cases} 1.22 & \text{for vertical-wall abutment} \\ 1.0 & \text{for wing-wall abutment} \\ 0.73 & \text{for spill-through abutment with 2:1 slope (horizontal to vertical slope)} \\ 0.59 & \text{for spill-through abutment with 3:1 slope,} \end{cases}$$

K_2 is the correction factor for the abutment skew defined by the following relations:

$$\begin{cases} 1.0\text{-}0.005|\theta - 90°| & \text{for } 60° \le \theta \le 120° \\ 0.85 & \text{otherwise,} \end{cases}$$

where θ is the abutment-skew angle (figure 4-1), in degrees (°), with an abutment perpendicular to flow having a value of 90°, an abutment pointing downstream having a value less than 90°, and an abutment pointing upstream having a value greater than 90°,

K_G is the correction factor for the channel geometry defined by the following values:

$$\begin{cases} 1.0 & \text{for compound channel} \\ 0.42 & \text{for rectangular channel,} \end{cases}$$

K_L is the correction factor for the abutment location defined by the following relations:

$$\begin{cases} \text{-}0.23\dfrac{B_f - L}{y_{f1}} + 1.35 & \text{for } \dfrac{B_f - L}{y_{f1}} < 1.5 \\ 1.0 & \text{otherwise,} \end{cases}$$

where

B_f is the floodplain width (figure 4-1), in feet,

L is the abutment length (figure 4-1), in feet, and

y_{f1} is as previously defined,

K_p is the correction factor for pressure flow defined by the following relations:

$$\begin{cases} 0.92(d_1/d_{deck})+1.0 & \text{for } d_1/d_{deck} < 1.0 \\ 0.21(d_1/d_{deck})^2\text{-}1.27(d_1/d_{deck})+2.97 & \text{for } 1.0 \le d_1/d_{deck} \le 3.0 \\ 1.0 & \text{for } 3.0 \le d_1/d_{deck}, \end{cases}$$

where

d_1 is the distance from water surface to the low chord of the bridge at the upstream face of the bridge (figure 4-2), in feet, and

d_{deck} is the distance from high steel to the low chord of the bridge deck blocking flow, in feet (figure 4-2),

K_{Re} is the correction factor for the Reynolds number defined by the relation:

$$1/0.0327Re_{f2}^{0.28},$$

where

Re_{f2} is the Reynolds number around the abutment toe, equal to $\frac{V_{f2}y_{f1}}{\nu}$,

where

ν is the kinematic viscosity of water ($1.08\text{x}10^{-5}$ ft^2/s at 20° Celsius),

and the other variables are as previously defined.

Fr_{f2} is the Froude number around the abutment toe, equal to $\frac{V_{f2}}{\sqrt{gy_{f1}}}$,

where

g is the acceleration due to gravity, in feet per second squared,

y_{f1} is as previously defined, and

V_{f2} is the velocity around the toe of the abutment, in feet per second,

Fr_{fc} is the critical Froude number around the abutment toe, equal to $\frac{V_c}{\sqrt{gy_{f1}}}$,

where

V_c is the critical velocity for the floodplain sediment, or for the case of protruding abutments, the main-channel sediment, in feet per second,

and the other variables are as previously defined.

Briaud et al. (2009) developed an empirical relation for evaluating V_c in cohesive sediments and later expanded this relation for non-cohesive sediments, thus extending the applicability of the NCHRP 24-15(2) method to cohesive and non-cohesive sediments. The empirical relation, described later in the report, is a lower-bound envelope curve of critical velocity as determined from EFA tests of field samples. A more accurate estimate of V_c for a given bridge site could be obtained from EFA tests of soil samples at the site of interest, likely yielding more accurate assessments of abutment scour. This should be kept in mind when reviewing the results associated with the NCHRP 24-15(2) prediction method.

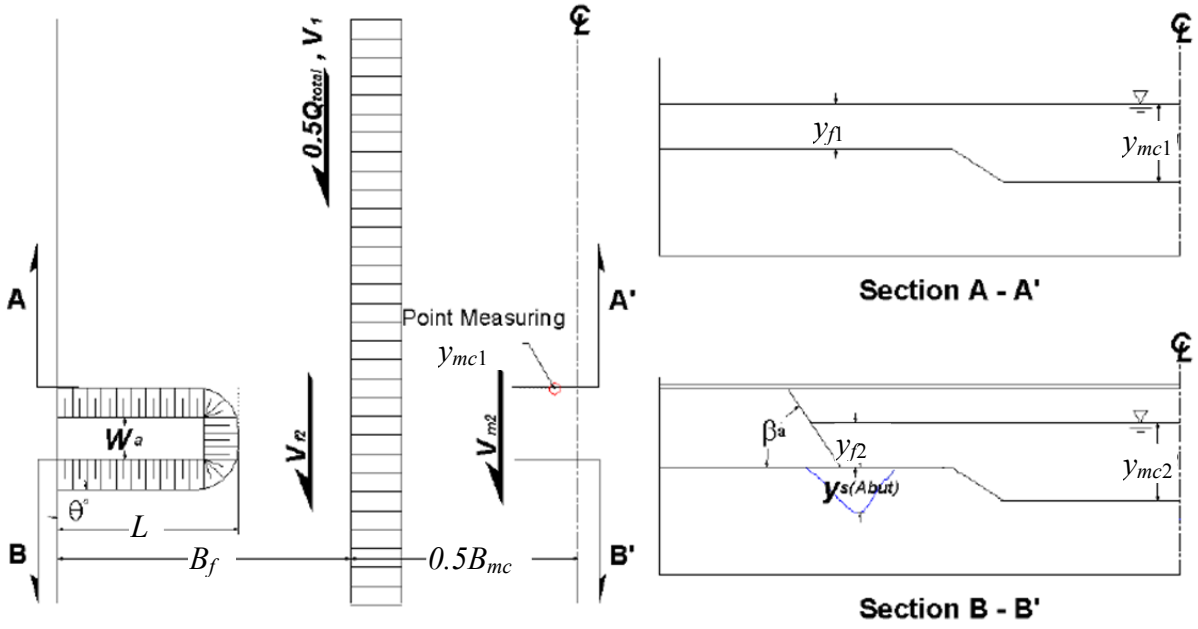

Figure 4-1. Definition of selected abutment-scour variables associated with the NCHRP 24-15(2) method (from Briaud et al. 2011).

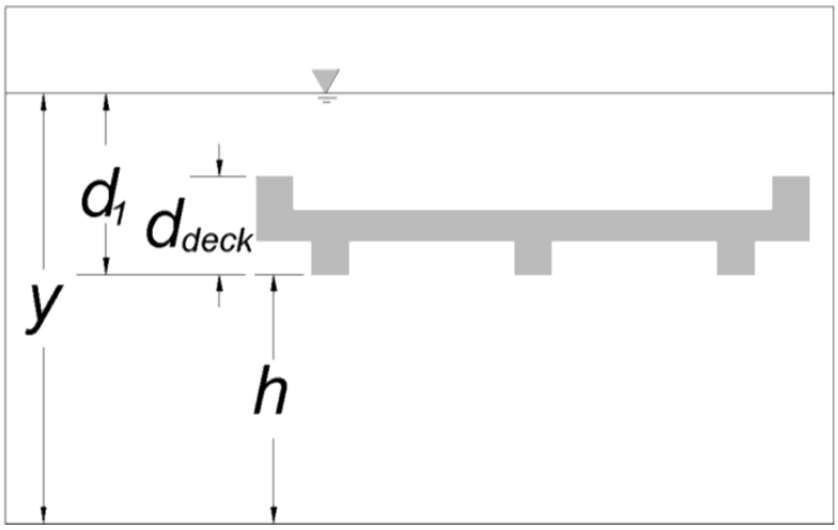

Figure 4-2. Definition of variables associated with pressure flow (from Briaud et al. 2011).

4.3 General Procedure for Application of NCHRP 24-15(2) to the Laboratory and the USGS Field Data

Briaud et al. (2011) provide guidance for applying equation 4-1. As with any scour prediction equation, some judgment is required in its application; therefore, a brief review of the steps used in applying the NCHRP 24-15(2) method to the laboratory and USGS field data follows.

1. **Compile laboratory and USGS field data**

   The laboratory and USGS field data previously described (tables 1-1 and 1-3) were reviewed, and pertinent data for the NCHRP 24-15(2) method were entered into a spreadsheet. These data included selected hydraulic, sediment, and bridge-geometry characteristics as described in table 2-1.

2. **Determine the correction factors for the abutment of interest**

   For most sites, the correction factors in equation 4-1 could be readily determined. However, some sites had characteristics differing from those of the laboratory models used in NCHRP 24-15(2) and required some judgment in determining the correction factors. The Reynolds number correction factor uses hydraulic properties and is discussed in item 8 below. Comments regarding the determination of the other correction factor follow.

   - K_1

     Vertical-wall and wing-wall abutments have abutment-shape correction factors with values of 1.22 and 1.0, respectively. (Note: No vertical-wall abutments were in the field data.) For spill-through abutments, there are two possible abutment-shape correction factors, 0.73 and 0.59, for spill-through slopes of 2:1 and 3:1, respectively. Most of the laboratory and field data have spill-through slopes of 2:1 or steeper. For spill-through slopes steeper than 2:1, a correction factor value of 0.73 was assumed. Additionally, where a spill-through slope was not provided in the database, the site was assumed to have a slope of 2:1 or steeper.

- ***K_2***

  The abutment-skew correction factor can be readily determined from the relations presented in equation 4-1, and no special consideration was required.

- ***K_G***

  The correction factor for channel geometry only has two cases, rectangular and compound channels. For the laboratory data, the channel-geometry classification is clearly specified and the values of K_G can be readily determined. For the field data, some judgment is required to determine the channel-geometry classification. Sites with well-defined channels were classified as compound channels. Floodplain relief bridges and swamps with poorly defined channels were classified as rectangular channels.

- ***K_L***

  The abutment-location correction factor accounts for increased turbulence and scour when the abutment toe is located near the channel bank. The largest value for this correction factor (1.35) occurs when the abutment toe is located at the channel bank. For most cases, the abutment-location correction factor can be readily determined from the relations presented in equation 4-1. However, the NCHRP 24-15(2) method did not evaluate the case for an abutment protruding into the main channel. In such cases, the maximum abutment-location correction factor of 1.35 was assumed to be applicable. Some sites had very small abutment setbacks of approximately 2 ft or less. In such cases, it was assumed that the abutment was set at the channel bank, and K_L was assigned a value of 1.35.

- ***K_p***

  The pressure-flow correction factor can be readily determined from the relations presented in equation 4-1. No pressure-flow cases are in the laboratory data. In contrast, some pressure-flow sites are in the USGS field data. These sites had limited data regarding the bridge deck geometry, and this information was used to approximate the variables (d_1 and d_{deck}, figure 4-2) required for evaluating the pressure-flow correction factor.

3. Determine the floodplain flow depth (y_{f1}) upstream from abutment

Two general cases must be considered when defining y_{f1}, including (1) setback abutments located on the floodplain (figure 1-3) and (2) abutments protruding into the main channel (figure 1-7). Figure 4-1 provides a schematic showing y_{f1} and its general location at the approach cross section.

Abutments located on the floodplain:

The NCHRP 24-15(2) method was developed for the case of abutments located on the floodplain, including bankline and setback abutments. In such cases, the following approach was used to define y_{f1}. For the laboratory data, the approach flow depth on the floodplain was used to represent y_{f1}. For USGS field sites with a defined channel and floodplain, the average flow depth on the upstream left or right floodplain, corresponding to the abutment of interest, was used to represent y_{f1}. For relief bridges located on a floodplain, the average flow depth on the upstream floodplain was used to represent y_{f1}. For sites crossing a swamp with a poorly defined channel, the average flow depth across the swamp was used to represent y_{f1}.

Abutments protruding into the main channel:

In the case of abutments protruding into the main channel, it was recommended that the flow depth in the main channel (y_{mc1} in figure 4-1) be used to represent y_{f1} (J.-L. Briaud, oral commun., March 5, 2014). This approach was applied to the laboratory and field data.

4. Determine the flow velocity (V_{f2}) around the toe of the abutment

For determining flow velocity around the toe of the abutment, Briaud et al. (2009; 2011) recommend using the method incorporated into the Maryland State Highway Administration's (2014) ABSCOUR program as defined in the following relations. (See figure 4-3 for definition of short and long setbacks.)

$$V_{f2} = \begin{cases} \frac{0.5Q}{A_2}, \text{for short setback } (B_f - L \leq 5y_{m1}), \\ \frac{Q_{fp1}}{A_{f2}}, \text{for long setback } (L \leq 0.25\, B_f), \\ \text{for intermediate setback, use a linearly interpolated velocity between the following values:} \\ \frac{0.5Q}{A_2}, \text{for } (B_f - L) = 5y_{m1} \text{ and } \frac{Q_{fp1}}{A_{f2}}, \text{for } L = 0.25\, B_f \end{cases} \quad (4\text{-}2)$$

where

$0.5Q$ is the flow associated with the approach floodplain of interest and half the approach main channel ($Q_{f1} + 0.5Q_{mc1}$), in cubic feet per second,

A_2 is flow area for the overbank of interest and half the main channel at the contracted section, in square feet,

A_{f2} is the flow area on the overbank of interest at the contracted section, in square feet,

y_{mc1} is the flow depth in the approach main channel, and

other variables are as previously defined.

The above approach is for sites with a defined channel and floodplain, but must be slightly modified for sites with rectangular channels, such as a relief bridge or swampy channel. For laboratory data with a rectangular channel, V_{f2} was determined as the average flow velocity through the contracted cross section. Similarly, for relief bridges and bridges crossing swamps with poorly defined channels, V_{f2} was determined as the average flow velocity through the bridge opening. Additionally, when both abutments are set at the bank or protrude into the main channel, V_{f2} was determined as the average flow velocity through the bridge opening. As noted in report section 2.3, the average flow velocity through the bridge probably is a reasonable value for estimating the flow velocity near the abutment at short-length bridges. As the bridge length increases, however, the average flow velocity probably begins to underestimate the larger flow velocity near the abutment. Therefore, to minimize the risk of underestimating the flow velocity at longer bridges, a factor of 1.2 was applied to the average velocity for bridges

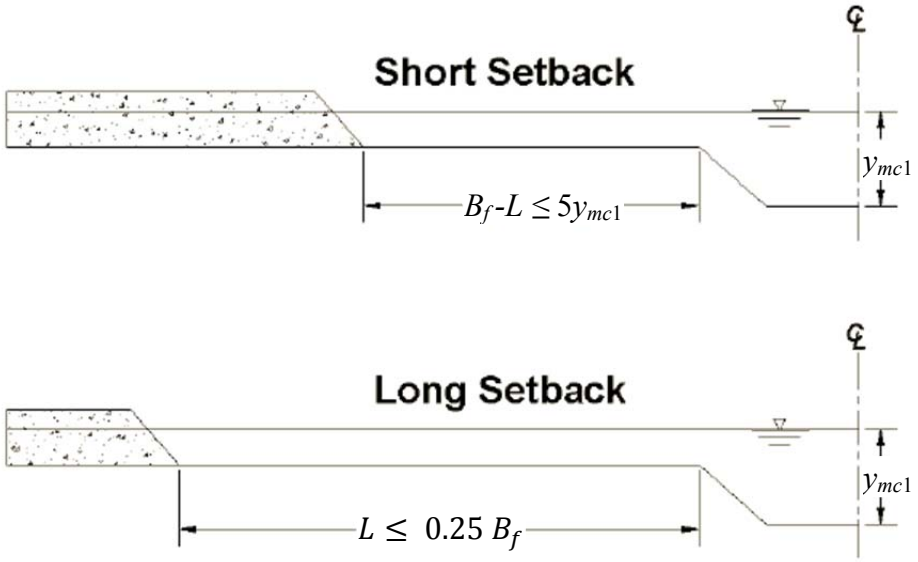

Figure 4-3. Definition of short and long setback abutments (modified from Briaud et al. 2009).

larger than 240 ft. Additional details regarding the rationale for using this factor can be found in report section 2.3.

5. **Determine the Froude number (Fr_{f2}) around the toe of the abutment**

   The value of Fr_{f2} is calculated by using y_{f1} and V_{f2} as determined in steps 3 and 4, respectively.

6. **Determine the floodplain sediment critical velocity (V_c) around the toe of the abutment**

   As noted in chapter 3 of this report, there are various methods for estimating the sediment critical velocity. Briaud et al. (2009) developed an empirical method for estimating V_c for cohesive and non-cohesive sediments as shown in figure 4-4, and recommended that these relations be used in the current investigation (J.-L. Briaud, oral commun., March 5, 2014). (Note: The following equations have units of meters per second that must be

converted to feet per second.) For sediments having a *D50* greater than or equal to 0.1 mm, the following equation was used:

$$V_c = 0.35\ D50^{0.45}, \quad (4\text{-}3)$$

where

V_c is the sediment critical velocity, in meters per second, and

D50 is the median grain size for the sediment, in millimeters.

For sediments having a *D50* less than 0.1 mm, the lower-bound equation in figure 4-4, as follows, was used:

$$V_c = 0.1\ D50^{-0.2}, \quad (4\text{-}4)$$

where all variables are as previously defined. A *D50* representative of the floodplain or main-channel sediments was used at floodplain setback abutments and protruding abutments, respectively. The relation in figure 4-4 is a lower-bound curve of critical velocity as determined from EFA tests of field samples. A more accurate estimate of V_c for a given bridge site could be obtained from EFA tests of soil samples at the site of interest, likely yielding more accurate assessments of abutment scour. This should be kept in mind when reviewing the results associated with the NCHRP 24-15(2) prediction method.

7. Determine the critical Froude number (Fr_{fc}) around the toe of the abutment

The value of Fr_{fc} is calculated by using y_{f1} and V_c as determined in steps 3 and 6, respectively.

8. Determine the Reynolds number correction factor (K_{Re}) around the toe of the abutment

The value of Re_{f2} is calculated by using y_{f1} and V_{f2} as determined in steps 3 and 4, respectively. This value is then used in the relation for computing K_{Re} as described in equation 4-1.

9. Determine the relative and absolute abutment-scour depth

The variables determined in the previous steps were applied to equation 4-1 to determine the relative and absolute scour depths.

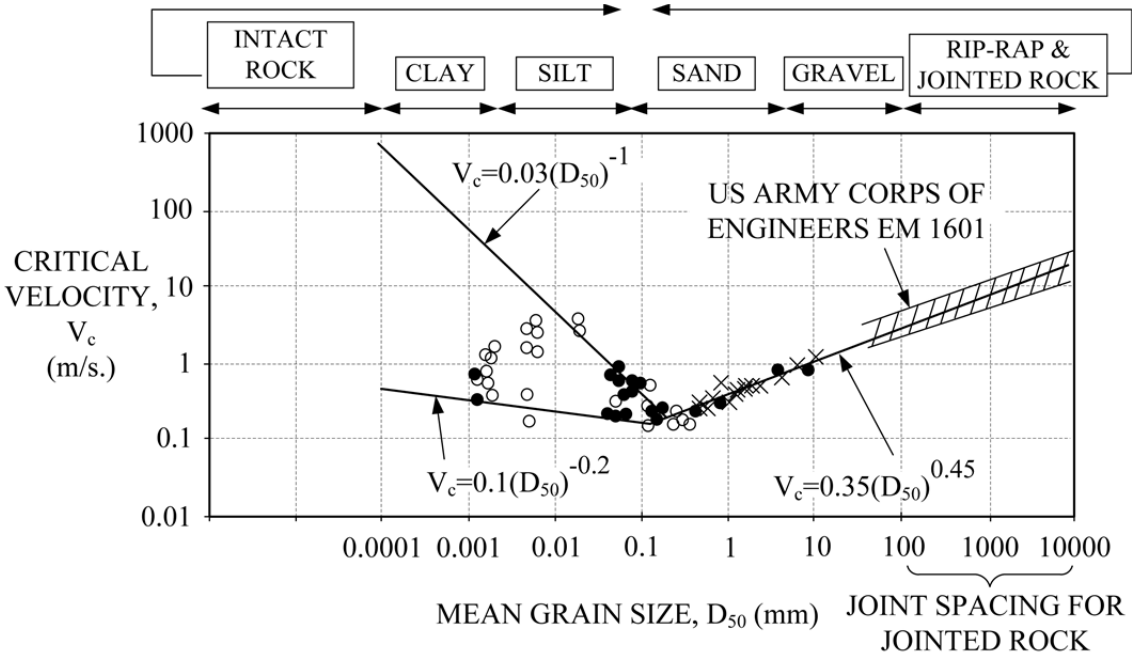

Figure 4-4. Relation of median grain size and sediment critical velocity (from Briaud et al. 2011).

CHAPTER 5

APPLICATION OF THE NCHRP 24-15(2) PREDICTION METHOD TO LABORATORY AND FIELD DATA

5.1 Introduction

The NCHRP 24-15(2) abutment-scour prediction method was originally developed for predicting abutment scour in cohesive sediments, but was extended to include abutment scour in non-cohesive sediments (Briaud et al. 2009; 2011). The NCHRP 24-15(2) method provides two procedures for predicting abutment scour, including (1) a time-dependent estimate requiring detailed site information (primarily for cohesive sediments) that provides a refined estimate of scour, and (2) the maximum scour depth estimate requiring less detailed data (for cohesive and non-cohesive sediments). Briaud et al. (2009; 2011) note that currently no laboratory or field abutment-scour databases include the detailed data required to evaluate the time-dependent method in cohesive sediments. Therefore, any performance evaluation of the NCHRP 24-15(2) abutment-scour prediction method with existing laboratory and field data must be limited to use of the maximum scour-depth equation. This was the approach used in the current (2015) investigation, and this limitation should be kept in mind when evaluating the results in this report. The maximum scour-depth equation was originally developed for predicting abutment scour in cohesive sediments by using an empirical relation for evaluating the sediment critical velocity for cohesive sediments. This empirical relation for sediment critical velocity was later expanded for non-cohesive sediments (see figure 4-4), thus extending the applicability of the NCHRP 24-15(2) method to cohesive and non-cohesive sediments. Therefore, cohesive and non-cohesive data are used in the evaluation of the NCHRP 24-15(2) method.

The procedure described in chapter 4 was used to apply the NCHRP 24-15(2) abutment-scour prediction method to the selected laboratory (table 1-3) and field (table 1-1) abutment-scour data. The results from this application were incorporated into selected scatter plots to display the relations of predicted and measured scour, as well as prediction residuals with respect to selected

explanatory variables. If a prediction equation is capturing the trends of the data, then the relation of the predicted and measured scour will tend to follow the line of agreement, with predicted scour increasing as measured scour increases. The relation of prediction residuals with respect to an explanatory variable will help identify prediction bias associated with that variable. If prediction residuals display a sloped trend with respect to a given explanatory variable, some prediction bias with respect to that variable is likely. Boxplots of the prediction residuals for the laboratory and field data are presented in chapter 6 and compared with the prediction residuals of the NCHRP 24-20 method. The boxplots display the distribution of the prediction residuals by quartiles, providing a simple but useful tool for evaluating the performance of each method and comparing their performance. A table of summary statistics for these boxplots also is provided in chapter 6 in order to quantify the trends in the boxplots.

The performance of the NCHRP 24-15(2) maximum scour-depth equation presented in the following sections of this report represents the combined influence of the equation, the prescribed application procedure, and the data, each having inherent limitations. These limitations will undoubtedly introduce uncertainty into the results; however, the larger number of laboratory (table 1-3) and field (table 1-1) data should be adequate to provide valuable insights into the general performance of the equation. The results associated with the laboratory data are presented first, followed by the results of the field data.

5.2 Analysis of the Laboratory Data

The NCHRP 24-15(2) method was initially evaluated with the laboratory measurements of abutment scour listed in table 1-3. The analysis included a comparison of predicted and measured scour, an evaluation of the relative influence of selected variables in the NCHRP 24-15(2) equation (equation 4-1) on predicted scour, and an evaluation of prediction residuals with respect to selected equation variables. The analysis of the laboratory data is presented in the following report sections.

5.2.1 Relation of Measured and Predicted Scour

Figure 5-1A shows the relation of measured abutment-scour depth to predicted scour for the application of the NCHRP 24-15(2) method to the laboratory data listed in table 1-3. (For clarity, a truncated portion of the graph in figure 5-1A is shown in figure 5-1B.) The data in figure 5-1 are grouped by data source, abutment shape, and bed transport condition. Live-bed scour conditions are represented by the solid symbols, with hollow symbols representing clear-water scour conditions. The Palaviccini (1993) data are associated with rectangular channels, while the other data, with a few exceptions [5 data points in Briaud et al. (2009) and 12 in Ettema et al. (2010)], are associated with compound channels. The Briaud et al. (2009) data are associated with cohesive sediments, while the other laboratory data represent non-cohesive sediments. The laboratory data in figure 5-1 represent abutment scour from a variety of experimental conditions; therefore, the scatter displayed in the data is not unreasonable. To provide insights into equation performance with respect to abutment shape, figures 5-2 through 5-4 present the data grouped by abutment shape, including vertical-wall, spill-through, and wing-wall abutments, respectively. Additionally, data are grouped by live-bed and clear-water scour conditions in figures 5-5 and 5-6 to provide insights into equation performance with respect to bed transport conditions. Some notable trends in these figures include:

- The largest overpredictions for the Sturm (2004) data (3 data points in figure 5-2 and 2 data points in figure 5-3) and the Ettema et al. (2010) data (5 data points in figure 5-3 and 4 data points in figure 5-4) are associated with abutments located at the channel bank or that protrude into the main channel. The abutment-location correction factor (K_L) in equation 4-1 for these types of abutments is 1.35, which will produce larger values of predicted scour depth. A more detailed analysis of these data is presented later in this chapter.
- The live-bed data tend to produce larger overpredictions, particularly in the Palaviccini (1993) vertical-wall abutment data (figures 5-1 and 5-5). As noted later, the live-bed data often have large Froude numbers at the abutment (Fr_{f2}) which tend to produce larger scour predictions when applied in equation 4-1. As previously noted, the Ettema et al.

(2010) live-bed data (figures 5-3 and 5-4) are associated with bankline or protruding abutments that also contribute to the larger scour predictions for these data.

- A review of figure 5-4 shows that three of the wing-wall abutments for the Briaud et al. (2009) data have overpredictions that are much larger than overpredictions for the other data. These three data points are associated with compound channels where the channel-geometry correction factor (K_G) in equation 4-1 has a value of 1.0. In contrast, the other five Briaud et al. (2009) data points that have smaller overpredictions that fall closer to the line of agreement are associated with rectangular channels where K_G has a value of 0.42 that substantially reduces the magnitude of predicted scour. (Note: Most of the other data in figure 5-4 have rectangular channels with the exception of the Ettema et al. (2010) live-bed data.) All of the Briaud et al. (2009) data in figure 5-4 have similar hydraulic and geometric characteristics, with the primary difference being channel geometry. The trends for the Briaud et al. (2009) data in this figure indicate that K_G may not fully reflect the scour processes associated with differing channel geometries. The K_G correction factor is evaluated in more detail later in this report.
- A review of the live-bed and clear-water scour data (figures 5-5 and 5-6, respectively) indicates that the clear-water scour data have a much higher incident of underprediction. With only a few exceptions, the underpredictions are associated with rectangular channels. The channel-geometry correction factor (K_G) in equation 4-1 for rectangular channels is 0.42, which contributes to the underpredictions associated with these data. Additionally, the clear-water data often have smaller Froude numbers at the abutment, which tend to produce smaller scour predictions when applied in equation 4-1. A more detailed analysis of these data is presented later in this chapter.

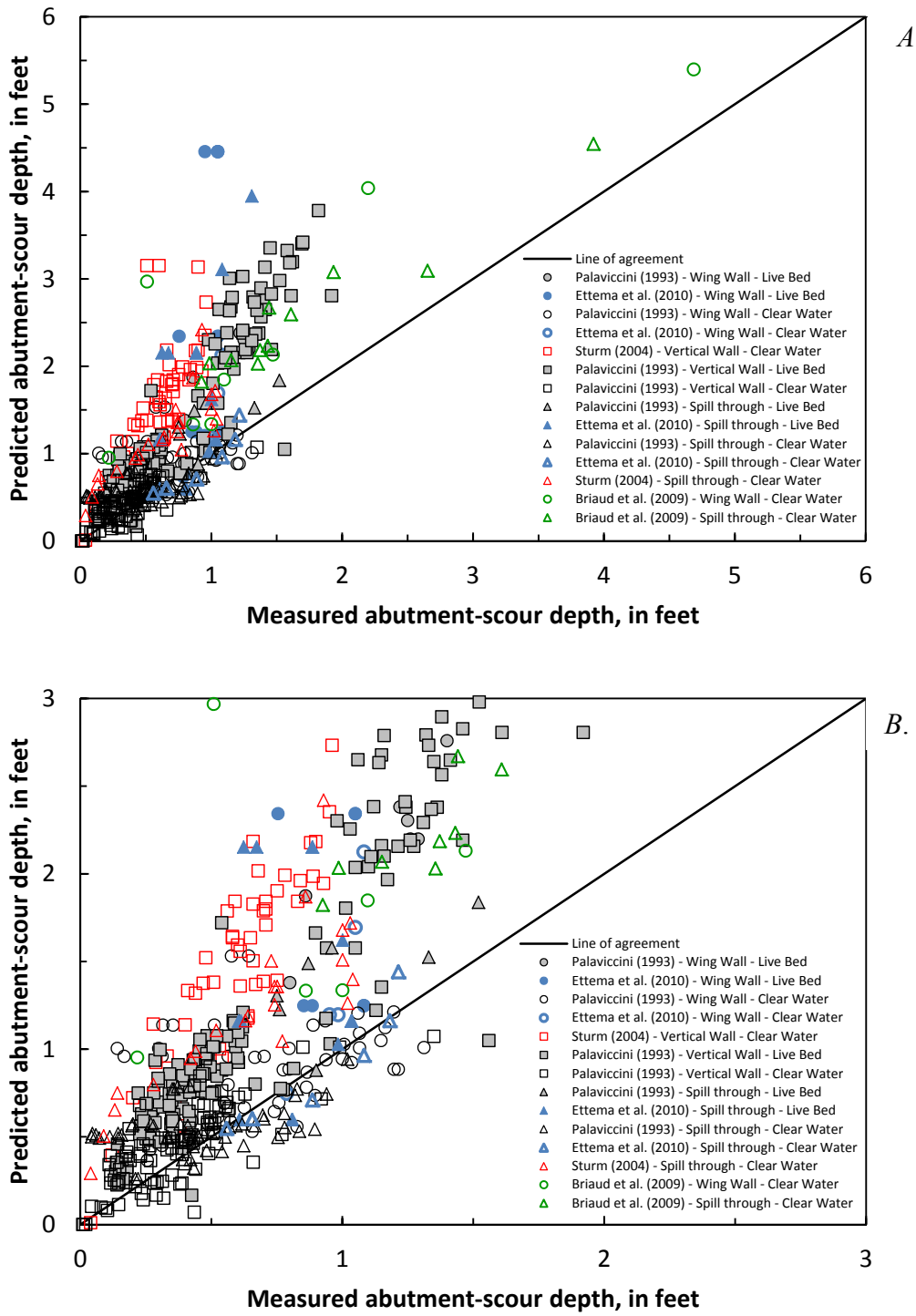

Figure 5-1. Relation of predicted and measured abutment-scour depth for (*A*) selected laboratory data, using the NCHRP 24-15(2) scour prediction method, and (*B*) the same data with a truncated scale.

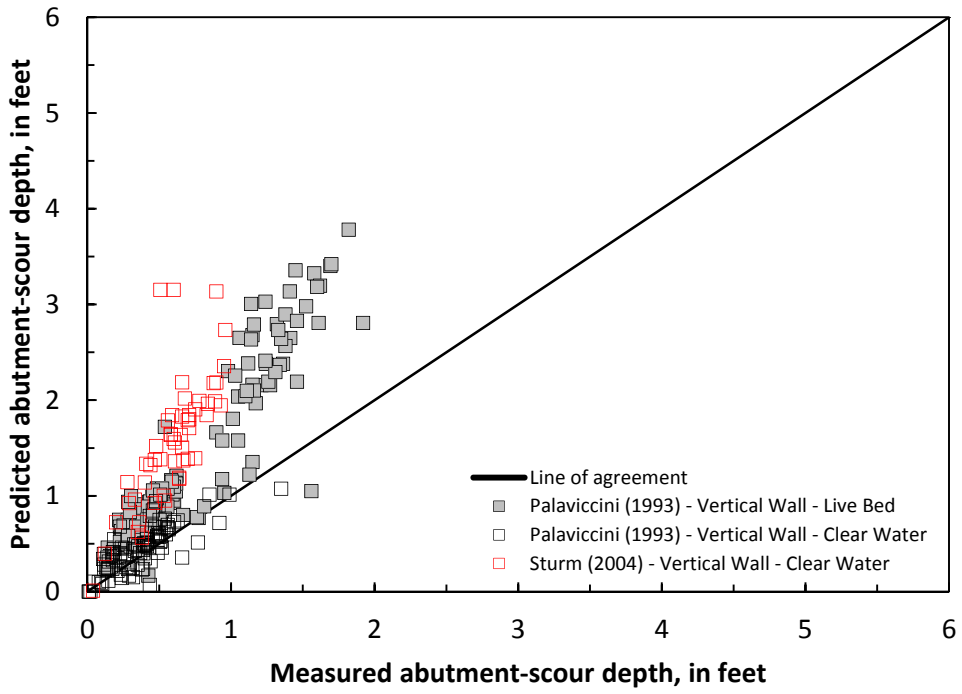

Figure 5-2. Relation of predicted and measured abutment-scour depth for selected laboratory data with vertical-wall abutments, using the NCHRP 24-15(2) scour prediction method.

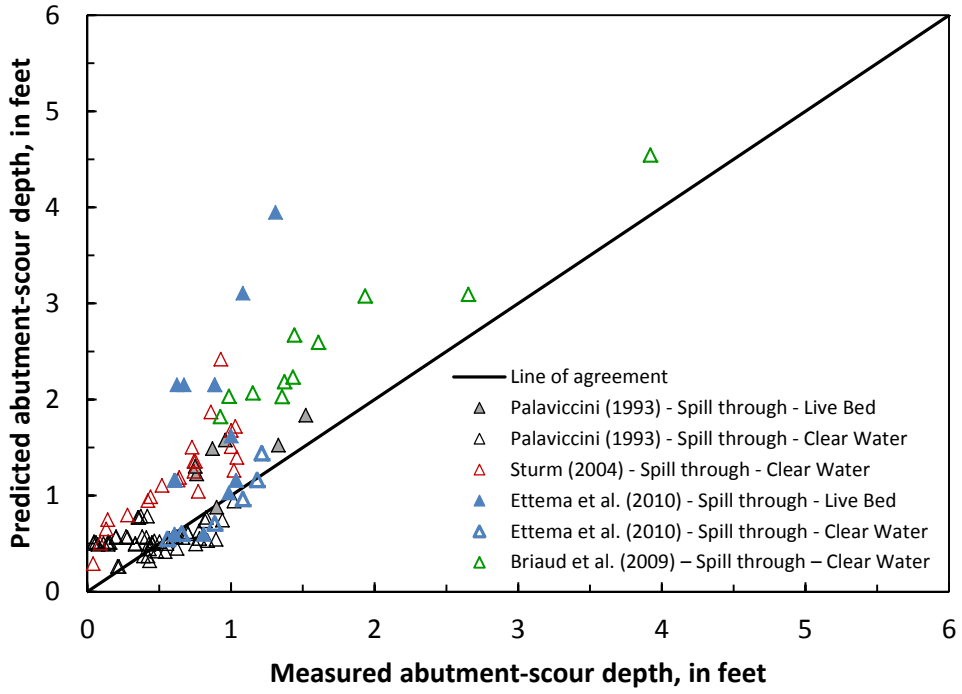

Figure 5-3. Relation of predicted and measured abutment-scour depth for selected laboratory data with spill-through abutments, using the NCHRP 24-15(2) scour prediction method.

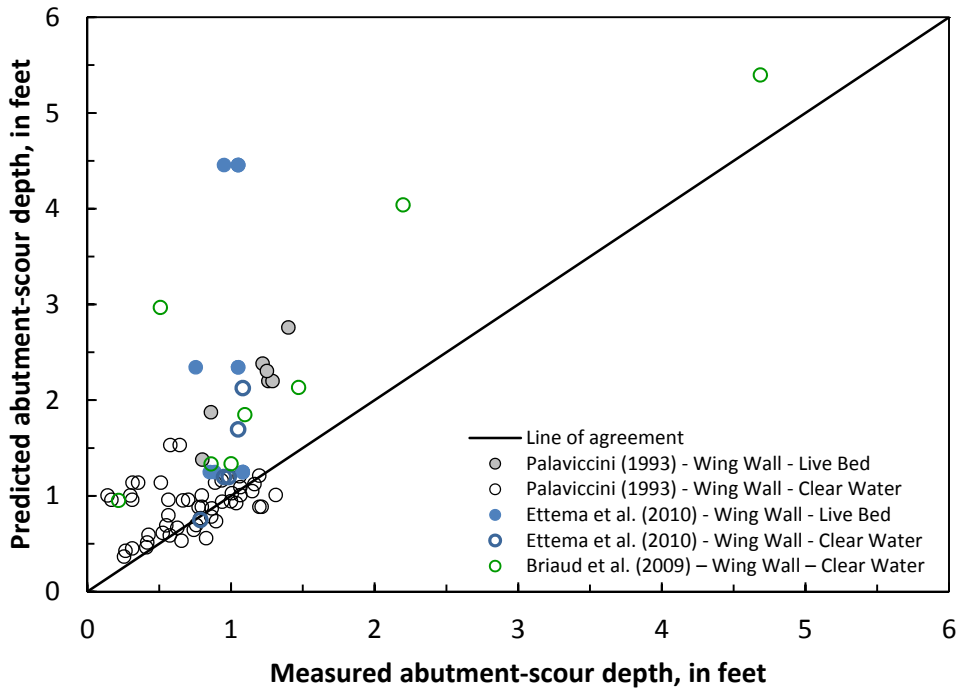

Figure 5-4. Relation of predicted and measured abutment-scour depth for selected laboratory data with wing-wall abutments, using the NCHRP 24-15(2) scour prediction method.

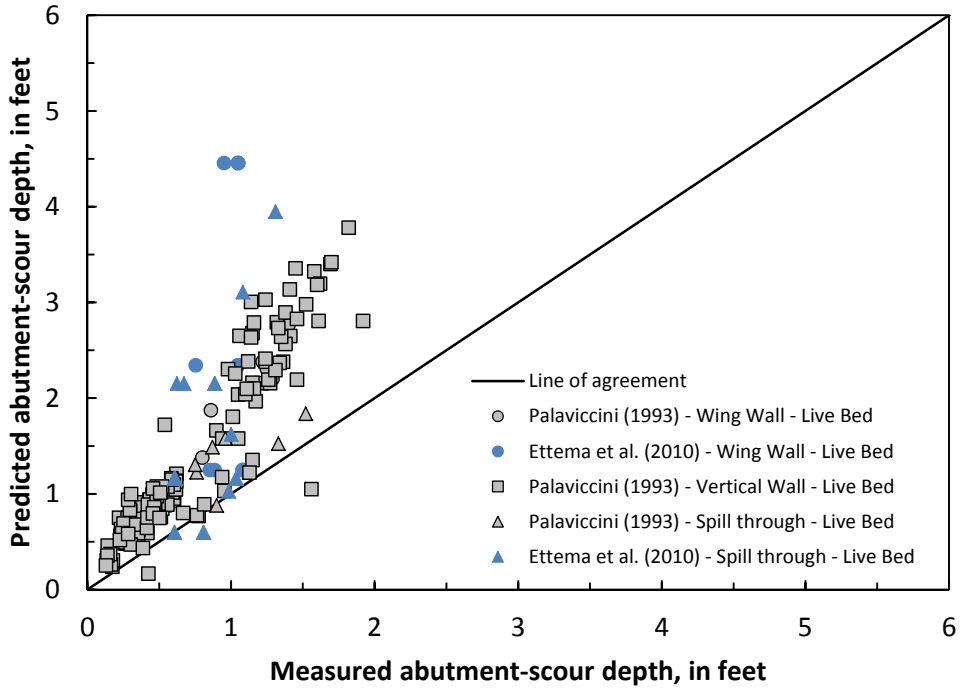

Figure 5-5. Relation of predicted and measured abutment-scour depth for selected laboratory data under live-bed transport condition, using the NCHRP 24-15(2) scour prediction method.

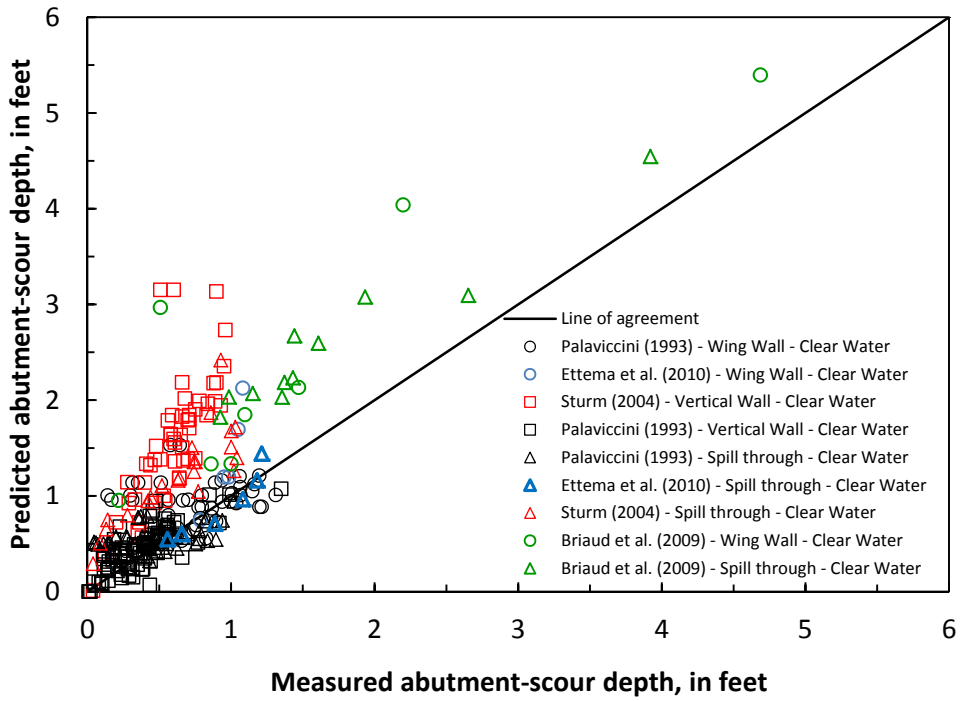

Figure 5-6. Relation of predicted and measured abutment-scour depth for selected laboratory data under clear-water transport condition, using the NCHRP 24-15(2) scour prediction method.

5.2.2 Influence of Selected Explanatory Variables on Predicted Scour

To provide some perspective on the influence of each explanatory variable in equation 4-1 on predicted scour, the following series of figures (figures 5-7 through 5-11) show the relation of predicted to measured scour as each explanatory variable is progressively added to the equation. The progression of adding the explanatory variables is as follows: $7.94(1.65Fr_{f2} - Fr_c)$, K_{Re}, K_1, K_G, and K_L. Some notable features regarding this series of figures include the following:

- The prediction pattern in figure 5-7 indicates that the core explanatory variable, $7.94(1.65Fr_{f2} - Fr_c)$, is reflecting the scour trends in the cohesive sediments from Briaud et al. (2009) better than the other non-cohesive laboratory data. There is a strong trend of overprediction in the non-cohesive data that increases with increasing measured scour.
- The progression from figure 5-7 to 5-8 highlights the influence that the Reynolds number correction factor, K_{Re}, has on the magnitude of predicted scour. The range for K_{Re} for the

laboratory data is from 0.9 to 2.5 with an average value of 1.58, indicating that K_{Re} will tend to increase predicted scour by about 60 percent on average.

- The progression from figure 5-8 to 5-9 highlights the influence of K_1 on predicted scour, with vertical-wall abutments having increased predicted scour and spill-through abutments having decreased predicted scour.
- The progression from figure 5-9 to 5-10 highlights the influence of K_G on predicted scour for rectangular channels, substantially reducing the overprediction, but increasing the frequency and magnitude of underprediction for such channels. All of the Palaviccini (1993) data are associated with rectangular channels, and the influence of K_G is strongly displayed in these data.
- The progression from figure 5-10 to 5-11 highlights the influence of K_L on predicted scour for bankline and protruding abutments, substantially increasing the overprediction for such abutments. Additionally, the underprediction associated with bankline and protruding abutments without the K_L adjustment (figure 5-10) is infrequent, while overprediction with the K_L adjustment (figure 5-11) can be excessive at times. This pattern indicates that K_L is likely not critical in reducing underprediction at such abutments. The K_L correction factor is evaluated in more detail later in this report.

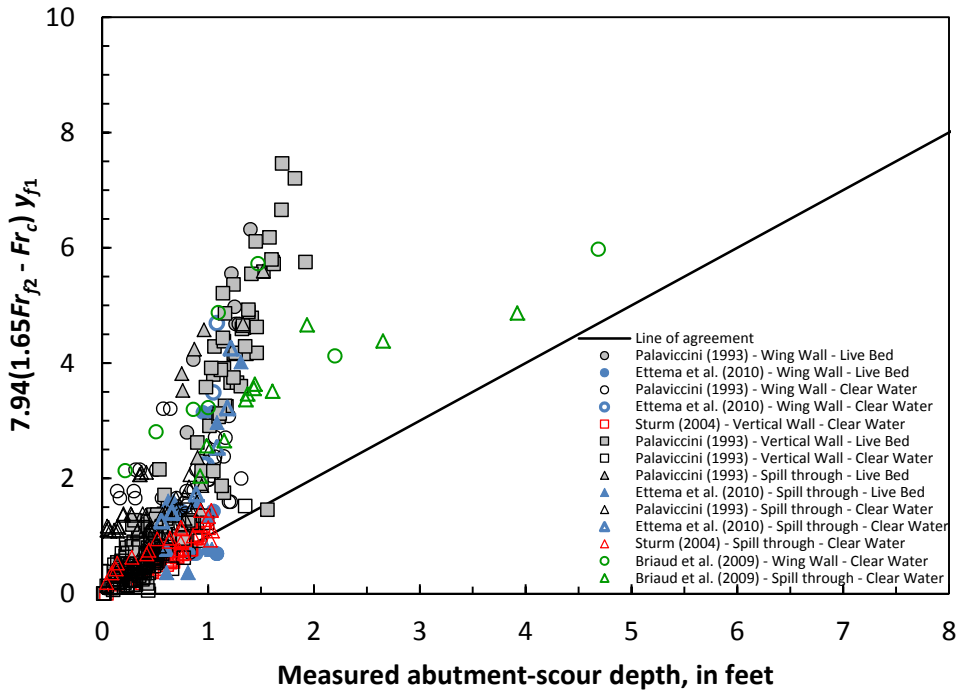

Figure 5-7. Relation of predicted and measured abutment-scour depth based on the selected equation parameters, 7.94(1.65Fr_{f2} - Fr_c), for the NCHRP 24-15(2) scour prediction method.

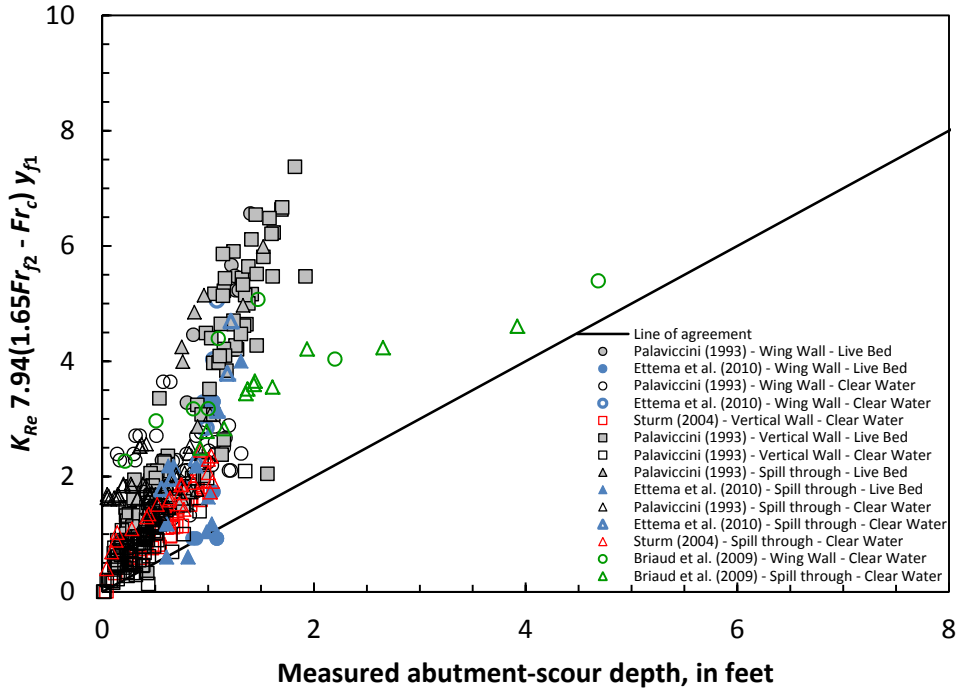

Figure 5-8. Relation of predicted and measured abutment-scour depth based on the selected equation parameters, K_{Re} 7.94(1.65Fr_{f2} - Fr_c), for the NCHRP 24-15(2) scour prediction method.

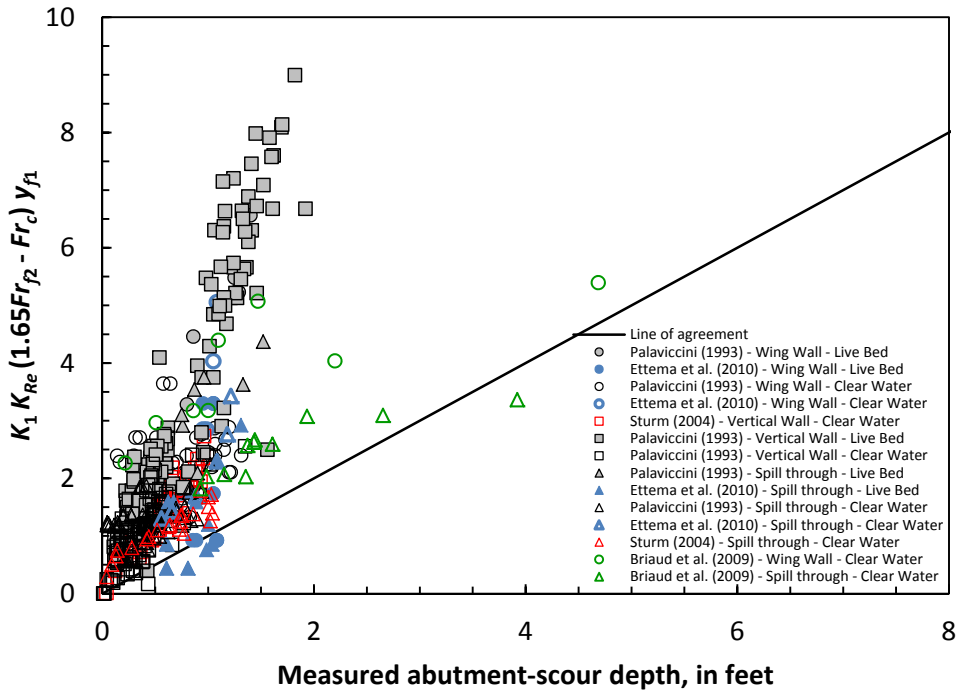

Figure 5-9. Relation of predicted and measured abutment-scour depth based on the selected equation parameters, $K_1 K_{Re}$ 7.94(1.65Fr_{f2} - Fr_c), for the NCHRP 24-15(2) scour prediction method.

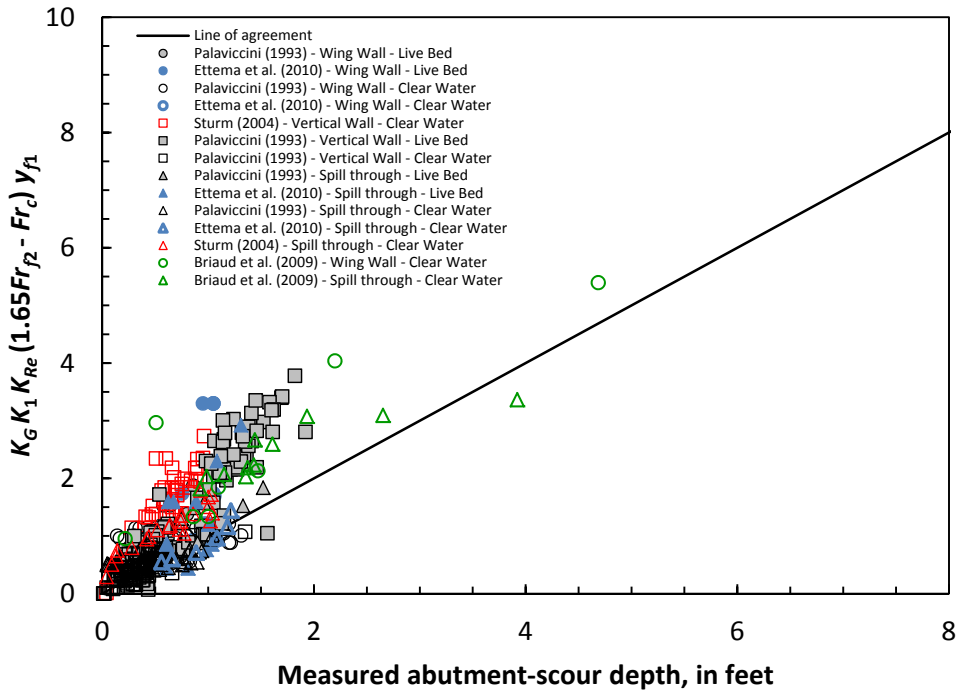

Figure 5-10. Relation of predicted and measured abutment-scour depth based on the selected equation parameters, $K_G K_1 K_{Re}$ 7.94(1.65Fr_{f2} - Fr_c), for the NCHRP 24-15(2) scour prediction method.

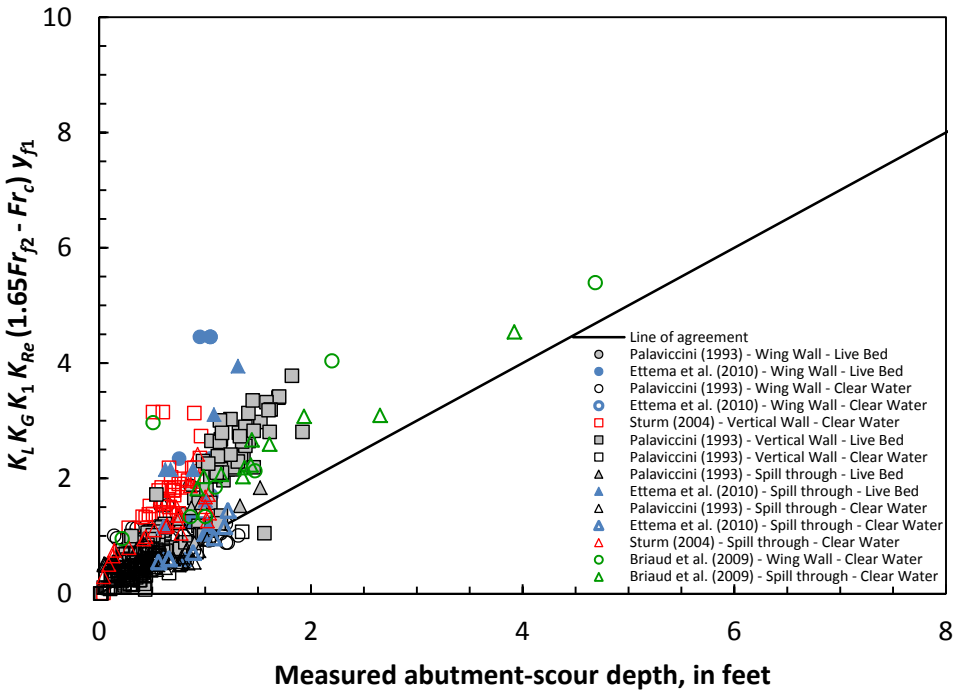

Figure 5-11. Relation of predicted and measured abutment-scour depth based on the selected equation parameters, $K_L\ K_G\ K_1\ K_{Re}\ 7.94(1.65Fr_{f2} - Fr_c)$, for the NCHRP 24-15(2) scour prediction method.

5.2.3 Prediction Residuals with Respect to Selected Explanatory Variables

Figures 5-12 through 5-21 show the prediction residuals (predicted minus measured scour) for the laboratory data in relation to selected explanatory variables, including *D50*, V_c, Fr_c, Fr_{f2}, $7.94(1.65Fr_{f2} - Fr_c)$, Re_{f2}, K_{Re}, and the correction factors in equation 4-1, respectively. The data symbols used in these plots are identical to those used in figures 5-1 through 5-6. These plots were reviewed to identify potential trends regarding under- and overprediction, and a discussion of these plots follows.

i. Prediction Residuals with Respect to *D50*, V_c, and Fr_c

The NCHRP 24-15(2) method uses the sediment critical Froude number (Fr_c) as part of the computational algorithm (equation 4-1). The determination of Fr_c requires an estimate of the sediment critical velocity (V_c) determined by the relation in figure 4-4 in conjunction with the *D50*. The relation of the prediction residuals with respect to *D50*, V_c, and Fr_c are shown in figures 5-12 through 5-14, respectively. The residuals with respect to V_c in figure 5-13A include all of the data, with figure 5-13B showing only the clear-water data. The residuals show that the NCHRP 24-15(2) method tends to overpredict the laboratory data, at times, excessively. Some underprediction is associated with clear-water scour conditions in non-cohesive sediments with rectangular channels. As noted previously, this underprediction, in part, is caused by the smaller K_G value of 0.42 associated with rectangular channels. Additionally, the largest overpredictions for the Sturm (2004) and Ettema et al. (2010) data are associated with bankline or protruding abutments that tend to produce larger scour predictions because of the larger K_L value of 1.35. Because of the influence of other variables on predicted scour, it is difficult to isolate the influence of *D50*, V_c, and Fr_c, and there generally does not appear to be a strong trend in the residuals. However, figures 5-13 and 5-14 indicate some increase in the frequency and magnitude of underprediction as V_c and Fr_c decrease. The determination of V_c in the NCHRP 24-15(2) method is based on the relation developed by Briaud et al. (2011) as shown in figure 4-4. A comparison of V_c determined from figure 4-4 to that determined by the HEC-18 (Arneson et al. 2012) method, based on the Laursen (1963) critical-velocity equation, is shown in figure 5-15. The comparison indicates that the Briaud et al. (2009) method tends to produce smaller

values for V_c than the Laursen (1963) equation with the exception of the larger *D50*s associated with the Sturm (2004) data. If the larger values of V_c associated with the Laursen (1963) equation are applied to the NCHRP 24-15(2) method, the frequency and magnitude of overprediction will be slightly reduced, but the frequency and magnitude of underprediction will increase. The Laursen (1963) V_c values for the laboratory data were applied to the NCHRP 24-15(2) method, and the prediction residuals with respect to the Laursen (1963) V_c are shown in figure 5-16 confirming this trend. (Note: The *D50* value for the Briaud et al. (2009) data was set to 0.2 mm for application to the Laursen (1963) V_c equation.) The trends in figure 5-16 indicate that application of the Laursen (1963) critical-velocity equation to the NCHRP 24-15(2) method likely would not improve performance.

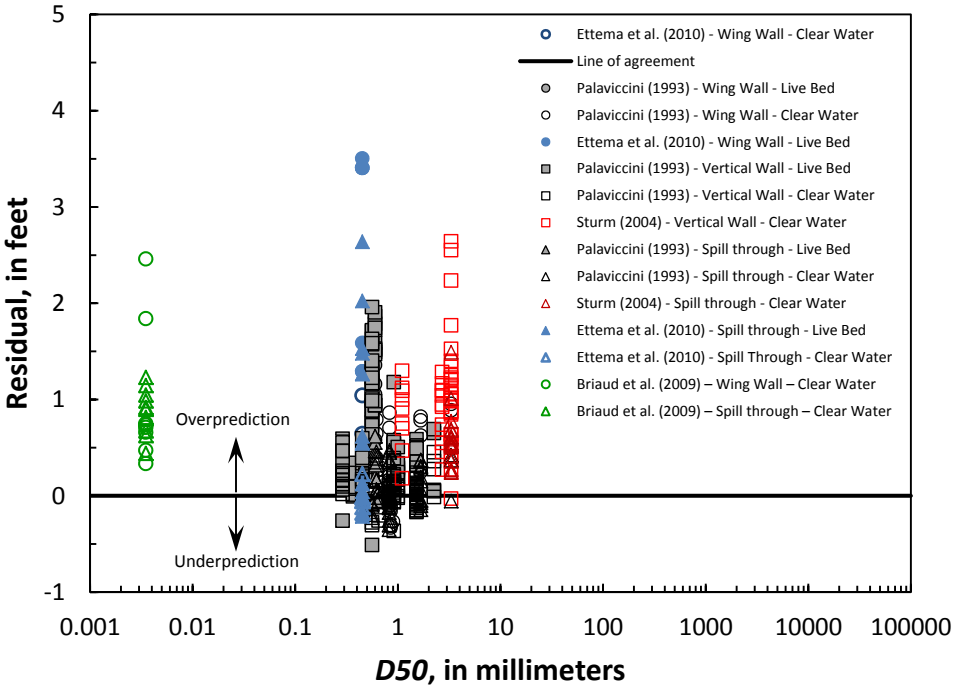

Figure 5-12. Relation of prediction residuals and the median sediment size (*D50*) for selected laboratory data, using the NCHRP 24-15(2) scour prediction method.

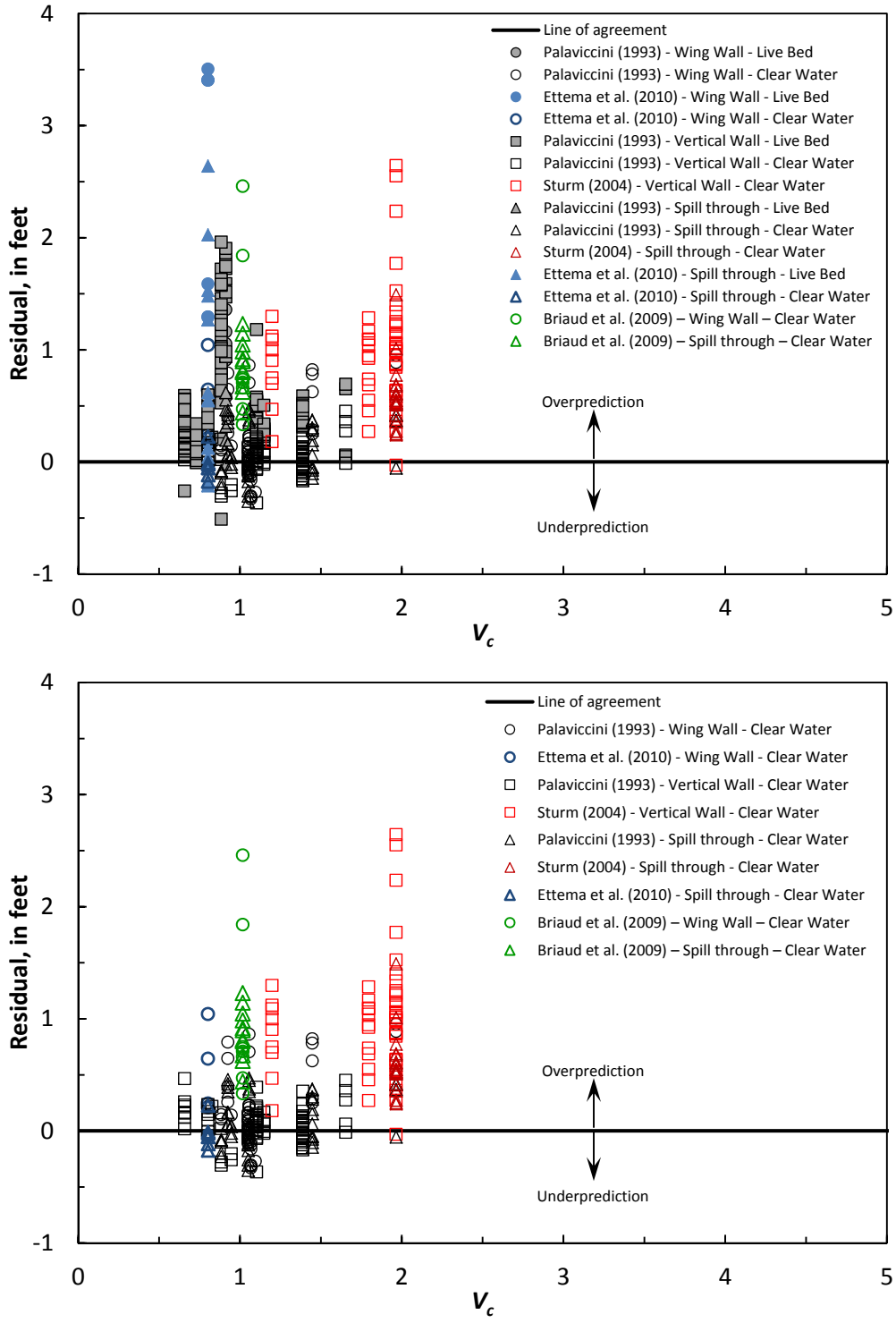

Figure 5-13. Relation of prediction residuals and the Briaud et al. (2009) sediment critical velocity (V_c) for selected laboratory data, using the NCHRP 24-15(2) scour prediction method, including (*A*) all of the data and (*B*) only clear-water scour data.

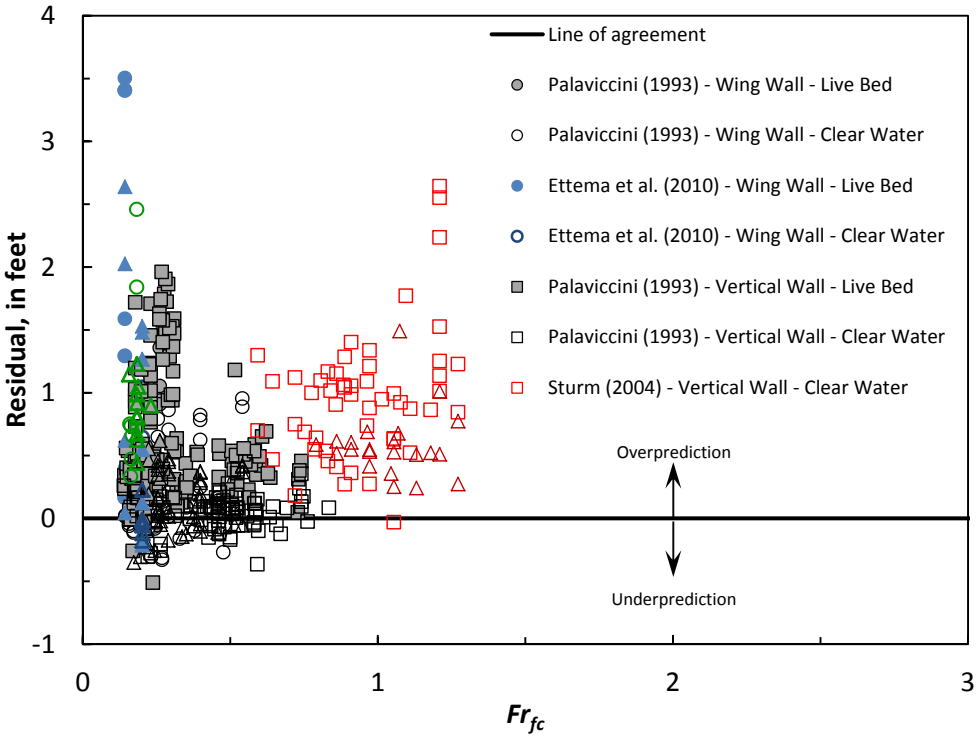

Figure 5- 14. Relation of prediction residuals and the sediment critical-velocity Froude number (Fr_c) for selected laboratory data, using the NCHRP 24-15(2) scour prediction method.

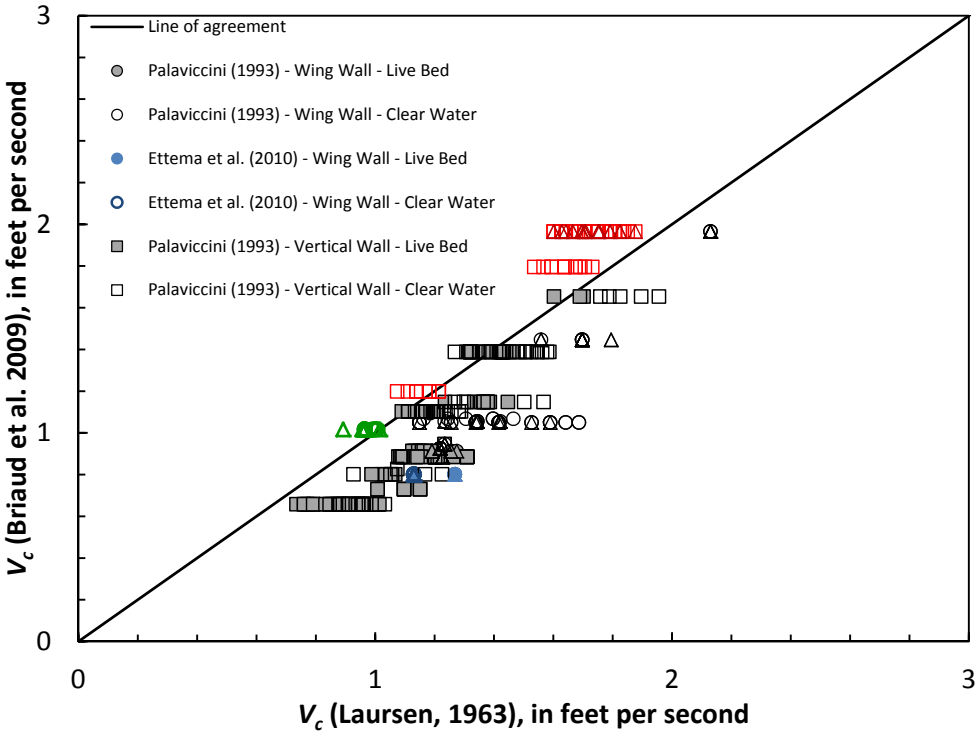

Figure 5-15. Comparison of the Briaud et al. (2009) and the Laursen (1963) sediment critical velocity (V_c) for selected laboratory data.

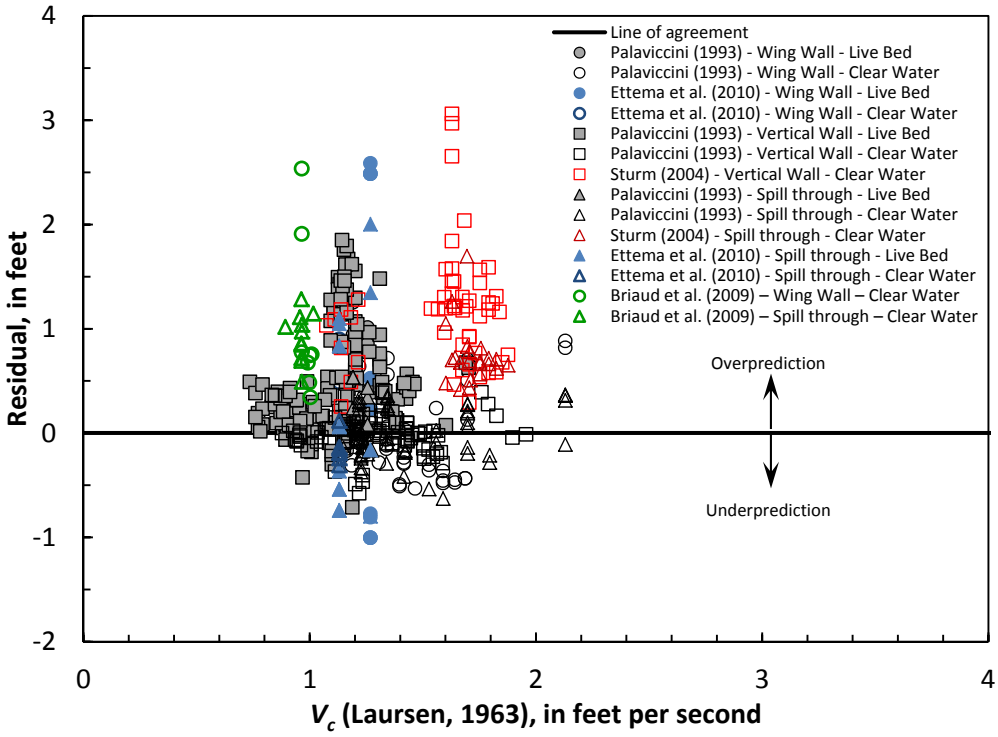

Figure 5-16. Relation of prediction residuals and the Laursen (1963) sediment critical velocity (V_c) for selected laboratory data, using the NCHRP 24-15(2) scour prediction method in conjunction with the Laursen (1963) V_c.

ii. Prediction Residuals with Respect to Fr_{f2} and $7.94(1.65Fr_{f2} - Fr_c)$

The core explanatory variable for the NCHRP 24-15(2) method is the parameter $7.94(1.65Fr_{f2} - Fr_c)$ that uses the Froude number at the abutment (Fr_{f2}) and the critical-velocity Froude number (Fr_c). The relation of the prediction residuals with respect to Fr_{f2} and the parameter $7.94(1.65Fr_{f2} - Fr_c)$ is shown in figures 5-17 and 5-18, respectively. The residuals display a strong relation with respect to both of these explanatory variables, indicating that the magnitude of overprediction increases as these explanatory variables increase. While the magnitude of the underprediction is smaller than the overprediction, the trends also indicate that the frequency and magnitude of underprediction increase with decreasing values of Fr_{f2} and $7.94(1.65Fr_{f2} - Fr_c)$ below about 0.75 and 5, respectively. The largest overpredictions for the Sturm (2004) and Ettema et al. (2010) data are associated with bankline or protruding abutments that have larger estimates of scour depth because the abutment-location correction factor (K_L) has a value of 1.35.

A review of figures 5-17 and 5-18 highlights that the range for these explanatory variables for the Briaud et al. (2009) data is smaller than that of the other laboratory data. For Fr_{f2} and $7.94(1.65Fr_{f2} - Fr_c)$, the values for the Briaud et al. (2009) data range from 0.23 to 0.58 and 1.78 to 6.20, respectively. In contrast, the other laboratory data range from 0.07 to 1.78 and 0.03 to 21.19, respectively, for Fr_{f2} and $7.94(1.65Fr_{f2} - Fr_c)$. Excluding the previously noted bankline and protruding abutments, the largest overpredictions and underpredictions in figures 5-17 and 5-18 are associated with values of these explanatory variables that are outside of the range of the Briaud et al. (2009) data used to develop the NCHRP 24-15(2) prediction method, indicating that caution should be used when applying the method beyond the range of the Briaud et al. (2009) data.

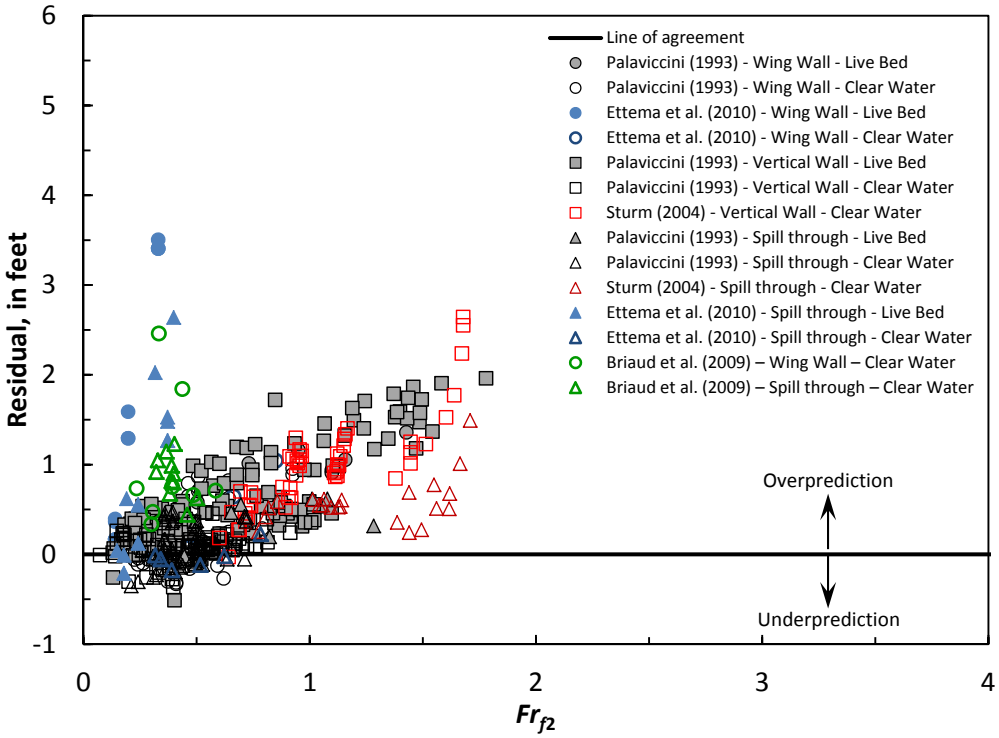

Figure 5-17. Relation of prediction residuals and the Froude number (Fr_{f2}) at the abutment for selected laboratory data, using the NCHRP 24-15(2) scour prediction method.

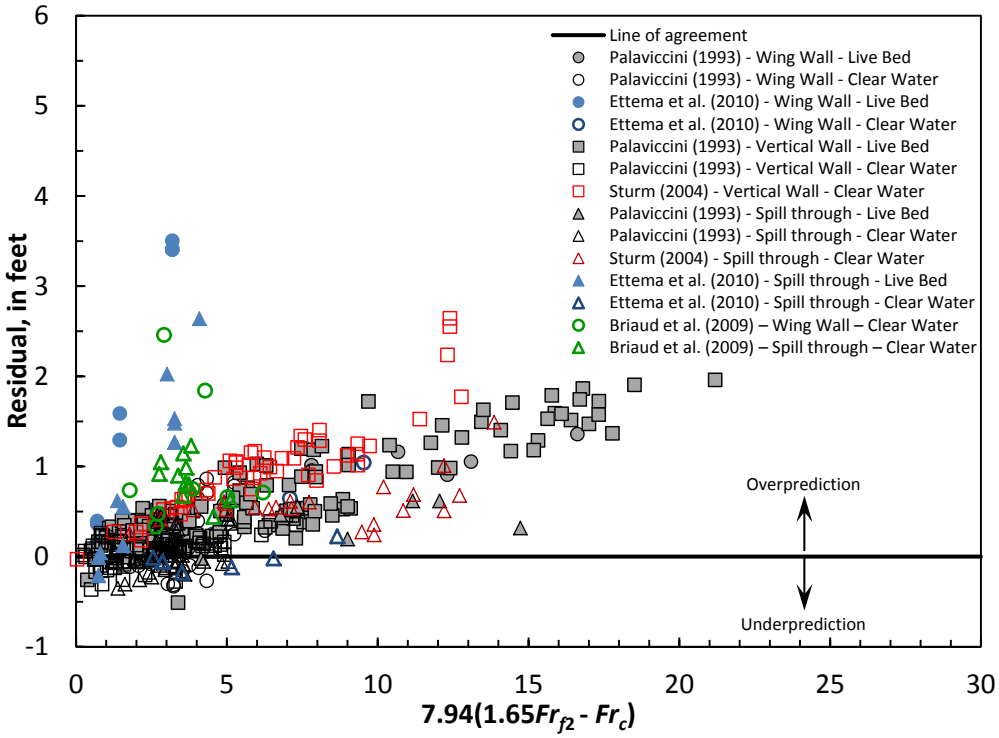

Figure 5-18. Relation of prediction residuals and the Froude number parameter, $7.94(1.65Fr_{f2} - Fr_c)$, for selected laboratory data, using the NCHRP 24-15(2) scour prediction method.

iii. Prediction Residuals with Respect to Re_{f2} and K_{Re}

The NCHRP 24-15(2) method incorporates a correction factor for the Reynolds number at the abutment (Re_{f2}), expressed as K_{Re}. In a literature review of previous investigations of abutment scour, Sturm et al. (2011) provided a list of 19 selected abutment-scour prediction equations developed during the period from 1961 to 2010. A review of these equations indicates that none, with the exception of the NCHRP 24-15(2) equation, include the Reynolds number as an explanatory variable. Melville and Coleman (2000) and Sturm et al. (2011) note that viscous effects, as incorporated in the Reynolds number, can be neglected in the derivation of abutment- and contraction-scour equations because of the large values for Reynolds numbers typically associated with prototype turbulent flows. This provides some explanation for the absence of the Reynolds number from the other abutment-scour equations, and suggests that its inclusion in the NCHRP 24-15(2) method is problematic.

The relation of the prediction residuals with respect to Re_{f2} is shown in figure 5-19A, which displays a trend indicating that the magnitude of overprediction increases as Re_{f2} increases. While the magnitude of the underprediction is smaller than the overprediction, there is a similar trend of increasing magnitude of underprediction with increasing Re_{f2}. The Sturm (2004) data have larger residuals than the other data within the same range of Re_{f2}. This difference is primarily attributed to the channel-geometry correction factor, K_G, with the Sturm (2004) data having compound channels with a K_G value of 1.0 in contrast to most of the other data in the same range of Re_{f2} and having rectangular channels with a K_G value of 0.42. To highlight the trend in the residuals, figure 5-19B shows the same data as in figure 5-19A without the Sturm (2004) data. All of the Palaviccini (1993) data have rectangular channels with a common K_G value of 0.42, and the increased overprediction with increasing Re_{f2} is observable.

To provide perspective on how the Reynolds number correction factor K_{Re} varies with Re_{f2}, figure 5-20 shows a plot of K_{Re} with respect to arbitrary values of Re_{f2}. The plot indicates that K_{Re} is inversely proportional to Re_{f2}, decreasing as Re_{f2} increases. The range of Re_{f2} for the Briaud et al. (2009) data, all of the laboratory data, and the field data are shown in the figure, with Re_{f2} ranging from about 98,000 to 310,000 for the Briaud data, 7,000 to 310,000 for all of

the laboratory data, and 220,000 to 12,000,000 for the field data. Correspondingly, the values for K_{Re} range from about 0.9 to 1.2 for the Briaud data, 0.9 to 2.5 for all of the laboratory data, and 0.3 to 1 for the field data. The ranges of Re_{f2} and K_{Re} for the other laboratory data and the field data are beyond that of the Briaud et al. (2009) data used to develop the NCHRP 24-15(2) equation, and this may affect equation performance for these datasets. Of particular concern for the field data application is that values for K_{Re} will be lower than those associated with the Briaud et al. (2009) data used to develop the NCHRP 24-15(2) equation potentially causing some underprediction. The relation of the prediction residuals with respect to K_{Re} is shown in figure 5-21. The residuals display a trend indicating that the magnitude of overprediction decreases as K_{Re} increases. The trend also indicates that the frequency and magnitude of underprediction decrease with increasing values of K_{Re}. The residual patterns in figures 5-19 and 5-21 indicate that the Reynolds number correction factor has some influence on equation performance. However, as noted in the previous section, the parameter $7.94(1.65Fr_{f2} - Fr_c)$ also has an influence on equation performance, making it difficult to separate the influence of these two explanatory variables. This is further compounded by the fact that both $7.94(1.65Fr_{f2} - Fr_c)$ and K_{Re} are determined by use of flow depth and flow velocity, indicating that their influence on equation performance is interrelated.

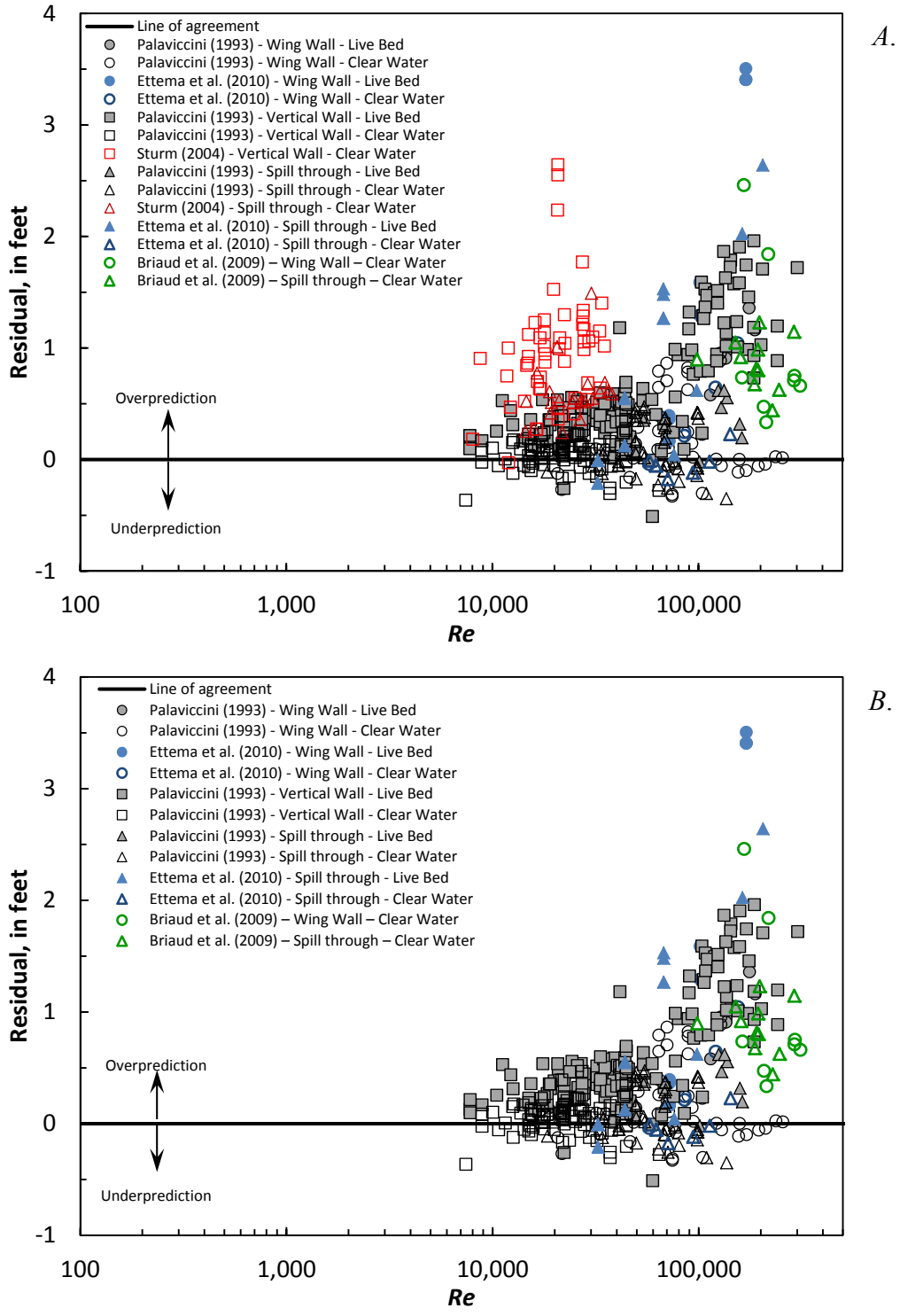

Figure 5-19. Relation of prediction residuals and the Reynolds number at the abutment (Re_{f2}) for selected laboratory data, using the NCHRP 24-15(2) scour prediction method, including (*A*) all of the data, and (*B*) without the Sturm (2004) data.

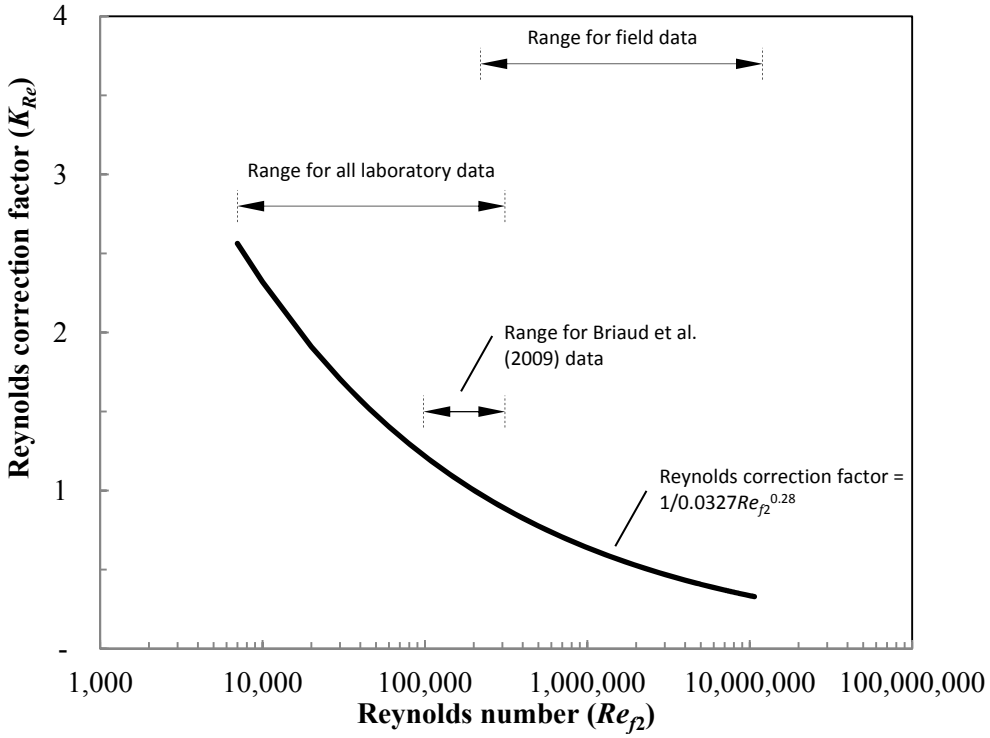

Figure 5-20 Relation of the Reynolds number at the abutment (Re_{f2}) and the Reynolds number correction factor, K_{Re}, for the NCHRP 24-15(2) scour prediction method.

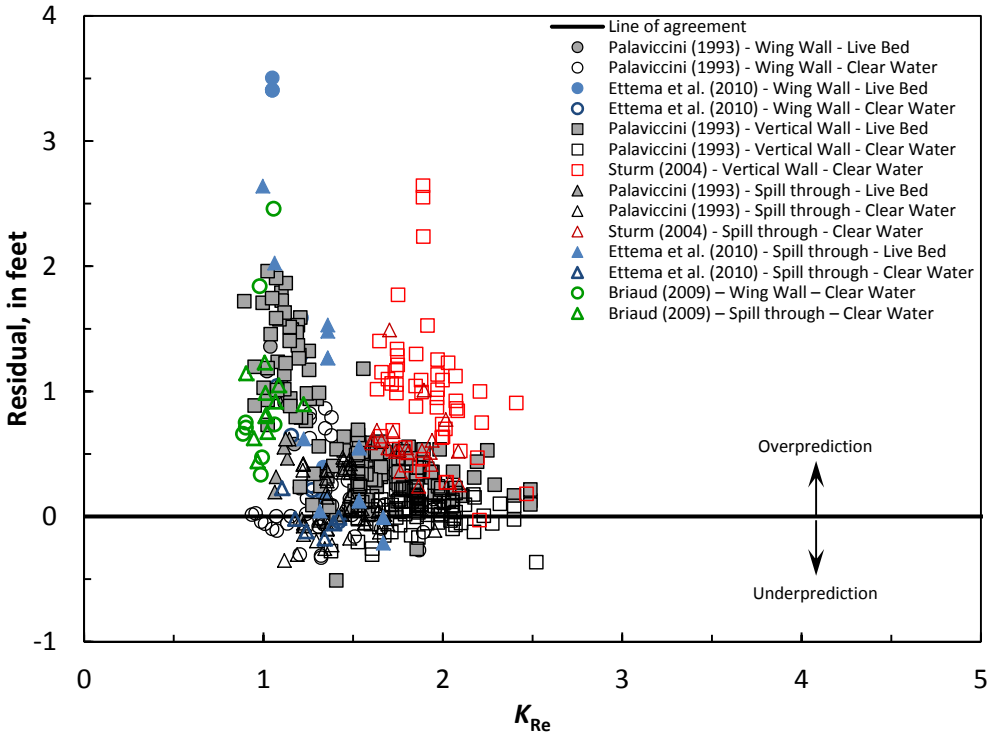

Figure 5-21. Relation of prediction residuals and the Reynolds number correction factor, K_{Re}, for selected laboratory data, using the NCHRP 24-15(2) scour prediction method.

iv. Prediction Residuals with Respect to K_1, K_2, K_G, and K_L

The NCHRP 24-15(2) method incorporates correction factors for abutment shape (K_1), abutment skew (K_2), channel geometry (K_G), and abutment location (K_L). In order to display the residual trends with respect to each correction factor, subsets of the laboratory data must be selected that have varying values for the correction factor of interest, with the other correction factors having constant values. The following is a review of each correction factor and an evaluation of residual trends for selected data subsets.

Abutment-shape correction factor (K_1)

Briaud et al. (2009) used 3 abutment shapes in their investigation including a 45-degree wing-wall abutment, a spill-through abutment with a 2:1 slope, and a spill-through abutment with a 3:1 slope. Using the 45-degree wing wall as the standard shape for normalizing the data, Briaud et al. (2009) assigned K_1 values of 1.0, 0.73, and 0.59 to these abutment shapes, respectively. In previous investigations of abutment scour (Froehlich, 1989; Melville, 1992), the vertical-wall abutment shape was often used as the normalizing shape leading to different values of K_1 than those developed by Briaud et al. (2009). In the case of the Froehlich (1989) study, correction factors for vertical-wall, wing-wall, and spill-through abutments were 1.0, 0.82, and 0.55, respectively. Briaud et al. (2009) note that it is possible to convert the Froehlich (1989) correction factors so that the wing-wall abutment is the normalizing shape by dividing the values by 0.82. This adjustment to the Froehlich (1989) correction factors leads to correction factor values of 1.22, 1.0, and 0.67 for vertical-wall, wing-wall, and spill-through abutments, respectively. These adjusted values, normalized to the wing-wall abutment shape, are comparable to those developed by Briaud et al. (2009), providing support for the validity of the K_1 values.

The Palaviccini (1993) dataset is the largest subset of the laboratory data that includes vertical-wall, wing-wall, and spill-through abutments with common values of K_2, K_G, and K_L. For these data, K_2 is 1.0, K_G is 0.42 for the rectangular channels, and K_L is 1.0. The relation of the prediction residuals with respect to K_1 is shown in figure 5-22. While other variables contribute to the residual patterns in this figure, the upper bound of the residuals decreases as

the value of K_1 decreases, reflecting the influence of K_1 on equation performance. The underprediction in figure 5-22 is primarily caused by the channel correction factor, K_G, being 0.42 for rectangular channels and should not be associated with the influence of K_1.

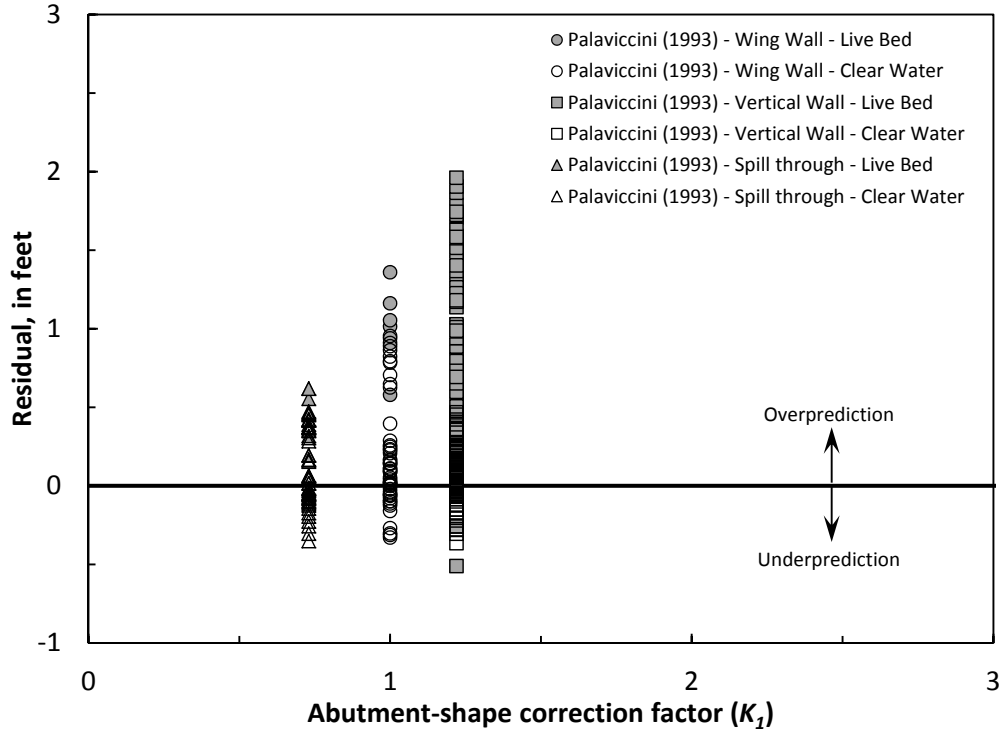

Figure 5-22. Relation of prediction residuals and the abutment-shape correction factor, K_1, for selected laboratory data, using the NCHRP 24-15(2) scour prediction method.

Abutment-skew correction factor (K_2)

Only two abutment-scour measurements in the laboratory data were associated with a skewed abutment, and therefore, a plot of the residuals associated with K_2 was of minimal benefit and not included in the report. However, a brief review of the K_2 correction factor follows. Based on the work of earlier investigations, such as Froehlich (1989) and Melville (1992), it generally has been accepted that skewed abutments pointing downstream produce smaller scour depths, while skewed abutments pointing upstream produce larger scour depths. Based on this previous work, the magnitude of the decrease or increase in scour depth is about 5 percent for moderate skews and about 10 percent for severe skews. The findings of the Briaud et al. (2009) investigation are somewhat contrary to these previous studies, with scour depth decreasing by as much as 15 percent regardless of the abutment orientation to flow. Based on this finding, the NCHRP 24-15(2) prediction method specifies that K_2 be set to a value of 0.85 for a skew angle of 30 degrees or greater from perpendicular, regardless of orientation to flow, with K_2 transitioning to a value of 1 as the abutment-skew angle approaches 0. Dongol (1993) notes that laboratory investigations by Kwan (1984) and Kandasamy (1985) found similar qualitative trends to those of Briaud et al. (2009), with reduced scour at skewed abutments regardless of orientation to flow, providing support for the general patterns in the Briaud et al. (2009) investigation. However, only two of the Briaud et al. (2009) data points are associated with skewed abutments, one pointing downstream and the other upstream. Because of the limited number of data, the relation for determining K_2 should be used with caution, and further investigation of the influence of skew on abutment-scour depth could be beneficial to confirm the equation for determining K_2.

Channel-geometry correction factor (K_G)

Briaud et al. (2009) concluded that channel geometry influences abutment-scour depth, with rectangular channels reducing scour by approximately 60 percent in comparison to compound channels. To account for this influence, a channel-geometry correction factor, K_G, was included in the NCHRP 24-15(2) scour prediction method, with K_G having a value of 1.0 for compound channels and 0.42 for rectangular channels. The relation of the prediction residuals for selected laboratory data with respect to K_G is shown in figures 5-23A through C. These data include the clear-water scour conditions for vertical-wall, wing-wall, and spill-through abutments for selected data, with values of K_2 and K_L equal to 1.0. The upper bound of the prediction residuals for the rectangular-channel data is smaller than that of the compound-channel data. The magnitude of this difference varies with abutment shape with the vertical- and wing-wall abutments having a larger difference than that of the spill-through abutments. The frequency and magnitude of underprediction is much larger for the rectangular-channel data than for the compound-channel data. To provide perspective on the influence of K_G, figure 5-24 shows the same data as in figure 5-23C, with the K_G value for the rectangular-channel data arbitrarily set to 1.0. This value of K_G for the rectangular-channel data removes most of the underpredictions. A review of figures 5-23A–C highlights how the NCHRP 24-15(2) method will yield frequent underpredictions for clear-water scour sites with rectangular channels. This is the pattern previously noted in figures 5-1 through 5-6, with most of the underprediction in those figures associated with clear-water scour conditions in rectangular channels. As noted later in the report, this pattern is of concern for the field data where floodplain relief bridges and bridges crossing swamps with poorly defined channels are classified as rectangular channels under clear-water scour conditions and also have frequent and, at times, large underprediction.

Figure 5-25 presents the relation from Briaud et al. (2009) that was used to analyze the influence of channel geometry on abutment-scour depth and, in turn, develop the K_G correction factor. As can be seen, a relation indicates that rectangular channels in the Briaud et al. (2009) data have smaller scour depths than compound channels. (Note: Only two of the three compound-channel data points, the largest of the relative scour values, are shown in

figure 5-25. The other 5 data points are associated with rectangular channels, and only the 2 data points that form the lower envelope of the rectangular-channel data are shown as circular symbols.) Because of the complex nature of scour, it is often difficult to isolate the influence of a single variable, and this is likely the case with regard to the influence of channel geometry. A review of the data in figure 5-25 indicates that hydraulic conditions are likely contributing to this pattern rather than just the channel geometry, and this is discussed below.

Figure 5-26 shows the relation of relative-scour depth to the total flow using the same data in figure 5-25 along with the one additional compound-channel data point. (Note: All of the rectangular- and compound-channel data are identified with distinct symbols in figure 5-26.) The flow for all of the rectangular-channel data is approximately 15 cubic feet per second (ft^3/s), whereas the three compound-channel data points have flows ranging from about 15 to 27 ft^3/s. The compound-channel data with a flow of about 15 ft^3/s are comparable to the flow rate of the rectangular channels, and also have a relative-scour depth comparable to the rectangular channels. In contrast, the two compound-channel data with larger flows have larger relative-scour depths, indicating that the differing scour patterns between the compound and rectangular channels likely are a function of flow rather than channel geometry. While additional research on the influence of channel geometry is warranted, the relations in figure 5-25 indicate that it may be appropriate to use a value of 1.0 for K_G at rectangular channels. This is further supported by the work of Melville (1992) and Melville and Coleman (2000). While these studies acknowledge the influence of channel geometry on scour depth, they indicate that rectangular channels produce the largest scour depth, contrary to the findings of the Briaud et al. (2009) study. Based on the work of Melville (1992) and Melville and Coleman (2000), it would seem appropriate to use a value of 1.0 for K_G at rectangular channels rather than a value of 0.42.

To provide understanding of how a change in K_G for rectangular channels will affect equation performance, figure 5-27 shows the same data as shown in figure 5-1A with K_G for rectangular channels set to 1.0. In this situation, underprediction for clear-water scour data at rectangular channels is largely removed. As noted later in the report, this is an important

feature for application of the field data to the NCHRP 24-15(2) method. However, there is large overprediction for the live-bed rectangular-channel data, with some excessive values. Figure 5-28 shows the residuals for the data in figure 5-27 with respect to the parameter $7.94(1.65Fr_{f2} - Fr_c)$ and highlights how the largest residuals are associated with live-bed scour data substantially beyond the range of $7.94(1.65Fr_{f2} - Fr_c)$ for the Briaud et al. (2009) data. For values of $7.94(1.65Fr_{f2} - Fr_c)$ near the range of the Briaud et al. (2009) data, the upper bound of the residuals is close to the upper bound associated with the Briaud et al. (2009) data, indicating that the performance of the rectangular channel, within the range of the Briaud et al. (2009) data, conforms to that of the compound channels when K_G is set to 1.0.

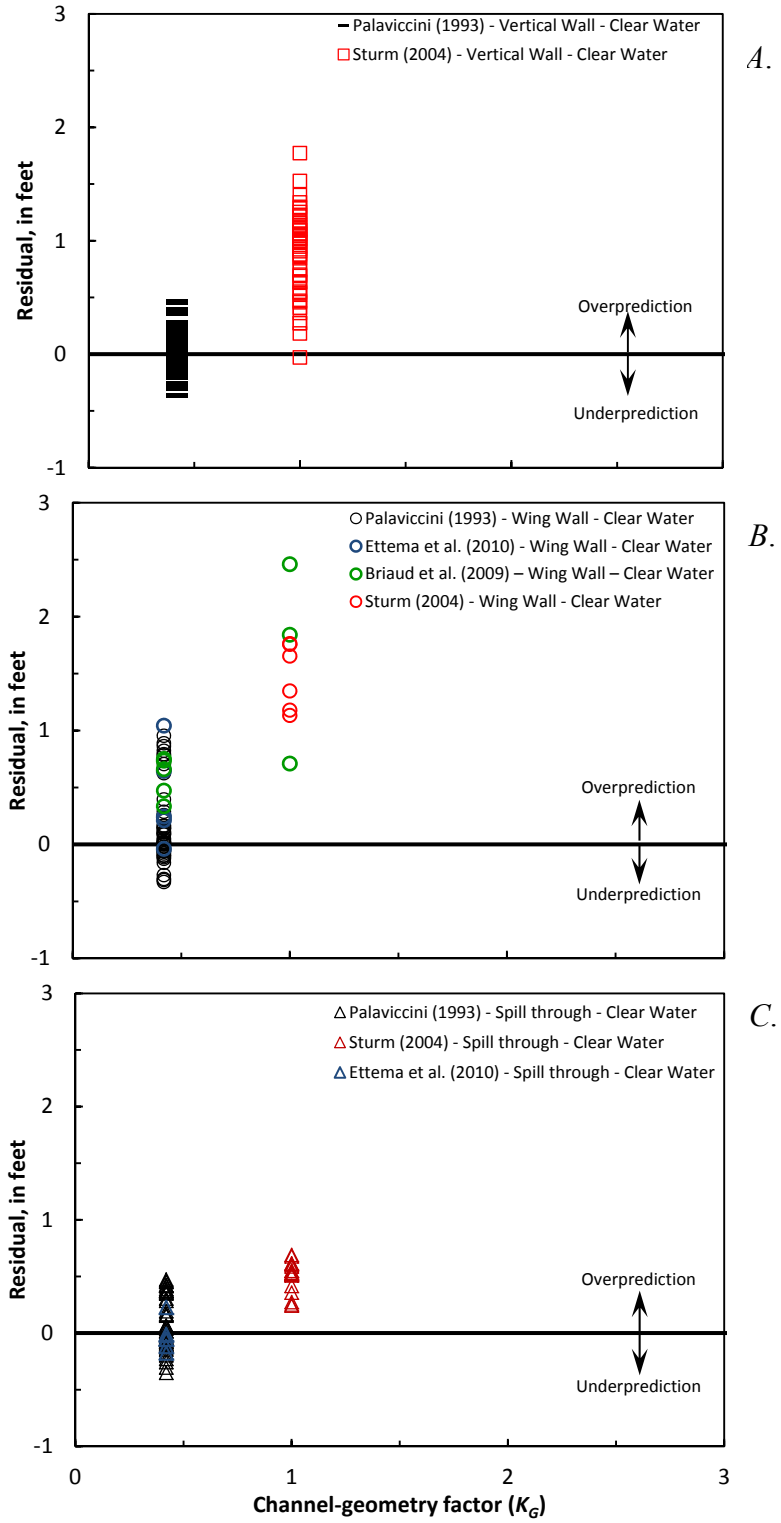

Figure 5-23. Relation of prediction residuals and the channel-geometry correction factor, K_G, using the NCHRP 24-15(2) scour prediction method for (*A*) vertical-wall abutments, (*B*) wing-wall abutments, and (*C*) spill-through abutments.

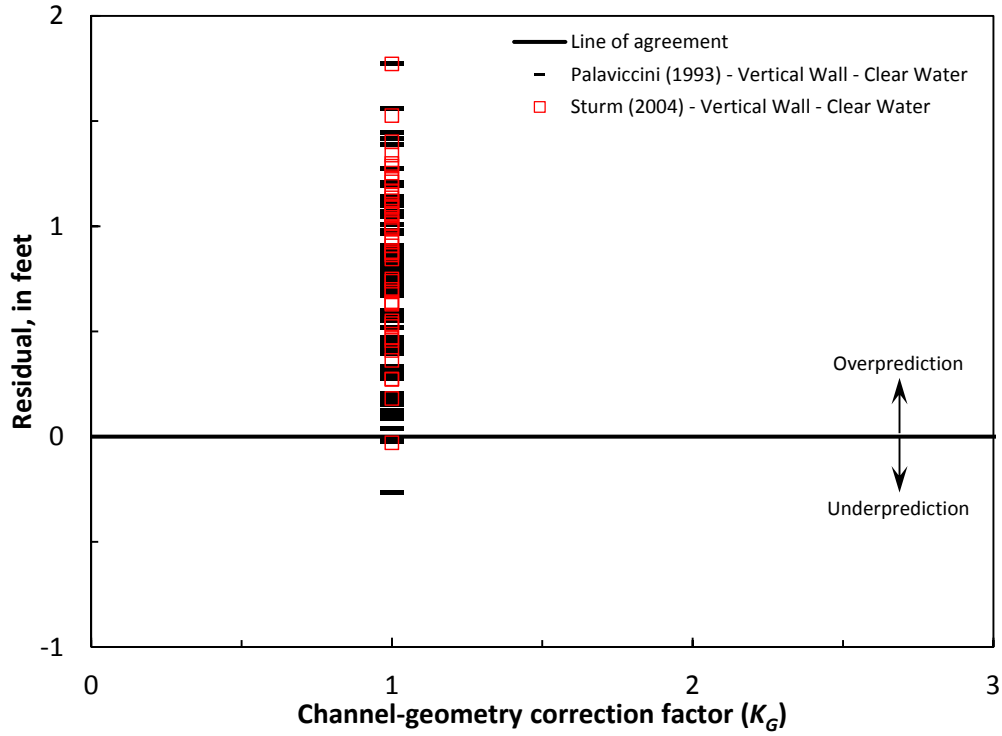

Figure 5-24. Relation of prediction residuals and the channel-geometry correction factor, K_G, using the NCHRP 24-15(2) scour prediction method for vertical-wall abutments and K_G for all data arbitrarily set to a value of 1.0.

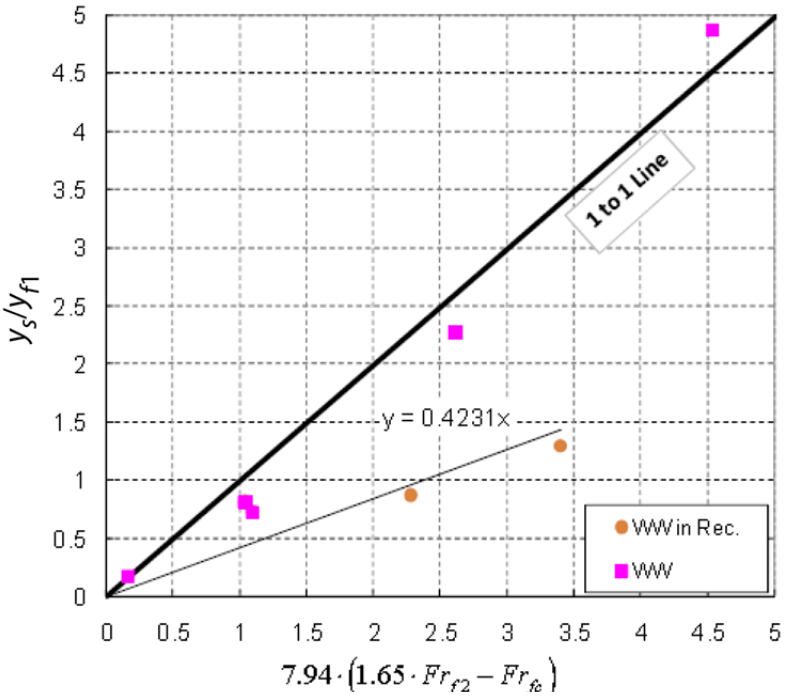

Figure 5-25. Relation of relative scour to the parameter, $7.94(1.65Fr_{f2} - Fr_c)$, used to develop the channel-geometry correction factor, K_G (from Briaud et al. 2009). (Note: The term "WW in Rec." refers to wing-wall abutment in a rectangular channel. The term "WW" refers to wing-wall abutment in a compound channel.

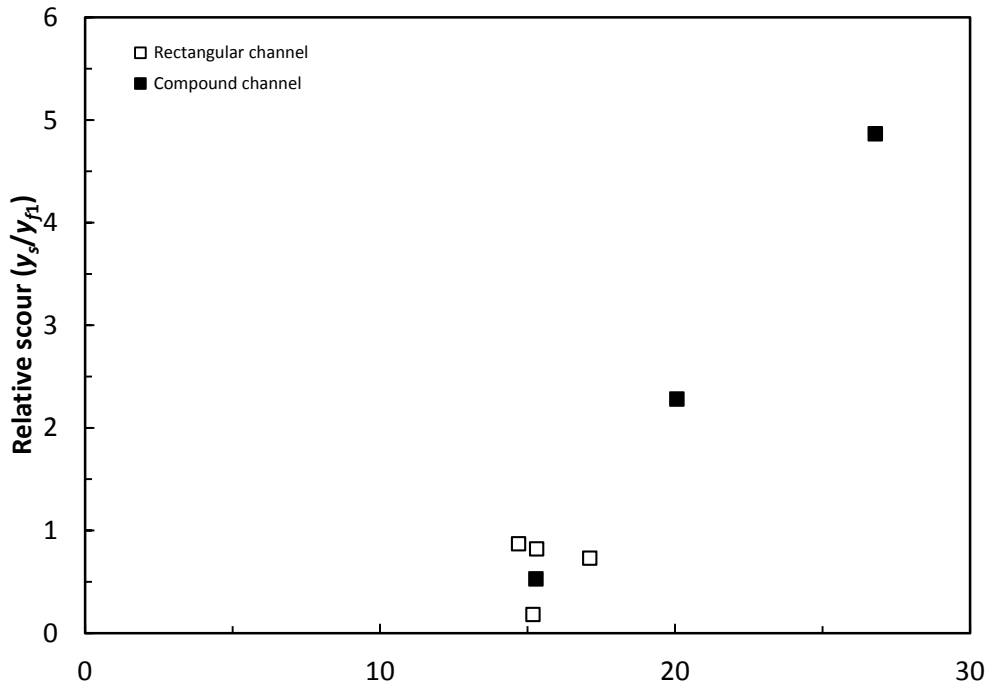

Figure 5-26. Relation of relative scour to flow for the rectangular- and compound-channel data used to evaluate the channel-correction factor, K_G for rectangular channels in the NCHRP 24-25(2) method.

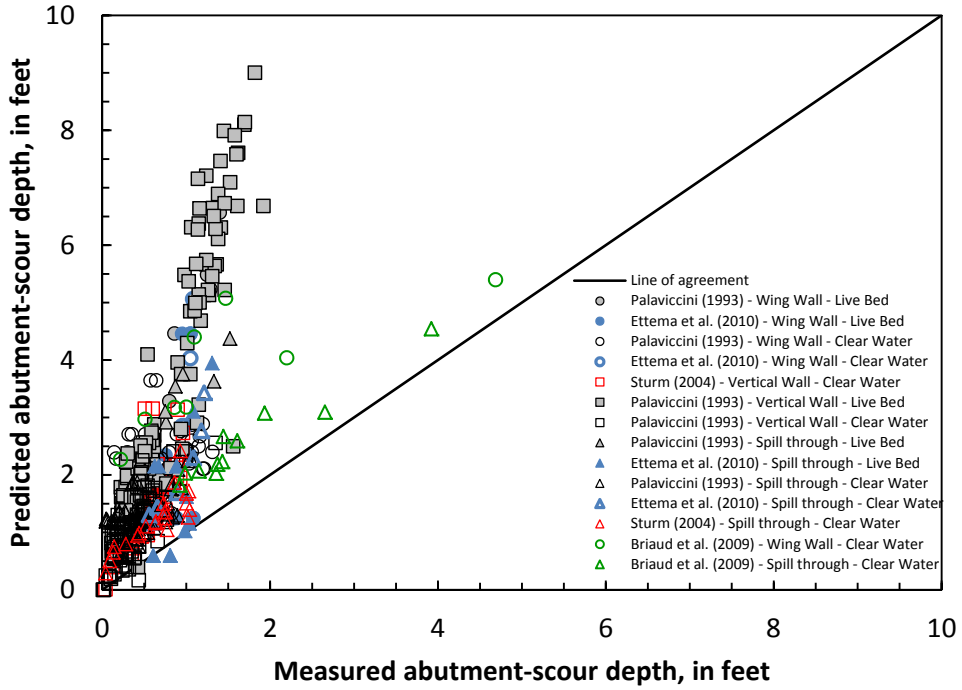

Figure 5-27. Relation of predicted and measured scour for selected laboratory data using the NCHRP 24-15(2) scour prediction method with all channel-geometry correction factors, K_G, arbitrarily set to a value of 1.0.

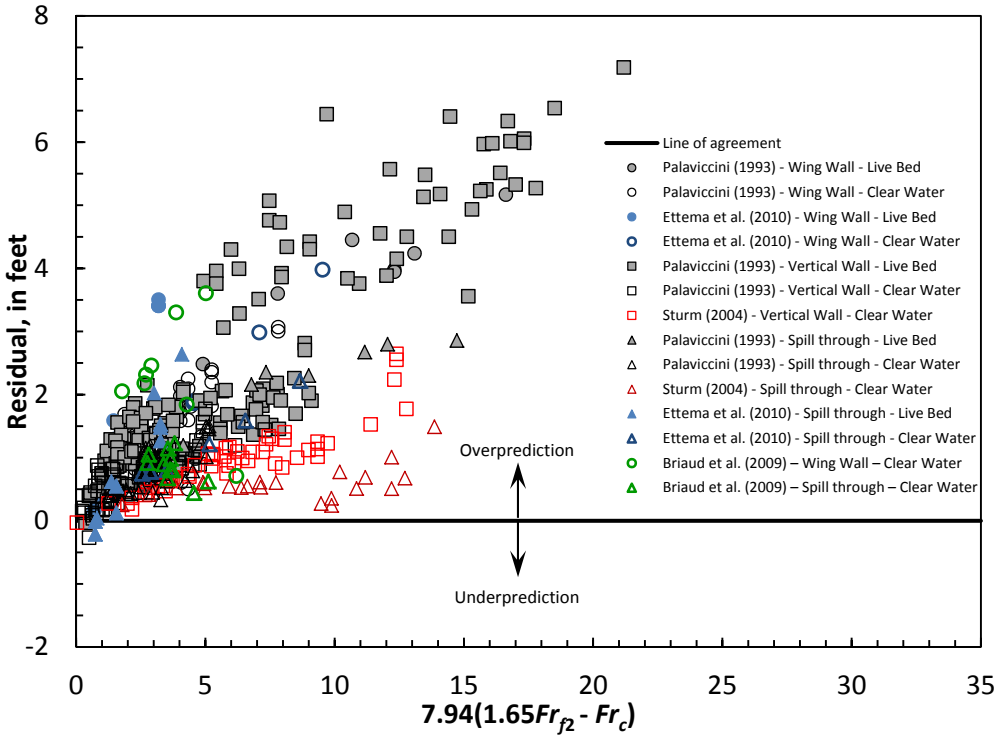

Figure 5-28. Relation of prediction residuals and the Froude number parameter, $7.94(1.65Fr_{f2} - Fr_c)$, using the NCHRP 24-15(2) scour prediction method and K_G for all data arbitrarily set to a value of 1.0.

Abutment-location correction factor (K_L)

The NCHRP 24-15(2) scour prediction method includes a correction factor for abutment location (K_L) with respect to the main channel. The maximum value for K_L is 1.35 and occurs when the abutment is located at the channel bank or protrudes into the main channel. The value of K_L transitions to 1.0 when the abutment toe is a distance of $1.5y_{f1}$ from the channel bank. As noted previously, the largest overpredictions in figure 5-1 in the Sturm (2004) and Ettema et al. (2010) data are associated with abutments located at the bank or protruding into the main channel. The relation of the prediction residuals with respect to K_L for vertical-wall and spill-through abutment data from Sturm (2004) is shown in figures 5-29A and B, respectively, and demonstrates the larger overprediction associated with bankline and protruding abutments.

Rather than using a correction factor for abutment location to account for scour associated with bankline and protruding abutments, an alternate method is to use the hydraulic characteristics associated with the channel rather than the floodplain. The standard method for applying the NCHRP 24-15(2) method (chapter 4) uses a combination of floodplain and channel hydraulics for bankline and protruding abutments. For protruding abutments, the flow depth and velocity used in equation 4-1 are associated with the main channel. Therefore, at such abutments it may be redundant to adjust the predicted scour depth for abutment location with a K_L value of 1.35. For bankline abutments, the flow depth and velocity reflect values associated with the floodplain and the main channel, respectively. For such abutments, it may be appropriate to use the flow depth in the main channel rather than the flow depth in the floodplain to account for the increased potential for scour, thereby removing the need to adjust the predicted scour depth for abutment location with a K_L value of 1.35. Figures 5-30A and B show the relation of measured abutment-scour depth to predicted scour for the laboratory data with bankline or protruding abutments, with figure 5-30A reflecting computations by using the standard method for applying the NCHRP 24-15(2) method with a K_L value of 1.35, and figure 5-30B reflecting computations by using the channel hydraulics with a K_L value of 1.0. In the case of the one point in the Briaud et al. (2009) data, using the channel hydraulics with a K_L value of 1.0 produces a minor

underprediction, indicating that the modified approach using the channel hydraulics may be appropriate. In the case of the Ettema et al. (2010) data, the magnitude of the overpredictions is decreased, with a small increase in the frequency and magnitude of underprediction. In the case of the Sturm (2004) data, the magnitude of the overpredictions increases for all of the data. This increased magnitude in overprediction can be attributed to the channel flow depths in the Sturm (2004) data being 6 to 8 times that of the floodplain flow depths. In contrast, the channel flow depths for the Ettema et al. (2010) and Briaud et al. (2009) data are approximately 2 times the floodplain flow depths. The prediction patterns in figures 5-30A and B indicate that using the channel hydraulics with a K_L value of 1.0 is reasonable where ratios of channel to floodplain flow depths are approximately 2, but can become excessive as that ratio increases. Because the number of data in figure 5-30 is relatively small, additional research of this matter would be advisable.

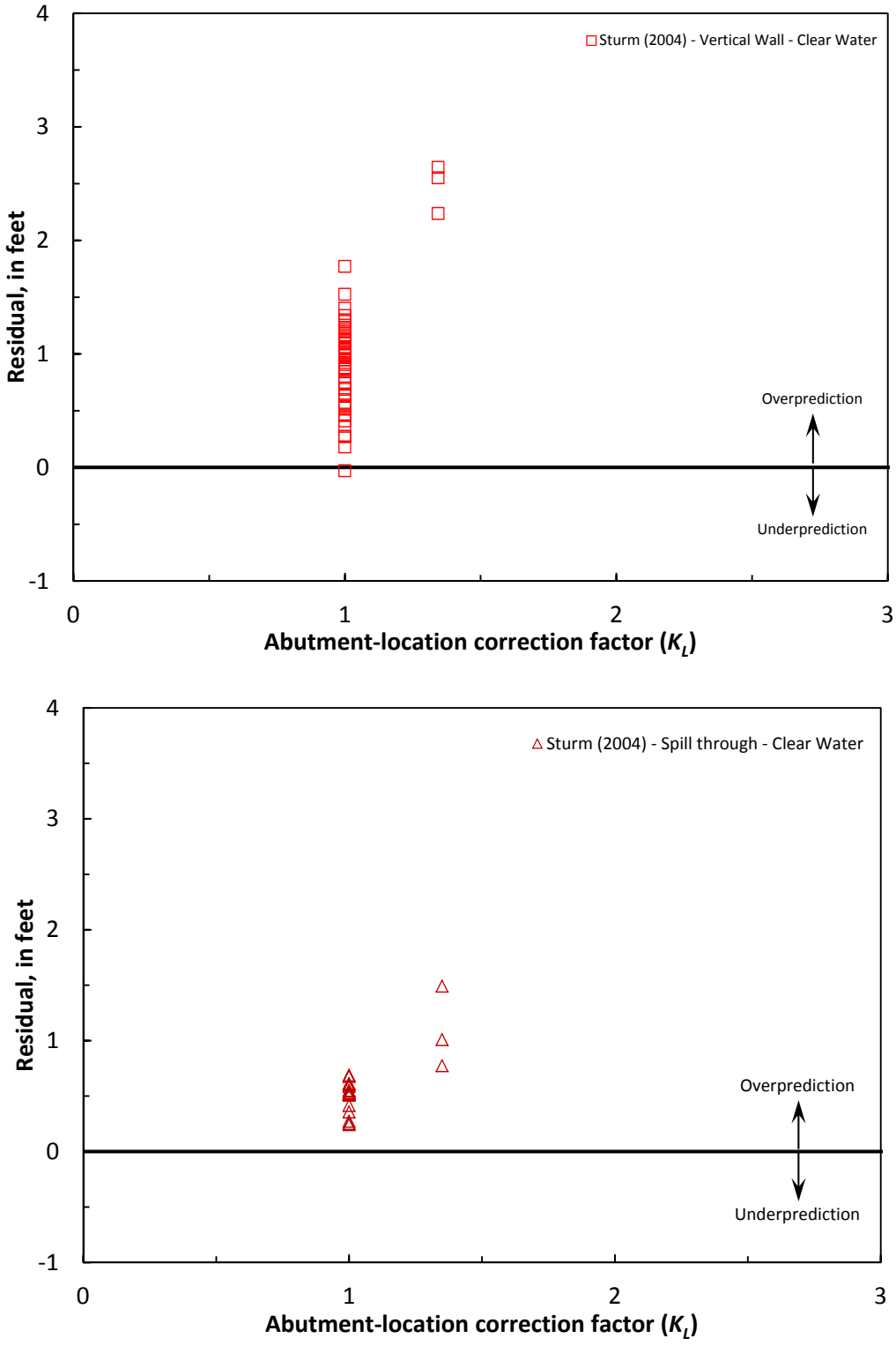

Figure 5-29. Relation of prediction residuals and the abutment-location correction factor, K_L, using the NCHRP 24-15(2) scour prediction method for (*A*) vertical-wall abutments and (*B*) spill-through abutments.

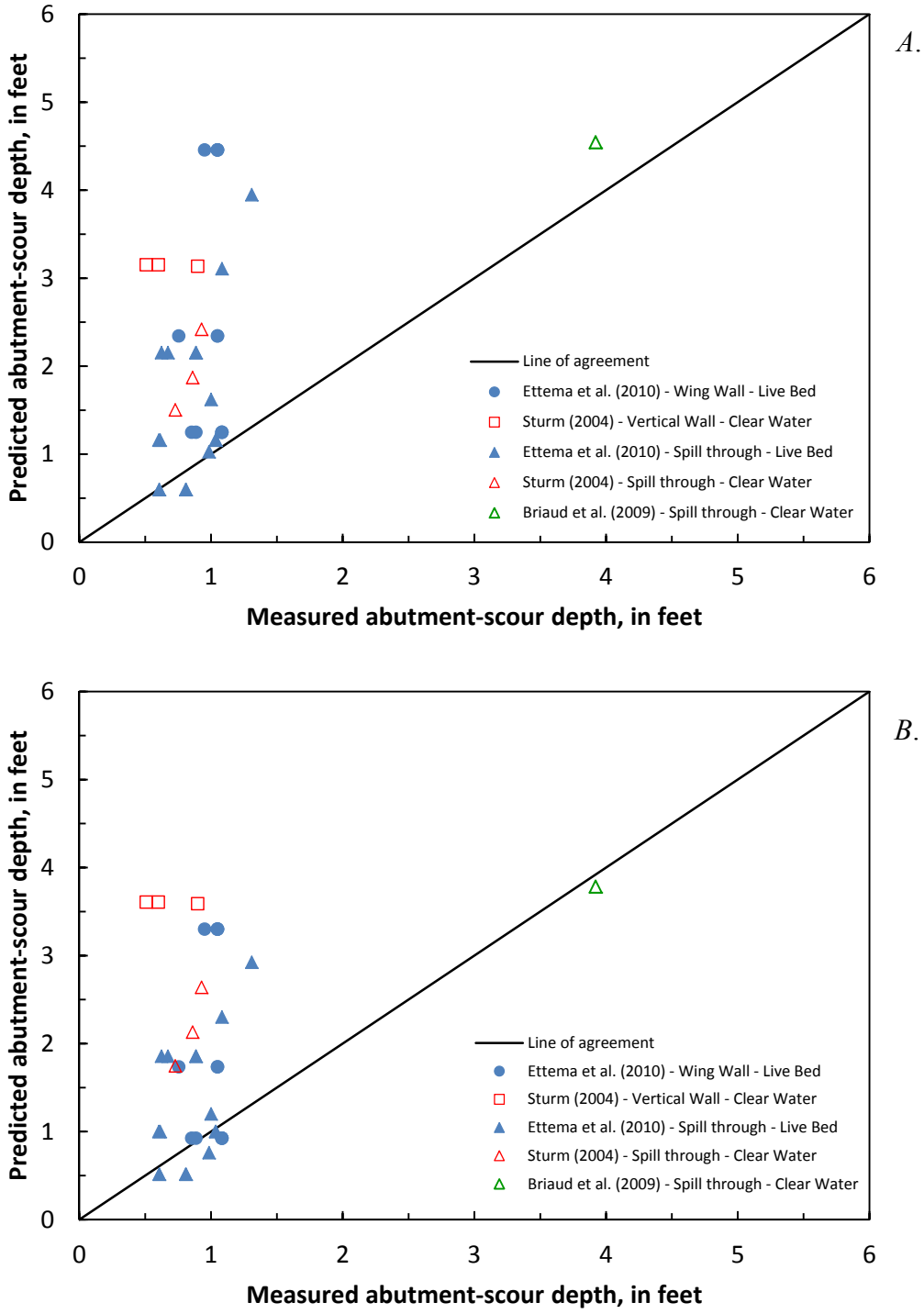

Figure 5-30. Relation of predicted and measured scour for selected laboratory data using the NCHRP 24-15(2) scour prediction method with (*A*) K_L equal to 1.35 and (*B*) K_L equal to 1.0 and using the main-channel hydraulics.

Pressure-flow correction factor (K_p)

No laboratory data were associated with pressure flow; therefore, no assessment was made of this correction factor. However, a brief review of the K_p correction factor follows. The K_p correction factor for the NCHRP 24-15(2) method was developed from numerical model simulations. The value of K_p is 1 just at the onset of pressure flow when the water surface comes in contact with the low chord of the bridge. As the water surface moves above the low chord, the value of K_p increases, reaching a maximum value of 1.92 when the water surface reaches the top of the bridge deck. The value of K_p diminishes as the water surface moves above the bridge deck and becomes 1 when the ratio of the water depth above the low chord to that of the bridge-deck thickness reaches a value of 3.0. For pressure-flow conditions, Briaud et al. (2009) recommend using the flow depth from the channel bottom to the low chord rather than the free-surface flow depth, and acknowledge that K_p will be conservative. The K_p correction factor can be as large as 1.92, which will substantially increase the predicted scour depth. There are 46 bridges in the field data with pressure-flow conditions, and values of K_p at these sites range from 1.1 to 1.92, with a median value of 1.56.

5.3 Analysis of the USGS Field Data

The NCHRP 24-15(2) method was evaluated with the field measurements of abutment scour listed in table 1-1. The analysis included a comparison of predicted and measured scour, an evaluation of the relative influence of selected variables in the NCHRP 24-15(2) equation (equation 4-1) on predicted scour, an evaluation of prediction residuals with respect to selected equation variables, and alternate methods to possibly improve the performance of the NCHRP 24-15(2) method. The analysis is presented in the following report sections.

5.3.1 Relation of Measured and Predicted Scour

Figure 5-31 shows the relation of measured abutment-scour depth to predicted scour for the application of the NCHRP 24-15(2) method to the USGS field data listed in table 1-1. The application method is described in chapter 4 of this report. The field data in this figure are grouped as presented in table 1-1, with the exception that a subset of 41 South Carolina measurements associated with floodplain relief bridges and swampy sites with poorly defined channels were plotted as an additional group. Most of the data in this subset are located in the Coastal Plain of South Carolina, with the exception of two data points located in the Piedmont. (Refer to report section 3.3 for additional information regarding this subset of data.) As with the analysis of the NCHRP 24-20 method, sites listed in table 3-1 are identified in figure 5-31 using the associated site number. The site characteristics associated with sites 7 through 9 (table 3-1) are inconsequential in the analysis of NCHRP 24-15(2) and were not identified. Other graphs in this analysis will identify the sites listed in table 3-1 in a similar manner. To better visualize the trends in figure 5-31, the data points associated with each data group are shown in figure 5-32 as a series of plots. All of the field data are shown as hollow circles, with the selected data groups identified with solid circles. The lower gradient and wide floodplain streams associated with the South Carolina Relief/Swamp Bridge data and the Coastal Plain data are shown in figures 5-32A and B, respectively. The frequent underprediction in these data can be attributed, in part, to lower Froude numbers and frequent rectangular channels having a K_G correction factor of 0.42. A similar pattern of underprediction associated with these characteristics was noted in the analysis of the laboratory data and is described in more detail in the analysis of the residuals.

For the cohesive sediments of the South Carolina Piedmont (figure 5-32C), underprediction is infrequent, and the magnitude of the underprediction is not frequently excessive. The NCHRP 24-15(2) method was developed for cohesive soils and the reasonable performance with the South Carolina Piedmont data indicates it is applicable to such sediments. The largest overprediction for the Piedmont data (approximately 25 ft) is associated with pressure flow having a K_p correction factor of 1.68. The next three largest overpredictions (approximately 15 ft or greater) are associated with larger Froude numbers which, in the laboratory analysis, tended to have a larger frequency and magnitude of overprediction. The Maine data (figure 5-32D) have the most excessive overprediction for the field data. This excessive overprediction can be attributed, in part, to larger Froude numbers, more frequent occurrence of pressure flow with K_p correction factors greater than 1.0, and protruding abutments for all of the data with abutment-location correction factors, K_L, of 1.35. If the value of K_L is set to 1.0 for the Maine data, the excessive overprediction is substantially improved. The few underpredictions in figure 5-32D are associated with smaller Froude numbers, which tend to produce more frequent underpredictions. For the cohesive sediments of the Alabama data (figure 5-32E), there is frequent underprediction. All of the Alabama data are associated with rectangular channels, and the underprediction can be attributed, in part, to the lower K_G correction factor of 0.42 for such channels. If the value of K_G was set to 1.0 for the Alabama data, the performance of the data would be similar to that of the South Carolina Piedmont data with minimal underprediction. The NBSD data are shown in figure 5-32F. Most of these data, including the 2 largest overpredictions, are associated with protruding abutments with K_L correction factors of 1.35. As with the Maine data, if the value of K_L is set to 1.0 for the NBSD data, the magnitude of the overprediction is reduced with minimal underprediction.

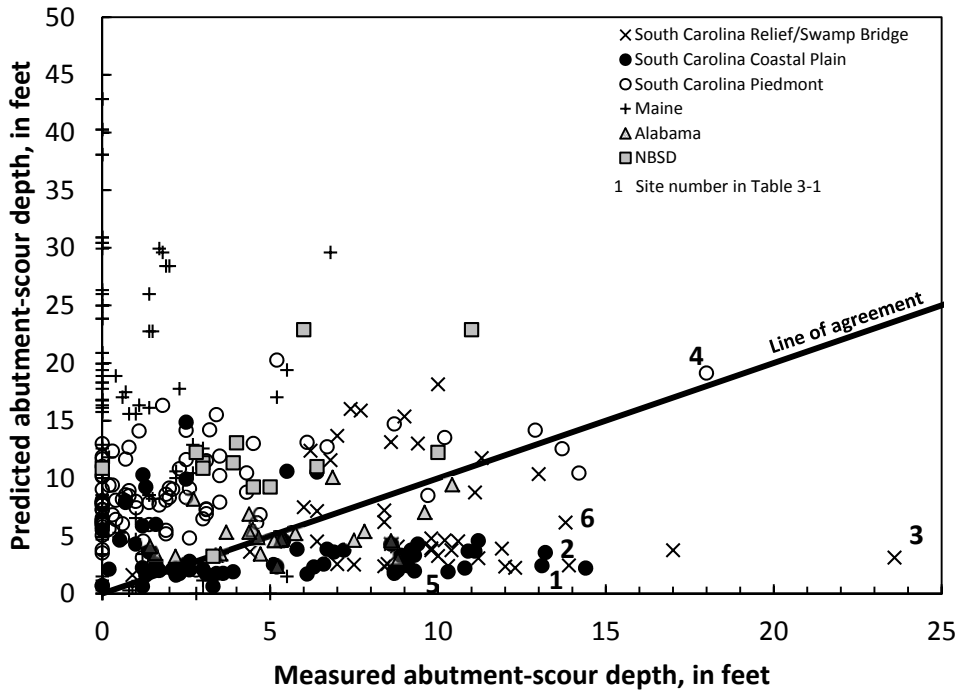

Figure 5-31. Relation of predicted and measured abutment-scour depth for selected field data using the NCHRP 24-15(2) scour prediction method.

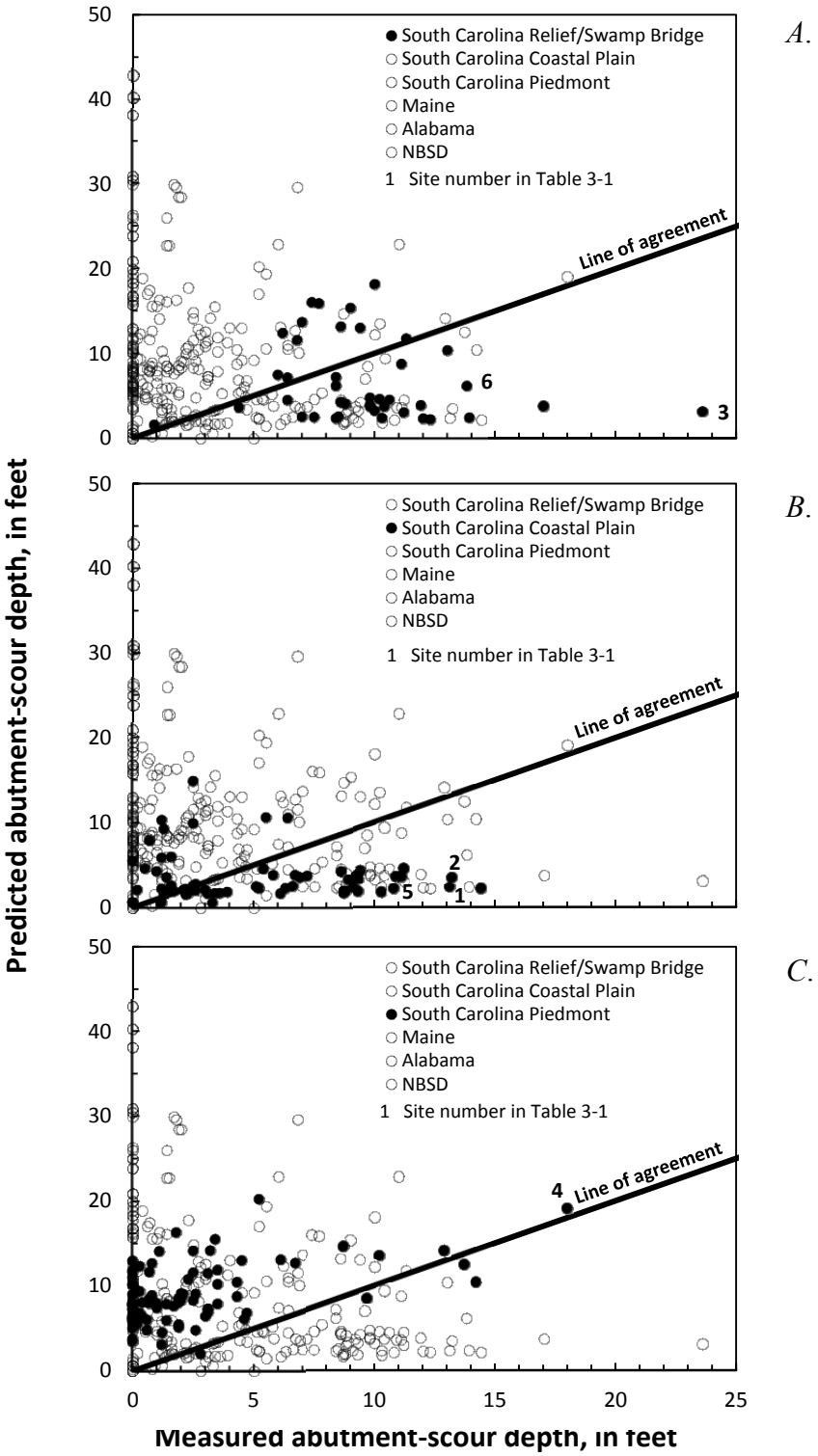

Figure 5-32. Relation of measured and predicted abutment-scour depth for selected field data using the NCHRP 24-15(2) scour prediction method for the (A) South Carolina Relief/Swamp Bridge, (B) South Carolina Coastal Plain, (C) South Carolina Piedmont, (D) Maine, (E) Alabama, and (F) NBSD data.

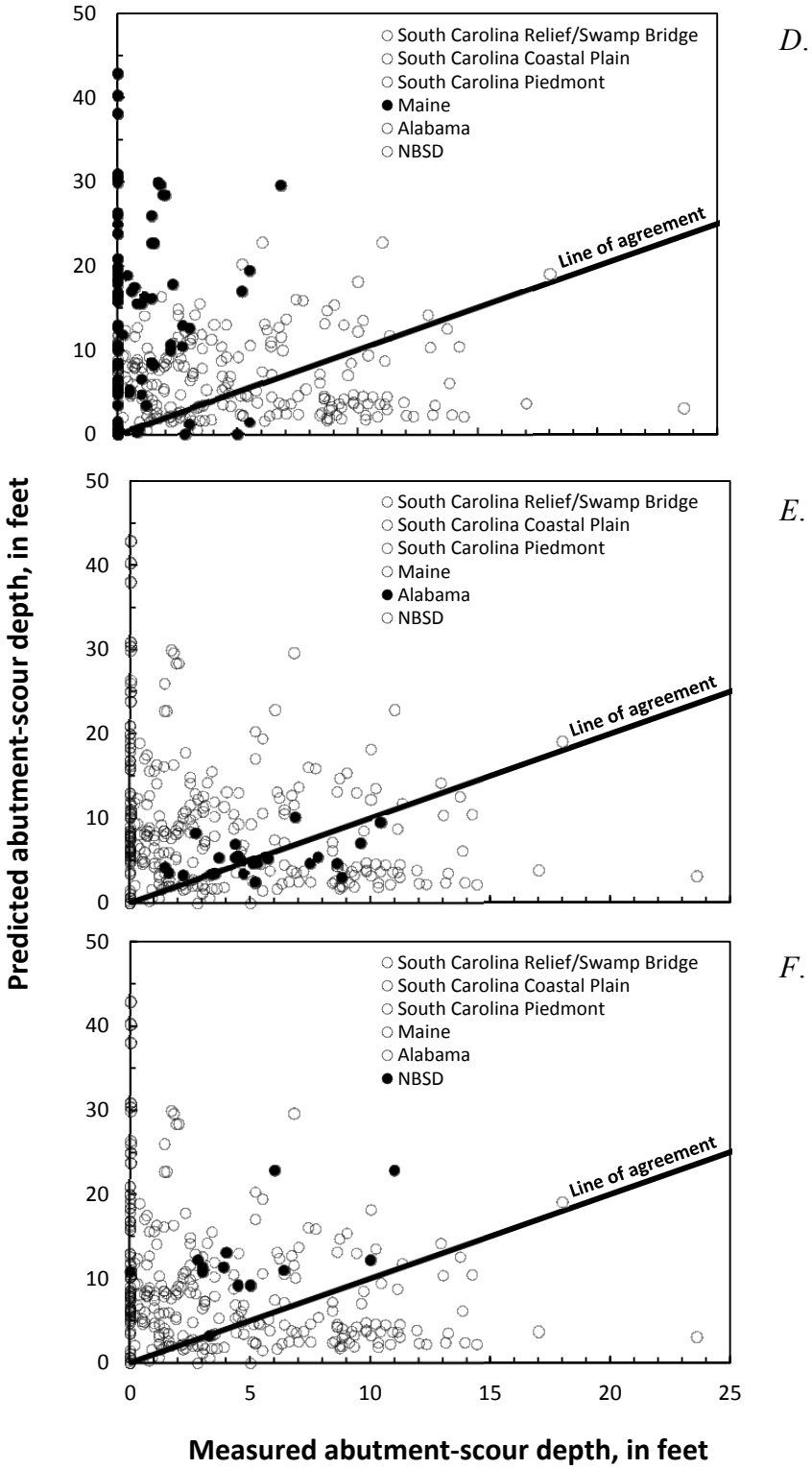

Figure 5-32. - Continued. Relation of measured and predicted abutment-scour depth for selected field data using the NCHRP 24-15(2) scour prediction method for the (A) South Carolina Relief/Swamp Bridges, (B) South Carolina Coastal Plain, (C) South Carolina Piedmont, (D) Maine, (E) Alabama, and (F) NBSD data.

5.3.2 Influence of Selected Explanatory Variables on Predicted Scour

To provide some perspective on the influence of each explanatory variable in equation 4-1 on predicted scour for the field data, the following series of figures (figures 5-33 through 5-39) show the relation of predicted to measured scour as each explanatory variable is progressively added to the equation. (This series of plots is shown for the laboratory data in report section 5.2.2.) The progression of adding the explanatory variables is as follows: $7.94(1.65Fr_{f2} - Fr_c)$, K_{Re}, K_1, K_2, K_G, K_L, and K_p. Some notable features regarding this series of figures are as follows:

- The prediction pattern in figure 5-33 essentially shows no underprediction, but large overprediction that at times is excessive. While overprediction can be excessive, the prediction patterns indicate that the core explanatory variable, $7.94(1.65Fr_{f2} - Fr_c)$, is capturing, in some measure, the trends of the field data, with predicted scour increasing as measured scour increases. The largest overpredictions in the Maine data are associated with large values of Fr_{f2} and small values of Fr_c, which yield large estimates of scour when applied to $7.94(1.65Fr_{f2} - Fr_c)$. It is notable that the non-cohesive sediments of the South Carolina Coastal Plain and the Relief/Swamp Bridges perform best and that the Pee Dee River at I-95, with the largest measured scour depth, is not underpredicted. In contrast, the cohesive sediments of the South Carolina Piedmont tend to have higher estimates of scour.
- The progression from figure 5-33 to 5-34 highlights how the Reynolds number parameter, K_{Re}, substantially reduces the magnitude of predicted scour, producing underprediction in the lower gradient streams of the Coastal Plain and Relief/Swamp Bridges. (Note: The vertical scales on figures 5-33 and 5-34 are different to accommodate the differing data ranges.) The range for K_{Re} for the field data is from 0.3 to 0.98, with an average value of 0.49, indicating that K_{Re} will tend to decrease predicted scour by about 50 percent on average. This trend is in contrast to the laboratory data where the range of K_{Re} is larger and increases predicted scour by about 60 percent on average (report section 5.2.2). As noted in report section 5.2.3(iii), the range of the Reynolds number for the field data is much larger than that of the Briaud et al. (2009) data, which produces smaller values of K_{Re} (figure 5-20) and thus smaller values of predicted scour.

- The progression from figure 5-34 to 5-35 highlights the influence of K_1 on predicted scour, with spill-through abutments showing a decrease in the magnitude of predicted scour and, therefore, an increase in underprediction. The increased underprediction is most noticeable in the lower gradient streams of the Coastal Plain and Relief/Swamp Bridges.
- The progression from figure 5-35 to 5-36 highlights the influence of K_2 on predicted scour, moderately reducing predicted scour at skewed abutments.
- The progression from figure 5-36 to 5-37 highlights the influence of K_G on predicted scour for rectangular channels, substantially increasing the frequency and magnitude of underprediction for such channels. This increased underprediction is associated with the lower gradient streams of the Coastal Plain and Relief/Swamp Bridges, as well as the relief bridges in the Alabama data, where rectangular channels are common.
- The progression from figure 5-37 to 5-38 highlights the influence of K_L on predicted scour for bankline and protruding abutments, substantially increasing the overprediction for such abutments. The increased overprediction is largely associated with the Maine and NBSD data and with some of the Relief/Swamp Bridges of South Carolina. (Note: Most of the swamp bridges in South Carolina do not have main channels. However, a few sites have small defined channels where the abutments are at the bankline or protrude into the small channel.)
- The progression from figure 5-38 to 5-39 highlights the influence of K_p on predicted scour for pressure-flow conditions, increasing the value of predicted scour. The increased overprediction is largely associated with the Maine and Alabama data, with some in the NBSD and South Carolina data.

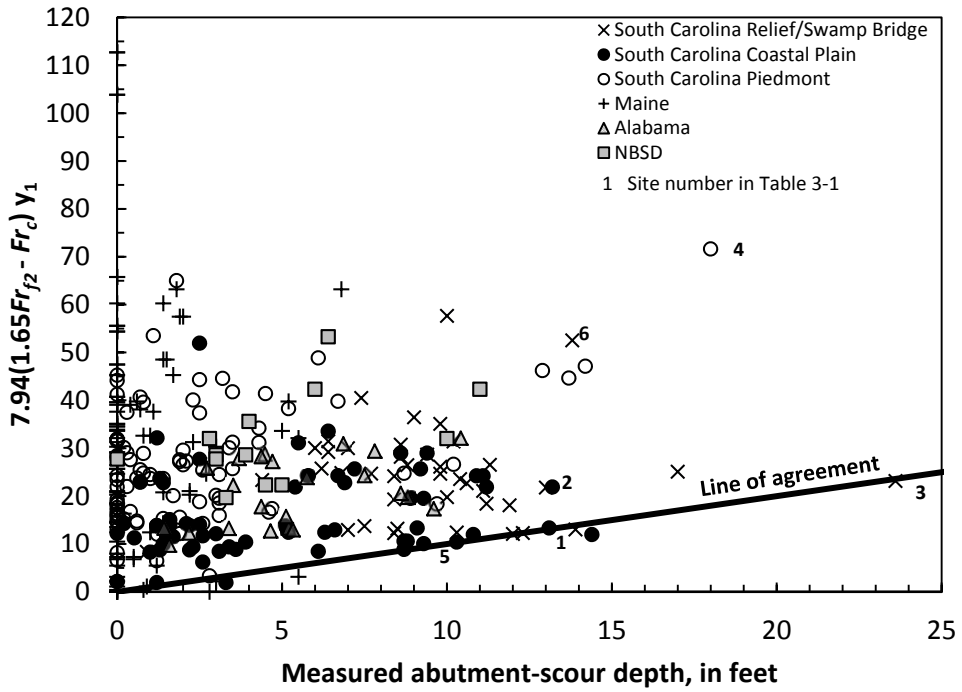

Figure 5-33. Relation of predicted and measured abutment-scour depth based on the selected equation parameter, $7.94(1.65Fr_{f2} - Fr_c)$, for the NCHRP 24-15(2) scour prediction method.

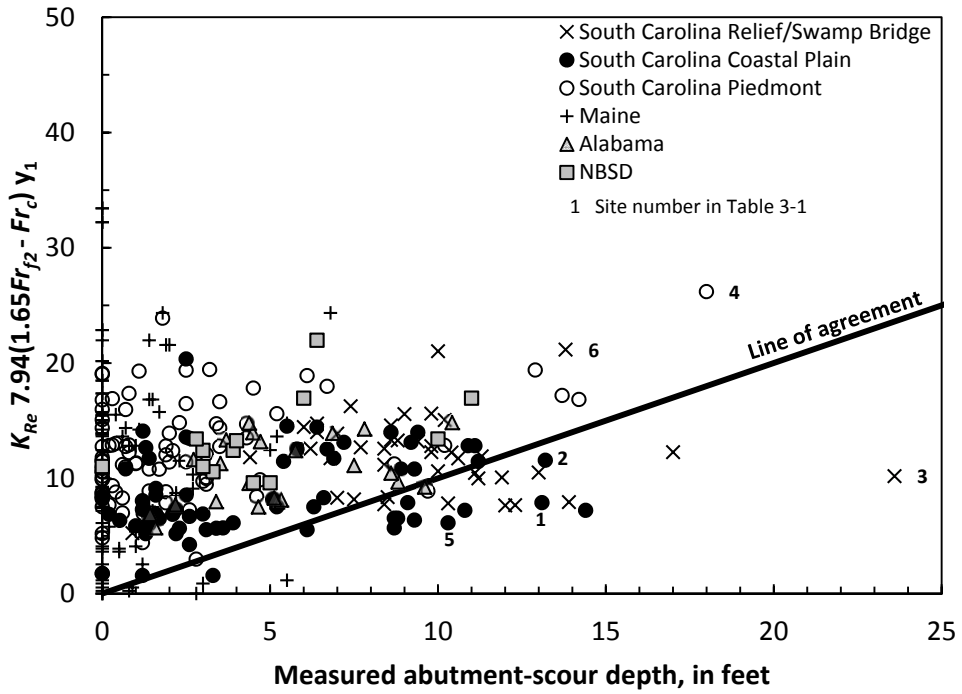

Figure 5-34. Relation of predicted and measured abutment-scour depth based on the selected equation parameters, K_{Re} 7.94(1.65Fr_{f2} - Fr_c), for the NCHRP 24-15(2) scour prediction method.

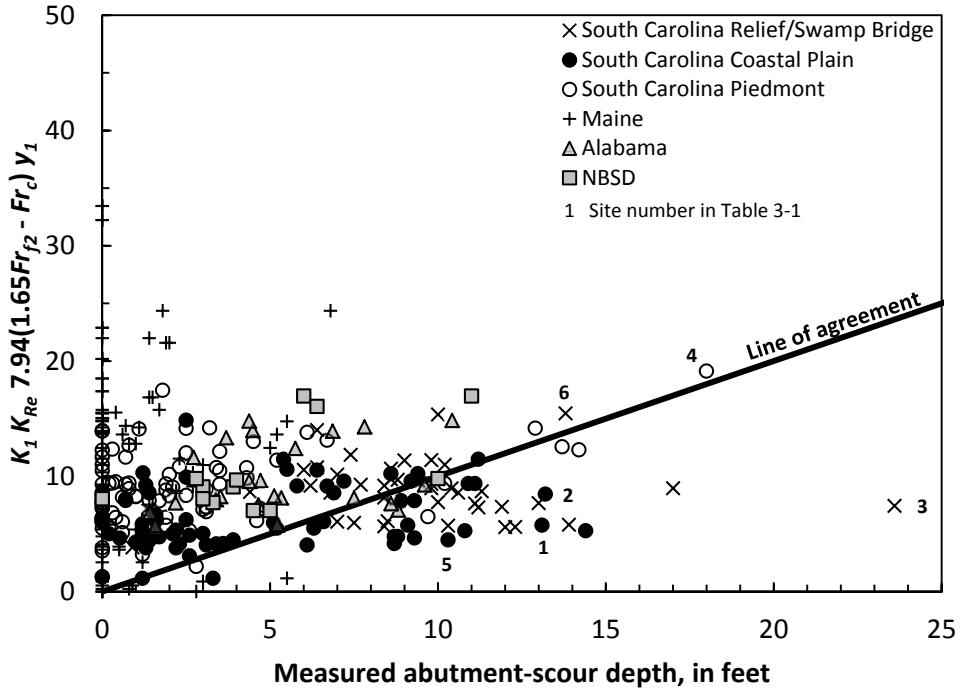

Figure 5-35. Relation of predicted and measured abutment-scour depth based on the selected equation parameters, K_1 K_{Re} 7.94(1.65Fr_{f2} - Fr_c), for the NCHRP 24-15(2) scour prediction method.

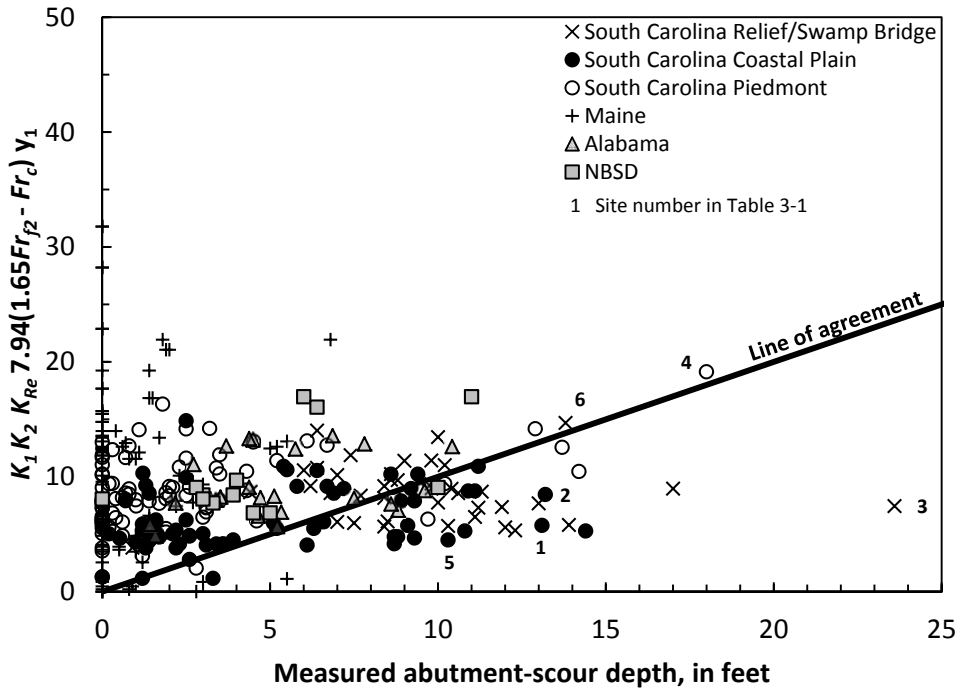

Figure 5-36. Relation of predicted and measured abutment-scour depth based on the selected equation parameters, K_1 K_2 K_{Re} 7.94(1.65Fr_{f2} - Fr_c), for the NCHRP 24-15(2) scour prediction method.

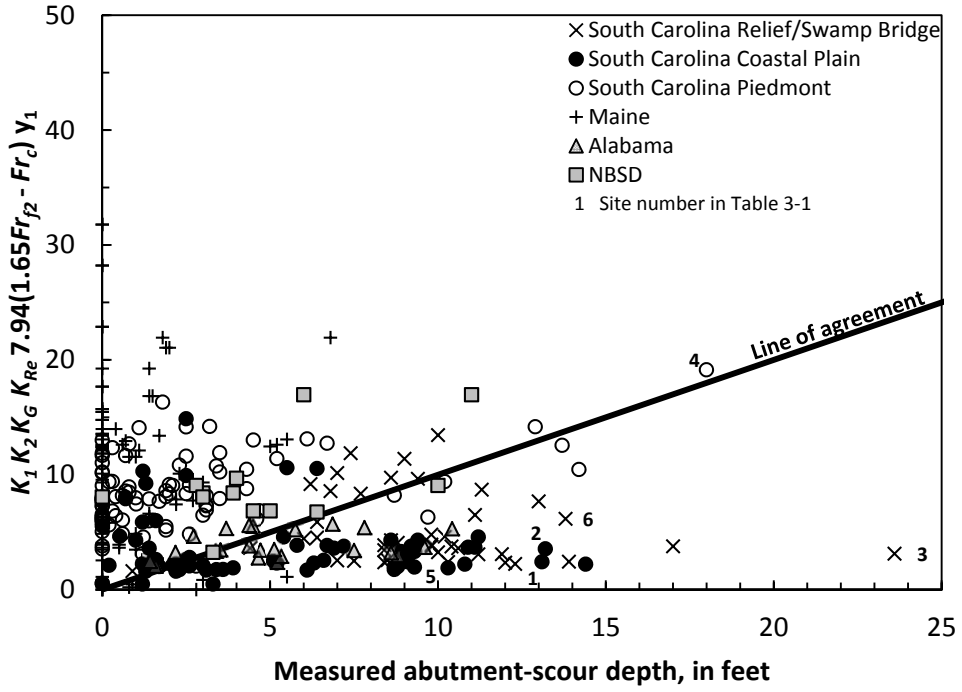

Figure 5-37. Relation of predicted and measured abutment-scour depth based on the selected equation parameters, K_1 K_2 K_G K_{Re} 7.94(1.65Fr_{f2} - Fr_c), for the NCHRP 24-15(2) scour prediction method.

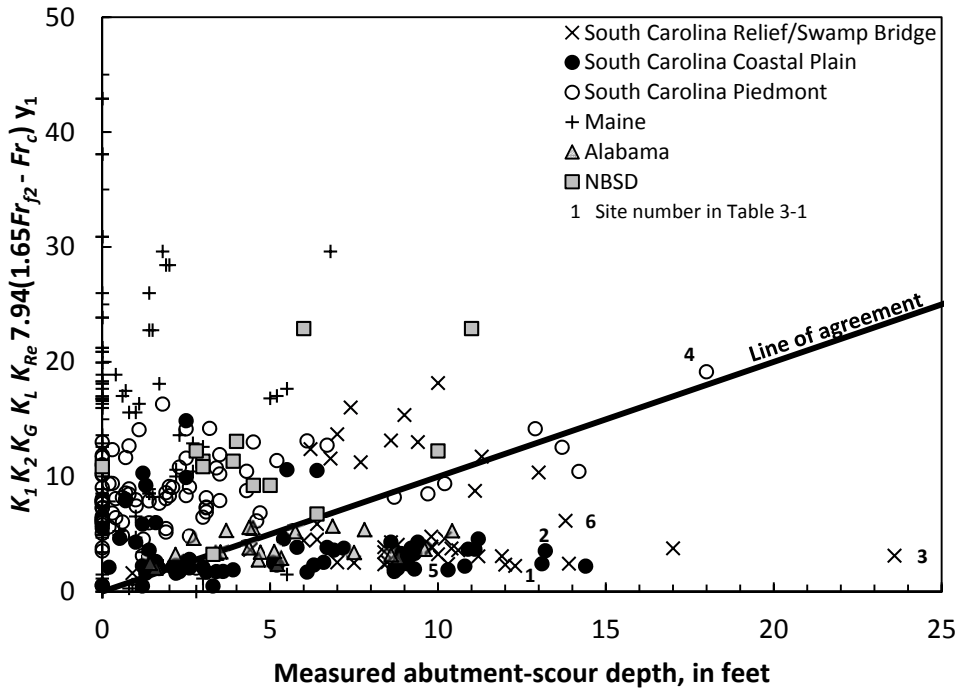

Figure 5-38. Relation of predicted and measured abutment-scour depth based on the selected equation parameters, $K_1\ K_2\ K_G\ K_L\ K_{Re}\ 7.94(1.65Fr_{f2} - Fr_c)$, for the NCHRP 24-15(2) scour prediction method.

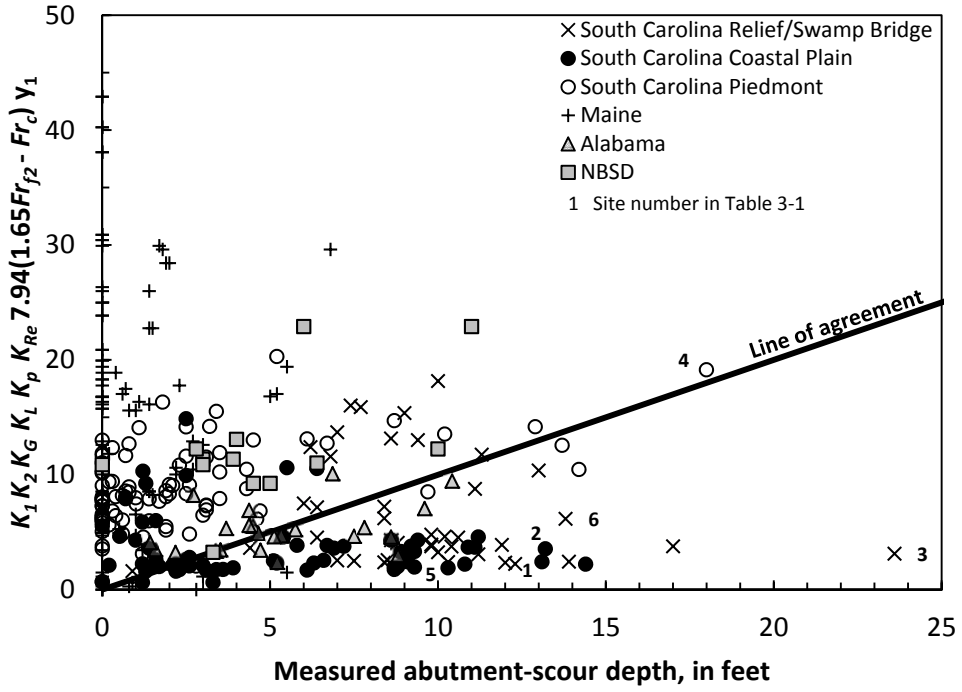

Figure 5-39. Relation of predicted and measured abutment-scour depth based on the selected equation parameters, $K_1\ K_2\ K_G\ K_L\ K_P\ K_{Re}\ 7.94(1.65Fr_{f2} - Fr_c)$, for the NCHRP 24-15(2) scour prediction method.

5.3.3 Prediction Residuals with Respect to Selected Explanatory Variables

Figures 5-40 through 5-48 show the prediction residuals (predicted minus measured scour) for the field data in relation to selected explanatory variables, including *D50*, Fr_c, Fr_{f2}, $7.94(1.65Fr_{f2} - Fr_c)$, Re_{f2}, K_{Re}, and the correction factors in equation 4-1, respectively. The data symbols used in these plots are identical to those used in figure 5-31. These plots were reviewed to identify potential trends regarding under- and overprediction, and a discussion of these plots follows.

i. Prediction Residuals with Respect to *D50*, V_c, and Fr_c

As described previously, the NCHRP 24-15(2) method (equation 4-1) uses Fr_c, which is a function of V_c as determined from the relation in figure 4-4 in conjunction with the *D50*. The relation of the prediction residuals with respect to *D50*, V_c, and Fr_c are shown in figures 5-40 through 5-42, respectively. Because of the influence of other variables on predicted scour, it is difficult to isolate the influence of *D50*, V_c, and Fr_c, and as with the laboratory data, there does not appear to be a strong trend in the residuals. However, as seen in the laboratory data (report section 5.2.3), there is an increase in the frequency and magnitude of underprediction as V_c and Fr_c decrease. While most of the underprediction in the Alabama and South Carolina data is associated with rectangular channels having a $K_G = 0.42$, it would appear that the variable Fr_c in equation 4-1 also is associated with this trend. The trends in the field and laboratory data both indicate that the frequency and magnitude of underprediction are small for larger sediment grain sizes. To isolate possible residual trends, figure 5-40B shows a subset of the South Carolina Piedmont data with data associated with rectangular channels, protruding abutments, and pressure flow removed. A subset of the Maine data, all associated with protruding abutments, but with the pressure-flow data removed, also is shown in figure 5-40B. The South Carolina Piedmont data show a trend with an increase in the upper bound of overprediction as *D50* increases to about 0.1 mm, which is the breakpoint between the cohesive and non-cohesive V_c equations in figure 4-4. This trend is not discernable in the laboratory data because the range of *D50* below 0.1 mm is limited to one grain size (report section 5.2.3). The Maine data also show a trend with overprediction diminishing with increasing *D50* and some underprediction for the largest *D50*s. The larger magnitude of overprediction in the Maine data, in contrast to the South

Carolina data, can be attributed to the larger Froude numbers and protruding abutments. These trends are not discernable in the laboratory data because the range of *D50* is smaller than that of the Maine field data (report section 5.2.3).

The results presented in figures 5-40 through 5-42 are based on the empirical relation for V_c as shown in figure 4-4, which represents a lower-bound curve of critical-velocity as determined from EFA tests of field samples (Briaud et al. 2009; 2011; report section 4.2). A more accurate measurement of V_c for a given bridge site could be obtained from EFA tests of soil samples from that site, possibly improving the performance results for NCHRP 24-15(2). Figure 4-4 shows a large range of data for cohesive sediments (*D50* < 0.1 mm), indicating that EFA tests for cohesive sediments would likely yield larger estimates of V_c and therefore, smaller estimates of abutment scour. The NCHRP 24-15(2) method produces minimal underprediction in cohesive sediments (see the cohesive data of the South Carolina Piedmont in figure 5-40), and therefore, a V_c determined from an EFA test of a field sample may reduce overprediction in such sediments. However, it also is possible that a V_c determined from an EFA test may yield more frequent underprediction for sites with cohesive sediments. While a V_c determined from an EFA test may yield better results for the non-cohesive data, other factors are contributing to the underprediction in the South Carolina Coastal Plain and Relief/Swamp Bridge data and to the overprediction in the Maine data. These factors are discussed later in this report section.

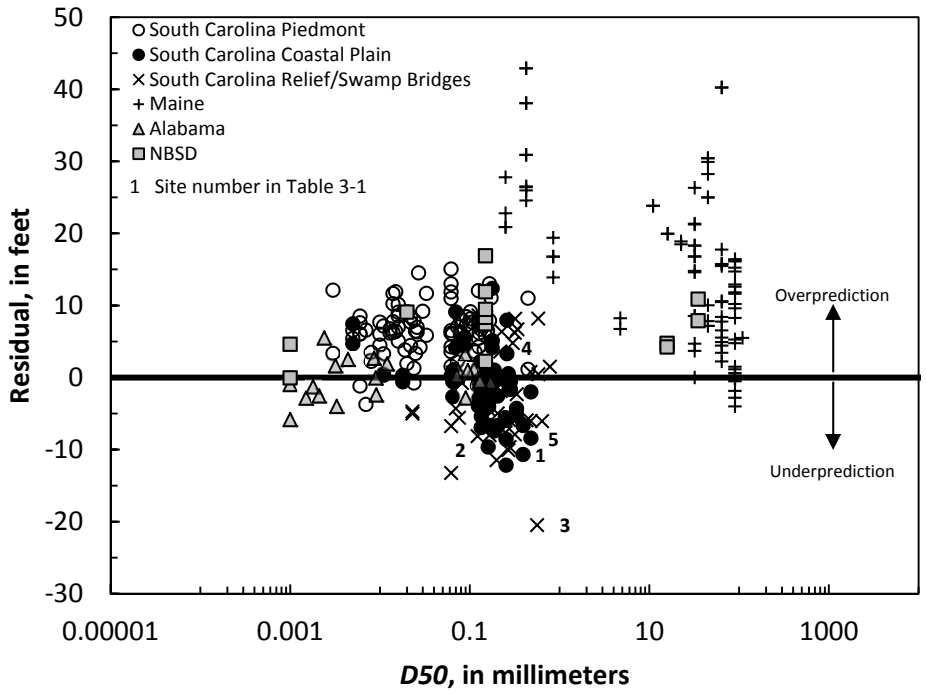

A.

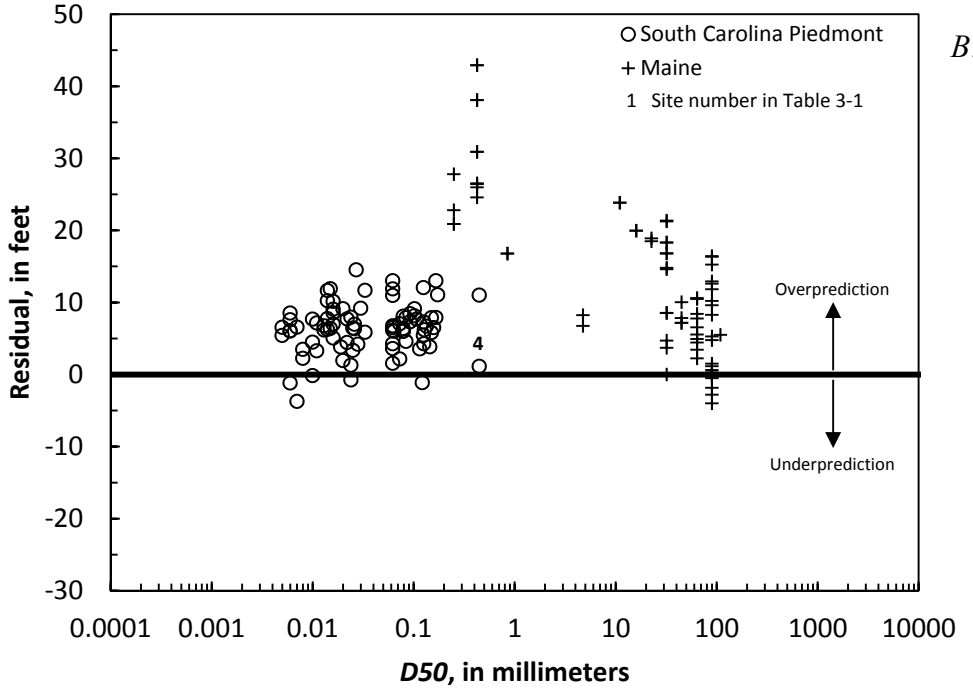

B.

Figure 5-40. Relation of prediction residuals and the median sediment size (*D50*) for selected field data, using the NCHRP 24-15(2) scour prediction method, including (*A*) all of the data, and (*B*) selected data from the South Carolina Piedmont and Maine data.

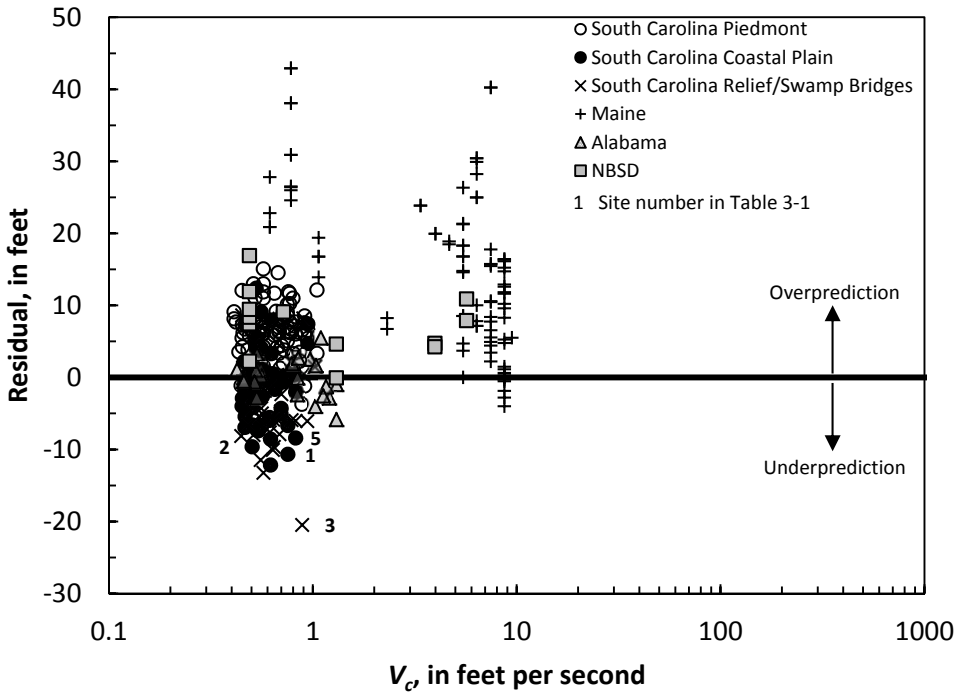

Figure 5-41. Relation of prediction residuals and the critical velocity (V_c) for selected field data, using the NCHRP 24-15(2) scour prediction method.

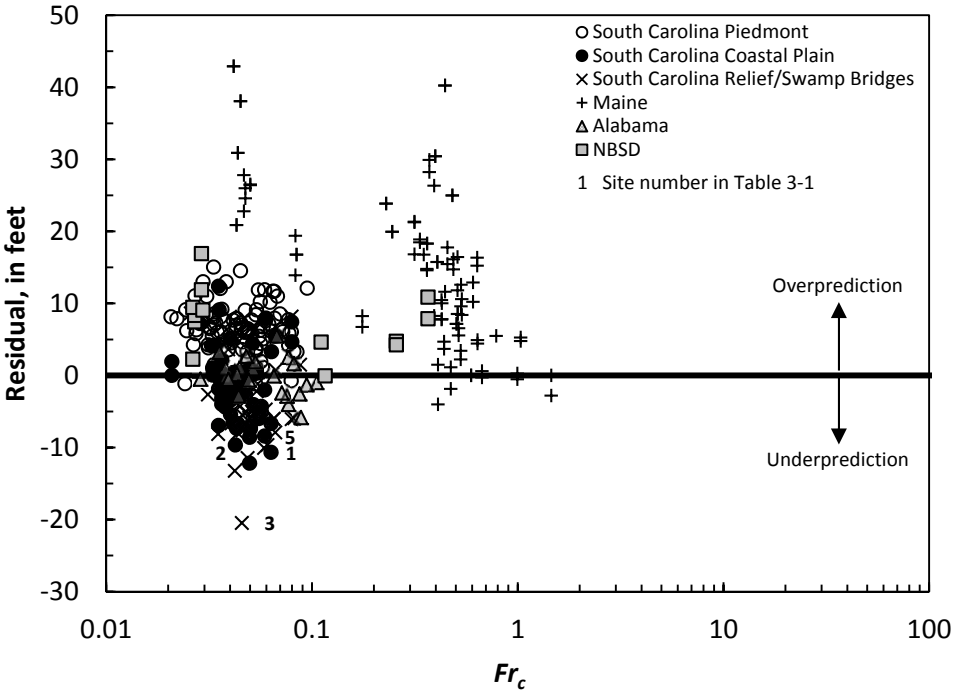

Figure 5-42. Relation of prediction residuals and the sediment critical-velocity Froude number (Fr_c) for selected field data, using the NCHRP 24-15(2) scour prediction method.

ii. Prediction Residuals with Respect to Fr_{f2} and $7.94(1.65Fr_{f2} - Fr_c)$

The relation of the prediction residuals with respect to Fr_{f2} and the parameter $7.94(1.65Fr_{f2} - Fr_c)$, the core explanatory variable for the NCHRP 24-15(2) method, is shown in figures 5-43 and 5-44, respectively. As with the laboratory data (report section 5.2.3), the residuals display a strong trend with respect to both of these variables, indicating that the magnitude of overprediction tends to increase as these variables increase. The overprediction is prominent in the Maine data, where steeper gradient streams have larger values of Fr_{f2} and $7.94(1.65Fr_{f2} - Fr_c)$. The residual trends also indicate that the frequency and magnitude of underprediction increase with decreasing values of Fr_{f2} and $7.94(1.65Fr_{f2} - Fr_c)$ below about 0.75 and 8, respectively. This underprediction is prominent in the South Carolina Coastal Plain and Relief/Swamp Bridge data, where lower gradient streams have smaller values of Fr_{f2} and $7.94(1.65Fr_{f2} - Fr_c)$. The general patterns in figures 5-43 and 5-44 also are confirmed by the laboratory data (report section 5.2.3). The underprediction and overprediction in figures 5-43 and 5-44 are pronounced for data associated with rectangular channels having a K_G value of 0.42, and at protruding abutments with a K_L value of 1.35, respectively. However, if K_G and K_L are set to a value of 1.0 for all of the field data, the previously noted trends are still prominent, as can be seen in figures 5-45 and 5-46. (Note: Similar trends also are evident in the laboratory data if K_G and K_L are set to a value of 1.0.) While other variables influence the residual patterns in figures 5-43 through 5-46, it would appear there is a strong relation in the residuals with respect to K_G and K_L. Another possible factor that contributes, in part, to the underprediction in the South Carolina Coastal Plain and Relief/Swamp Bridge data, is the less accurate estimates of the flow velocity at the abutment from one-dimensional flow models. Many of these data are associated with swamps or floodplain relief bridges where the average flow velocity through the bridge opening, amplified by a value of 1.2 for longer bridges (chapter 4), was used to approximate the velocity at the abutment. This method may underestimate flow velocity at the abutment producing underestimation of scour. Better estimates of the flow velocity at the abutment, such as from a two-dimensional model, would likely reduce the magnitude and frequency of underprediction in these data.

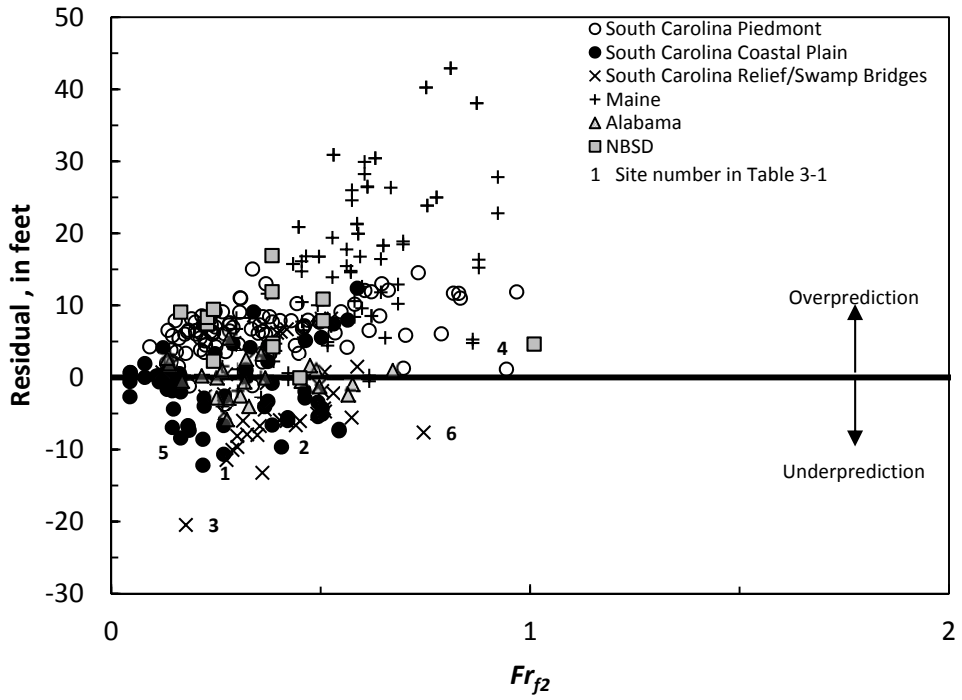

Figure 5-43. Relation of prediction residuals and the Froude number (Fr_{f2}) at the abutment for selected field data, using the NCHRP 24-15(2) scour prediction method.

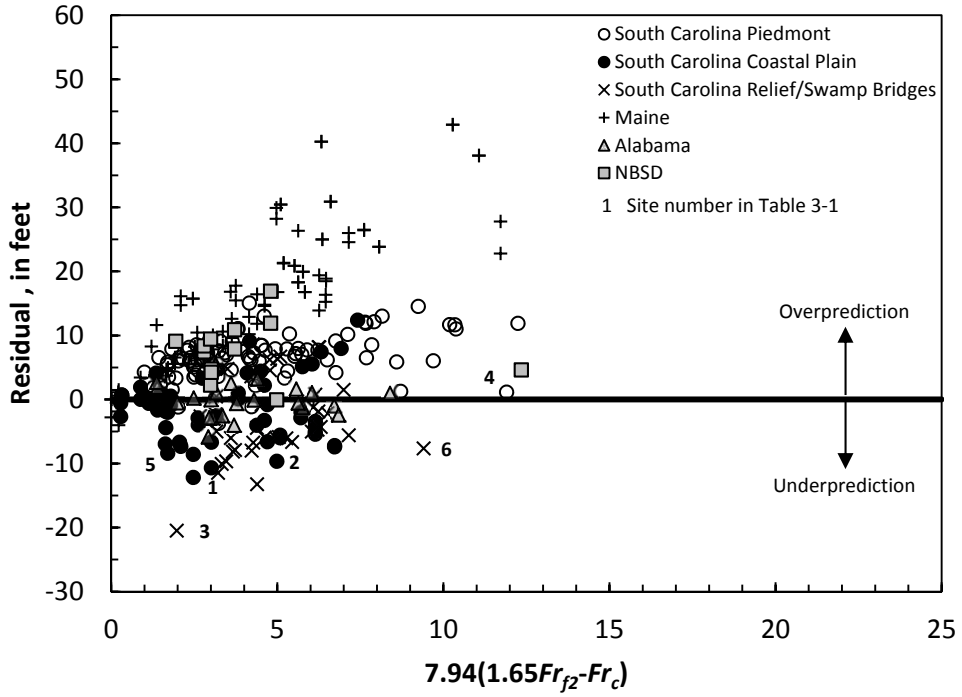

Figure 5-44. Relation of prediction residuals and the Froude number parameter, $7.94(1.65Fr_{f2} - Fr_c)$, for selected field data, using the NCHRP 24-15(2) scour prediction method.

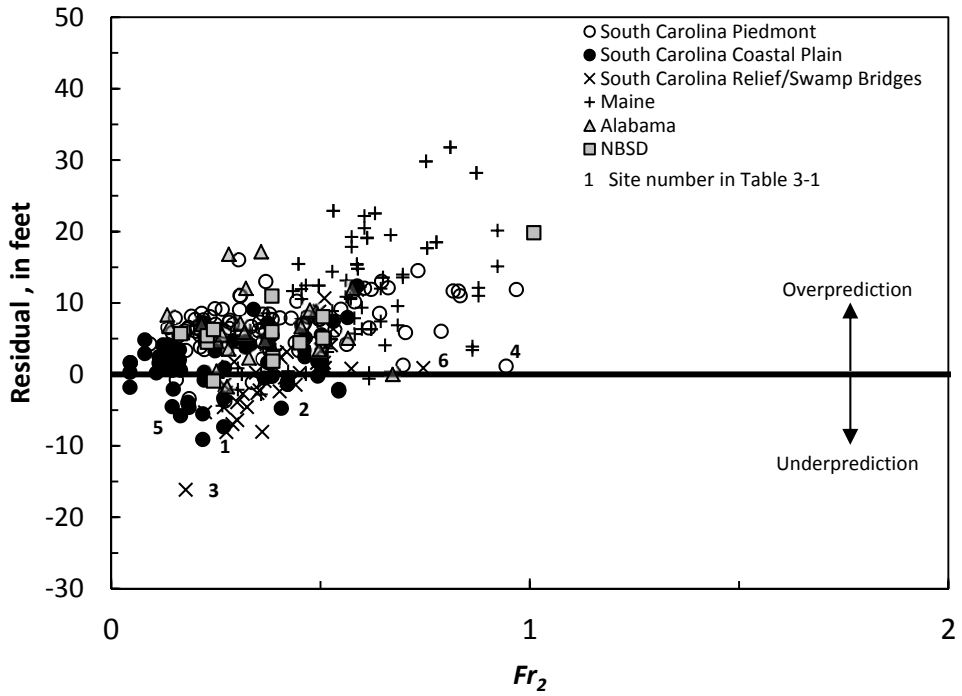

Figure 5-45. Relation of prediction residuals and the Froude number (Fr_{f2}) at the abutment for selected field data, using the NCHRP 24-15(2) scour prediction method and setting K_G and K_L to a value of 1.0.

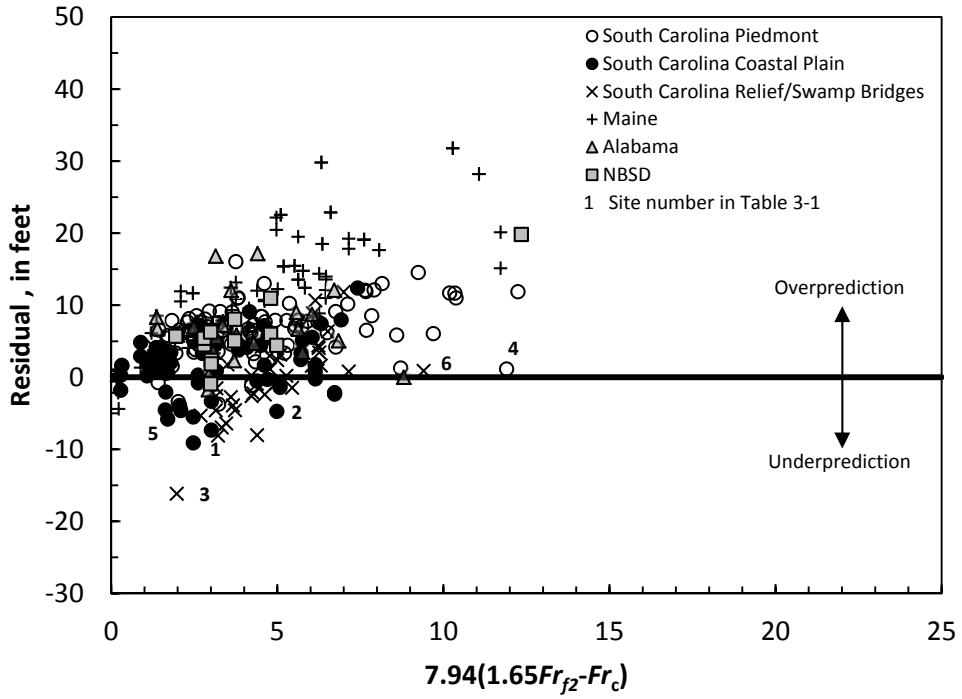

Figure 5-46. Relation of prediction residuals and the Froude number parameter, $7.94(1.65Fr_{f2} - Fr_c)$, for selected field data, using the NCHRP 24-15(2) scour prediction method and setting K_G and K_L to a value of 1.0.

iii. Prediction Residuals with Respect to Re_{f2} and K_{Re}

The relation of the prediction residuals with respect to Re_{f2} and K_{Re} is shown in figures 5-47 and 5-48, respectively, indicating that the magnitude of overprediction increases as Re_{f2} increases, and conversely, as K_{Re} decreases. As noted previously, the largest overpredictions are associated with the steeper gradient streams of Maine, with the largest underpredictions associated with the lower gradient streams of the South Carolina Coastal Plain and Relief/Swamp Bridge data. While the overprediction and underprediction in the Maine and South Carolina data are influenced by protruding abutments and rectangular channels, respectively, analysis in the previous section indicates that the general residual patterns will be similar even if K_G and K_L are set to a value of 1.0 for all of the field data. While some differences exist, the analysis of the laboratory data (report section 5.2.3) generally confirms the patterns seen in figures 5-47 and 5-48.

The ranges of Re_{f2} and K_{Re} for the laboratory and field data differ from one another as can be seen in figure 5-20 (report section 5.2.3). The much larger values of Re_{f2} for the field data yield smaller values of K_{Re} than those associated with the laboratory data, which tend to produce smaller values of predicted relative scour leading to underprediction. The influence of K_{Re} towards reducing predicted scour in the field data is evident in the comparison of figures 5-33 and 5-34 in report section 5.3.2. For the Maine, NBSD, and South Carolina Piedmont data, underprediction is not a major concern, and the lower values of K_{Re} do not appear to produce much underprediction. However, the frequent underprediction for the non-cohesive sediments and lower gradient streams in the Coastal Plain and Relief/Swamp Bridges of South Carolina is of concern. To highlight the differing ranges of K_{Re} for the laboratory and field data, figure 5-49 shows the relation of the Reynolds number correction factor, K_{Re}, with respect to the parameter $7.94(1.65Fr_{f2} - Fr_c)$. The values of K_{Re} for the laboratory data are about 2 to 4 times larger than those of the field data, which will generally lead to smaller estimates of relative scour for the field data. While other factors contribute to the underprediction of the lower gradient streams in the Coastal Plain and Relief/Swamp Bridges of South Carolina, the lower values of K_{Re} likely contribute, in part, to the frequent underprediction associated with those data.

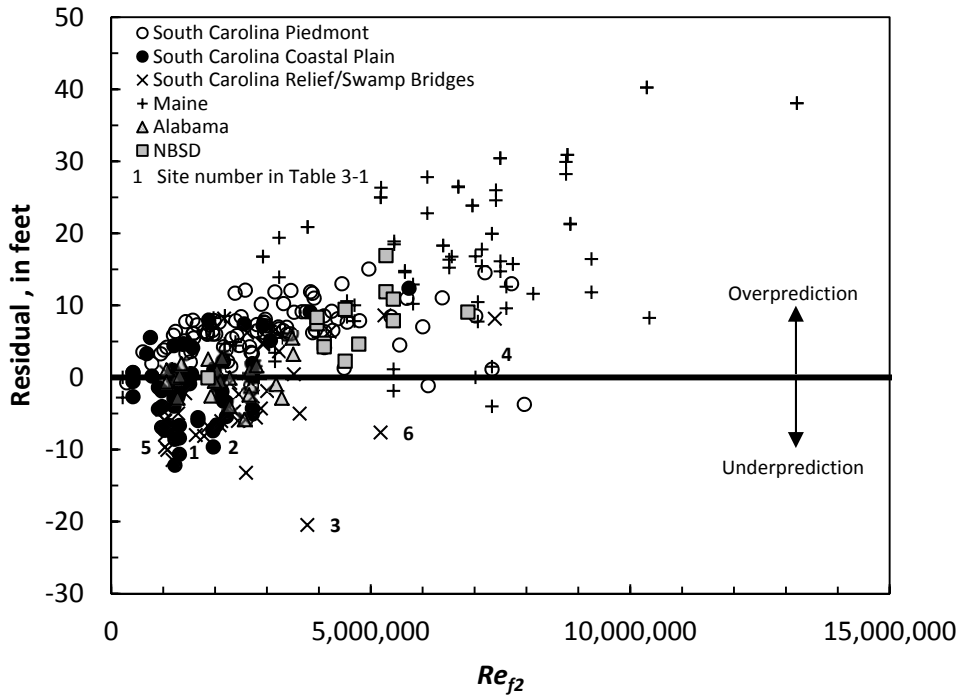

Figure 5-47. Relation of prediction residuals and the Reynolds number at the abutment (Re_{f2}) for selected field data, using the NCHRP 24-15(2) scour prediction method.

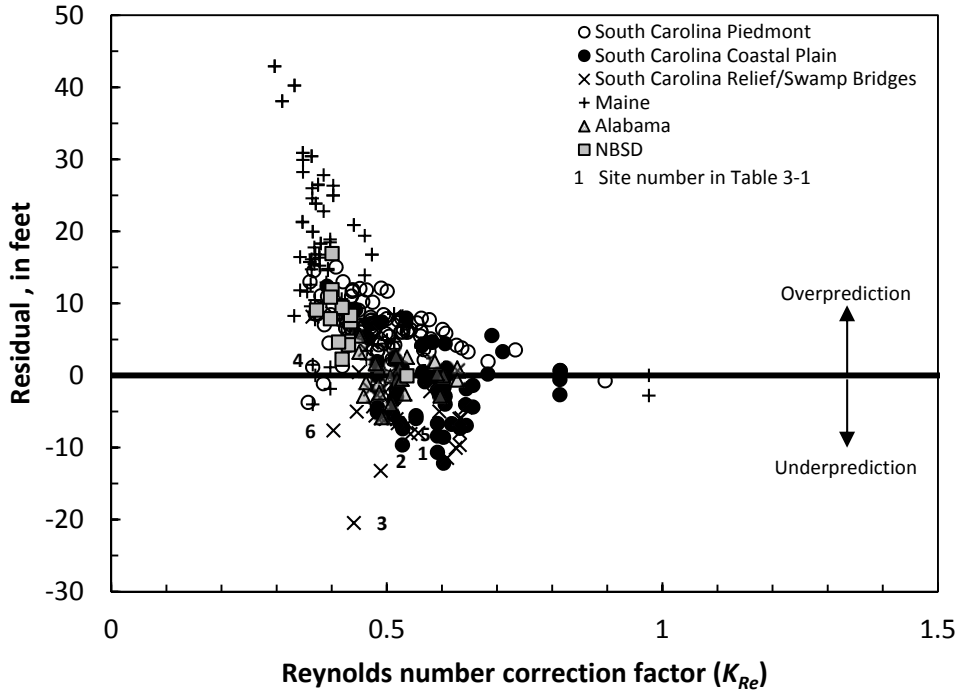

Figure 5-48. Relation of prediction residuals and the Reynolds number correction factor, K_{Re}, for selected field data, using the NCHRP 24-15(2) scour prediction method.

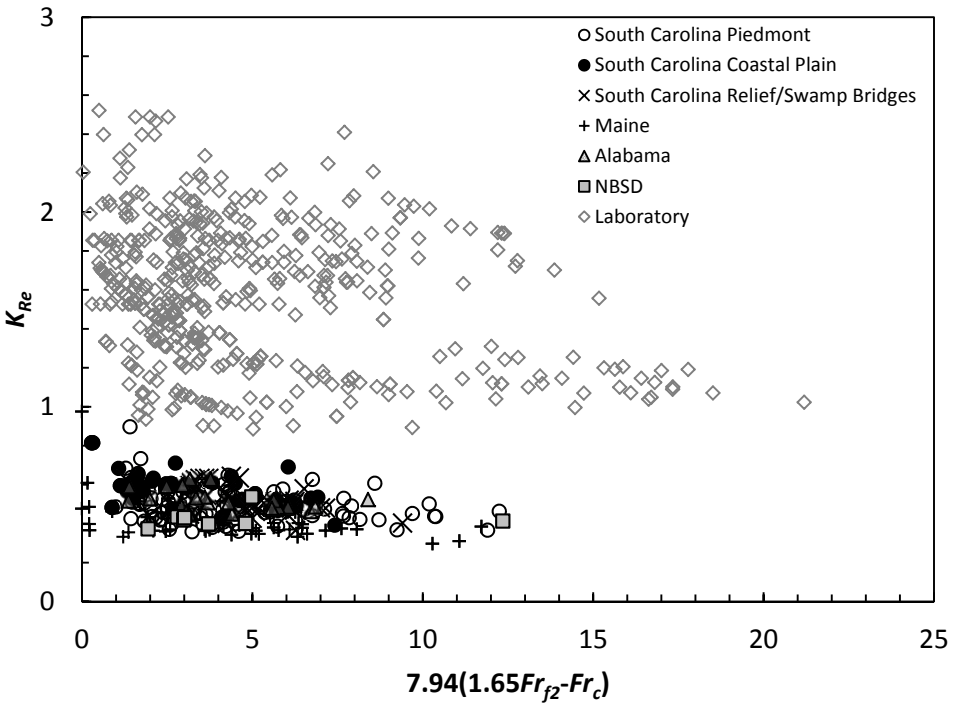

Figure 5-49. Relation of the Froude number parameter, $7.94(1.65Fr_{f2} - Fr_c)$, and the Reynolds number correction factor, K_{Re}, for selected field data.

iv. Prediction Residuals with Respect to K_1, K_2, K_G, K_L, and K_p

The diverse combination of the correction factors K_1, K_2, K_G, K_L, and K_p within the field data make it difficult to display the influence of a given correction factor with respect to prediction residuals, and therefore, no residual plots are shown. Report section 5.3.2 provides a series of figures that progressively adds each correction factor to the predicted scour, illustrating the influence of these correction factors within the field data. Some comments on the influence of these correction factors on predicted scour within the field data follow.

Abutment-shape correction factor (K_1)

The 2 abutment shapes in the field data are wing-wall and spill-through abutments, with most of the spill-through abutments associated with the South Carolina and NBSD data. Figures 5-34 and 5-35, in report section 5.3.2, show predicted scour without and with K_1, respectively, providing a good illustration of the influence of this correction factor on predicted scour within the field data. Wing-wall abutments have a K_1 value of 1.0 and,

therefore, no change in predicted scour. Spill-through abutments with a K_1 value of 0.73 will have a reduction in predicted scour.

Abutment-skew correction factor (K_2)

A brief review of this correction factor is presented in report section 5.2.3 in the analysis of the laboratory data. For skewed abutments, this correction factor will reduce predicted scour by up to 15 percent, regardless of abutment orientation to flow. Figures 5-35 and 5-36, in report section 5.3.2, show predicted scour without and with K_2, respectively, providing a good illustration of the influence of this correction factor on predicted scour within the field data.

Channel-geometry correction factor (K_G)

For rectangular channels, this correction factor will reduce predicted scour by nearly 60 percent. Figures 5-36 and 5-37, in report section 5.3.2, show predicted scour without and with K_G, respectively, providing a good illustration of the influence of this correction factor on predicted scour within the field data. Predicted scour values for rectangular channels have a larger frequency and magnitude of underprediction than predicted scour in compounds. This increased underprediction is associated with the lower gradient streams of the Coastal Plain and Relief/Swamp Bridges, as well as the relief bridges in the Alabama data, where rectangular channels are common. A review of this correction factor was provided in report section 5.2.3 in the analysis of the laboratory data, with a general recommendation that K_G at rectangular channels be given a value of 1.0 rather than 0.42 in order to minimize underprediction.

To provide understanding of how changing K_G from 0.42 to 1.0 for rectangular channels will affect equation performance with the field data, figure 5-50 shows the same data as in figure 5-31 with K_G for rectangular channels set to a value of 1.0. The underprediction associated with the Alabama data is largely removed. About half of the Alabama data are associated with pressure flow, and the larger overpredictions can be attributed to pressure-flow conditions. For the South Carolina Coastal Plain and Relief/Swamp Bridges, underprediction

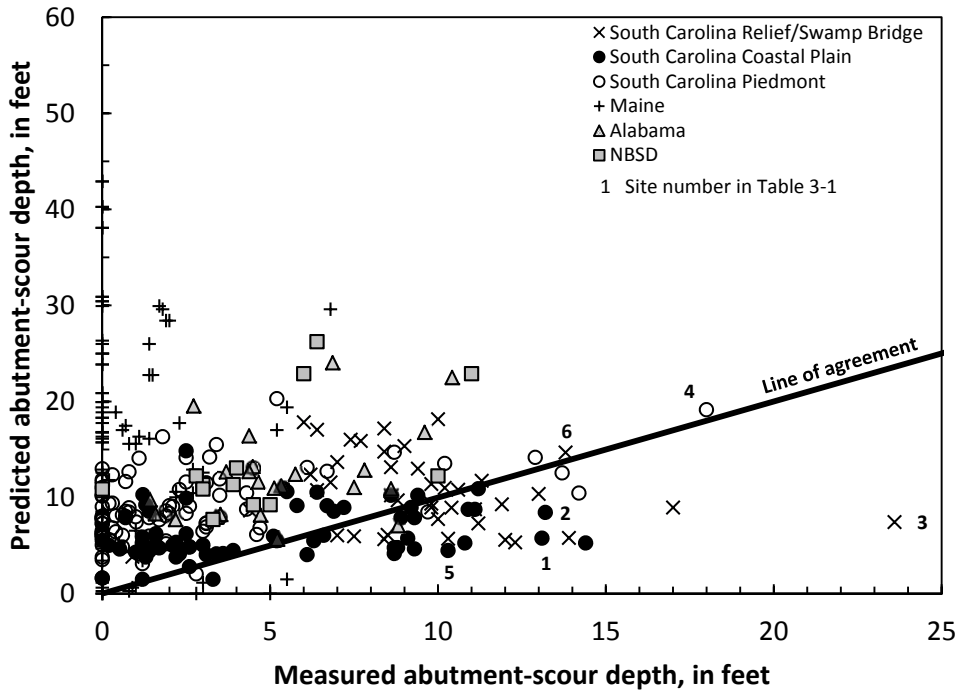

Figure 5-50. Relation of predicted and measured abutment-scour depth for selected field data using the NCHRP 24-15(2) scour prediction method, with the channel-geometry correction factor, K_G, set to a value of 1.0 for rectangular channels.

is diminished; however, substantial underprediction with some increase in overprediction is still present. The patterns in figure 5-50 indicate that using a K_G value of 1.0 for rectangular channels will tend to reduce underpredictions and appears to be a reasonable modification to the NCHRP 24-15(2) method.

Abutment-location correction factor (K_L)

The NCHRP 24-15(2) scour prediction method includes a correction factor for abutment location (K_L) to account for potential increased scour for abutments near the channel bank or protruding into the channel. The maximum value for K_L is 1.35 and occurs when the abutment is located at the channel bank or protrudes into the main channel. As noted in the analysis of the laboratory data (report section 5.2.3), predicted scour associated with K_L values of 1.35 produces some of the largest overpredictions. Figures 5-37 and 5-38, in report section 5.3.2, show predicted scour without and with K_L, respectively, providing a good

illustration of the influence of this correction factor on predicted scour within the field data. The Maine and NBSD data have frequent protruding abutments, and the K_L correction factor increases the overprediction for these data, excessively so for the Maine data. Figure 5-37 shows predicted scour without K_L and shows little underprediction for the Maine and NBSD data, indicating that its inclusion is not critical in reducing underprediction at bankline and protruding abutments. This general pattern also was confirmed in the analysis of the laboratory data (report section 5.2.3).

An alternate method to account for the potential increases in scour for abutments near the main channel is to use the hydraulic data associated with the channel, therefore, removing the need for the abutment correction factor K_L. This method was tested with the laboratory data, and details regarding the method can be found in report section 5.2.3. The same approach was tested with field data associated with bankline or protruding abutments. Figures 5-51A and B show the relation of measured abutment-scour depth to predicted scour for the field data with bankline or protruding abutments, with figure 5-51A reflecting computations using the standard method for applying the NCHRP 24-15(2) method with a K_L value of 1.35, and figure 5-51B reflecting computations using the channel hydraulics with a K_L value of 1.0. A comparison of these figures indicates that using the channel hydraulic data with a K_L value of 1.0 reduces the magnitude of the overpredictions with only a small increase in the frequency and magnitude of underprediction, indicating that it likely is a reasonable alternative to account for the potential increases in scour for abutments near the main channel.

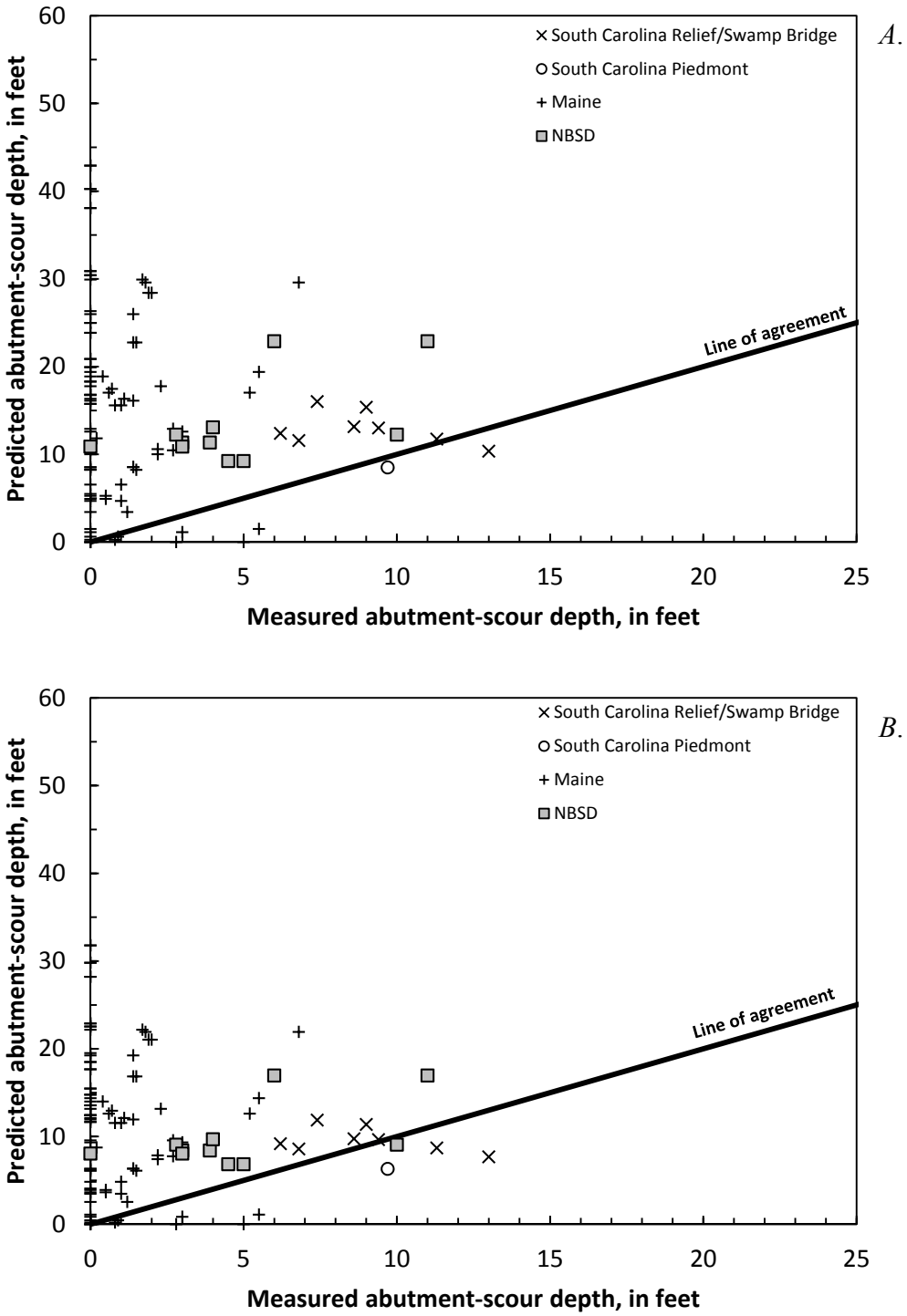

Figure 5-51. Relation of predicted and measured abutment-scour depth for selected field data using the NCHRP 24-15(2) scour prediction method, with (A) K_L equal to 1.35 and (B) K_L equal to 1.0 and using the main-channel hydraulics.

Pressure-flow correction factor (K_p)

The K_p correction factor for the NCHRP 24-15(2) method accounts for increased scour associated with pressure flow and was developed from numerical model simulations. In the field data, 46 bridges have pressure-flow conditions, and values of K_p at these sites range from 1.1 to 1.92, with a median value of 1.56. Figures 5-38 and 5-39, in report section 5.3.2, show predicted scour without and with K_p, respectively, providing a good illustration of the influence of this correction factor on predicted scour within the field data. Because K_p can have values as large as 1.92, it can substantially increase predicted scour.

v. Prediction Residuals with Respect to Relative Abutment Length (L/y_{f1})

Melville (1992) noted that the influence of abutment shape diminishes as abutment length increases, and for longer abutments, scour depths in non-cohesive sediments approach those for a vertical wall regardless of abutment shape. Melville (1992) noted that when L/y_{f1} equaled or exceeded a value of 25 (classified as a long abutment), the abutment-shape correction factors for spill-through and wing-wall abutments become comparable to those for a vertical-wall abutment. Figure 5-52 shows the relation of the prediction residuals and L/y_{f1} and identifies the abutment-length classifications developed by Melville (1992). The residual patterns indicate that the underpredictions in the South Carolina Coastal Plain and Relief/Swamp Bridge data are all associated with long abutments, indicating that it may be appropriate to adjust the abutment-shape correction factor (K_1) for these data to reflect that of a vertical wall (K_1=1.22). Because most of the South Carolina Coastal Plain and Relief/Swamp Bridge data are associated with spill-through abutments, this adjustment tends to increase predicted scour, thereby reducing underprediction. Figure 5-53 shows the relation of predicted and measured scour with a value of 1.22 assigned to K_1, for the South Carolina Coastal Plain and Relief/Swamp Bridge data, if L/y_{f1} was greater than or equal to 25. In addition to this adjustment, the values for K_G and K_L for all of the field data were assigned a value of 1.0 to minimize the underprediction and overprediction associated with these correction factors, as described previously. The modification of the abutment-shape correction factor, as recommended by Melville (1992), was applied only to the South Carolina Coastal Plain and Relief/Swamp Bridge data because of the poor performance of

these data. Additionally, these data are associated with non-cohesive sediments in the sand range, as were the Melville (1992) data, which have a higher potential for scour. Application of Melville's (1992) modified abutment-shape correction factor to the other field data would substantially increase overprediction and therefore was not applied. The results shown in figure 5-53 indicate improvement in the performance of the South Carolina Coastal Plain and Relief/Swamp Bridge data, indicating that the application of Melville's (1992) modified abutment-shape correction factor for long abutments may be appropriate for those data. In addition to adjusting predicted scour for abutment length, better estimates of the flow velocity at the abutment, such as from a two-dimensional model, would likely further reduce the magnitude and frequency of underprediction in these data.

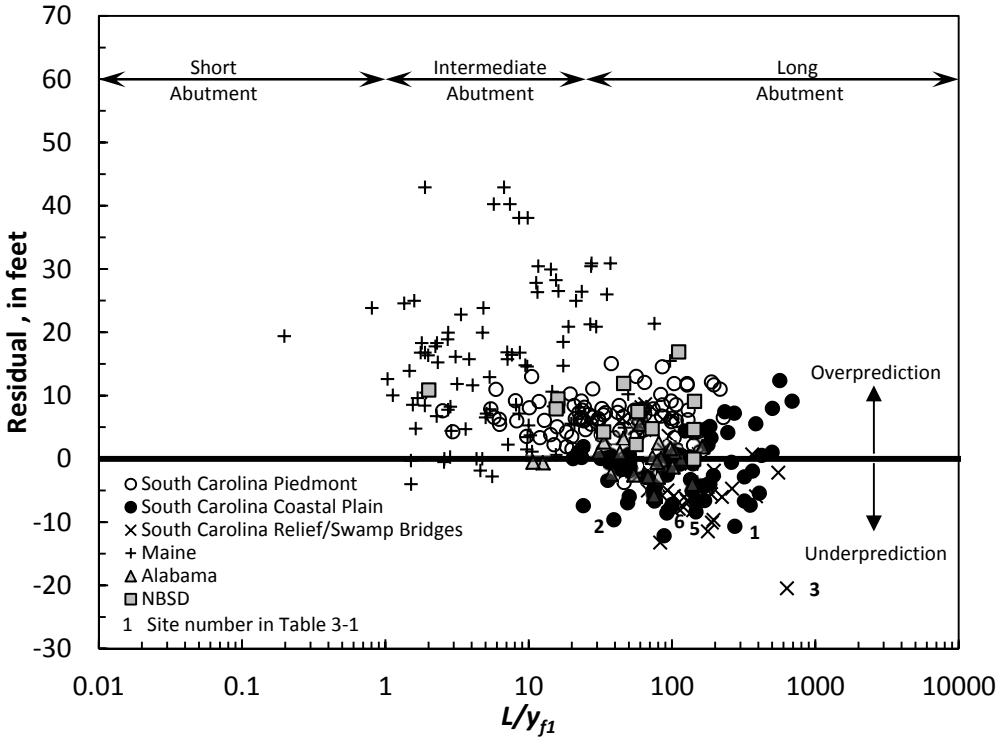

Figure 5-52. Relation of prediction residuals and the relative abutment length (L/y_{f1}) for selected field data, using the NCHRP 24-15(2) scour prediction method.

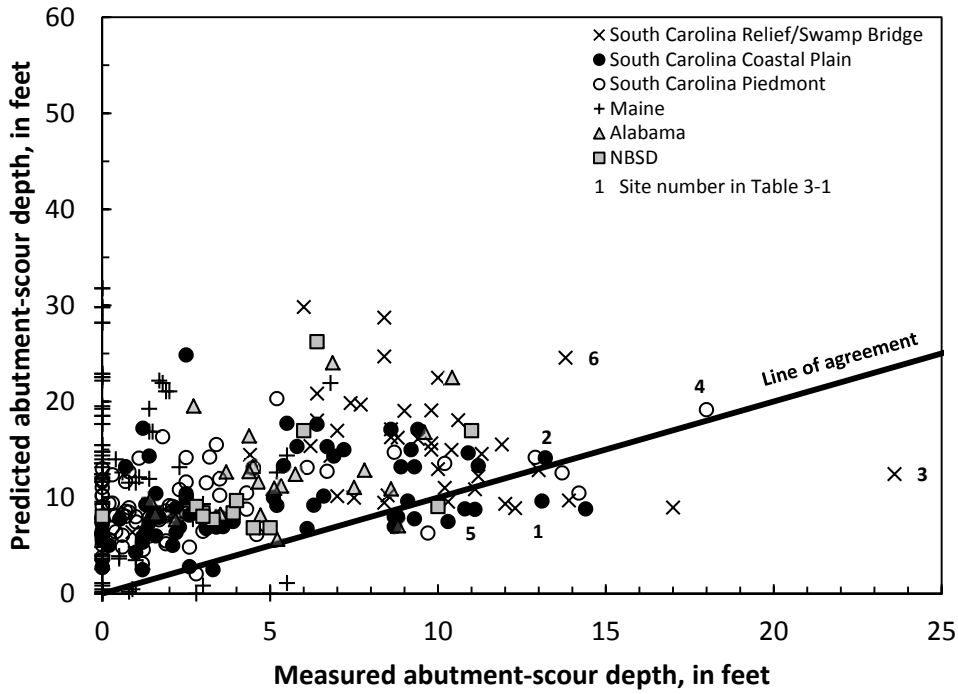

Figure 5-53. Relation of predicted and measured abutment-scour depth for selected field data using the NCHRP 24-15(2) scour prediction method, with K_G and K_L set to a value of 1.0, and K_1 set to a value of 1.22 for the South Carolina Coastal Plain and Relief/Swamp Bridge data if the relative abutment length was greater than or equal to 25.

5.3.4 Prediction Trends for Cohesive and Non-Cohesive Sediments

Figures 5-54 and 5-55 show the same data as shown in figures 5-31 and 5-40A, respectively, with the data grouped by the categories of cohesive and non-cohesive sediments. The trends in figure 5-54 and 5-55 indicate that the cohesive sediments perform better than the non-cohesive sediments having a smaller frequency and magnitude of underprediction and less excessive overprediction. The NCHRP 24-15(2) method was developed for cohesive sediments; therefore, the better performance with the cohesive sediments would seem reasonable. Of the 32 underpredictions in the cohesive sediments, 27 are associated with rectangular channels with a correction factor K_G of 0.42. If K_G is assigned a value of 1.0 for these data, then most of these underpredictions are removed.

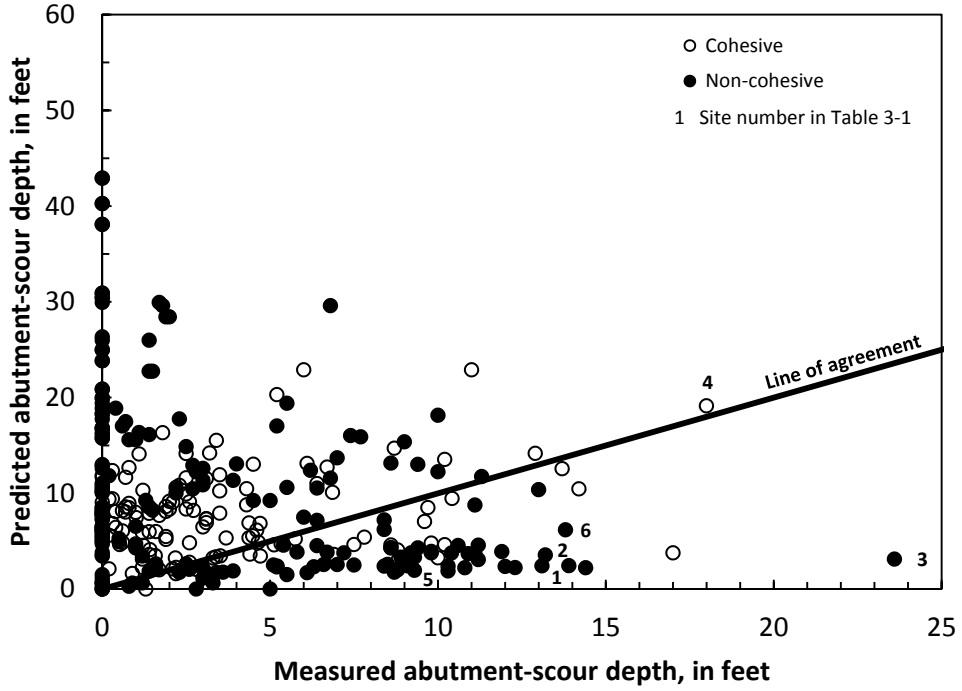

Figure 5-54. Relation of predicted and measured abutment-scour depth for selected field data grouped by cohesive and non-cohesive sediments, using the NCHRP 24-15(2) scour prediction method.

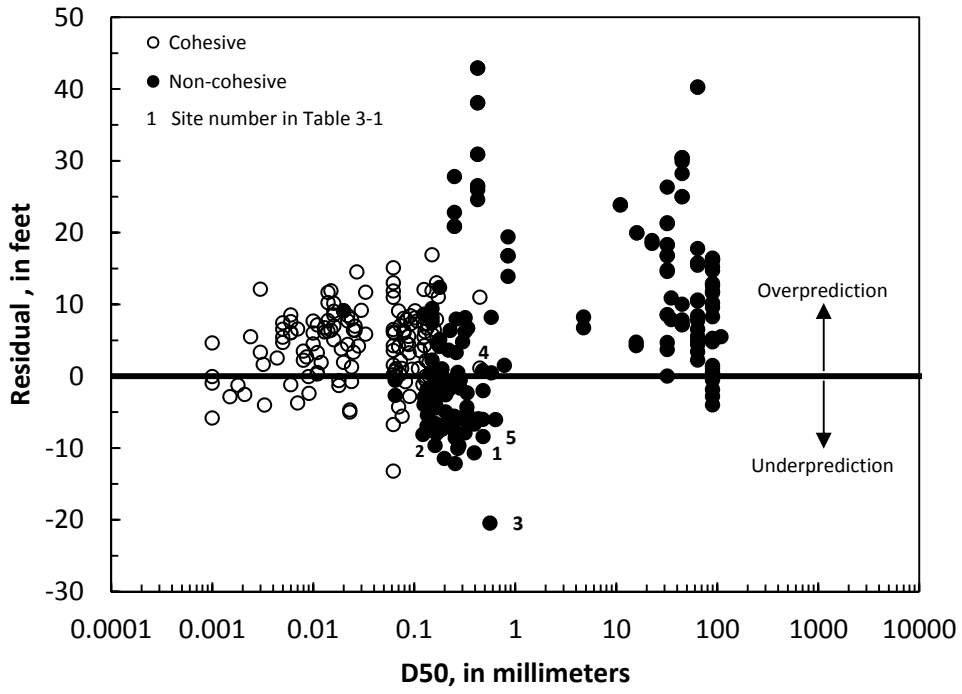

Figure 5- 55. Relation of prediction residuals and the median sediment size (*D50*) for selected field data grouped by cohesive and non-cohesive sediments, using the NCHRP 24-15(2) scour prediction method.

5.3.5 Alternate Critical-Velocity Methods for Estimating Clear-Water Contraction Scour

By using a similar approach to the analysis of the NCHRP 24-20 equation, alternate methods for determining V_c were applied to the NCHRP 24-15(2) to determine their influence on equation performance. These alternate methods include Fortier and Scobey (1926), Laursen (1963), Neill (1973), and Vanoni (1975). A brief description of these alternate critical-velocity methods can be found in report section 3.6. Figure 5-56 shows the relation of predicted scour to measured scour for the data grouped by cohesive and non-cohesive sediments. The Neill (1973) method is not shown in Figure 5-56 but performs similarly to the other methods. Figure 5-57 shows the relation of prediction residuals (predicted minus measured scour) with respect to the median grain size. While there are some differences, the results displayed in these figures indicate that scour prediction, with respect to the alternate critical-velocity methods, is not highly sensitive to the estimate of critical velocity. The influence of V_c in the NCHRP 24-15(2) method (equation 4-1) is embedded in the parameter $7.94(1.65Fr_{f2} - Fr_c)$ and therefore, predicted scour and V_c are not directly proportional. The value of $1.65Fr_{f2}$ is typically larger than Fr_c, has the stronger influence on determining the value $7.94(1.65Fr_{f2} - Fr_c)$, and diminishes the influence of V_c on predicted scour.

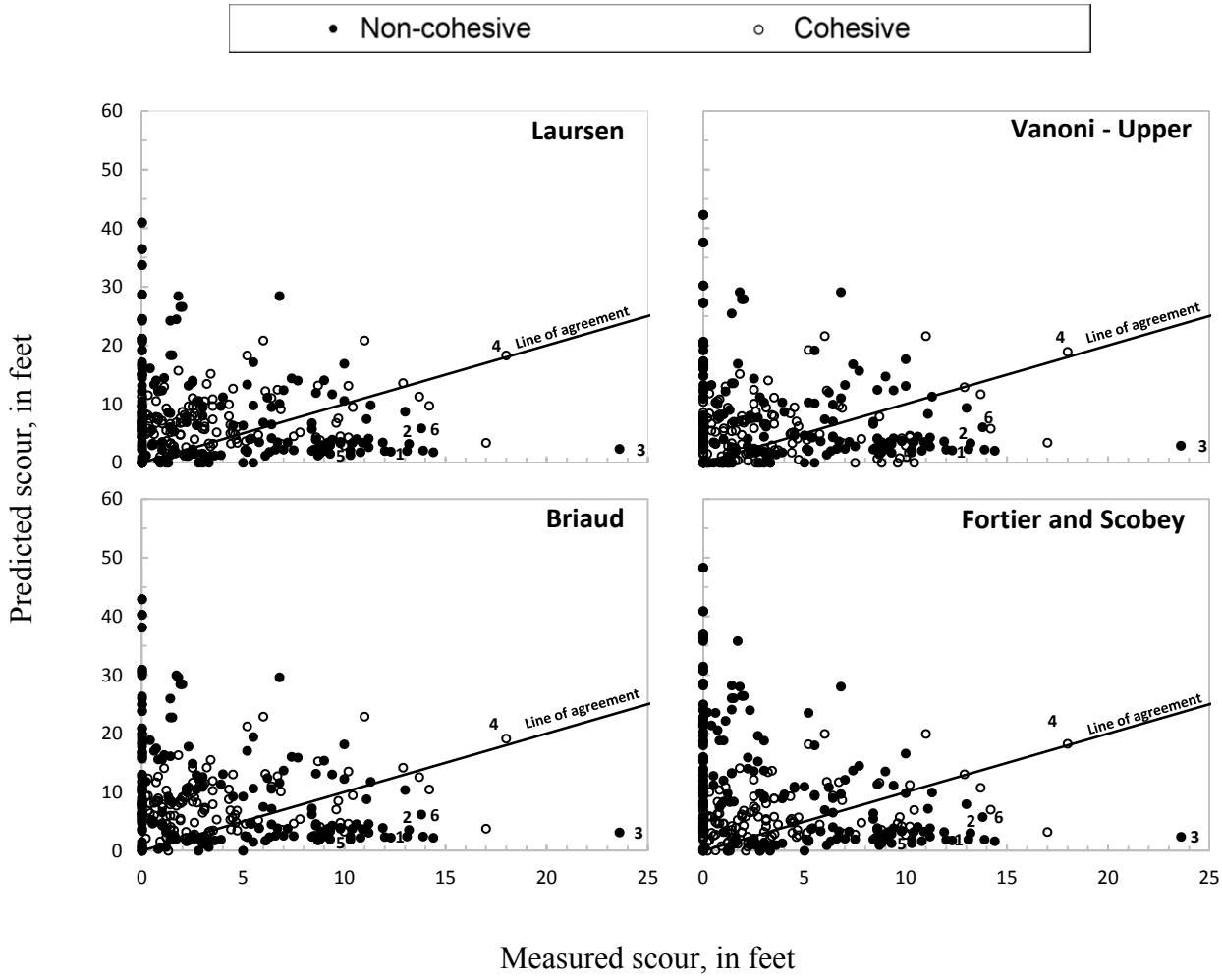

Figure 5- 56. Relation of predicted and measured abutment-scour depth for the NCHRP 24-15(2) scour prediction method using field data and selected critical-velocity methods.

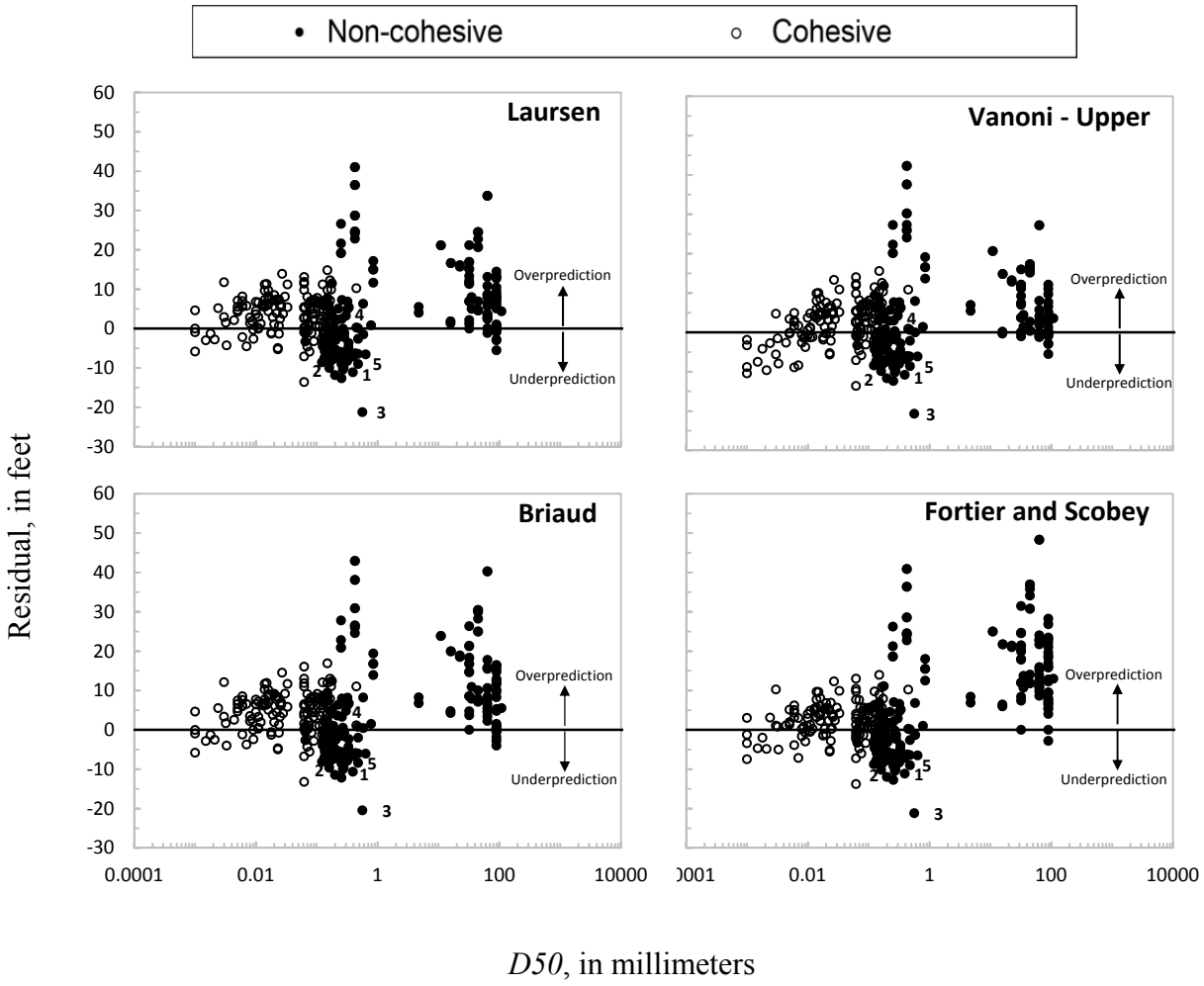

Figure 5- 57. Relation of the median grain size (*D50*) and the abutment-scour prediction residual for the NCHRP 24-15(2) scour prediction method using field data and selected critical-velocity methods.

5.4 Assessment of the NCHRP 24-15(2) Prediction Method

Based on the review of the NCHRP 24-15(2) prediction method (Briaud et al. 2009; 2011) and the analysis associated with the laboratory and USGS field data, a limited assessment of the method is presented, including noted strengths and weakness, suggested modifications for improved performance along with additional analysis for further verification of the method's performance, and limited guidance for applying the method. The complexity of scour processes at abutments and the limitations of the data used in this analysis make it difficult to fully evaluate the performance of the NCHRP 24-15(2) prediction method. The following comments should be viewed in light of this challenge.

5.4.1 Strengths

The strengths of the NCHRP 24-15(2) abutment-scour prediction method include the following:

1. **Simple equation form similar to the Froehlich (1989) equation:**

   The NCHRP 24-15(2) equation consists of a simple format that uses a series of empirical expressions to account for the influence of a given variable on scour depth. The general equation format is similar to the Froehlich (1989) abutment-scour equation, and the NCHRP 24-15(2) and Froehlich (1989) equations have some similar equation parameters. The similarity in equation form to the familiar Froehlich (1989) equation should make application of the NCHRP 24-15(2) equation fairly intuitive to the practitioner.

2. **While excessive overprediction occurs, the core explanatory variable, $7.94(1.65Fr_{f2} - Fr_c)$, approximates the trend of the field data with minimal underprediction:**

   The prediction patterns in figure 5-33 indicate that the core explanatory variable, $7.94(1.65Fr_{f2} - Fr_c)$, captures, in some measure, the trends of the field data because predicted scour increases as measured scour increases. While overprediction can be excessive, there is essentially no underprediction.

3. **Method performs reasonably well in cohesive sediments:**

   The NCHRP 24-15(2) method was originally developed for predicting abutment scour in cohesive sediments and performs best in those types of sediments. This is particularly evident in the cohesive sediments of the South Carolina Piedmont (figure 5-32C). The cohesive data for Alabama (figure 5-32E) have more frequent underprediction than the South Carolina Piermont data because they are associated with rectangular channels with a channel-geometry correction factor, K_G, that tends to cause underprediction of scour (see report sections 5.2.4(iv) and 5.3.4). Modification of this correction factor, as noted later in this report section, will improve performance with the Alabama data.

4. **Includes a time-dependent method for a refined estimate of scour in cohesive sediments:**

   While not evaluated in the current (2015) investigation, the NCHRP 24-15(2) method includes a time-dependent method for estimating abutment scour in cohesive sediments, providing a refined, and likely smaller, estimate of abutment scour.

5.4.2 Weaknesses

The weaknesses of the NCHRP 24-15(2) abutment-scour prediction method include the following:

1. **The method in its current format performs poorly in non-cohesive sediments:**

   The NCHRP 24-15(2) method was originally developed for predicting scour in cohesive sediments, but was extended to include prediction for non-cohesive sediments. While performance in cohesive sediments is reasonable, the method in its current format performs poorly (figure 5-54) with substantial underprediction. If certain parameters within the method are modified, performance in non-cohesive sediments improves substantially.

2. **The derivation of the method largely relies on empirical relations:**

The derivation of the NCHRP 24-15(2) maximum abutment-scour equation (equation 4-1) largely relies on empirical relations to define all of the equation's explanatory variables and does not strongly incorporate the evaluation of physics-based processes as part of the derivation. This approach is not unusual and has been used in the derivation of various scour prediction methods, with the Froehlich (1989) equation being a good example of an empirically-derived equation. A weakness of this approach is that uncertainty in the equation performance increases when applied to sites substantially beyond the range of the data used to develop the equation. Therefore, some caution must be used when applying the NCHRP 24-15(2) method to sites outside the range of the dimensionless variables associated with the laboratory data used to develop the method (table 1-4).

3. **Selected correction factors need further evaluation and modification:**

The analysis of the NCHRP 24-15(2) method indicates that the poor performance in the non-cohesive sediments is related, in part, to poor definition of some of the correction factors, including the correction factors for channel geometry, abutment location, and abutment shape. Selected modifications of these correction factors were evaluated with the NCHRP 24-15(2) method, and performance with the non-cohesive data improved. These preliminary modifications are noted for consideration in the following section, but they should be evaluated further before incorporation into the NCHRP 24-25(2) method.

5.4.3 Recommendations for Improving Method

The analysis of the NCHRP 24-15(2) method indicated that equation performance could improve with modification to selected correction factors. These recommendations are based on a limited analysis and therefore, may need additional evaluation prior to incorporating into the NCHRP 24-15(2) method.

1. **Modification of the correction factor for channel geometry, K_G:**

   The correction factor for channel geometry, K_G, for rectangular channels has a value of 0.42, which increases the frequency and magnitude of underprediction at such sites. In the field data, bridges associated with swamps and floodplain relief bridges were classified as rectangular channels and have a much higher incidence of underprediction (see report sections 5.3.2 and 5.3.3). The work of Melville (1992) and of Melville and Coleman (2000) indicates that a value of 1.0 for K_G at rectangular channels may be appropriate, and this was tested in the field data (figure 5-50). Results of the test reduced the incidence of underprediction, with some increase in overprediction. Consideration should be given to modifying K_G to a value of 1.0 for rectangular channels.

2. **Modification of the correction factor for abutment location, K_L:**

   The correction factor for abutment location, K_L, accounts for potential increased scour for abutments near the channel bank or protruding into the channel. Such sites are associated with some of the largest overpredictions in the laboratory and field data (see report sections 5.2.3 and 5.3.3). An alternate method to account for the potential increases in scour is to use the hydraulic data associated with the channel, therefore removing the need for the abutment-location correction factor K_L. This alternate method was tested with selected laboratory and field data (figures 5-30 and 5-51, respectively) and was generally found to reduce the magnitude of the overprediction at such sites with only a small increase in the frequency and magnitude of underprediction, indicating that it probably is a reasonable alternative to account for the potential increases in scour for abutments near the main channel. Consideration should be given to accounting for scour

at bankline and protruding abutments by using the channel hydraulic data rather than the abutment-location correction factor K_L.

3. **Modification of the correction factor for abutment shape, K_1:**

   The correction factor for abutment shape, K_1, accounts for the influence of abutment shape on scour depth, with streamlined shapes, such as a spill-through abutment, producing smaller scour depths than blunt shapes, such as a vertical wall. As noted by Melville (1992), the reduction in scour depth derived from streamlined abutment shapes diminishes as abutment length increases, and for longer abutments, scour depths approach those for a vertical wall regardless of abutment shape. The largest underpredictions in the field data are associated with the long abutments of the South Carolina Coastal Plain and Relief/Swamp Bridge data (figure 5-52) with all but 3 data points having spill-through abutments with K_1 values of 0.73. Based on the work of Melville (1992), the K_1 value for these data should be adjusted to that of a vertical wall (1.22), which would substantially reduce underprediction (figure 5-53). Applying this abutment-shape adjustment to the cohesive sediments of the South Carolina Piedmont and Alabama data will substantially increase overprediction and therefore, may not be appropriate. However, for the non-cohesive sandy sediments of the South Carolina Coastal Plain and Relief/Swamp Bridge data, this adjustment seems appropriate. Consideration should be given to incorporating Melville's (1992) abutment-shape adjustment for long abutments, in particular at sites with non-cohesive sediments similar to those of the Coastal Plain of South Carolina. While this adjustment does not appear to be as critical at sites with cohesive sediments, it would be beneficial to give some consideration to its application at such sites.

4. **Further evaluation of the correction factor for abutment skew, K_2:**

   Only two abutment-scour measurements in the NCHRP 24-15(2) laboratory data were associated with a skewed abutment, with one measurement having an abutment pointing downstream and the other pointing upstream. Because of the limited number of data, the relation for determining K_2 should be used with caution, and further investigation of the

influence of skew on abutment-scour depth would be beneficial to confirm the equation for determining K_2 (see report section 5.2.3(iv) for additional details).

5. **Further evaluation of the Reynolds number correction factor:**

   It is generally accepted that viscous effects, as incorporated in the Reynolds number, can be neglected in the derivation of abutment- and contraction-scour equations (Melville and Coleman, 2000; Sturm et al. 2011; see report section 5.2.3), thus making its inclusion in the NCHRP 24-15(2) method problematic. The Reynolds number correction factor for the NCHRP 24-15(2) equation was derived from a limited set of laboratory data, including the NCHRP 24-15(2) measurements in cohesive sediments and previously published measurements in non-cohesive sediments. Because of the limited nature of the data used to develop this parameter, in conjunction with the previously noted observation that viscous effects, and thus Reynolds numbers, can be neglected in the derivation of abutment-scour equations, further evaluation of the Reynolds number correction factor for the NCHRP 24-15(2) equation is justified. Additionally, the Reynolds numbers associated with the field data are often much larger than those of the laboratory data used to develop the NCHRP 24-15(2) equation (figure 5-20). In the empirical relation for K_{Re}, large Reynolds numbers yield smaller values of the Reynolds number correction factor for equation 4-1, which will tend to produce smaller values of predicted scour. A comparison of figures 5-33 and 5-34 shows how K_{Re} substantially reduces predicted scour in the field data. Additionally, figure 5-49 highlights the different ranges of K_{Re} for the laboratory and field data, showing the values for the field data to be much lower. As a general rule, empirical and semi-empirical equations should be applied to sites having characteristics similar to the range of the explanatory variables used to develop the equation and should be used with caution when site conditions exceed that range. Because most of the Re_{f2} values associated with the field data are substantially outside the range of the laboratory data, in conjunction with the previously noted concerns, further consideration should be given to testing and, if necessary, removing or modifying the Reynolds number correction factor.

6. **Evaluate the influence of V_c determined from EFA tests**

The NCHRP 24-25(2) maximum abutment-scour depth equation uses an estimate of V_c based on the empirical relation shown in figure 4-4. This relation is a lower-bound curve of critical velocity as determined from EFA tests of field samples (Briaud et al. 2009; 2011; report section 4.2). A more accurate measurement of V_c for a given bridge site could be obtained from EFA tests of soil samples from that site, possibly improving the performance results for NCHRP 24-15(2). Because of the scour-resistant nature of cohesive sediments, EFA tests may particularly reduce the overprediction associated with these types of sediments. Therefore, it may be beneficial to test selected sites with such data to evaluate the sensitivity of the method to the determination of V_c.

7. **Safety factor**

In its current format, the prediction patterns associated with the NCHRP 24-15(2) method indicate a measure of uncertainty with frequent underprediction for larger measurements of scour (figure 5-54). Therefore, to minimize underprediction, consideration should be given to the incorporation of a safety factor.

8. **Evaluating sensitivity to flow velocity:**

Some of the underprediction in the non-cohesive sediments in the USGS field data (figure 5-54) is likely caused by inaccurate estimates of the flow velocity from one-dimensional flow models. It is thought that better estimates of flow velocity near the abutment likely would improve performance, perhaps substantially. This assumption could be evaluated by selecting a strategic sample of sites from the USGS field database, developing two-dimensional flow models for the sites, and applying the better estimates of flow velocity to the NCHRP 24-15(2) method. This analysis would help identify how sensitive the NCHRP 24-15(2) method is to the estimate of flow velocity at the abutment, providing direction for improving equation performance.

5.4.4 General Application Guidance

This guidance for application of the NCHRP 24-15(2) method is not exhaustive and is not intended to supersede the guidance in Briaud et al. (2009; 2011):

1. **Estimate of the maximum flow velocity near the abutment:**

   The maximum flow velocity at the abutment is an important variable in the NCHRP 24-15(2) prediction method. A two-dimensional flow model will provide the most accurate assessment of this variable. At bridge sites with a well-defined main channel, the NCHRP 24-15(2) prediction method (chapter 4) provides a method to estimate a conservative value of the maximum flow velocity at the abutment from a one-dimensional flow model. However, this method tends to underpredict flow velocity at the abutment for swamps and floodplain relief bridges, and a two-dimensional flow model is a better tool for making this assessment. If a one-dimensional flow model is used at such a site, engineering judgment should be used to estimate the larger velocity associated with contracted flow at an abutment. In general, conservative, but reasonable, estimates of the velocity should be used.

2. **Evaluation of sediments:**

   The surface and subsurface sediments at a site influence the potential for abutment-scour depth, and giving consideration to this matter is important when evaluating scour at a bridge site. Scour depth is often limited by cohesive sediments or by subsurface scour-resistant layers (see report section 1.2.5). However, field conditions where the depth of the erodible sediments is very large may allow for large scour depths to develop beyond those measured in the USGS field data. Because of the complexity of soil conditions in the field, a multidisciplinary team, including geotechnical, structural, and hydraulic engineers, should be used to assess the potential influence of soil conditions on scour.

3. **Long abutments and large contractions:**

Long abutments and large flow contractions have high potential for scour, and the underprediction in the USGS field data is often associated with these types of site characteristics. When such sites are being analyzed with the NCHRP 24-15(2) method, it is important to use judgment and a strong measure of conservatism in the assessment. Conservative estimates of flow velocity near the abutment, along with some type of safety factor, would be advisable.

4. **Application to cohesive sediments (*D50* < 0.1 mm)**

As noted previously (report section 5.3.4), the NCHRP 24-15(2) method performs reasonably well with cohesive sediments. The cohesive data for Alabama will perform well if K_G is modified as noted previously in report section 5.4.3. The NCHRP 24-15(2) method was originally developed for cohesive sediments; therefore, the better performance with these types of sediments would seem logical. The analysis of cohesive sediments presented in this report primarily reflects the field characteristics associated with the South Carolina Piedmont and Alabama data. Performance of the NCHRP 24-15(2) method in cohesive sediments may vary for sites that have characteristics beyond the range of the South Carolina Piedmont and Alabama data. Table 1-1 provides a summary of site characteristics associated with these data that can be used to evaluate if a site of interest has characteristics similar to the South Carolina and Alabama data. Additionally, the reports associated with these data (Benedict, 2003; Lee and Hedgecock, 2008) can be referenced.

5. **Application to coarse sediments in the small, steep-gradient streams of Maine (*D50* > 10 mm)**

The small streams of Maine with steep gradients and coarse sediments (*D50* > 10 mm) have minimal underprediction, but at times excessive overprediction. The overprediction is related to a number of factors, including the large values of Fr_{f2} and protruding

abutments. A frequent incident of pressure flow in the Maine data will increase predicted scour. Overprediction associated with protruding abutments can be reduced by using the channel hydraulic data rather than the abutment-location correction factor, K_L, as was demonstrated in figure 5-51. The analysis of steep-gradient and coarse-sediment streams presented in this report primarily reflects the characteristics associated with the Maine data. Performance of the NCHRP 24-15(2) method for steep-gradient and coarse-sediment streams may vary for sites that have characteristics beyond the range of the Maine data. Table 1-1 provides a summary of site characteristics associated with these data that can be used to evaluate if a site of interest has characteristics similar to the Maine data. Additionally, reference can be made to the report associated with these data (Lombard and Hodgkins, 2008).

6. Application to non-cohesive sediments in the low-gradient streams of South Carolina

As noted previously, the NCHRP 24-15(2) method has frequent underprediction with many of the South Carolina Coastal Plain and Relief/Swamp Bridges. These data are generally associated with lower gradient streams with non-cohesive sandy sediments. Wide floodplains are common at these sites, and bridges often create large contractions of flow and thus a high potential for scour. These sites have some of the largest measured scour depths in the field database (table 1-1), and underprediction where large scour depths frequently occur is of concern. To minimize underprediction at such sites, consideration should be given to modification of the correction factors K_1, K_G, and K_L, as previously noted. Additionally, conservative estimates of the flow velocity at the abutment minimize the potential for underprediction, and the use of a two-dimensional flow model may be advisable. Note that the core explanatory variable, $7.94(1.65Fr_{f2} - Fr_c)$, provides a conservative estimate of abutment scour in the South Carolina Coastal Plain and Relief/Swamp Bridges (figure 5-33) with essentially no underprediction and offers an alternative method for predicting abutment scour at sites with these characteristics. Performance of the NCHRP 24-15(2) method in sandy, non-cohesive sediments may vary for sites that have characteristics beyond the range of the South

Carolina Coastal Plain data. Table 1-1 provides a summary of site characteristics associated with these data that can be used to evaluate if a site of interest has characteristics similar to the South Carolina data, and reference can be made to Benedict (2003) for additional information.

CHAPTER 6

COMPARISON OF RESULTS FOR NCHRP 24-20 AND NCHRP 24-15(2) AND CONCLUSIONS

6.1 Introduction

Summary statistics of prediction residuals provide a useful way to compare the performance of selected prediction methods. Therefore, the summary statistics of the laboratory- and field-data prediction residuals associated with the analysis of the NCHRP 24-20 and 24-15(2) prediction methods were computed and tabulated in tables 6-1 and 6-2, respectively. (Note: The field data for the South Carolina Coastal Plain and the Relief/Swamp Bridge data, with two exceptions, are located in the South Carolina Coastal Plain and were combined into one group called the South Carolina Coastal Plain for the purposes of this report section. The two exceptions are swampy relief bridges in the Piedmont that have similar characteristics to those of the Coastal Plain data.) The summary statistics of the prediction residuals include the minimum, mean, and maximum values, along with the 25th, 50th, and 75th percentile values. Additionally, boxplots for the same data listed in tables 6-1 and 6-2 were developed and are shown in figures 6-1 and 6-2, providing a useful visual presentation of the prediction residuals. Positive values of the prediction residuals in the boxplots represent overprediction, and negative values represent underprediction. The scatter plots of the prediction residuals, presented earlier in the report, display the trend of the prediction residuals with respect to a given variable, providing insights regarding prediction trends associated with that variable. The boxplots cannot display such trends, but provide a general understanding of equation performance and a simple tool for comparing the performance of multiple equations. The boxplots and data in tables 6-1 and 6-2, with respect to the laboratory and field data, are reviewed below.

6.2 Performance in the Laboratory Data

The prediction-residual boxplots in figure 6-1 indicate that the performance of the NCHRP 24-20 and NCHRP 24-15(2) prediction methods, with respect to the laboratory data, are similar in the

frequency of overprediction, with approximately 75 percent or more of the data having overpredictions. The exception to this is the performance of the Sturm (2004) data with the NCHRP 24-20 prediction method, where underprediction is more frequent, and comments on this pattern will be noted later. The boxplots also indicate that the NCHRP 24-15(2) prediction method generally has larger prediction residuals (larger overpredictions) than the NCHRP 24-20 prediction method. The magnitude of the larger overpredictions can be assessed from a review of the data in table 6-1 and is discussed in the following sections.

6.2.1 Residual Patterns Associated with the NCHRP 24-20 Prediction Method

Some particular observations regarding the residuals in the NCHRP 24-20 prediction method are as follows:

- The Ettema et al. (2010) data have the best performance within the laboratory data, with no underpredictions and the smallest range for the residuals. Because these data were used to develop the NCHRP 24-20 prediction method, the pattern is to be expected and demonstrates that the NCHRP 24-20 method reflects well the trends of the data from the investigation.
- The largest overpredictions in the NCHRP 24-20 prediction method are associated with the cohesive sediments of the Briaud et al. (2009) data. The NCHRP 24-20 prediction method was developed for scour prediction in non-cohesive sediments, and the larger overpredictions in cohesive sediments are to be expected (report section 3.5). This pattern also is observed in the field data, as is noted later.
- The largest and most frequent underpredictions are associated with the Sturm (2004) data. The Sturm (2004) data represent rigid abutments/embankments that have rigid substructures that extend below the bed. The rigid abutment models tend to produce larger scour depths than the erodible models of the NCHRP 24-20 investigation, and this difference contributes to the performance patterns. Additionally, a review of tables 1-3 and 1-4 highlights the different ranges of data characteristics for the Sturm (2004) data and the Ettema et al. (2010) data used to develop the NCHRP 24-20 prediction method. The Sturm (2004) data include relatively long, vertical-wall abutments that are beyond the range and characteristics of the data used to develop the NCHRP 24-20 prediction

method, providing some explanation for the differing performance. Furthermore, the Sturm (2004) data have the smallest flow depths (tables 1-3 and 1-4) within the laboratory data, which tend to produce smaller values of predicted scour when applied to the NCHRP 24-20 prediction method.

- Excluding the Sturm (2004) data, the non-cohesive data for Palaviccini (1993) and Ettema et al. (2010) have a similar range of prediction residuals between the 25th and 75th percentile (figure 6-1), with the live-bed Palaviccini (1993) data having the largest range. A review of tables 1-3 and 1-4 highlights the similar ranges of data characteristics for these two datasets, providing some explanation for their similar performance for the NCHRP 24-20 prediction method.

6.2.2 Residual Patterns Associated with the NCHRP 24-15(2) Prediction Method

Some particular observations regarding the residuals in the NCHRP 24-15(2) prediction method are as follows:

- The Briaud et al. (2009) data have no underprediction, but do have a fairly large range for the prediction residuals. Because these data were used to develop the NCHRP 24-15(2) prediction method, the pattern of no underprediction is to be expected. However, the large range of the residuals, with several large overpredictions, indicates that the NCHRP 24-15(2) method, in its current form, does not fully capture the trends of these data.
- The largest overpredictions in the NCHRP 24-15(2) prediction method are in the Sturm (2004) and Ettema et al. (2010) data, displayed as outliers in figure 6-1. These data are associated with protruding abutments that tend to produce larger overpredictions of scour in the NCHRP 24-15(2) prediction method (report section 5.2.3), than abutments set back from the channel. Approximately 70 percent of the Ettema et al. (2010) data have protruding abutments, which will tend to have larger overpredictions of scour when applied to the NCHRP 24-25(2) method. This is the primary reason why the boxplot of the Ettema et al. (2010) data is skewed towards large overpredictions.

- The NCHRP 24-15(2) prediction method produces larger overpredictions of scour in the Sturm (2004) data in comparison to the NCHRP 24-20 prediction method. These data are associated with larger values of Fr_{f2} that tend to produce larger overpredictions of scour in the NCHRP 24-15(2) prediction method (report section 5.2.3).
- The Palaviccini (1993) data have some of the largest underpredictions which, in part, are related to having rectangular channels with a channel-geometry correction factor of 0.42. The Palaviccini (1993) live-bed data have larger overpredictions than the clear-water data because many of the live-bed data have larger Fr_{f2} values that tend to produce larger scour predictions in the NCHRP 24-15(2) prediction method (report section 5.2.3).

Table 6-1. Summary statistics for the laboratory-data prediction residuals for the NCHRP 24-20 and 24-15(2) scour prediction methods.

	Live-Bed Scour Prediction Residuals		Clear-Water Scour Prediction Residuals		Scour Prediction Residuals		Scour Prediction Residuals		Scour Prediction Residuals	
Data Source:	**Palaviccini (1993)**		**Palaviccini (1993)**		**Sturm (2004)**		**Briaud et al. (2009)**		**Ettema et al. (2010)**	
Prediction Method:	NCHRP 24-20	NCHRP 24-15(2)	NCHRP 24-20	NCHRP 24-15(2)	NCHRP 24-20	NCHRP 24-15(2)	NCHRP 24-20	NCHRP 24-15(2)	NCHRP 24-20	NCHRP 24-15(2)
Units:	(feet)		(feet)		(feet)		(feet)		(feet)	
Number of data points:	164		191		74		19		40	
Minimum:	-0.73	-0.51	-0.51	-0.36	-0.91	-0.03	-1.99	0.33	0.02	-0.21
25th percentile:	-0.11	0.31	-0.10	-0.05	-0.57	0.53	0.28	0.67	0.10	-0.01
Mean:	0.25	0.63	0.09	0.10	-0.37	0.86	0.72	0.92	0.20	0.82
Median:	0.21	0.48	0.00	0.08	-0.33	0.77	0.60	0.80	0.15	0.30
75th percentile:	0.58	0.94	0.25	0.19	-0.20	1.09	1.14	1.02	0.31	1.29
Maximum:	1.74	1.96	1.24	0.95	0.20	2.64	2.72	2.46	0.50	3.50
Standard deviation:	0.54	0.49	0.27	0.23	0.27	0.49	1.22	0.50	0.14	1.11

Table 6-2. Summary statistics for the field-data prediction residuals for the NCHRP 24-20 and 24-15(2) scour prediction methods.

	Scour Prediction Residuals		Scour Prediction Residuals		Scour Prediction Residuals		Scour Prediction Residuals		Scour Prediction Residuals	
Data Source:	**South Carolina Piedmont**		**South Carolina Coastal Plain**		**Maine**		**Alabama**		**NBSD**	
Prediction Method:	NCHRP 24-20	NCHRP 24-15(2)	NCHRP 24-20	NCHRP 24-15(2)	NCHRP 24-20	NCHRP 24-15(2)	NCHRP 24-20	NCHRP 24-15(2)	NCHRP 24-20	NCHRP 24-15(2)
Units:	(feet)		(feet)		(feet)		(feet)		(feet)	
Number of data points:	90		106		93		23		13	
Minimum:	-4.98	-3.74	-16.50	-20.47	-6.47	-5.00	-0.18	-5.84	-2.06	-0.06
25th percentile:	8.29	4.44	-1.57	-6.01	0.02	6.55	2.93	-1.84	0.38	4.61
Mean:	13.62	6.55	1.90	-1.93	3.85	14.96	6.84	-0.16	5.61	7.51
Median:	12.37	6.52	1.61	-1.99	2.63	14.79	5.85	-0.06	4.59	7.87
75th percentile:	17.96	8.35	4.42	0.76	5.21	21.35	9.86	1.36	6.35	9.44
Maximum:	40.17	14.52	17.29	12.79	29.02	42.91	17.47	5.49	22.40	16.89
Standard deviation:	8.18	3.49	4.97	5.69	7.08	11.38	4.99	2.57	6.85	4.45

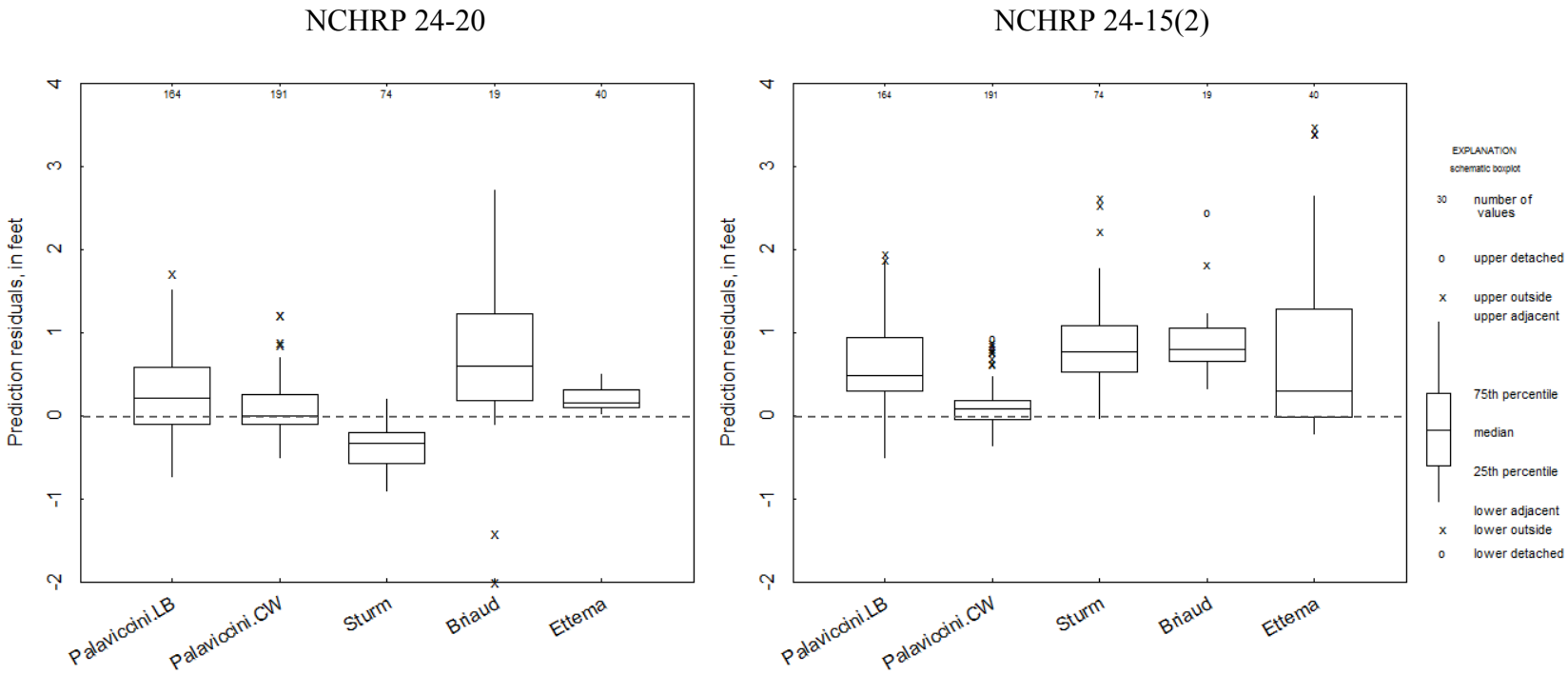

Figure 6-1. Boxplots for the laboratory-data prediction residuals for the NCHRP 24-20 and 24-15(2) scour prediction methods. (Note: The terms "LB" and "CW" refer to live-bed and clear-water scour, respectively.)

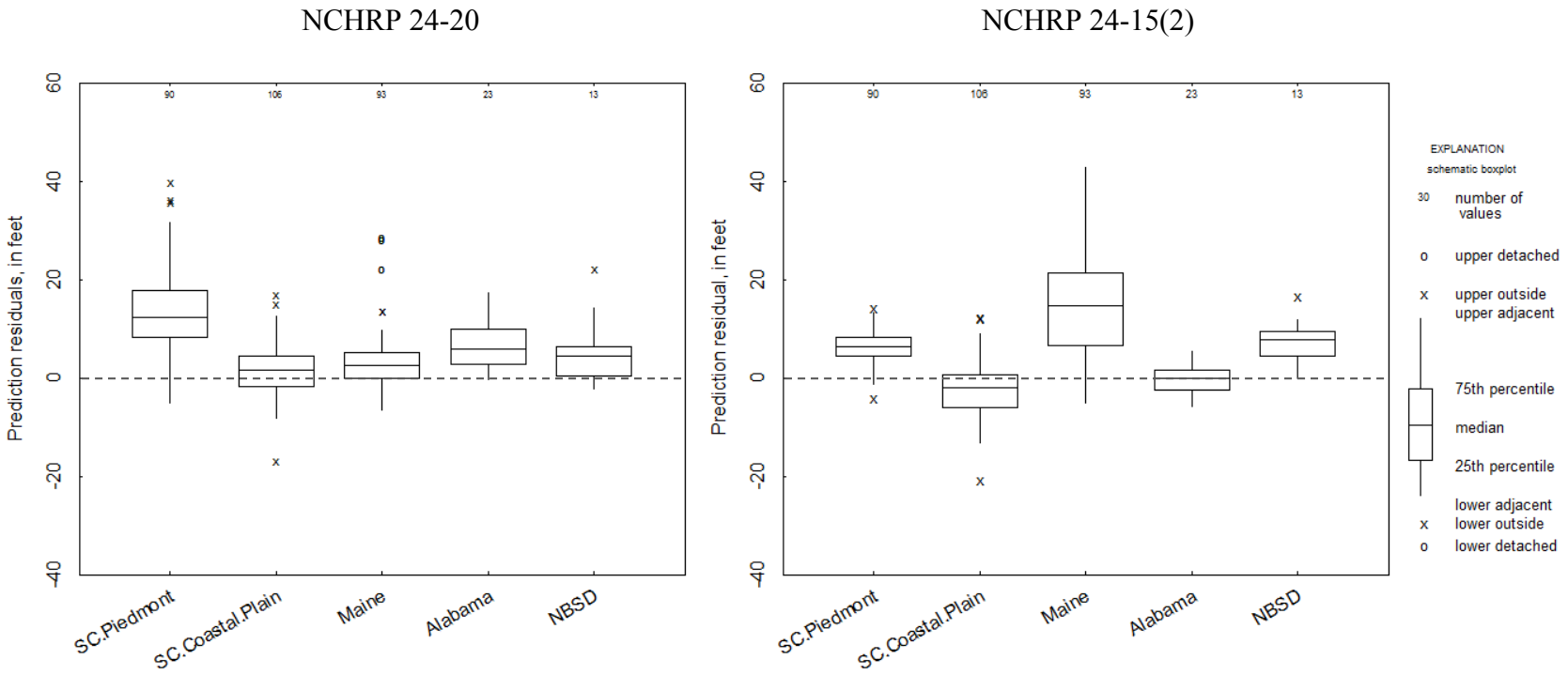

Figure 6-2. Boxplots for the field-data prediction residuals for the NCHRP 24-20 and 24-15(2) scour prediction methods.

6.3 Performance in the Field Data

Similar to the performance of the laboratory data, the prediction-residual boxplots in figure 6-2 indicate that the performance of the NCHRP 24-15(2) and NCHRP 24-20 prediction methods, with respect to the field data, tend to produce overpredictions, with approximately 75 percent or more of the data having overpredictions. The exception to this is the performance of the South Carolina Coastal Plain and Alabama data with the NCHRP 24-15(2) prediction method; comments on this pattern are noted later.

6.3.1 Residual Patterns Associated with the NCHRP 24-20 Prediction Method

Some particular observations regarding the residuals in the NCHRP 24-20 prediction method are as follows:

- The largest overpredictions in the NCHRP 24-20 prediction method are associated with the cohesive sediments of the South Carolina Piedmont. The current formulation of the NCHRP 24-20 prediction method was developed for scour prediction in non-cohesive sediments, and the larger overprediction in cohesive sediments is to be expected. The cohesive sediments of the Alabama data also produce larger predicted scour depths than the non-cohesive sediment data, but not as large as the predicted scour depths of the South Carolina Piedmont data. The Alabama data consist of all floodplain relief bridges that must use the average flow velocity through the bridge, rather than the more conservative estimate of velocity associated with the SBR method (chapter 2), providing some explanation for the smaller scour predictions. Large overpredictions also were noted in the cohesive sediments of the Briaud et al. (2009) laboratory data (figure 6-1). The prediction patterns in the cohesive sediments of the laboratory and field data indicate that the NCHRP 24-20 prediction method, originally developed for scour prediction in non-cohesive sediments, tends to produce large, and at times excessive, overprediction in cohesive sediments. Alternate critical-velocity methods were tested in the NCHRP 24-20 prediction method (report section 3.5), and while overprediction was substantially reduced in the cohesive sediments, underprediction increased.

- The patterns of the prediction residuals for the non-cohesive sediments of the South Carolina Coastal Plain, Maine, and NBSD data are similar, with the 25th percentile, mean, median, and 75th percentile having comparable values (table 6-2). These data include non-cohesive sediments ranging from small sand sizes up to coarse gravel, indicating that the NCHRP 24-20 prediction method performs in a similar manner over a wide range of non-cohesive sediment sizes, and is most applicable to non-cohesive sediments. The relations of predicted and measured scour for the non-cohesive sediments of the laboratory and field data (figures 3-1 and 3-25, respectively) generally show an approximate symmetric scatter of the predicted values around the line of agreement, indicating that the NCHRP 24-20 prediction method, on average, is reflecting the general trends of the measured data for these types of sediments. However, the laboratory and field data both indicate a trend of more frequent underprediction as the scour depth increases. In particular, there is more frequent underprediction of scour in the field data for measured abutment-scour depths of approximately 10 ft and larger. This trend is highlighted in figure 6-3 where boxplots of the prediction residuals grouped by cohesive and non-cohesive sediments, and by measured scour depth less than or greater than 10 ft, are shown. For both sediment categories, the frequency and magnitude of underprediction with the NCHRP 24-20 method is larger for the category of measured scour depths greater than 10 ft, and is most severe in the non-cohesive sediments. Table 6-3 provides the summary statistics for the data in figure 6-3, again highlighting this trend. The underpredictions associated with the non-cohesive data, in part, may be associated with poor estimates of the flow velocity at the abutment as determined from one-dimensional flow models. Performance would likely improve with better estimates of the flow velocity from two-dimensional flow models. Additionally, most of the underpredictions in the non-cohesive sediments are associated with relatively long spill-through abutments, and incorporation of an adjustment for long abutments based on the work of Melville (1992) likely will improve performance at these sites. Because of the potential for underprediction for larger measured scour depths, caution and judgment is required in the application of the NCHRP 24-20 prediction method to non-cohesive sediments.

- Recommendations for ways to potentially improve the performance of the NCHRP 24-20 are presented in report section 5.7

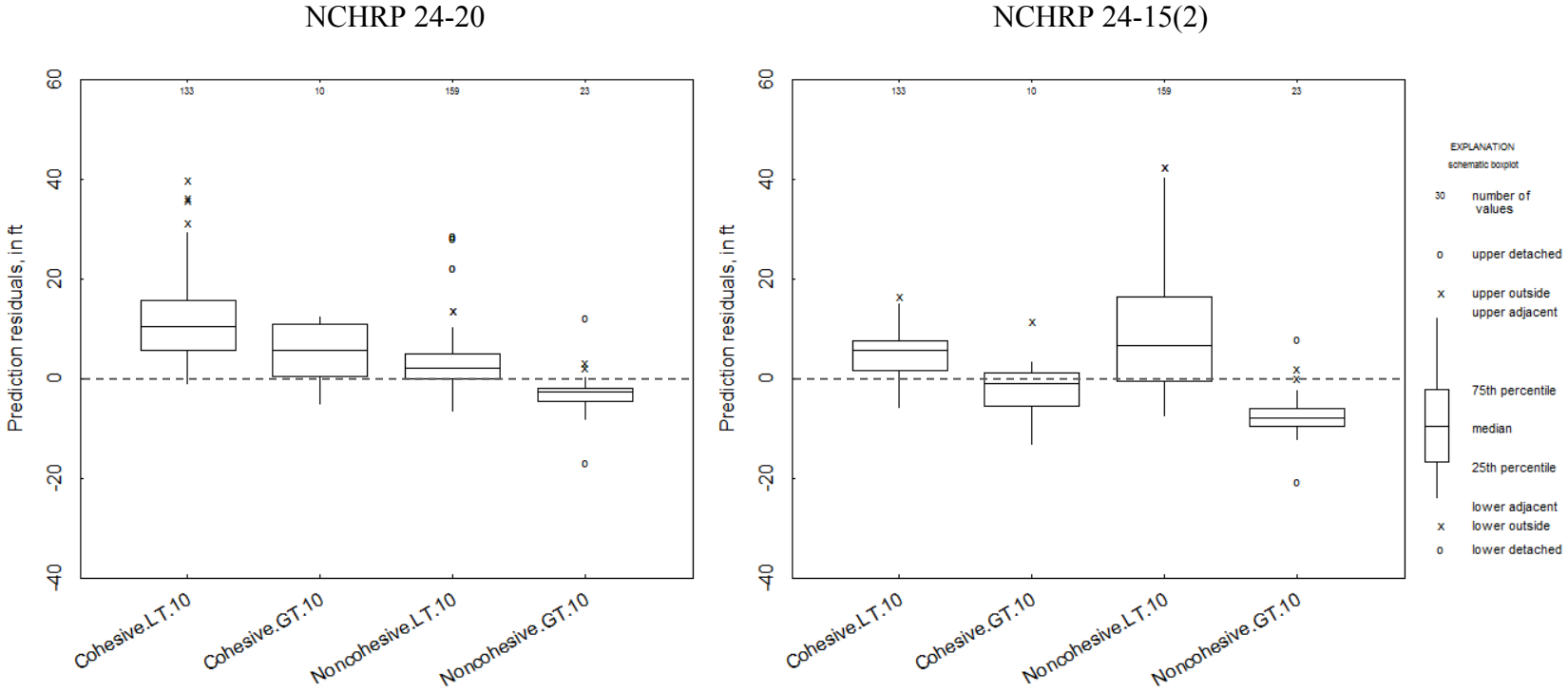

Figure 6-3. Boxplots for the field-data prediction residuals for the NCHRP 24-20 and 24-15(2) scour prediction methods, grouped by cohesive and non-cohesive sediments, and by measured scour depth less than (LT) or greater than (GT) 10 feet.

Table 6-3. Summary statistics for the field-data prediction residuals for the NCHRP 24-20 and 24-15(2) scour prediction methods, grouped by cohesive and non-cohesive sediments, and by measured scour depth less than (LT) or greater than (GT) 10 feet.

	Cohesive sediments with measured scour less than 10 feet		Cohesive sediments with measured scour greater than or equal to 10 feet		Non-cohesive sediments with measured scour less than 10 feet		Non-cohesive sediments with measured scour greater than or equal to 10 feet	
Prediction Method:	NCHRP 24-20	NCHRP 24-15(2)	NCHRP 24-20	NCHRP 24-15(2)	NCHRP 24-20	NCHRP 24-15(2)	NCHRP 24-20	NCHRP 24-15(2)
Units:	(feet)		(feet)		(feet)		(feet)	
Number of data:	133		10		159		23	
Minimum:	-0.87	-5.84	-4.98	-13.23	-6.47	-7.34	-16.50	-20.47
25th percentile:	5.77	1.54	0.38	-5.58	0.00	-0.56	-4.53	-9.65
Mean:	11.53	0.84	5.38	0.38	3.10	0.82	-2.76	1.00
Median:	10.52	5.80	5.61	-1.06	2.07	6.69	-2.55	-7.90
75th percentile:	15.79	7.68	11.07	1.27	5.06	16.43	-1.84	-6.06
Maximum:	40.17	16.89	12.48	11.89	29.02	42.91	12.61	8.15
Standard deviation:	7.89	4.52	5.89	6.70	5.86	11.85	5.14	5.58

6.3.2 Residual Relations Associated with the NCHRP 24-15(2) Prediction Method

Some particular observations regarding the residuals in the NCHRP 24-15(2) prediction method are as follows:

- The Maine data have the largest overpredictions in the NCHRP 24-15(2) prediction method. This overprediction is attributed to larger Fr_{f2} values and protruding abutments, both of which tend to produce larger scour predictions in the NCHRP 24-15(2) prediction method. As demonstrated in report section 5.3.3, using the channel hydraulic data as an alternative to the abutment-location correction factor for protruding abutments will reduce the magnitude of overprediction and improve performance in the Maine data.
- The South Carolina Coastal Plain and Alabama data have the highest frequency of underprediction. This underprediction, in part, may be associated with poor estimates of the flow velocity at the abutment as determined from one-dimensional flow models, and performance would likely improve with better estimates of the flow velocity from two-dimensional flow models. Additionally, these data have a high frequency of floodplain relief bridges and swamps with poorly defined channels that were classified as rectangular channels. The channel-geometry correction factor for such sites is 0.42, which will tend to produce more frequent underprediction. As demonstrated in report section 5.3.3, modifying the channel-geometry correction factor from a value of 0.42 to 1.0 for rectangular channels will diminish the frequency and magnitude of underprediction in the South Carolina data and remove underprediction from the Alabama data. Recommendations for modifying selected correction factors in the NCHRP 24-15(2) prediction method are presented in report section 5.4, and these modifications substantially improve performance in the South Carolina Coastal Plain data.
- The cohesive sediments of the South Carolina Piedmont data have infrequent underprediction. The range of the overprediction is relatively small, with a mean prediction residual of 6.5 ft, and the 75th percentile and maximum values are 8.4 ft and 14.5 ft, respectively (table 6-2). The underprediction associated with the cohesive

sediments of the Alabama data, as noted previously, is caused by the correction factor of 0.42 for rectangular channels, which when modified to a value of 1.0, the underprediction is removed (report section 5.3.3). The performance of the South Carolina Piedmont data and the Alabama data, modified as suggested, indicates that the NCHRP 24-15(2) prediction method will likely perform well in cohesive sediments. The NCHRP 24-15(2) prediction method was originally developed for cohesive sediments, so the better performance with the South Carolina Piedmont and Alabama data would seem logical.

- As noted for the NCHRP 24-20 prediction method, there is more frequent underprediction of scour in the field data for measured abutment-scour depths of approximately 10 ft and larger than for measured abutment-scour depths less than 10 ft. This trend is highlighted in the boxplots shown in figure 6-3 and in the summary statistics for the prediction residuals in table 6.3 (see report section 6.3.1 for descriptions of figure 6-3 and table 6-3), where the frequency and magnitude of underprediction with the NCHRP 24-15(2) method are larger for the category of measured scour depths greater than 10 ft, and is most severe in the non-cohesive sediments. As noted for the NCHRP 24-20 method, the underprediction is likely caused by a number of factors, including poor estimates of the flow velocity at the abutment as determined from one-dimensional flow models and relatively long spill-through abutments that tend to produce larger scour depths. Performance would likely improve with better estimates of the flow velocity from two-dimensional flow models and with the incorporation of an adjustment for long abutments based on the work of Melville (1992). Additionally, many of the non-cohesive data are associated with rectangular channels that tend to underpredict scour because the channel-geometry correction factor is 0.42. Modifying this correction factor to 1.0 will substantially improve performance. Because of the potential for underprediction for larger measured scour depths, caution and judgment are required in the application of the NCHRP 24-15(2) prediction method to non-cohesive sediments.
- Recommendations for ways to potentially improve the performance of the NCHRP 24-15(2) method are presented in report section 5.4.

6.4 Conclusions

The NCHRP 24-15(2) and NCHRP 24-20 investigations represent extensive efforts to develop conceptual models for abutment scour in cohesive and non-cohesive sediments, collect laboratory data, evaluate those data, and develop new methods for predicting abutment scour. The conceptual models, along with the data collected in these investigations, provide a valuable resource to assist the engineer in evaluating abutment scour. The focus of the current investigation was to evaluate the performance of these newly developed equations by using laboratory and field data. As described earlier in the report, the laboratory and field data have inherent weaknesses and limitations (chapter 1), and the results presented in this report will in some measure be a function of those limitations. Therefore, caution and judgment should be used in the evaluation, interpretation, and application of the findings in this report. However, the large amount of data used in the investigation (tables 1-1 and 1-3) is sufficient to provide a general understanding of each equation's performance, providing helpful information to those using these equations. A general summary of conclusions based on the results from this report is presented in the following report sections.

The NCHRP Project 24-27(2) (Sturm et al. 2011) reviewed selected abutment-scour research, including the NCHRP 24-15(2) and NCHRP 24-20 prediction methods and made general recommendations for abutment-scour design. The following quotation from that report provides insights to the challenges that still exist for scour prediction at abutments.

> *Given this state of our current understanding of abutment/contraction scour, or lack thereof, it is very difficult to develop design-specific recommendations at this time. Some important strides forward have been made in the past decade, but there remains much to be learned before we have arrived at the more settled and defined state of knowledge that currently exists with respect to pier scour.*

While the challenges of predicting abutment scour are real, Sturm et al. (2011) provide some general and useful recommendations for abutment-scour design, as well as further research (see chapter 7 of that report). The conclusions of the current (2015) investigation should be considered in light of these recommendations.

6.4.1 Summary of Conclusions for NCHRP 24-20

Report section 3.7 provides a description of selected strengths and weaknesses associated with the NCHRP 24-20 prediction method, and some of the more notable characteristics are summarized below. One strength of the NCHRP 24-20 method is its simple conceptual model derived from physical processes, in which abutment scour is considered a function of contraction scour. The simplicity of the model provides a logical explanation of the relation between abutment and contraction scour, and its derivation from physical processes should make the method applicable to a broad range of field conditions. The current formulation of the NCHRP 24-20 method uses Laursen's (1960; 1963) familiar and widely accepted contraction-scour equations, which should make application of the NCHRP 24-20 method fairly intuitive to the practitioner.

The performance of the NCHRP 24-20 method, as shown in figure 3-25, indicates that the method is reflecting the general trend of the non-cohesive field data, with predicted scour depth increasing as measured scour depth increases, particularly for measured scour depths less than about 10 ft. This pattern suggests that the NCHRP 24-20 method is, in some measure, capturing the scour processes for the non-cohesive field data within this range. The boxplots in figure 6-2 also highlight the performance pattern in the non-cohesive sediments. However, as measured scour depth increases beyond 10 ft, underprediction also increases (figure 6-3), which is of concern. Multiple factors likely contribute to this pattern of underprediction, including limitations associated with the field and laboratory data. With regard to the field data, poor estimates of flow velocities at the abutment from one-dimensional flow models likely causes some of the underprediction, and performance would likely improve with better velocity estimates from two-dimensional flow models. With regard to the laboratory data, the erodible abutment/embankment models used to develop the NCHRP 24-20 method for Scour Condition B (figure 3-21) eroded, producing smaller scour depths than rigid or intact abutments. Because the USGS field data with Scour Condition B reflect intact abutments (see report section 3.4), the NCHRP 24-20 method may tend to underpredict scour at such abutments, producing some of the underprediction seen in figure 3-25. While eroded abutments and failed embankments are common in the field, many abutments/embankments will remain intact during a flood. Because of the differing scour patterns between erodible and intact abutments, the practitioner will need

to evaluate the appropriateness of using the NCHRP 24-20 prediction method for abutments with Scour Condition B. (See report section 3.4 for additional details.) A way to address this concern would be the inclusion of an appropriate abutment-scour countermeasure, which is recommended as a standard design procedure by Sturm et al. (2011) for all new abutment designs. With respect to cohesive sediments, the boxplots in figure 6-2 show the infrequent underprediction for the cohesive sediments of the South Carolina Piedmont and Alabama, but overprediction that at times is excessive, especially in the South Carolina Piedmont data. Additional information on the strengths and weaknesses of the NCHRP 24-20 method can be found in report section 3.7.

While the underprediction in the non-cohesive sediments and the noted limitations associated with the NCHRP 24-20 method are a concern, the prediction patterns in the non-cohesive sediments displayed in figure 3-2 indicate that the method is reflecting the general trends of abutment scour in the field and that further research and evaluation will likely yield improved performance. Some specific areas for further evaluation are noted in report section 3.7.3 and include:

- Evaluating the sensitivity to flow velocity by using two-dimensional flow models at selected sites in the USGS field data.

- Evaluating the influence of relatively long abutments to determine if incorporating an adjustment factor (Melville, 1992; Melville and Coleman, 2000) in the NCHRP 24-20 for such abutments would be appropriate to minimize the potential for underprediction.

- Evaluating the amplification factor for field conditions where the abutment and embankment remains intact.

- Developing an appropriate safety factor.

- Developing an equation formulation appropriate for cohesive sediments.

- Evaluating the current, simplified contraction-scour equations to improve these methods that in turn will improve abutment-scour prediction.

Limited guidance for applying the NCHRP 24-20 method is presented in report section 3.7.4. This guidance is not exhaustive and is not intended to supersede the guidance in HEC-18 or NCHRP 24-20. Additionally, the practitioner will need to evaluate the appropriateness of using the NCHRP 24-20 method for the given design criteria and site conditions. The guidance provides some cautions regarding the estimate of flow velocity at the abutment, evaluation of scour potential at long abutments and large flow contractions, and the influence of soil conditions on scour at a given site. Additionally, limited guidance is provided for applying the NCHRP 24-20 method to sites with cohesive sediments similar to the South Carolina Piedmont and Alabama data, steep-gradient streams with coarse sediments similar to the Maine data, and low-gradient streams with non-cohesive sediments similar to the South Carolina Coastal Plain data. The performance of the NCHRP 24-20 prediction method, as presented in this report, is based on the range of site conditions associated with the field data in table 1-1, and uncertainty of the equation performance increases as site conditions approach the limits or deviate from those listed in table 1-1.

6.4.2 Summary of Conclusions for NCHRP 24-15(2)

Report section 5.4 provides a description of selected strengths and weaknesses associated with the NCHRP 24-15(2) prediction method, and some of the more notable characteristics are summarized here. The NCHRP 24-15(2) method consists of a simple equation format similar to the Froehlich (1989) abutment-scour equation, which should make application of the method fairly intuitive. The prediction method was developed for cohesive sediments, and results from this investigation indicate that the equation in its original form will perform best in those types of sediments. The boxplots in figure 6-2 and the scatter plot in figure 5-32C highlight the good performance in the cohesive sediments of the South Carolina Piedmont, and similar performance occurs in the cohesive sediments of the Alabama data (figure 5-50) when the recommended modification for rectangular channels is made. The equation in its original form does not perform as well in the non-cohesive sediments (figure 5-54), with substantial underprediction in the low-gradient streams of the South Carolina Coastal Plain (figures 5-32A and B) and substantial overprediction in the steep-gradient streams with coarse sediments of Maine (figure 5-32D). Similar to the performance in the NCHRP 24-20 prediction method, the underprediction in the South Carolina Coastal Plain, in part, is likely associated with poor estimates of the flow

velocity at the abutment as determined from one-dimensional flow models, and performance would likely improve with better estimates of the flow velocity from two-dimensional flow models. However, other factors likely contribute to this pattern. It is notable that the core explanatory variable, $7.94(1.65Fr_{f2} - Fr_c)$, provides a conservative estimate of abutment scour in the low-gradient streams of the South Carolina Coastal Plain (figure 5-33) with essentially no underprediction.

A review of the correction factors in the NCHRP 24-15(2) prediction method indicates that further evaluation and modification of some of these factors may lead to improved performance. Specific recommendations are presented in report section 5.4.3, including the following:

- Modifying the value of the channel-geometry correction factor, K_G, for rectangular channels from 0.42 to 1.0.

- Using the channel hydraulic data rather than the abutment-location correction factor, K_L, to account for the potential increase in scour at bankline and protruding abutments.

- Incorporating an adjustment to the abutment shape correction factor, K_1, to account for the potential increase of scour associated with long abutments as described in Melville (1992). (Note: The modification only was applied to the South Carolina Coastal Plain data as described in report section 5.4.)

- Further evaluating the correction factor for abutment skew, K_2, because of the limited data used to develop the factor.

- Further evaluating the Reynolds number correction factor, K_{Re}, to address some of the problematic issues described in report section 5.4.3.

- Evaluating the influence on predicted scour for V_c as determined from an EFA test in contrast to V_c as determined from figure 4-4.

- Evaluating the sensitivity to flow velocity by using two-dimensional flow models at selected sites in the USGS field data.

- Developing an appropriate safety factor.

Limited guidance for applying the NCHRP 24-15(2) method is presented in report section 5.4.4. This guidance is not exhaustive and is not intended to supersede the guidance in Briaud et al. (2009, 2011). Additionally, the practitioner will need to evaluate the appropriateness of using the NCHRP 24-15(2) method for the given design criteria and site conditions. The guidance provides some cautions regarding the estimate of flow velocity at the abutment, evaluation of scour potential at long abutments and large flow contractions, and the influence of soil conditions on scour at a given site. Additionally, limited guidance is provided for applying the NCHRP 24-15(2) method to sites with cohesive sediments similar to the South Carolina Piedmont and Alabama data, steep-gradient streams with coarse sediments similar to the Maine data, and low-gradient streams with non-cohesive sediments similar to the South Carolina Coastal Plain data. The performance of the NCHRP 24-15(2) prediction method as presented in this report is based on the range of site conditions associated with the field data in table 1-1, and uncertainty of the equation performance increases as site conditions approach the limits or deviate from those listed in table 1-1.

REFERENCES

Arneson, L.A., Zevenbergen, L.W., Lagasse, P.F., and Clopper, P.E. (2012). "Evaluating Scour at Bridges." *Hydraulic Engineering Circular* No. 18, 5th Ed., Federal Highway Administration, Arlington, VA.

Benedict, S.T. (2003). "Clear-water abutment and contraction scour in the Coastal Plain and Piedmont Provinces of South Carolina, 1996-99." Water-Resources Investigations *Report* 03-4064, U. S. Geological Survey, Columbia, South Carolina.

Benedict, S.T. (2010). "Evaluation of Maryland abutment scour equation through selected threshold velocity methods." *Transportation Research Record*, No. 2195, pp. 153-167.

Benedict, S.T., and Caldwell, A.W. (2006). "Development and evaluation of clear-water pier and contraction scour envelope curves in the Coastal Plain and Piedmont Provinces of South Carolina." Scientific Investigations *Report* 5289, U. S. Geological Survey, Reston, VA.

Benedict, S.T., Deshpande, N., Aziz, N.M., and Conrads, P.A. (2006). "Trends of abutment-scour prediction equations applied to 144 field sites in South Carolina." Open-File *Report* 03-295, U. S. Geological Survey, Reston, VA.

Benedict, S.T., Deshpande, N., and Aziz, N.M. (2007). "Evaluation of abutment scour prediction equations with field data" *Transportation Research Record*, No. 2025, pp. 118-126.

Briaud, J.-L., Ting, F., Chen, H.-C., Gudavalli, R., Kwak, K., Philogene, B., Han, S.-W., Perugu, S., Wei, G.S., Nurtjahyo, P., Cao, Y.W., and Li, Y. (1999 (a)). "SRICOS: Prediction of Scour Rate at Bridge Piers." TTI Report no. 2937-1 to the Texas DOT, Texas A&M University, College Station, Texas, USA.

Briaud, J.-L., Ting, F., Chen, H.C., Gudavalli, S.R., Perugu, S., and Wei, G. (1999 (b)). "SRICOS: Prediction of Scour Rate in Cohesive Soils at Bridge Piers." ASCE Journal of Geotechnical and Geoenvironmental Engineering Vol. 125, pp. 237-246.

Briaud, J.-L., Chen, H.-C., Li, Y., Nurtjahyo, P., and Wang, J. (2004). "Complex Pier Scour and Contraction Scour in Cohesive Soils." NCHRP report 516, Transportation Research Board, Washington, D.C.

Briaud, J.-L., Chen, H.-C., Chang, K.-A., Oh, S.J., and Chen, X. (2009). "Abutment Scour in Cohesive Material." NCHRP Report 24-15(2), Transportation Research Board, National Research Council, Washington, D.C.

Briaud, J.-L., Chen, H.-C., Chang, K.-A., Oh, S.J., Chen, S., Wang J., Li Y., Kwak K., Nartjaho P., Gudavalli R., Wei W., Perugu S., Cao, Y.W., and Ting, F. (2011). "The SRICOS–EFA method." Summary Report, Texas A&M University.

Brice, J.C., Blodgett, J.C., and Others (1978). "Countermeasures for hydraulic problems at bridges, volume 2—Case histories for sites 1-283." *Report* No. FHWA-RD-78-163, Federal Highway Administration, Arlington, VA.

Chang, F., and Davis, S. (1998). "Maryland SHA procedure for estimating scour at bridge abutments, part 2—Clear water scour," Proc. of Water Resources Engineering, '98, ASCE, Memphis, TN, pp. 169-173.

Chang, F., and Davis, S. (1999). "Maryland SHA procedure for estimating scour at bridge waterways, part 1—Live bed scour." In *Stream Stability and Scour at Highway Bridges*, (Eds) Richardson, E. and Lagasse, P., American Society of Civil Engineers, Reston VA, pp. 401-4011.

Conaway, J.S. (2006). "Comparison of long-term streambed scour monitoring data with modeled values at the Knik River, Alaska," *Proc.* 3rd International Conference on Scour and Erosion at Amsterdam, Holland.

Conaway, J.S., and Brabets, T.P. (2011). "Streamflow and streambed scour in 2010 at bridge 339, Copper River, Alaska." In *Studies by the U.S. Geological Survey in Alaska, 2010* (Eds) Dumoulin, J.A., and Dusel-Bacon," Professional *Paper* 1784-C, U. S. Geological Survey, Reston, VA.

Culbertson, D.M., Young, L.E., and Brice, J.C. (1967). "Scour and fill in alluvial channels with particular reference to bridge sites." Open-File *Report* 1967, U.S. Geological Survey.

Dongol, D.M. (1993). "Local scour at abutments." Report 544, Dept. of Civil Engineering, University of Auckland, Auckland, New Zealand.

Ettema, R., Nakato, T., and Muste, N. (2010). "Estimation of scour depth at bridge abutments." Draft final report, NCHRP Report 24-20, National Cooperative Highway Research Program, Transportation Research Board, Washington, D.C.

Ettema, R., Yorozuya, A., Nakato, T., and Muste, M. (2005). "A practical approach to estimating realistic depths of abutment scour." *The 2005 Mid-Continent Transportation Research Symposium*, Iowa State University, Ames, IA.

Fortier, S. and Scobey, F.C. (1926). "Permissible canal velocities," ASCE, *Transactions*, Vol. 89, Paper No. 1588, pp. 940–984.

Froehlich, D.C. (1989). "Local scour at bridge abutments," Proc. ASCE National Hydraulic Conference, Colorado Springs, Colorado, pp. 13-18.

Hayes, D.C. (1996). "Scour at bridge sites in Delaware, Maryland, and Virginia." Water-Resources Investigations *Report* 96-4089, U.S. Geological Survey, Richmond, Virginia.

Kandasamy, J.K. (1985). "Local scour at skewed abutments." Report No. 375, School of Engineering, University of Auckland, Auckland, New Zealand.

Kwan, T.F. (1984). "Study of abutment scour." Report 328, Department of Civil Engineering, University of Auckland, Auckland, New Zealand.

Lagasse, P.F., Clopper, P.E., Zevenbergen, L.W, and Ruff, J.F. (2006). "Riprap design criteria, recommended specifications, and quality control." Report 568, National Cooperative Highway Research Program, Transportation Research Board, Washington, D.C.

Lagasse, P.F., Clopper, P.E., Pagán-Ortiz, J.E., Zevenbergen, L.W., Arneson, L.A., Schall, J.D., and Girard, L.G. (2009). "Bridge scour and stream instability countermeasures experience, selection, and design guidance." *Hydraulic Engineering Circular* No. 23, 3rd Ed., Federal Highway Administration, Arlington, VA.

Laursen, E.M. (1960). "Scour at bridge crossings." *J. Hydr. Div.*, ASCE, 86(2), 39-54.

Laursen, E.M. (1963). "An analysis of relief bridge scour." *J. Hydr. Div.*, ASCE, 86(2), 93-118.

Lee, K.G., and Hedgecock, T.S. (2008). "Clear-water contraction scour at selected bridge sites in the Black Prairie Belt of the Coastal Plain in Alabama, 2006." Scientific Investigations *Report* 2007–5260 U. S. Geological Survey, Reston, VA.

Lombard, P.J., and Hodgkins, G.A. (2008). "Comparison of observed and predicted abutment scour at selected bridges in Maine." Scientific Investigations *Report* 2008–5099, U. S. Geological Survey, Reston, VA.

Maryland State Highway Administration, Office of Structures. (2014). ABSCOUR 10, the Maryland State Bridge Scour Program, November 2014.

Melville, B.W. (1992). "Local scour at bridge abutments." J. Hydr. Eng., ASCE, Vol. 118, No. 4, p. 615.

Melville, B.W. (1997). "Pier and abutment scour: Integrated approach." Journal of Hydraulic Engineering, ASCE, Vol. 123, No. 2, pp. 125-136.

Melville, B.W., and Coleman, S.E. (2000). "Bridge Scour." Water Resources Publications, Colorado, U.S.A., 550 p.

Morales, R., and Ettema, R. (2013). "Insights from depth-averaged numerical simulation of flow at bridge abutments in compound channels," ASCE Journal of Hydraulic Engineering, Vol. 139, No. 5, pp. 470-481.

Mueller, D.S., Miller, R.L., and Wilson, J.T. (1993). "Historical and potential scour around bridge piers and abutments of selected stream crossings in Indiana." Water-Resources Investigations *Report* 93-4066, U.S. Geological Survey, Indianapolis, IN.

National Bridge Inventory Database (NBI). (2012). Federal Highway Administration, Washington, D.C.

Neill, C.R. (1973). "*Guide to Bridge Hydraulics*." Roads and Transportation Assoc. of Canada, Univ. of Toronto Press, Toronto, Canada.

Palaviccini, M. (1993). "Predictor model for bridge abutments." PhD Thesis, The Catholic University of America, Washington, D.C.

Parola, A.C., Hagerty, D.J., and Kamojjala, S. (1998). "Highway infrastructure damage caused by the 1993 Upper Mississippi River basin flooding." NCHRP Report 417. National Cooperative Highway Research Program, Transportation Research Board, Washington, D.C.

Richardson, E.V., and Davis, S.R. (2001). "Evaluating Scour at Bridges." *Hydraulic Engineering Circular* No. 18, 4th Ed., Federal Highway Administration, Arlington, VA.

Shearman, J.O. (1990). "User's manual for WSPRO—A computer model for water-surface profile computations." Report No. FHWA-IP-89-027, Federal Highway Administration, McLean, VA.

Sturm, T.W. (2004). "Enhanced abutment scour studies for compound channels." *Report* No. FHWA-RD-99-156, Federal Highway Administration, McLean, VA.

Sturm, T.W. (2006). "Scour around Bankline and Setback Abutments in Compound Channels." Journal of Hydraulic Engineering, ASCE, Vol. 132, No. 1, pp. 21-32.

Sturm, T.W., Ettema, R., and, Melville, B.W. (2011). "Evaluation of bridge-scour research: Abutment and contraction scour processes and prediction." We-Only Document 181, National Cooperative Highway Research Program, Transportation Research Board, Washington, D.C.

U.S. Army Corps of Engineers, (2001). "HEC–RAS River Analysis System, Hydraulic Reference Manual." ver. 3.1.3, Hydrologic Engineering Center, Davis, CA.

U.S. Geological Survey (2001). "National bridge scour database." (http://water.usgs.gov/osw/techniques/bs/BSDMS/index.html).

Vanoni, V.A. (ed.). (1975). *Sedimentation Engineering*, *ASCE Manuals and Reports on Engineering Practices*, ASCE 54, New York, NY.

Wagner, C.R., Mueller, D.S., Parola, A.C., Hagerty, D.J., and Benedict, S.T. (2006). "Scour at contracted bridges." We-Only Document 83, National Cooperative Highway Research Program, Transportation Research Board, Washington, D.C.

Yang, T.Y. (1996). "Sediment Transport Theory and Practice." McGraw-Hill, New York.